NUREG/CR–5118
SAND88–7155

Leak and Structural Test of Personnel Airlock for LWR Containments Subjected to Pressures and Temperatures Beyond Design Limits

Prepared by J. T. Julien, S. W. Peters

CBI Research Corporation

Sandia National Laboratories

Prepared for
U.S. Nuclear Regulatory Commission

AVAILABILITY NOTICE

Availability of Reference Materials Cited in NRC Publications

Most documents cited in NRC publications will be available from one of the following sources:

1. The NRC Public Document Room, 2120 L Street, NW, Lower Level, Washington, DC 20555

2. The Superintendent of Documents, U.S. Government Printing Office, P.O. Box 37082, Washington, DC 20013-7082

3. The National Technical Information Service, Springfield, VA 22161

Although the listing that follows represents the majority of documents cited in NRC publications, it is not intended to be exhaustive.

Referenced documents available for inspection and copying for a fee from the NRC Public Document Room include NRC correspondence and internal NRC memoranda; NRC Office of Inspection and Enforcement bulletins, circulars, information notices, inspection and investigation notices; Licensee Event Reports; vendor reports and correspondence; Commission papers; and applicant and licensee documents and correspondence.

The following documents in the NUREG series are available for purchase from the GPO Sales Program: formal NRC staff and contractor reports, NRC-sponsored conference proceedings, and NRC booklets and brochures. Also available are Regulatory Guides, NRC regulations in the *Code of Federal Regulations*, and *Nuclear Regulatory Commission Issuances*.

Documents available from the National Technical Information Service include NUREG series reports and technical reports prepared by other federal agencies and reports prepared by the Atomic Energy Commission, forerunner agency to the Nuclear Regulatory Commission.

Documents available from public and special technical libraries include all open literature items, such as books, journal and periodical articles, and transactions. *Federal Register* notices, federal and state legislation, and congressional reports can usually be obtained from these libraries.

Documents such as theses, dissertations, foreign reports and translations, and non-NRC conference proceedings are available for purchase from the organization sponsoring the publication cited.

Single copies of NRC draft reports are available free, to the extent of supply, upon written request to the Office of Information Resources Management, Distribution Section, U.S. Nuclear Regulatory Commission, Washington, DC 20555.

Copies of industry codes and standards used in a substantive manner in the NRC regulatory process are maintained at the NRC Library, 7920 Norfolk Avenue, Bethesda, Maryland, and are available there for reference use by the public. Codes and standards are usually copyrighted and may be purchased from the originating organization or, if they are American National Standards, from the American National Standards Institute, 1430 Broadway, New York, NY 10018.

NUREG/CR--5118

TI89 014540

Leak and Structural Test of Personnel Airlock for LWR Containments Subjected to Pressures and Temperatures Beyond Design Limits

Manuscript Completed: February 1989
Date Published: May 1989

Prepared by
J. T. Julien, S. W. Peters

CBI Research Corporation
1501 N. Division Street
Plainfield, IL 60544-8929

Under Contract to:
Sandia National Laboratories
Albuquerque, NM 87185

Prepared for
Division of Engineering
Office of Nuclear Regulatory Research
U.S. Nuclear Regulatory Commission
Washington, DC 20555
NRC FIN A1375

For sale by the Superintendent of Documents, U.S. Government Printing Office
Washington, D.C. 20402

Blank Page

ABSTRACT

As part of the U.S. Nuclear Regulatory Commission's (USNRC) Containment Integrity Program, tests were performed on a full-size personnel airlock for a nuclear containment building to determine its leakage potential and to measure its structural and thermal response. The airlock was subjected to conditions simulating severe accident conditions. Testing was performed by CBI Research Corporation (CBIRC) under contract to Sandia National Laboratories (SNL), which manages the Containment Integrity Program for the USNRC.

The objective of the test was to characterize the performance of airlock door seals when subjected to conditions that simulate a severe accident condition. The gaskets tested had a cross-section known as a "double dog-ear" configuration and were made from EPDM E603. The seals were aged at an accelerated rate to simulate aging that might occur during 40 years of continuous service and a loss of coolant accident (LOCA). The data obtained from this test will be used by SNL as a benchmark for development of analytical methods. Leak rate, strain, temperature, displacement, and pressure data were measured and recorded from over 330 transducers.

A total of nine tests were performed on the airlock. In the most rigorous of these tests, the airlock inner door was subjected to pressures and temperatures of 300 psig (2.07 MPa) and 850°F (454°C). The airlock was originally designed for a pressure of 60 psig (410 kPa) and 340°F (171°C). During the beyond-design-basis test, the inner door and bulkhead of the airlock were exposed to a maximum surface pressure of 300 psig (2.07 MPa) and a maximum surface temperature on the door of 783°F (417°C)

The remaining eight tests were performed at ambient temperatures and at air pressures on the airlock doors up to 69 psig (476 kPa). These tests were conducted to provide reference points for leakage under design conditions, to estimate the need for and effectiveness of the gaskets, and to characterize the post-severe accident behavior of the airlock.

Blank Page

TABLE OF CONTENTS

LIST OF FIGURES

LIST OF FIGURES (continued)

LIST OF FIGURES (continued)

LIST OF TABLES

Blank Page

ACKNOWLEDGMENTS

The project team would like to thank Mr. Jack Smith for his consulting efforts in implementing the use of the high temperature strain gages used in this test program. We would also like to thank Mr. Tom Ahl of CBI Industries, Inc. for his input and guidance in the area of personnel airlock gasket seals, and Mr. David Clauss of Sandia National Laboratories for his overall guidance and encouragement over the test program duration, and the SNL Peer Review group for their insightful comments which have helped to make this report a credit to the nuclear industry.

EXECUTIVE SUMMARY

The U.S. Nuclear Regulatory Commission (USNRC) has embarked on a program, known as the Containment Integrity Program, to establish behavior characteristics of light water reactor (LWR) containment buildings subjected to conditions beyond design basis. Sandia National Laboratories (SNL) manages the following four elements of this program:

(1) Tests of seals and mechanical penetrations,
(2) Scale model tests of containment buildings,
(3) Analysis and methodology development, and
(4) Electrical penetration assemblies.

The overall objective of these program elements is to develop test validated methods for predicting the performance of containment buildings subjected to severe accident conditions.

Personnel airlocks provide access into and out of containment buildings for maintenance and inspection crews, as well as for the transport of light equipment. The full-size airlock tested in this program was partially fabricated for the Union Electric Company's cancelled Callaway Unit 2. Construction of the airlock was completed for this test program.

The airlock consisted of a steel cylinder 19 ft-5/16 in (5.80 m) long with an inside diameter of 9 ft-10 in (3.00 m). Both ends of the cylinder are enclosed with reinforced bulkheads. The bulkheads are made of steel plate reinforced with structural stiffeners to resist bending loads created by the pressure loading on the bulkhead surface. A 6 ft-8 in (3.0 m) by 3 ft-6 in (1.1 m) rectangular doorway is located in the middle of each bulkhead and is framed by the primary bulkhead structural stiffeners. The reinforced steel doors that measure 7 ft-1/2 in (2.1 m) by 3 ft-10-1/2 in (1.2 m) complete the structural design. The door overlaps the bulkhead doorway opening. The overlapping surfaces of the door and bulkhead are machined and form the sealing surface for the gasket. A gland groove is machined into the door and contains the gasket. The door is located on the side opposite the bulkhead stiffeners.

The airlock was tested to provide benchmark data that can be used to validate analytical methods for predicting the performance of personnel airlocks subjected to loads beyond design. A major objective of this test program was to evaluate the leakage potential of the airlock door seals when subjected to conditions beyond the original design basis. Eight additional tests were performed at ambient temperature conditions to provide reference data for leakage under design conditions, to estimate the need for and effectiveness of the gaskets, and to characterize the post-severe accident behavior of an airlock. The experimental program was also designed to measure the structural and thermal behavior of a personnel airlock subjected to pressures and temperatures simulating severe accident conditions greater than design conditions.

The airlock door seals used were "double dog-ear" gaskets made of EPDM E603. The gaskets were subjected to an accelerated thermal aging process to simulate in-service radiation and thermal aging over a 40-year service life plus a loss-of-coolant-accident (LOCA). Radiation aging was not practical due to the size of the airlock. The equivalent thermal aging condition was determined by SNL using the Arrhenius model to obtain the life (as measured by compression set retention) corresponding to both radiation and thermal aging over the 40-year service life and a LOCA. Accelerated aging was achieved by heating the airlock door with the gasket seals installed and the doors closed and latched. The inner door gasket was maintained at an average temperature of 369°F (187°C) and the outer door gasket at an average temperature of 365°F (185°C). The duration of heating was approximately 172 hours for both doors.

As a result of the accelerated aging process, the gaskets were deformed to the point that the interspace gap and the original "double dog ear" cross-section were no longer recognizable. At several locations around the perimeter of the doors the gaskets flowed into the space between the doors and the adjacent bulkhead. This material between the door and the bulkhead prevented metal-to-metal contact between the door and bulkhead.*

The personnel airlock was extensively instrumented with 123 strain gages, 115 thermocouples, 88 displacement transducers, five pressure transducers, and flow meters. Data was acquired from 331 transducers.

A total of nine tests were performed on the airlock. In the most rigorous of these tests, the airlock inner door was subjected to pressures and temperatures beyond the design basis. The airlock was originally designed for a pressure of 60 psig (410 kPa) and 340°F (171°C). During the beyond design basis test, the inner door and bulkhead of the airlock were exposed to the following three load cycles:

- The first load cycle consisted of heating the air above the inner door to 400°F (204°C). In the test configuration "above the inner door" is equivalent to inside the containment building. The air temperature was allowed to stabilize and the pressure was increased to 300 psig (2.07 MPa) in 10 psi (69 kPa) increments. Pressure was decreased in 25 psi (17 kPa) increments.

- The second load cycle consisted of increasing the air temperature above the inner door from 400 to 800°F (204 to 427°C). The air temperature was allowed to stabilize, and the pressure was increased to 300 psig (2.07 MPa) in 10 psi (69 kPa) increments. Pressure was decreased in 25 psi (170 kPa) increments. As pressure was increased, the air temperature above the door dropped below 600°F (316°C).

- The third load cycle was implemented since the gasket survived the first two load cycles. The air temperature above the door was increased to

---

* The cross-sectional area of the double dog-ear gasket was designed to be slightly less than that of the gland the gasket was contained in so that metal-to-metal contact is achieved when the gasket is fully compressed.

850°F (454°C) and allowed to thermally soak for approximately 10 hours. Pressure was increased in 25 psi (170 kPa) increments until the gasket seal failed. The larger pressure increments were used to minimize heat loss during pressurization. The airlock was then pressurized to 300 psig (2.07 MPa).

During the first and second loading cycles the seals remained intact and there was no measurable leakage. During the third load cycle, the inner door gasket material became unstable, and at 151 psig (1.04 MPa) the inner door seal failed. The failure occurred suddenly and the gasket eroded quickly as the hot air rushed past. Upon further examination of the data, there was evidence the inner door seal was leaking very slowly prior to full failure. During the third pressurization cycle, at a pressure of 51.0 psig (352 kPa), the pressure in the airlock (between the inner and outer doors) began to increase. Pressures in the airlock cylinder increased from 2.3 to 6.5 psig (16.1 to 44.7 kPa) while the pressure on the inner door was increased from 51 to 149 psig (352 kPa to 1.02 MPa). There was a small increase in flow rate measured past the inner door, but it was not considered to be accurate in this low range. While increasing pressure from 149 psig (1.02 MPa) to 175 psig (1.21 MPa), the seal failed completely at a pressure of 151 psig (1.04 MPa). The gasket eroded quickly in the area of the failure, creating a larger leak opening. The gasket material remaining adjacent to the eroded gasket area was either powdery or charred and brittle, indicating that the gasket may have smoldered or ignited as outgassing of combustibles occurred during the third load cycle. When the seal failed, the maximum leak rate recorded was 706 SCFM (20,000 l/min), or 102% volume/day of a 1 million ft^3 (28,300 m^3) containment building. However, since leak rate was not recorded continuously during pressurization, it is possible that the instantaneous leak rates exceeded 706 SCFM (20,000 l/min) after the inner door seal failed.

The temperature profile measured on the door was fairly uniform except along the 0 and 180° axis, which had the lowest and highest temperatures, respectively. The test temperatures measured on the door were all near the temperature at which the seal material degrades and thus these elevated test temperatures are considered the major cause of the seal failure.

During heating from 400°F to 800°F (204 to 427°C), the inner door moved away from the bulkhead. The movement was significant, with the maximum increase in the gap between the inner door and bulkhead as much as 0.13 in. (3.3 mm). Restrained expansion of the gasket material is the only source of applied load that could force a separation of the inner door and bulkhead. The second pressurization cycle on the inner door closed the gap. The gap did not reopen to any significant amount during heating of the third load cycle.

Based on the above discussion the following summarize the test results:

(1) The airlock was designed for 60 psig (410 kPa) and 340°F (171°C). Testing exposed the airlock to 300 psig (2.07 MPa) and an air temperature above the inner door of 850°F (454°C). Although the gasket was degraded by an accelerated aging process, no leakage of the airlock door occurred for pressures from 0 to 300 psig (0 to 2.07 MPa) while the gasket was subjected to temperatures less than its ignition temperature (approximately 620°F (327°C)).

(2) Degradation and subsequent failure of the gasket seal was related to temperatures in excess of the temperatures at which EPDM E603 elastomer is stable. When the gasket failed it was quickly eroded by an onrush of hot air. The gasket was reduced to a powdery consistency in the area that the seal was breached.

(3) Test results indicate that the gasket expanded while increasing air temperature above the door from 400 to 800°F (204 to 427°C) causing significant upward deflection of the inner door and resulting in larger gaps between the inner door and bulkhead.

(4) The personnel airlock survived 300 psig (2.07 MPa) internal pressurization. All strain gages indicated elastic behavior throughout the airlock from stresses induced by the elevated pressures and temperatures.

(5) The condition of the gasket due to accelerated aging did not appear to affect sealing ability at high temperatures and pressures. However, extrusion of the gasket material between the inner door and bulkhead during accelerated aging and high temperature heating, as in Item (3) above, prevented metal-to-metal contact between the door and bulkhead.

(6) The outer door at 300 psig (2.07 MPa) did not leak. Temperatures measured on the outer door were below 200°F (93°C). Heat transfer conditions have an important effect on the temperature distribution. The temperature of the inner door and bulkhead reached an average surface temperature of approximately 611°F (322°C) when the air temperature was 800°F (427°C), even under forced convection conditions. The outer door and bulkhead temperatures were lower for this test than might be expected due to the effect of the airlock orientation.

1.0 INTRODUCTION

The safety of nuclear power plants in the very unlikely event of a severe accident depends on the performance of the containment system, which is the last engineered barrier to the release of radioactive material to the atmosphere. Personnel airlocks are an important component of most containment systems. A severe accident may generate loads (pressure and temperature) much greater than the design basis for the containment system. It is commonly assumed that the consequences of a severe accident are not significant unless leakage from the containment exceeds 10% volume/day,[1*] which then serves as the failure threshold. Performance parameters of interest include when, where, and how failure takes place and also the size of the leak area.

The U.S. Nuclear Regulatory Commission (USNRC) has been involved in sponsoring and developing a research and development effort known as the Containment Integrity Program. This program was developed with the ultimate goal of establishing performance characteristics of light water reactor (LWR) containment buildings subjected to pressure and temperature conditions beyond the original design conditions. Sandia National Laboratories (SNL) is currently managing the following four elements of this program:[2]

(1) Tests of seals and mechanical penetrations,
(2) Scale model tests of containment buildings,
(3) Analysis and methodology development, and
(4) Tests of electrical penetration assemblies.

The overall objective of these program elements is to develop methods for predicting the performance of containment buildings subjected to severe accident conditions. In a survey of containment penetrations conducted by Argonne National Laboratory,[3] personnel airlocks were identified as having a relatively high potential for leakage. Idaho National Engineering Laboratory came to similar conclusions in the analysis of specific containments and penetrations for the NUREG-1037 study.[4] Because of the complex structural behavior and uncertainty with respect to gasket performance in an actual penetration that must be accounted for in an analysis of personnel airlocks, experimental validation was needed. As part of this program, a full size personnel airlock was tested by CBI Research Corporation (CBIRC) to provide benchmark data that can be used to validate analytical methods for predicting the performance of personnel airlocks subjected to loads beyond design.

The purpose of the tests reported herein was to gather and interpret the following items of interest:

(1) Measure leak rate characteristics of aged gasket seals,
(2) Gather strain and deformation data on the airlock structural members and door gaskets,
(3) Gather temperature data on the personnel airlock, and
(4) Record and review the data at pressures and temperatures that exceed design pressures and temperatures.

---

* Superscript numbers refer to the numbered references in Section 10.0.

The severe accident was not based on an actual or hypothetical accident scenario. The pressures and temperatures that the test airlock was exposed to should be considered representative of severe accident profiles, but generic in nature. Although a great deal of valuable information has been generated, any extension of the test results must account for differences in airlock design and differing load scenarios. Also, other potential limit states for a given containment may be realized first.

1.1 Test Philosophy

Accident scenarios for LWR containments encompass a wide variety of pressure, temperature, and radiation exposure conditions that no single test can duplicate. Rather than defining a particular set of load conditions for a specific accident scenario, plausible loads were defined to determine the conditions under which significant leakage occurs. An upper bound of 300 psig (2.07 MPa) was established since, if the airlock withstood this pressure in an actual power plant installation, some other component of the containment system would likely have failed before this condition was reached.

Beyond design basis testing of the airlock needed to address the important effect of gasket performance on leakage; two different phases of gasket performance were considered. Two temperature plateaus were established. The first temperature plateau was at an air temperature above the door of 400°F (204°C). At this temperature, gasket performance is dictated by degradation due to thermal aging in addition to accelerated aging to which the gaskets were exposed. The second temperature plateau was at an air temperature above the door greater than 800°F (427°C). At this temperature gasket performance is dictated by the gasket material instability. It was important to separate the pressure and temperature loadings. At each of these thermal plateaus pressure was increased to a maximum of the upper bound.

Sizing of the orifice flow metering system was defined by typical design allowables for containment leakage. The design allowables for the flow metering system are from 0.1% to 25% volume/day (10% volume/day is considered to be a failure threshold[1]). For a 1 million ft^3 (28,300 m^3) containment at standard temperature and pressure, this corresponds to leak rates between 0.7 to 174 SCFM (19.8 to 4930 l/min).

The above discussion delineates the process by which parameters were defined for the beyond design basis test. Test conditions were dictated largely based on the containment accident scenario concept and acceptable conditions formulated from plausible limit-state loading.

1.2 Test Rationale

During severe accident conditions in an LWR containment, it is possible to have either a steam or dry air atmosphere. Additionally, there is no fixed rate of thermal and pressure loading. For this test program, there was no unique set of heat transfer conditions that were being duplicated. The intent was to expose the airlock inner door to a set of temperature and pressure conditions from which reasonable benchmark data could be gathered.

The orientation of the airlock and the use of air rather than steam as the pressure medium was dictated by the following:

(1) The test facility available for testing,
(2) Safety considerations,
(3) Instrumentation requirements, and
(4) Maximum pressure and temperature loading requirements.

The airlock was tested in a 40 ft (12 m) deep cell with the cylinder oriented vertically (the airlock doors in the horizontal plane). In the event of a catastrophic release of the pressure boundary, it was essential to ensure safety. With the airlock in the deep test cell, a failure could be safely contained with the exception of the area directly above the airlock. Rather than build a containment, an available structure was utilized.

The presence of steam in the airlock would have presented some difficult problems for instrumentation. Although strain gage and thermocouple elements are hermetically sealed, the displacement transducers used to measure displacements within the airlock were extremely sensitive to the presence of moisture in the air. In the event that the airlock developed a leak, meaningful leak rate measurements may not have been possible due to condensate in the piping and flow metering system.

A one-dimensional thermal analysis modeling the airlock door was performed to evaluate the natural convective heat transfer characteristics with the airlock oriented horizontally (with the doors in the vertical plane) and with the airlock oriented vertically (with the doors in the horizontal plane). The door was modeled as a flat plate using an equivalent thickness based on the mass of the door, stiffeners, and bulkhead. It was determined that the effect of orientation of the door was significant for the modeled configuration. At a pressure of 200 psia (1.38 MPa) and an air temperature of 700°F (371°C) (which were the upper limit test conditions originally planned) the average temperature of the door when in the vertical plane was 530°F (277°C). For the same pressure and temperature conditions, the average temperature of the door when oriented in the horizontal plane was 436°F (224°C). The temperature differential between these two conditions was 94°F (53°C). To offset the effects of the orientation of the door, a flow header was designed to blow preheated air onto the inner door seal area directly from the pressure inlet, thus providing forced convection heating. Heat transfer to the outer door was not considered in this analysis and is discussed qualitatively in a subsequent paragraph in this section.

Based on test results reported by SNL (after the initial thermal and pressure conditions were defined), it was determined that the temperature at which the gasket material (EPDM E603) becomes unstable is approximately 620°F (343°C)[5], which was much greater than the maximum of 530°F (277°C) predicted using the one-dimensional analysis. The one-dimensional model was used in a parametric study to determine the air temperature and pressure that would be necessary to increase the door temperature to the temperature at which the gasket becomes unstable and loses its sealing capability. With the air temperature increased to 800°F (427°C) and the air pressure increased to 300 psig (2.07 MPa), the predicted average door temperature increased to 637°F (336°C). The upper bound parameters were then re-defined (from 200 psia (1.38 kPa) and 700°F (371°C) to 300 psig (2.07 kPa) and 800°F (427°C)) to test the limit of the gasket seal and the airlock.

In an actual airlock installation, the door, hinge beam, bearing blocks, hinges, latching mechanism, and stiffeners on the door that are located within the containment are an obstacle in the path of natural convective flow considered above. Therefore, the door temperatures predicted in the analysis for a vertical flat plate are probably higher than what would actually occur. Within the airlock itself, the primary and secondary stiffeners are also obstacles at the inner door bulkhead such that secondary and tertiary convective flow loops within the boundaries of the bulkhead stiffeners could develop. This would limit the amount of convective heat transfer to the outer door. Inside the airlock the heated air moving across the vertical flat plate would likely lose its bouyancy before it reached the outer door as a result of heat losses through the airlock cylinder wall. In essence, the flow loop would reach an equilibrium state and would close before it reached the outer door. Within the actual airlock, the presence of the bulkhead stiffeners would further hamper convective air flow.

Comments in the preceding paragrph are based strictly on engineering judgement. A complete analysis would be required to validate or disprove the above supposition. However, the preceeding discussion demonstrates the rationale used to determine the major test parameters. The loading that the inner door and bulkhead were exposed to is an upper limit of temperatures and pressures that a similar in-service personnel airlock could possibly experience, which is consistent with the test philosophy described in Section 1.1.

1.3 General Test Plan

The beyond design basis test (Test 2C) has been discussed in detail in Section 1.1 of this chapter. There were eight additional tests performed. These tests were performed at ambient room temperature conditions and at pressures up to 15% beyond design. These ambient temperature tests were performed to:

(1) Establish a baseline leak rate to evaluate the effectiveness of the gaskets,
(2) Understand the effect of any permanent deformations that occurred during the beyond design basis test, and
(3) Provide a basis for comparison on the overall behavior of the airlock before and after the beyond design basis test.

The following is a description of the tests that were performed on the personnel airlock.

Test 1A - Leak rate test of the airlock inner door without the gasket. The inner door was subjected to a pressure of 69 psig (476 kPa) at ambient temperature.

Test 1B - Leak rate test of the airlock outer door without the gasket. The outer door was subjected to a pressure of 69 psig (476 kPa) at ambient temperature.

Test 1AA - Leak rate test of airlock inner door with accelerated aged gasket in place. The inner door was subjected to a pressure of 69 psig (476 kPa) at ambient temperatures. This test was not originally planned and was added to determine if the aged gasket seal could adequately seal the inner door and bulkhead closure. Repeat of Test 1A.

Test 1BB - Leak rate test of airlock outer door with accelerated aged gasket in place. The outer door was subjected to a pressure of 69 psig (476 kPa) at ambient temperature. This test was not originally planned and was added to determine if the aged gasket seal could adequately seal the outer door and bulkhead closure. Repeat of Test 1B.

Test 2A - Leak rate test of the airlock inner door with gasket in place and full instrumentation. The door was subjected to a pressure of 69 psig (476 kPa) at ambient temperature.

Test 2B - Leak rate test of the airlock outer door with gasket in place and full instrumentation. The door was subjected to a pressure of 69 psig (476 kPa) at ambient temperature.

Test 2C - Leak rate test of the entire personnel airlock assembly under severe accident conditons. Both doors were closed with gaskets in place. The inner door was subjected to simultaneous elevated temperatures and pressures.

Pressure and temperature systems accommodated the following maximum capacities:

- 300 psig (2.07 MPa)
- 800°F (427°C)
- 174 SCFM @ 300 psig (4930 l/min @ 2.07 MPa)
- 7°F/min @ 174 SCFM (3.9°C/min @ 4930 l/min).

Test 3A - Leak rate test of the airlock inner door without disturbing the gasket from Test 2C. The door was subjected to a pressure of 69 psig (476 kPa) at ambient temperature.

Test 3B - Leak rate test of the airlock outer door without disturbing the gasket from Test 2C. The door was subjected to a pressure of 69 psig (476 kPa) at ambient temperature.

2.0 PERSONNEL AIRLOCK AND TEST VESSELS

This section describes the details of the personnel airlock and the test chambers that capped both ends of the airlock cylinder.

2.1 Personnel Airlock

The personnel airlock was originally fabricated at CBI's Birmingham, Alabama fabrication facility. The airlock was designed and fabricated for the Union Electric Company's cancelled Callaway Unit 2 nuclear power generating facility. Under a separate contract with SNL, the partially fabricated airlock was completed.[6] This included:

(1) Attaching hinges necessary to mount the doors,
(2) Machining sealing surfaces of both doors and bulkheads,
(3) Attaching hold down fixtures necessary to hold both doors in place during pressurization (not the cam latching mechanism),
(4) Sealing all penetrations through bulkheads except the doors,
(5) Conducting a leak test of the airlock at 60 psig (410 kPa) (design pressure), and
(6) Providing two sets of double dog-ear gasket seals.

A full set of drawings and mill test reports for the airlock were also provided under the contract.

The airlock assembly was 19 ft-5/16 in. (5.8 m) long with an inside diameter of 9 ft-10 in. (3.0 m). The airlock was made from steel conforming to the minimum requirements of ASME Designation: SA 516 Grade 70 steel plate. As shown in Figures 2.1 through 2.5, the airlock can be divided into five major structural components: the inner door; the inner door bulkhead; the cylindrical body; the outer door; and the outer door bulkhead. The cylindrical body is made from a 5/8 in. (16 mm) thick steel plate.

The bulkhead assemblies consist of 1 in. (25 mm) thick heavily reinforced steel plate. These steel plates are welded to the inside wall of a cylindrical ring. The cylindrical rings are welded to the cylindrical body of the airlock. The cylindrical ring around the inner door bulkhead is 1 in. (25 mm) thick and the cylindrical ring around the outer door bulkhead is 5/8 in. (16 mm) thick. Cut and framed into the centers of both bulkheads are 6 ft-8 in. (2.0 m) high by 3 ft-6 in. (1.1 m) wide rectangular door openings. The doors are attached to the pressure sides of the bulkheads by means of a large hinge assembly. The doors overlap the doorway opening to provide a perimeter area for installation of the gasket seal and for transferring the pressure loadings into the bulkheads.

The inner and outer doors are identical in design. As shown in Figure 2.4, each door consists of a steel plate 1-1/2 in. (38.1 mm) thick. The plate measures 3 ft-10-1/2 in. by 7 ft-1/2 in. (1.18 x 2.15 m) as shown in Figures 2.1 and 2.2. The door overlaps the bulkhead doorway opening by 2-1/4 in. (57.2 mm). A gland to contain the gasket seal is machined in the door as shown in Figure 2.4. The surfaces of the bulkhead and the door that overlap are machined flat and form the sealing surface for the gasket. Surface finishes of the machined surfaces on the bulkhead and door are shown in Figure 2.2. The design requirements specify that when the door is closed without the

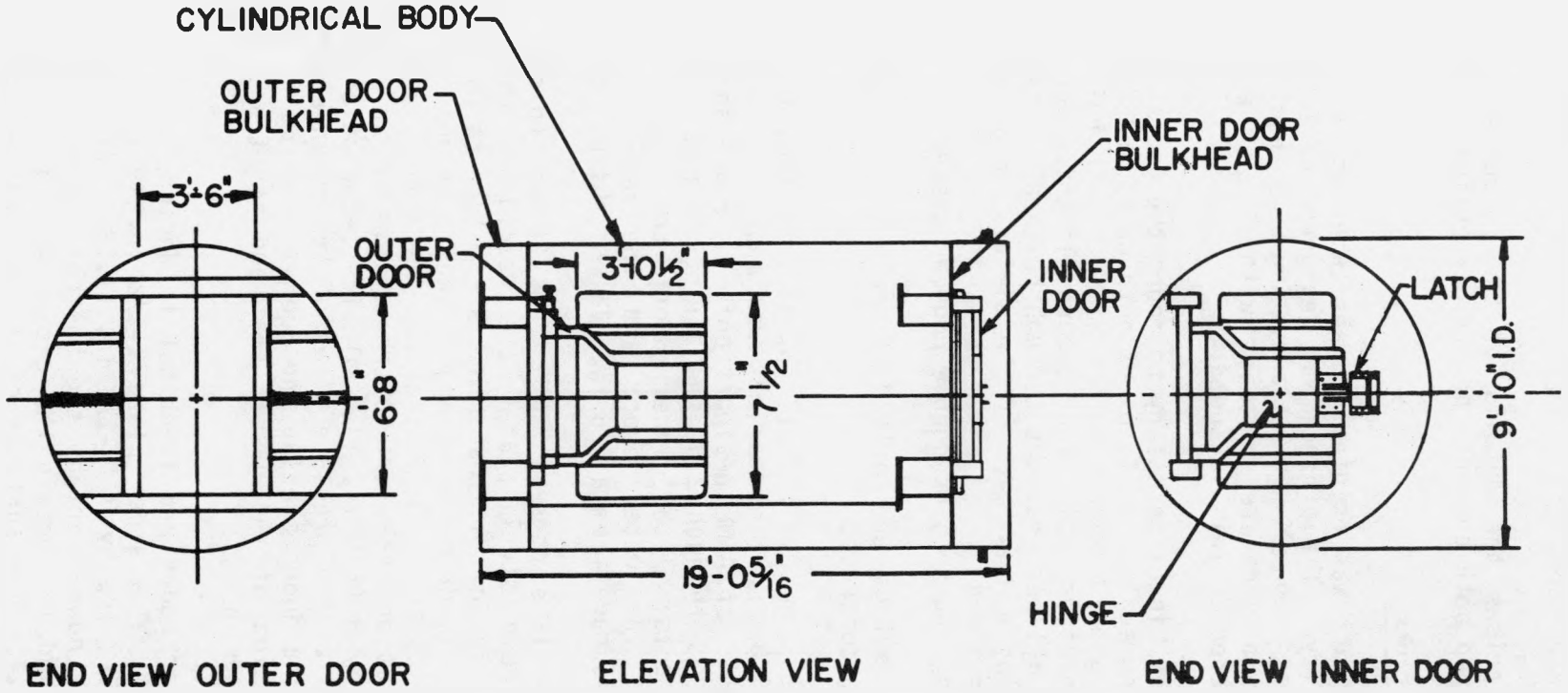

Figure 2.1 Personnel Airlock

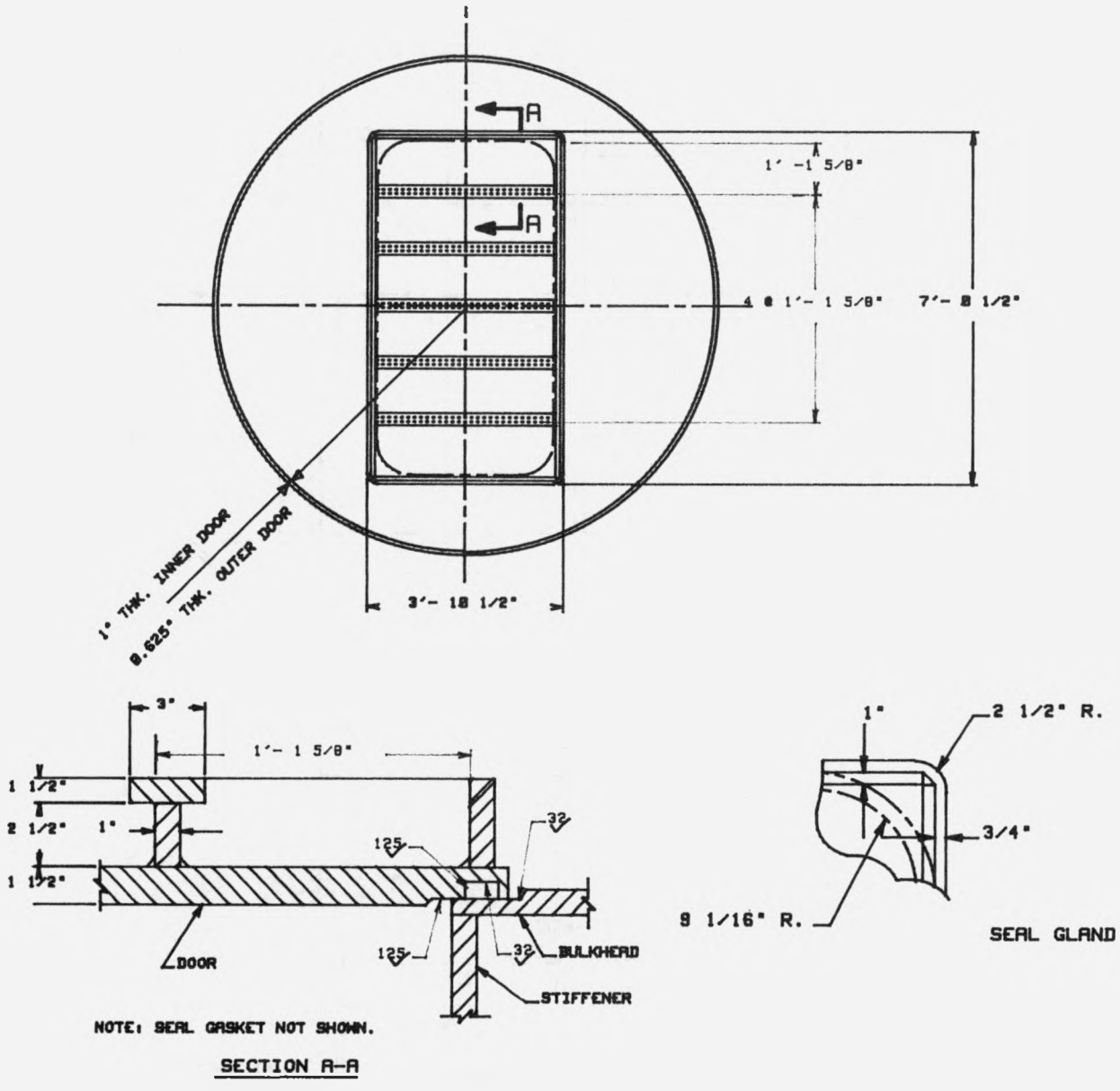

Figure 2.2 Elevation of Typical Bulkhead: Door Side

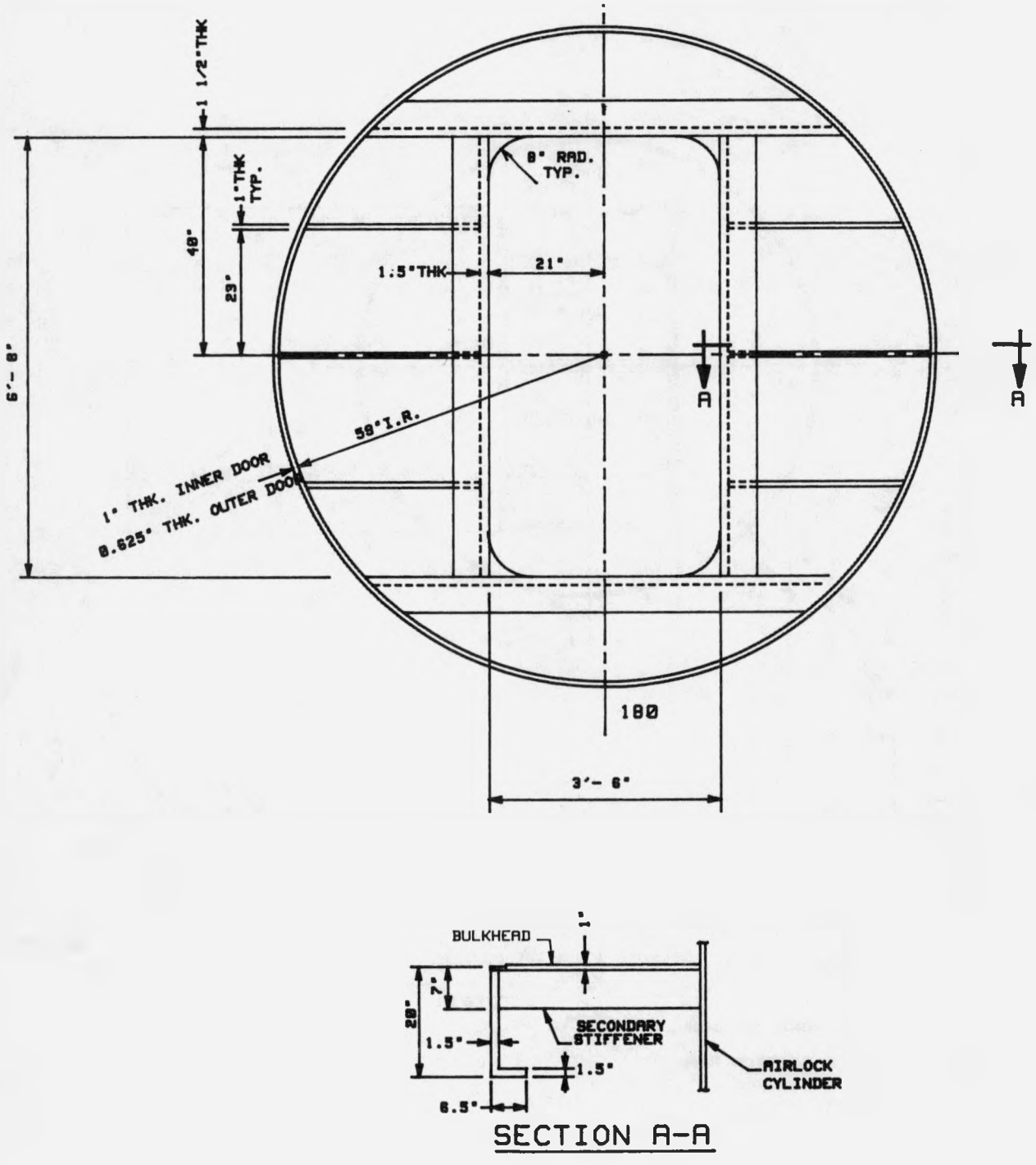

Figure 2.3 Elevation of Typical Bulkhead: Structural Stiffener Side

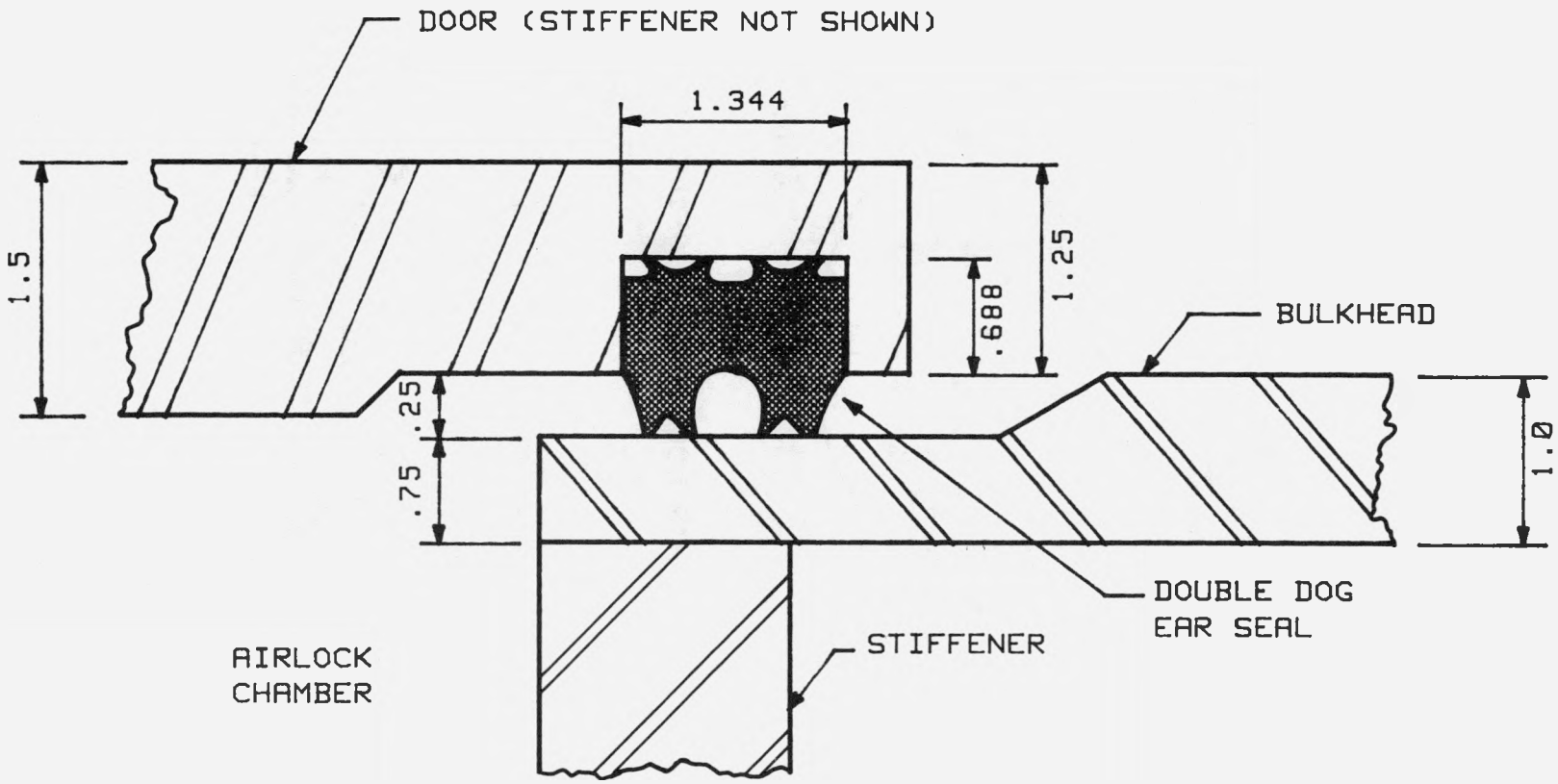

Figure 2.4 Seal Gland and Gasket Cross-Section Configuration

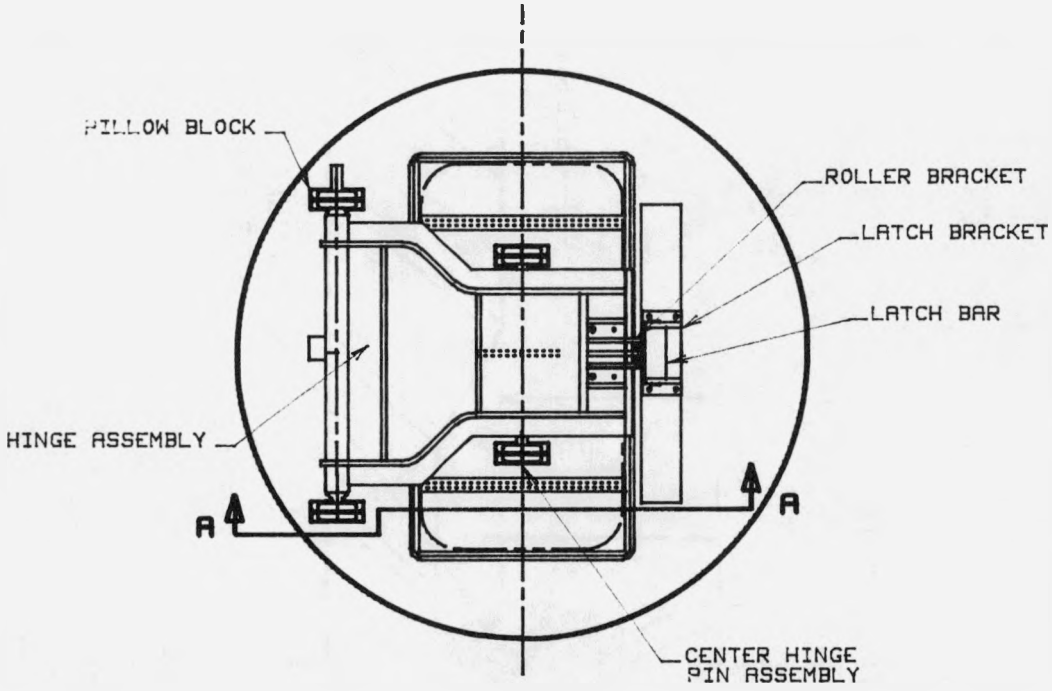

AIR LOCK DOOR PROFILE

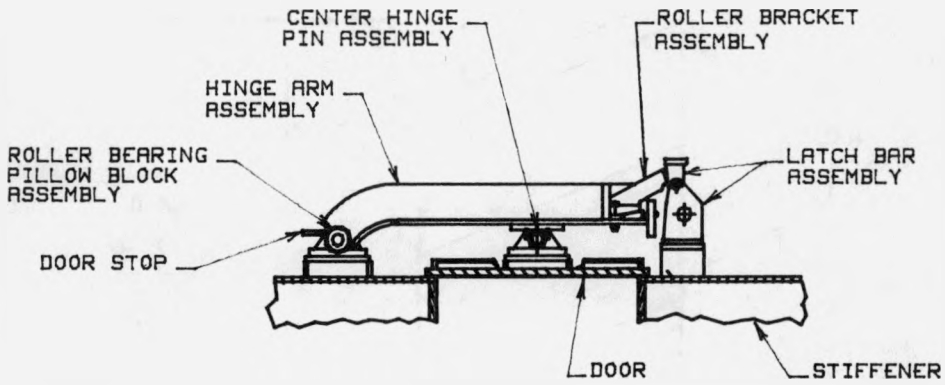

AIR LOCK SECTION A-A

Figure 2.5 Airlock Door Hinge Arm Assembly and Latch Mechanism

gasket seal in place, the gap between the machined surfaces of the bulkhead and door must be less than 0.005 in. (0.13 mm).

The door is reinforced with structural stiffeners that are attached on the opposite side of the seal surface. Reinforcing the door plate perimeter is a steel plate welded on edge. The stiffener is fillet welded to the door plate the entire length of the stiffener and has a full fusion weld at the corner where adjacent stiffeners meet. The stiffener around the perimeter is a steel plate with 4 x 1 in. (100 x 25 mm) cross-section. In the short direction of the interior portion of the door away from the edges, five "T" shaped structural members reinforce the door. The flange of the T-section is 3 x 1-1/2 in. (76 x 36 mm) and the web is 2-1/2 x 1 in. (64 x 25 mm) as shown in Figure 2.2. These structural members are spaced equally about the centerline of the door.

The door is hinged at a weldment located along the longitudinal centerline of the door. This attachment location allows rotational freedom so the door can seat properly against the bulkhead in the closed position. The center hinge pin assembly is attached to the bulkhead by a hinge arm assembly. The hinge arm assembly, shown in Figure 2.5, is attached to the bulkhead at the roller bearing pillow block assembly.

The door is latched using the latching mechanism that is attached to the bulkhead as shown in Figure 2.5. The latch consists of a roller bracket assembly that attaches to the hinge arm assembly and cantilevers over the bulkhead. The latching bar assembly, which is attached to the bulkhead, engages the roller bracket assembly roller bearing and applies a force on the door that causes the gasket to be compressed between the door and the bulkhead. Compression of the gasket between the door and bulkhead provides the initial seal for air pressures below 5.0 psig (34 kPa). At pressures of 5.0 psig (34 kPa) and above, the surface pressure applied to the door is sufficient to compress the gasket, and the latching mechanism may no longer be engaged.

The gasket cross-section is known as a "double dog-ear" and is patented by CBI Industries, Inc. (Patent No. 3,831,950). The gaskets used in this test were fabricated from an EPDM E603 compound and were manufactured by Presray.* The double dog-ear seal was designed to form an initial seal at low pressures. At elevated pressures the seal compresses, fills the voids in the gland left by the initial cross-section configuration, and forms a nearly solid rubber seal. In addition, with the gasket filling the machined gland in the door, the door and bulkhead can come into metal-to-metal contact.

2.2 Differences in Airlock Tested and Airlock in Service

There were a number of modifications that were made to the airlock to accommodate all of the test equipment, instrumentation, and orientation of the

* Mention of specific products and/or manufacturers in this document implies neither endorsement or preference nor disapproval of the use of a specific product for any purpose by the U.S. Government, any of its agencies, or Sandia National Laboratories.

airlock. These modifications will be discussed in the following section (Section 2.3). In this section, the main differences between the airlock used in this test and a similar airlock already in service are discussed.

Airlocks are normally oriented with the longitudinal axis parallel to the horizontal and with the doors opening into the containment building. The airlock tested was oriented with the cylinder longitudinal axis parallel to the vertical. The doors opened upward and the dead weight of the doors and hinge assemblies rested on the bulkhead when closed. The dead weight of the door is equivalent to about 2.0 psig (14 kPa) surface pressure on the door and precompresses the gasket seal between the door and bulkhead.

Normally there are floor plates in airlocks to provide a flat walking surface. This floor surface was not provided in the test airlock. The absence of this floor detail was not significant during testing. Instead, a ladder was used to gain access from the top of the outer door bulkhead to the underside of the inner door bulkhead. A section of grated flooring was suspended below the underside of the inner door bulkhead to serve as a work platform.

Personnel airlocks are normally welded into the containment building shell to form a leak tight barrier. The airlock tested had the normal interlock ring assembly installed, which acted as a reinforcing ring for the airlock cylinder. Interaction between the airlock and containment shell was not modeled in this test.

The door latch in an airlock in service is normally an automated system that is electronically controlled and has a manual backup system. Once the door is closed, the latch bracket engages the roller bracket assembly. Mechanical linkages and electrical wiring penetrate both the inner and outer door bulkheads. In the airlock tested, the door was latched manually, and all mechanical and electrical penetration were welded shut and leak tested. These closure details are shown in Figures 2.6 and 2.7. The mechanical and electrical penetrations were welded shut; these penetrations are a potential source of leakage from the containment into the airlock in an actual in-service airlock, which may require a separate investigation.

2.3 Modifications to Personnel Airlock

The airlock required a number of modifications for testing purposes. These modifications were made, where applicable, in accordance with the 1974 Edition of the ASME Boiler and Pressure Vessel Code (Section III).[7-10] These modifications included the addition of the following items:

(1) An access manhole,
(2) Nozzles for instrumentation leadwires,
(3) Pipe fittings in the cylinder wall,
(4) Drilled and tapped holes in the inner door bulkhead stiffener, and
(5) A shroud enclosing the inner doorway.

The manhole was added to obtain access to the airlock cylinder. The nozzles were added to route instrument leadwires into and out of the airlock. The nozzle cover plates, known as blind flanges, were drilled and tapped to accept various sized pipe threads. Conax high pressure and temperature fittings were

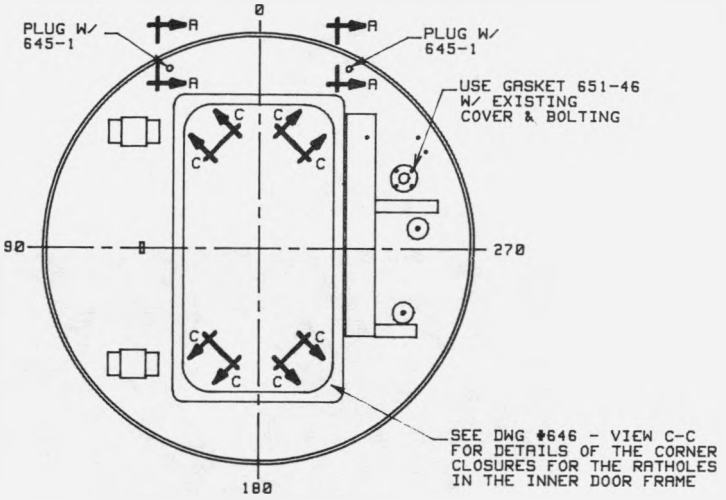

INNER DOOR BULKHEAD
PLAN VIEW

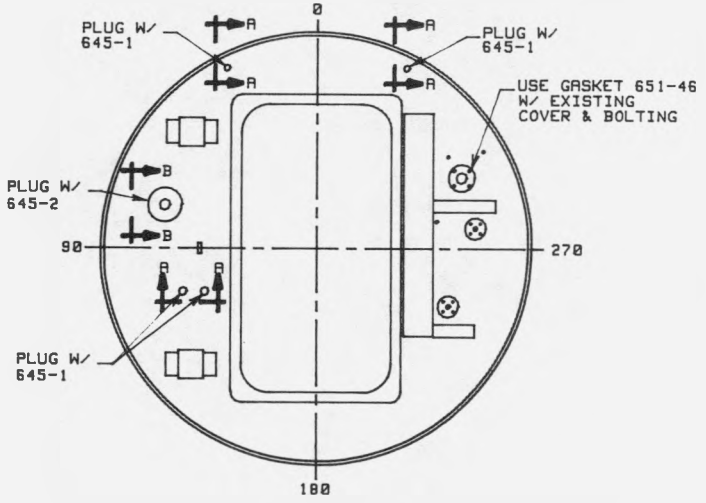

OUTER DOOR BULKHEAD
PLAN VIEW

SHIP PC	MARK	ASSM PC	DESCRIPTION	LENGTH FT	LENGTH IN	SPEC
6	645-1		PLATE 1 1/4"DIA.x 5/8"THK.			*
1	645-2		PLATE 3 1/2"DIA.x 5/8"THK.			*
2	651-46		GASKET FOR 3"DIA. 150# FLG.			DURABLA

* - A516 GR.70 (M/F-5/8" THK MTRL CUTOUT FROM AIRLOCK TO INSTALL NOZZLES FOR TESTING)

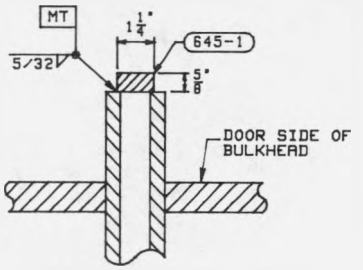

SECTION A-A
(SIMILAR FOR 6 LOCATIONS)

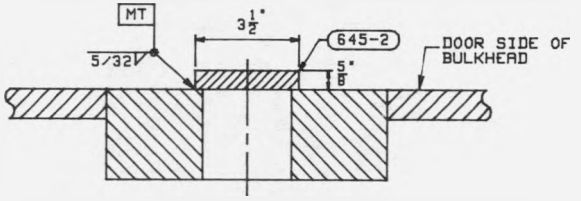

SECTION B-B
(1 LOCATION)

Figure 2.6 Closure Details of Bulkhead Penetrations

Figure 2.7 Typical Weldment of Bulkhead Closures

used to provide a leak tight barrier around the instrument leadwires. A shroud was attached across the inner door stiffeners below the inner door to capture air that had effectively leaked past the inner door seal. The shroud consisted of a five-sided sheet metal box (0.090 in. (2.3 mm) thick) 4 in. (100 mm) deep that overlapped the inner door opening. The box was reinforced with structural stiffeners to withstand bending stresses exerted due to the differential pressure between the door and inside the airlock. The shroud was designed to withstand a differential pressure of 10 psi (69 kPa). The shroud was welded to the structural steel stiffeners inside the airlock that frame the inner door. A flexible pipe was attached to the shroud and was connected to a fitting in the cylinder wall to allow movement due to thermal effects.

Threaded coupler pipe fittings were installed in the airlock cylinder walls. These pipe fittings were used for routing air that bypassed the inner door seal to the flow meters, returning air from the flow meters to the airlock, and pressurizing the airlock.

As a result of enclosing the inner door with the shroud box, the surface of the inner door within the airlock was inaccessible. Holes for instrument leadwires were drilled and tapped in the primary stiffener webs that framed the inner door as shown Figure 2.8. Instrument leadwires were routed through Conax high pressure and high temperature fittings to provide a leak tight barrier around the instrument leadwires.

2.4 Additional Structural Pressure Vessel Assemblies

The personnel airlock test required that enclosures be installed above the inner door bulkhead and below the outer door bulkhead. The following paragraphs describe these enclosures. The airlock and test assembly is shown in Figure 2.9.

2.4.1 Top Chamber Above the Inner Door Bulkhead (Chamber V-1)

The top chamber (Chamber V-1), located above the inner door bulkhead, was originally designed to pressurize the inner door bulkhead up to 200 psia (1.38 MPa) and withstand air temperatures up to 700°F (371°C). Chamber V-1 was fabricated in accordance with these requirements. A 2 in. (51 mm) thick layer of Kaowool insulation was installed to cover the entire inside surface of Chamber V-1 to protect the steel from elevated temperatures and to reduce heat loss. Based on a thermal analysis of the bulkhead,[11] it was determined that the gasket seal would not reach 620°F (327°C), which is the instability temperature of the gasket material, if the air temperature in Chamber V-1 was limited to 700°F (371°C). It was decided that the maximum air temperature be increased to 800°F (427°C) and the maximum pressure be increased to 300 psig (2.07 MPa). During the test, the maximum pressure that Chamber V-1 was exposed to was 300 psig (2.07 MPa) and the maximum air temperature above the inner door was approximately 850°F (454°C).

Chamber V-1 was fabricated from steel conforming to the minimum requirements of ASME Designation: SA516 Grade 70[8] and consisted of a cylindrical section 4 ft (1.22 m) long with an inside diameter of 9 ft-11-1/4 in. (3.03 m). The cylinder wall was 1 in. (25.4 mm) thick. The cylinder was capped with a 2:1 elliptical head. In the center of the elliptical head a 24 in. (610 mm) diameter manhole was located for access to the top side of the inner door and bulkhead.

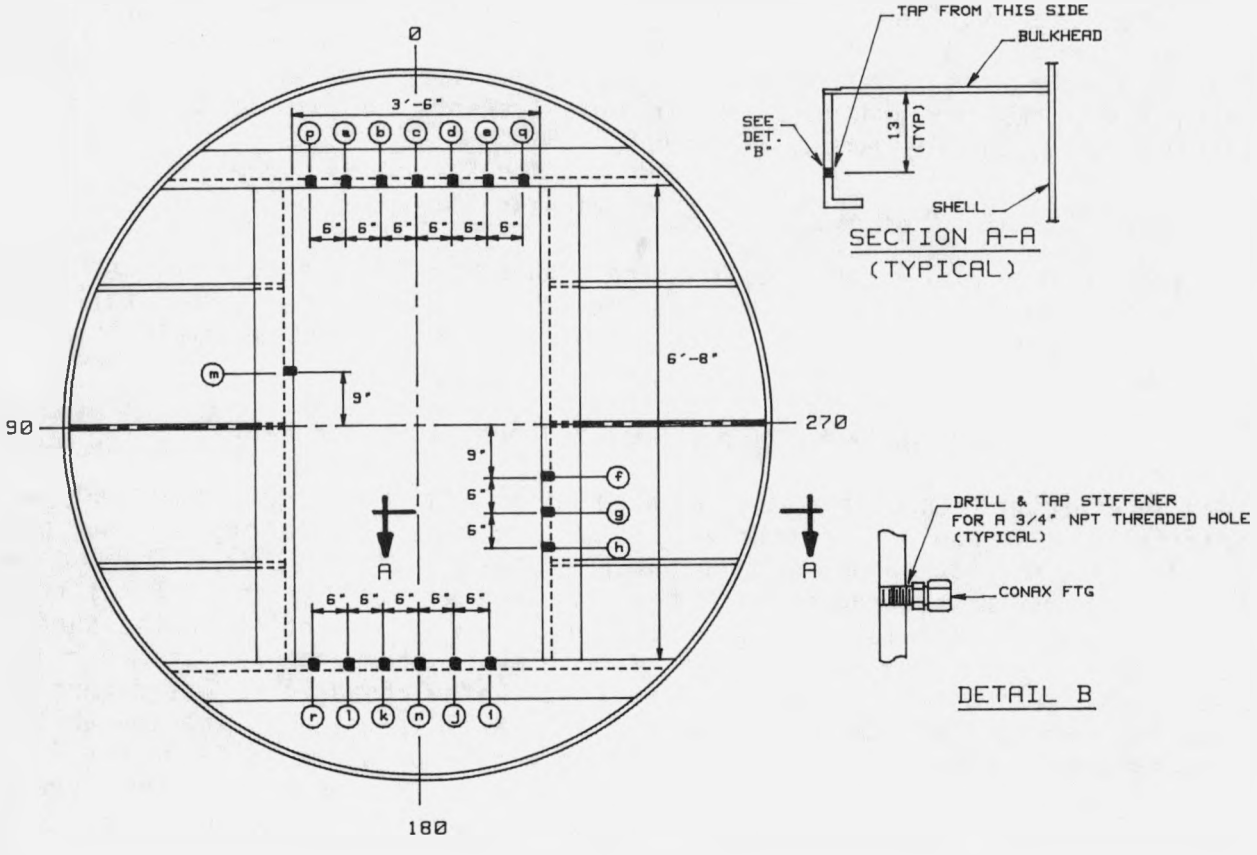

Figure 2.8 Inner Door Frame Penetrations for Conax Fittings

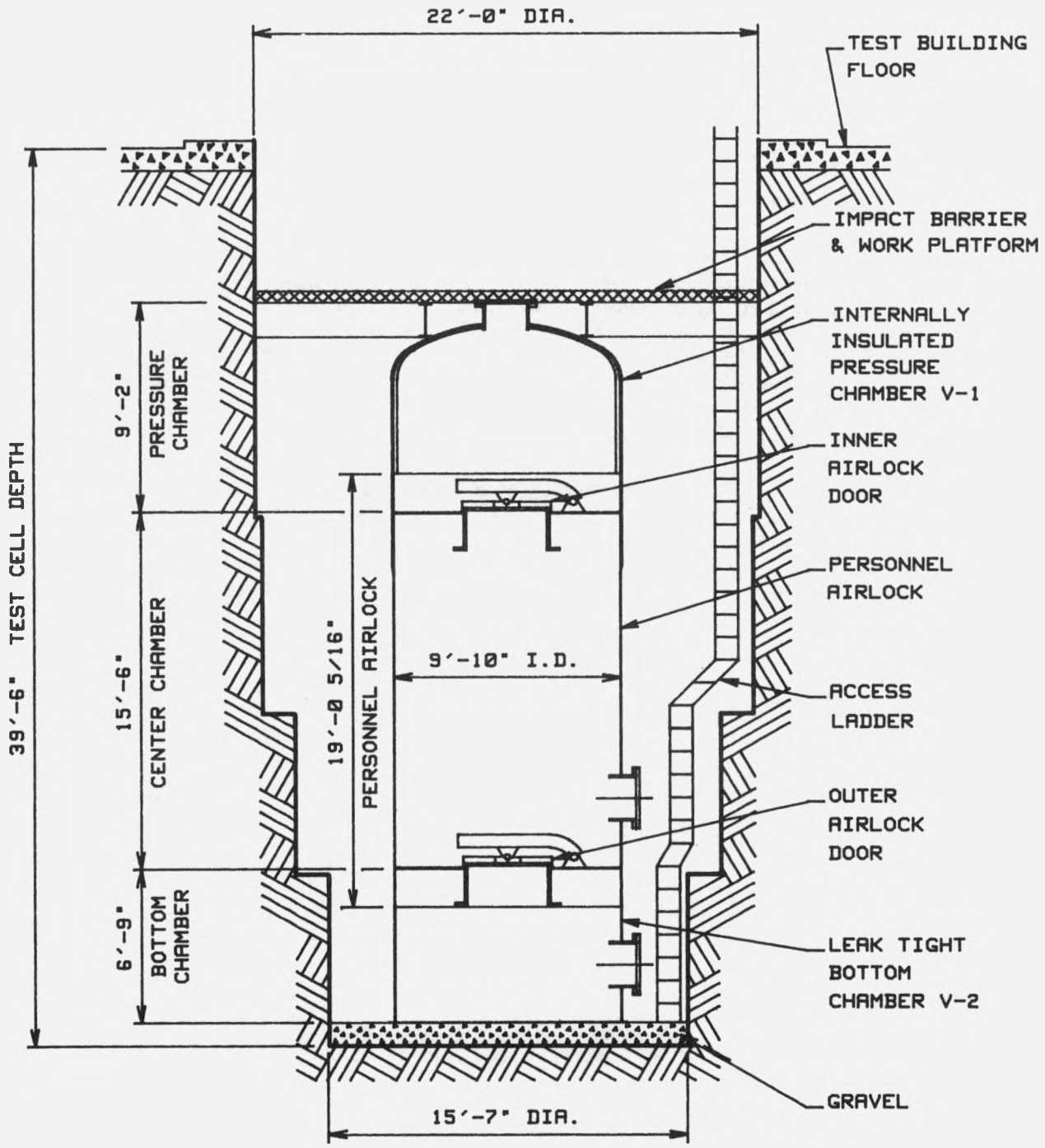

Figure 2.9 Airlock and Test Chambers in Deep Test Cell

Three 10 in. (254 mm) nozzles, similar to the nozzles in the airlock, were installed. Blind flange plates were drilled and tapped to accommodate instrument leadwires. Pipe fittings of varying sizes were welded to the cylinder wall for the following:

(1) Pressure inlet,
(2) Pressure outlet, and
(3) High voltage electrical feedthroughs.

On the inside, bracket assemblies were installed to support electric heaters and air outlet piping.

2.4.2 Bottom Chamber Below Outer Door Bulkhead (Chamber V-2)

Chamber V-2 provided two functions. One was to support the dead weight of the airlock and Chamber V-1. The other function was to capture any air that effectively bypassed the outer door seal and route it to a flow meter to measure the outer door leak rate. A 24 in. (610 mm) diameter manhole was provided as well as two 10 in. (254 mm) nozzles and one 3 in. (76 mm) pipe. The 10 in. (610 mm) nozzle blind flanges were drilled and tapped to accept various sized pipe threads. Conax fittings were used to provide a leak tight barrier around instrument leadwires.

Chamber V-2 was fabricated from steel plate conforming to the minimum requirements of ASTM Designation: A36 and consisted of a cylinder 5 ft (1.524 m) long with an inside diameter of 9 ft-10-1/4 in. (3.00 m). The cylinder wall was 1/4 in. (6.4 mm) thick. The bottom of the cylinder was sealed with a flat plate fabricated from two half circles of 1/4 in. (6.4 mm) thick steel plate. Chamber V-2 was designed for a pressure of 5 psig (34 kPa).

3.0 TEST SETUP AND CONTROL

The test setup required rigorous design and fabrication efforts before the first tests could be performed. The following paragraphs describe the test setup, including piping and insulation, pressurization and heating systems, and test controls for pressures and temperatures.

3.1 Test Setup

Figure 3.1 is an artist's rendering of the actual test setup.

3.1.1 System Piping

Transport of heated and pressurized air from the booster compressors to the test vessel and from the airlock to the flow meters was achieved using a system of valves and pipes. A process and instrument flow diagram for the entire piping system is shown in Figure 3.2. The valve positions are shown in Table 3.1.

3.1.1.1 Chamber V-1 Pressurization System Piping

The pipes were sized to provide the maximum anticipated flow rate of 174 SCFM (4930 l/min) at a pressure up to 300 psig (2.07 MPa). Pipes from the booster compressor to Chamber V-1 and the airlock were 1-1/2 in. (38 mm) schedule 80 pipe. A 3000 lb (13.33 kN) threaded coupling was welded to Chamber V-1 cylinder wall which penetrated the thickness of Chamber V-1. Inside Chamber V-1, the pressurization piping was continued into a distribution inlet header that was placed around the door seal surface, as shown in Figures 3.3 and 3.4. This header routed hot air such that it was blown directly on the seal area of the inner door and bulkhead. The inlet header was located approximately 7 in. (178 mm) above the inner door bulkhead. A total of fifty-two 1/4 in. (6.4 mm) diameter holes were distributed evenly over the entire length of the inlet header and oriented such that flow was directed towards the seal surface. Holes in the inlet header were provided to direct and distribute the heated air across the seal.

As part of the pressure control system air in Chamber V-1 could be vented to the outside of the test building to relieve pressures and to circulate heated air over the gasket. An outlet header, which had a hexagonal shape, was installed near the top of Chamber V-1. This was connected to a 3000 lb (13.3 kN) threaded coupling for a 1-1/2 in. (38 mm) schedule 80 pipe. There were a total of fifty-two 1/2 in. (12.7 mm) diameter holes distributed uniformly along the length of the outlet header. This particular system of piping was used in all phases of testing the airlock, however, they were bypassed during flow meter verification.

3.1.1.2 Inner Door Flow Path

To detect air leaking past the inner door seal, a leak rate measurement system was implemented. Air that bypassed the inner door seal was collected and routed through a flow metering system and either returned to the airlock or vented outside of the test building, as dictated by the test requirements.

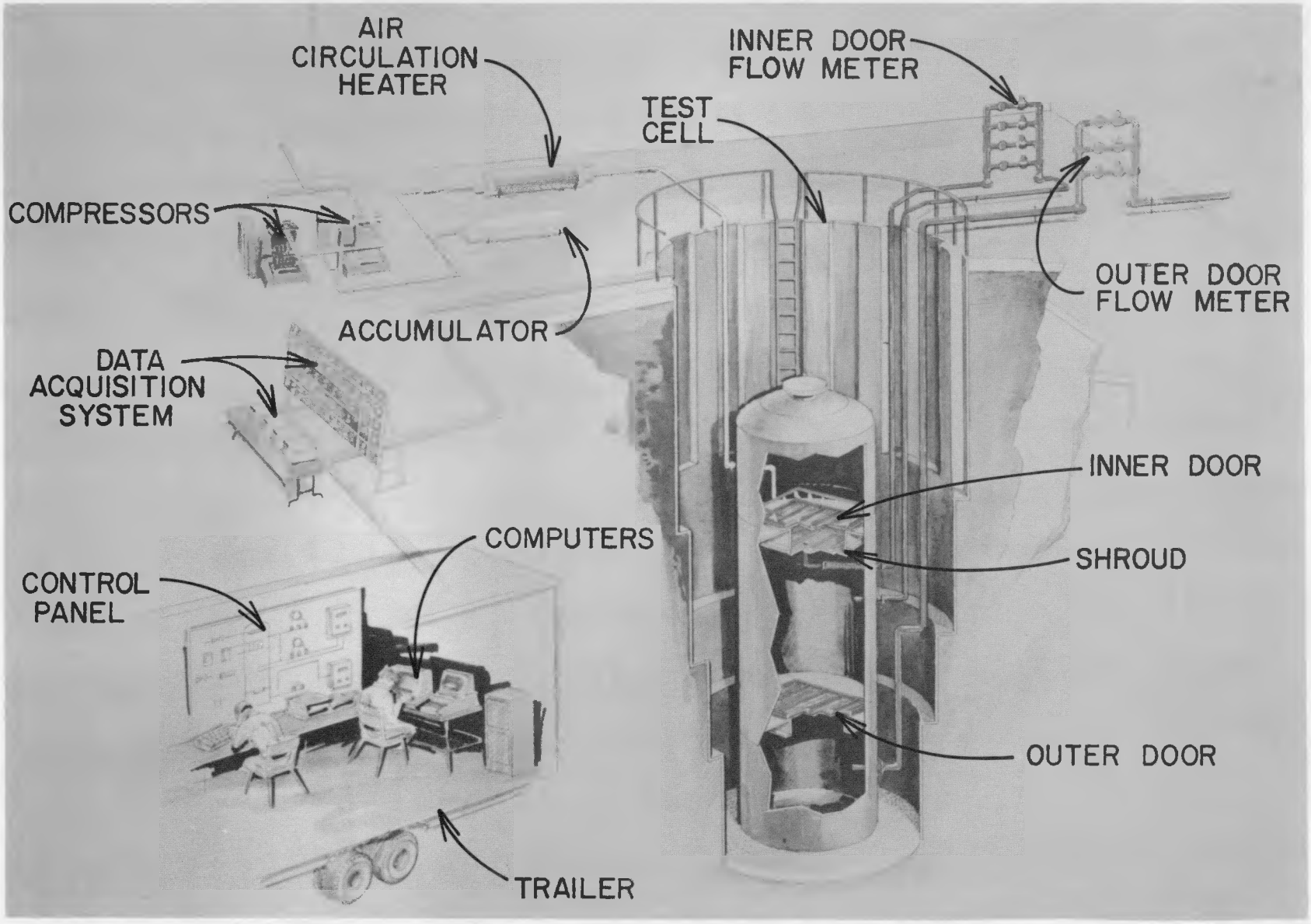

Figure 3.1 Test Setup

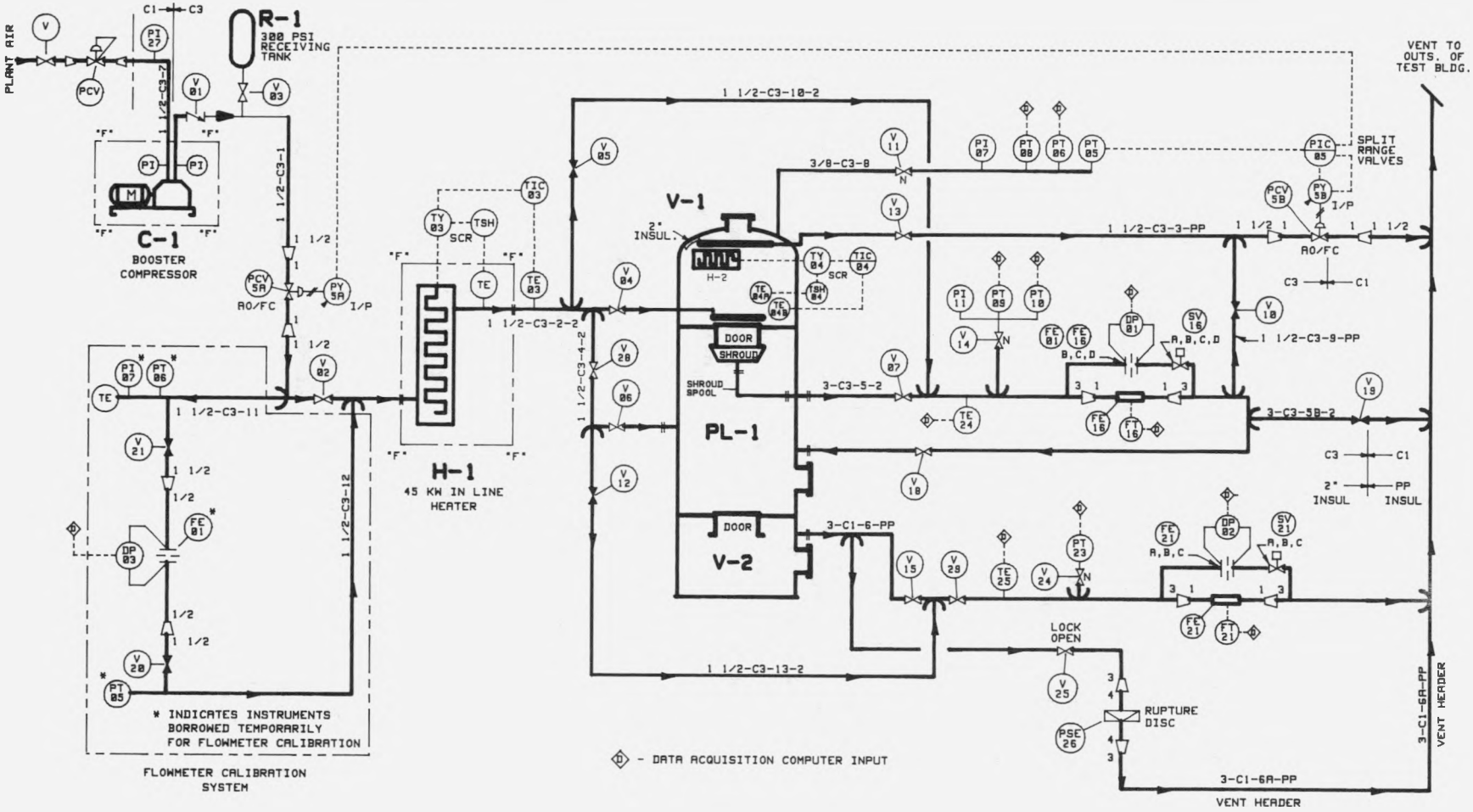

Figure 3.2 Overall Test Setup Process and Instrument Diagram

Table 3.1

Valve Position During Testing and Flow Meter Verification

VALVES	TEST NUMBER					FLOW METER CALIBRATION	
	1A & 1AA	1B & 1BB	2C	2A 3A	2B 3B	INNER DOOR FT-01	OUTER DOOR FT-01
V-1 (CHECK)	--	--	--	--	--	--	--
V-2 (NO)	OPEN	OPEN	OPEN	OPEN	OPEN	CLOSED	CLOSED
V-3 (NO)	OPEN	OPEN	OPEN	OPEN	OPEN	OPEN	OPEN
V-4 (NO)	OPEN	OPEN	OPEN	OPEN	OPEN	CLOSED	CLOSED
V-5 (NC)	CLOSED	CLOSED	CLOSED	CLOSED	CLOSED	OPEN	CLOSED
V-6 (NO)	OPEN	OPEN	CLOSED	OPEN	OPEN	CLOSED	CLOSED
V-7 (NO)	OPEN	OPEN	OPEN	OPEN	OPEN	CLOSED	CLOSED
---	--	--	--	--	--	--	--
---	--	--	--	--	--	--	--
V-10 (NC)	CLOSED	CLOSED	CLOSED	CLOSED	CLOSED	OPEN	CLOSED
V-11 (NO)	OPEN	OPEN	OPEN	OPEN	OPEN	CLOSED	CLOSED
V-12 (NC)	OPEN	CLOSED	CLOSED	OPEN	CLOSED	CLOSED	OPEN
V-13 (NO)	OPEN	OPEN	OPEN	OPEN	OPEN	CLOSED	CLOSED
V-14 (NO)	OPEN	OPEN	OPEN	OPEN	OPEN	OPEN	OPEN
V-15 (NO)	OPEN	OPEN	OPEN	OPEN	OPEN	CLOSED	CLOSED
---	--	--	--	--	--	--	--
V-17	--	--	--	--	--	--	--
V-18 (NO)	CLOSED	OPEN	OPEN	CLOSED	OPEN	CLOSED	CLOSED
V-19 (NC)	OPEN	CLOSED	CLOSED	OPEN	CLOSED	CLOSED	CLOSED
V-20 (NC)	CLOSED	CLOSED	CLOSED	CLOSED	CLOSED	OPEN	OPEN
V-21 (NC)	CLOSED	CLOSED	CLOSED	CLOSED	CLOSED	OPEN	OPEN
---	--	--	--	--	--	--	--
---	--	--	--	--	--	--	--
V-24 (NO)	OPEN	OPEN	OPEN	OPEN	OPEN	OPEN	OPEN
V-25 (NO)	OPEN	OPEN	OPEN	OPEN	OPEN	CLOSED	CLOSED
---	--	--	--	--	--	--	--
---	--	--	--	--	--	--	--
V-28 (NC)	CLOSED	OPEN	CLOSED	CLOSED	OPEN	CLOSED	OPEN
V-29 (NC)	CLOSED	OPEN	OPEN	CLOSED	OPEN	CLOSED	OPEN

NC - NORMALLY CLOSED
NO - NORMALLY OPEN

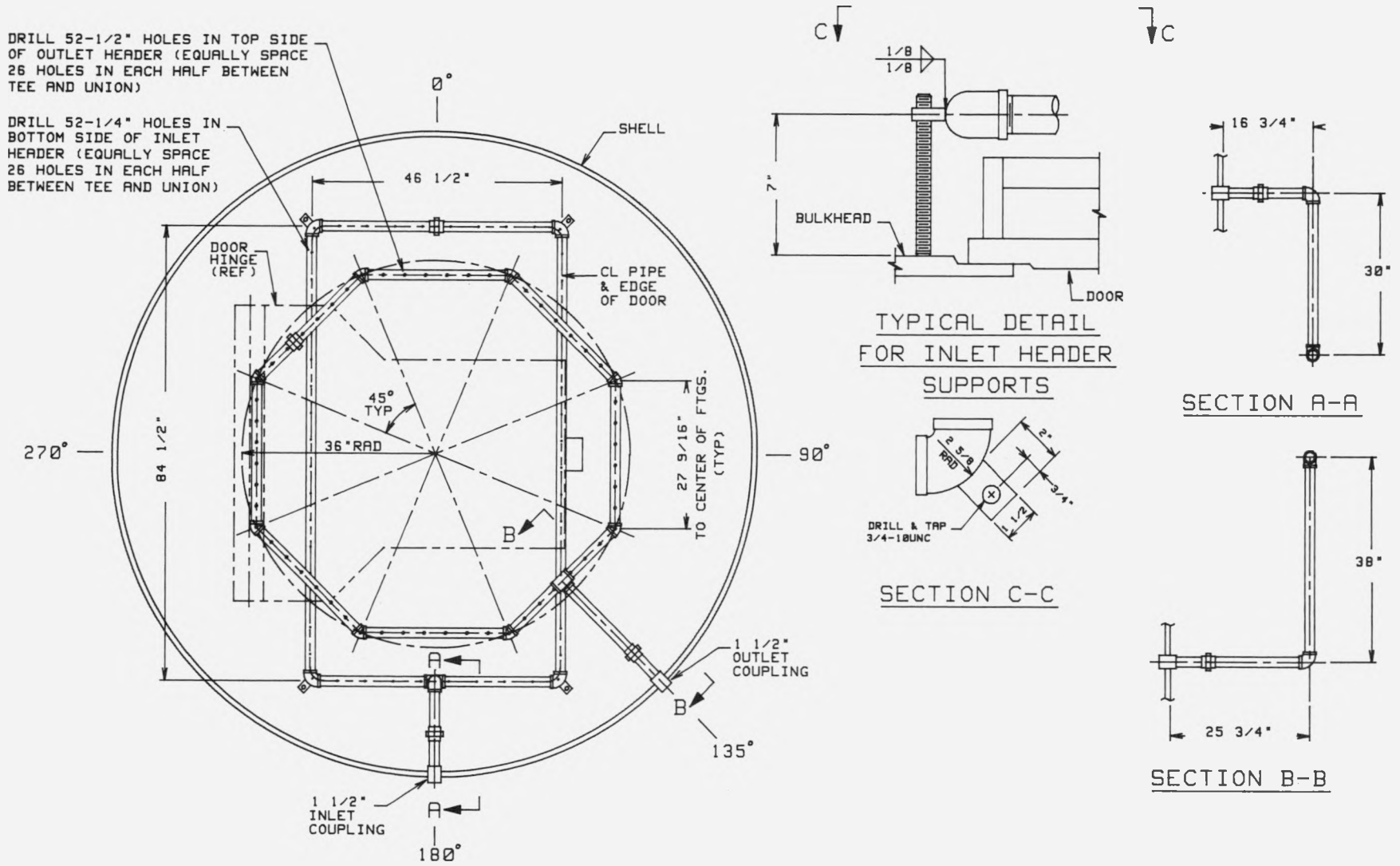

Figure 3.3 Inlet and Outlet Headers

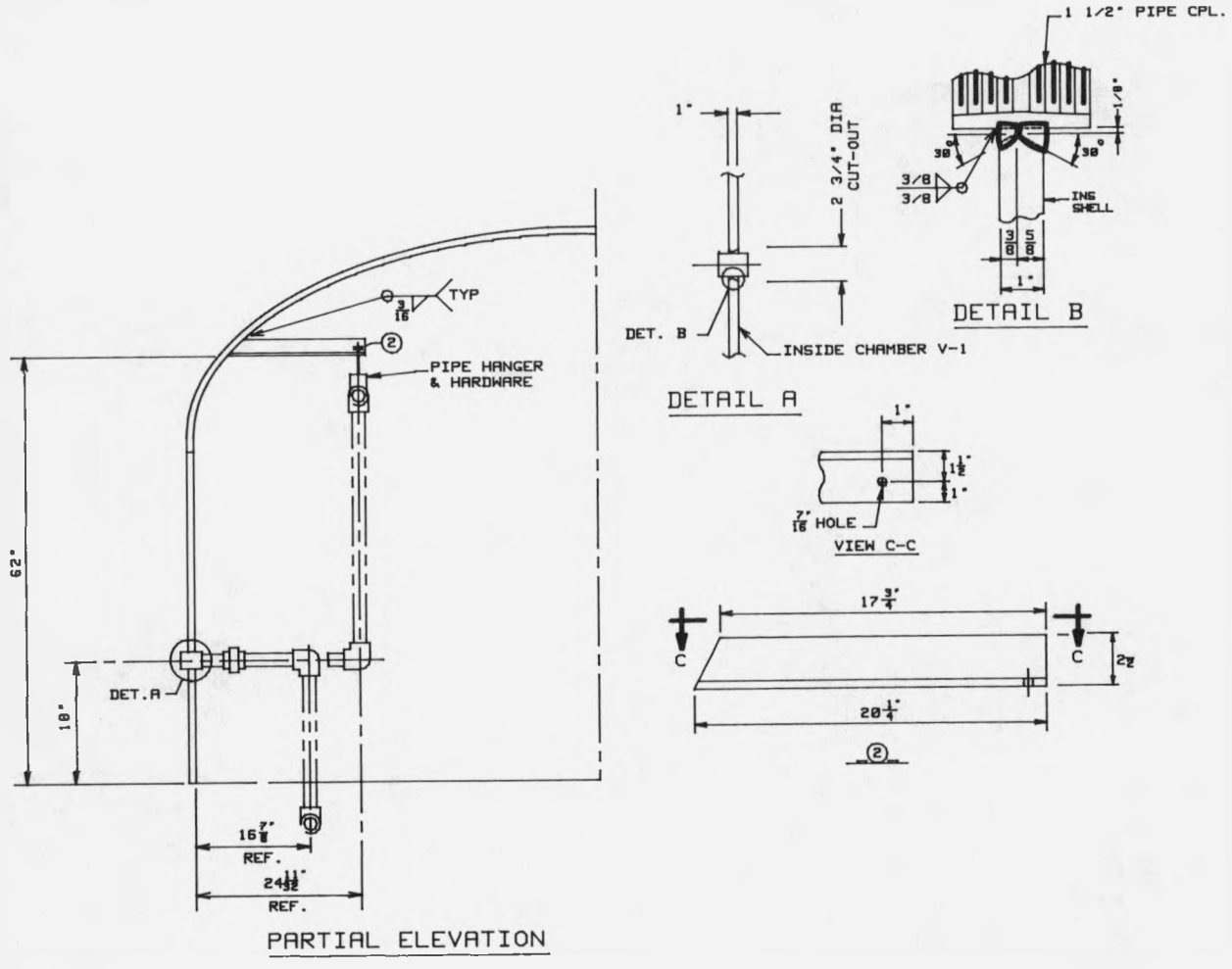

Figure 3.4 Partial Elevation of Chamber V-1 Detailing Inlet and Outlet Header Locations

Air leaking past the inner door was collected by a structural shroud that was welded to the primary structural stiffeners. The shroud was made up of 13 gauge sheet metal in the form of a reinforced five-sided box. The box was reinforced with 2 in. (51 mm) structural steel tubes. The shroud, as shown in Figure 3.5, had a single penetration for a 3 in. (76 mm) schedule 80 pipe which was welded to the shroud for a leak tight seal. This pipe directed leaking air to the flow meter. A Flexonics metal hose was attached to the pipe to allow for any movement due to thermal and pressure effects without applying significant loads on the shroud and piping. Piping from the Flexonics metal hose attached to a flanged fitting that went through the airlock cylinder wall turned vertically to run up the height of the deep test cell to a flow measurement system for the inner door. Depending on the test requirements, the leaking air was either vented to atmosphere or returned to the airlock.

At the four intersections of the primary stiffeners that make up the doorway frame, openings at the corners are typically left unwelded. These openings, known as "rat holes", are intentionally fabricated at this juncture to facilitate a quality weld as welding in a corner is difficult. The openings would have allowed air to bypass the inner door flow meters and escape directly into the airlock. Thus, each of the four corners of the inner door bulkhead were sealed as shown in Figure 3.6. The welds were tested to ensure leak tightness. The material used was a sheet metal with a thickness of 0.090 in. (2.3 mm), and did not provide any significant artificial stiffening of the bulkhead.

3.1.1.3 Outer Door Flow Path

To measure leakage of air past the outer door, air was collected in Chamber V-2 and routed via a 3 in. (76 mm) diameter schedule 80 pipe to a flow measurement system. Air that passed through the flow meter was then vented to atmosphere.

To ensure that Chamber V-2 was not overloaded (design pressure was 5 psig (35 kPa)) a rupture disk was installed as part of the piping.

3.1.1.4 Flow Meter Verification

Additional pipes and valves were installed to bypass the airlock test assembly so the flow meters could be verified for accuracy. This flow path can be traced using Figure 3.2 and Table 3.1.

3.1.1.5 Valving and Insulation

All valves for the piping system were manual with the exception of inlet and outlet Pressure Control Valves PCV-5A and PCV-5B. Those valves that could potentially be exposed to elevated temperatures were manufactured with high temperature packings. All valves with flanged fittings were sealed with Durabla high temperature gasket material. Those gaskets that did not have flanged fittings had welded connections to the pipes. Prior to testing of the airlock, the pipes and valves that would potentially see pressures up to 300 psig (2.07 MPa) were leak tested to a pressure of 345 psig (2.38 MPa).

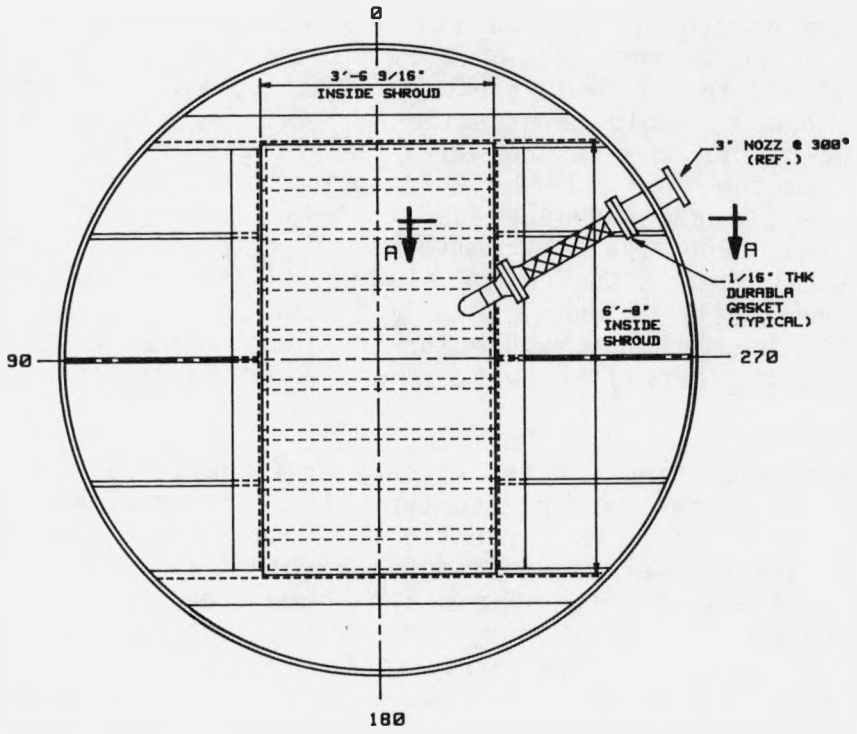

INVERTED PLAN
(UNDERSIDE OF INNER DOOR BULKHEAD)

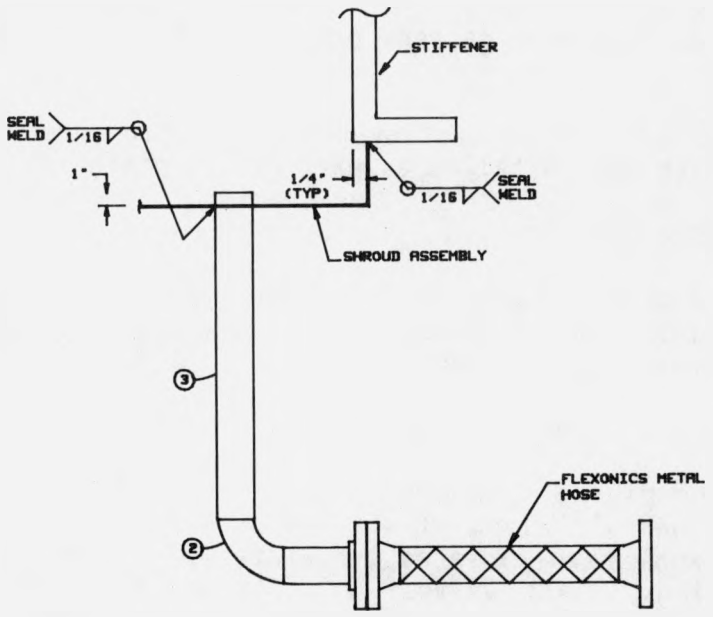

SECTION A-A
(PIPING ROTATED INTO VIEW)

Figure 3.5 Inner Door Shroud and Piping

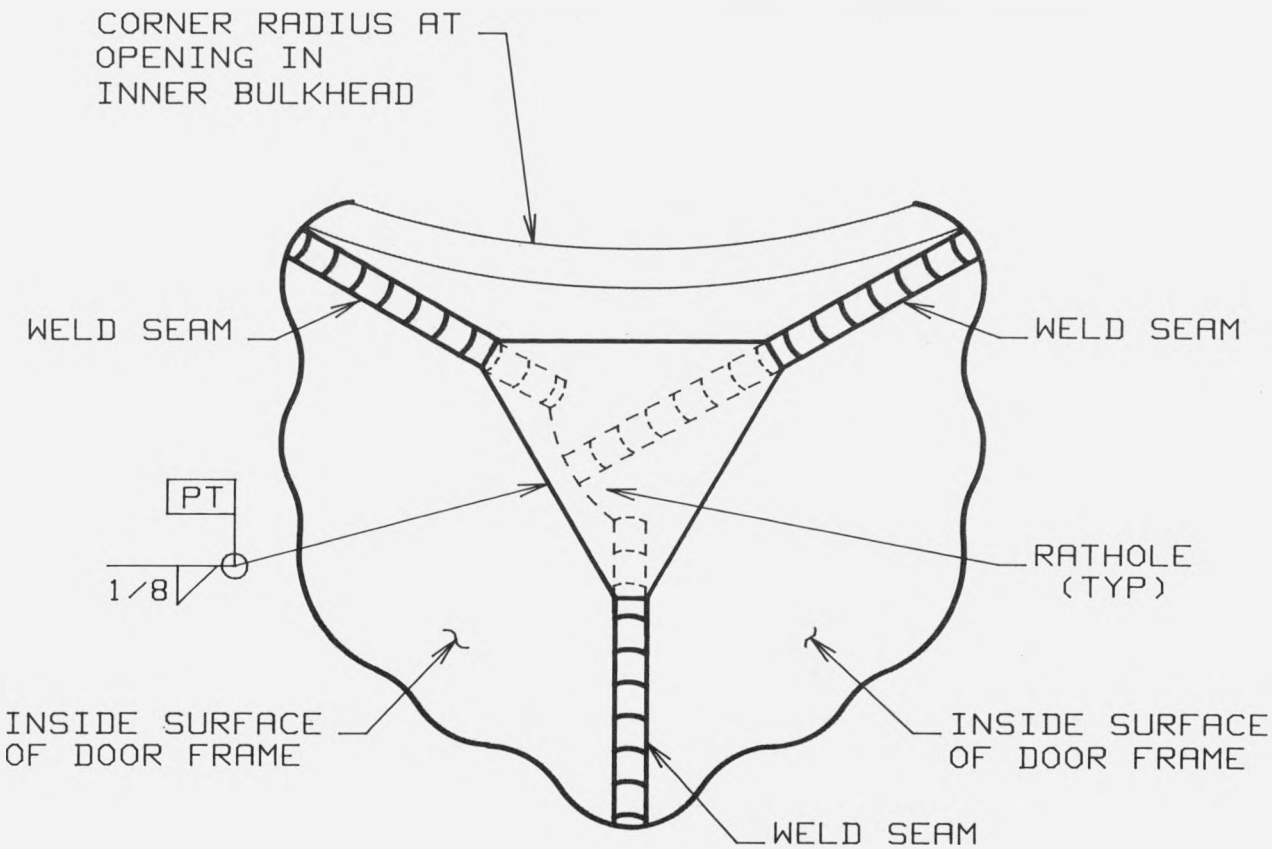

TYPICAL CORNER CLOSURE FOR
"RATHOLES" IN INNER DOOR STRUCTURAL STIFFENER

Figure 3.6 Corner Closure for Inner Door Structural Stiffener

After the leak checks were completed all piping that carried high temperature pressurized air was insulated. Insulation was used to minimize heat loss through the piping and provide personnel protection. Pipes that were welded to the airlock or Chamber V-1 or V-2 were insulated to the cylinder wall. Each valve and the flowmeters were also covered with insulation. Insulation in the high temperature areas consisted of 2 in. (51 mm) of fiberglass with a plastic casing enveloping the fiberglass. Other areas that could potentially become hot but to a lesser degree were also insulated for personnel protection.

3.1.2 Pressurization System

The pressurization sytem, shown in the upper left-hand corner of Figure 3.2, consisted of three main components. This included the plant air source, the booster compressors, and the receiving tank. With the exception of Test 2C, plant air pressure was sufficient. The maximum test pressure was 69 psig (476 kPa) in Tests 1A, 1B, 1AA, 1BB, 2A, 2B, and 3B. Test 3A was stopped after a pressure in Chamber V-1 of approximately 16 psig (110 kPa) was reached because the leak rate was greater than the plant air flow capacity.

For Test 2C, booster compressors were used to increase the plant air pressure from 90 to 300 psig (0.62 to 2.97 MPa). Although one booster compressor was sufficient to achieve the desired maximum pressure, the target flow rate of 174 SCFM (4927 l/min) could not be reached. As a result, two booster compressors, placed in parallel, and supplied with plant air were used. Air receiving tank R-1 was installed between the booster compressors C1 and pressure control valve PCV-5A. This receiving tank provided a volume into which air could be compressed and provided a reservoir of compressed air so that the booster compressors did not run continuously.

3.1.3 Heating System

Pressurized, heated air was supplied to Chamber V-1 for Test 2C (all other tests were performed at ambient temperatures). Air was routed through Pressure Control Valve PCV-5A to the Air Circulation Heater H-1. Heater H-1 was a 45 kW inline heater that preheated the air before it entered Chamber V-1. Heater H-1 is shown schematically in Figure 3.2.

To maintain the target air temperature above the inner door, twelve electrical resistance ribbon type heaters were installed as shown in Figures 3.7 and 3.8. The total power requirements for the twelve oven heaters in Chamber V-1 was 45 kW. The inside surface of Chamber V-1 was covered with a 2 in. (51 mm) layer of Kaowool insulation. The insulation reduced the overall heating requirements and protected Chamber V-1 from elevated temperatures.

3.2 Test Control

There were three parameters controlled during the test: pressure and temperature in Chamber V-1, and the outlet temperature from Heater H-1. The control panel shown in Figure 3.9 was used during the test. Dial pressure gages on the right were used as a visual guide. The same pressure lines had two pressure transducers for electronic monitoring. The pressure and temperature controllers are shown on the left. The two computers in the foreground were used for continuous monitoring and data acquisition, and also

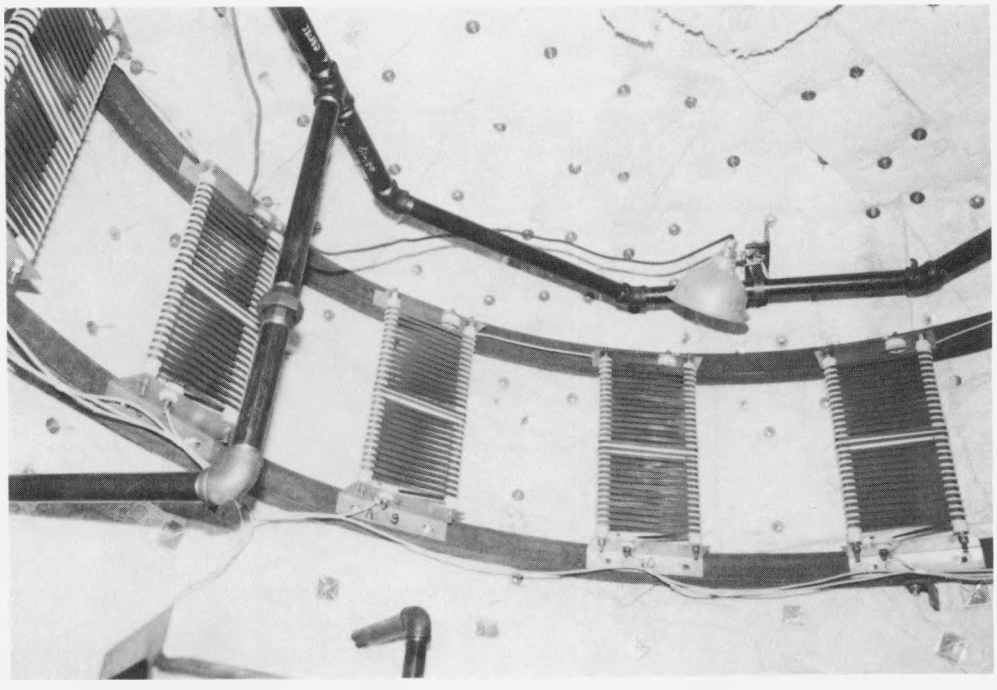

3.7 Heating Elements in Insulated Chamber V-1

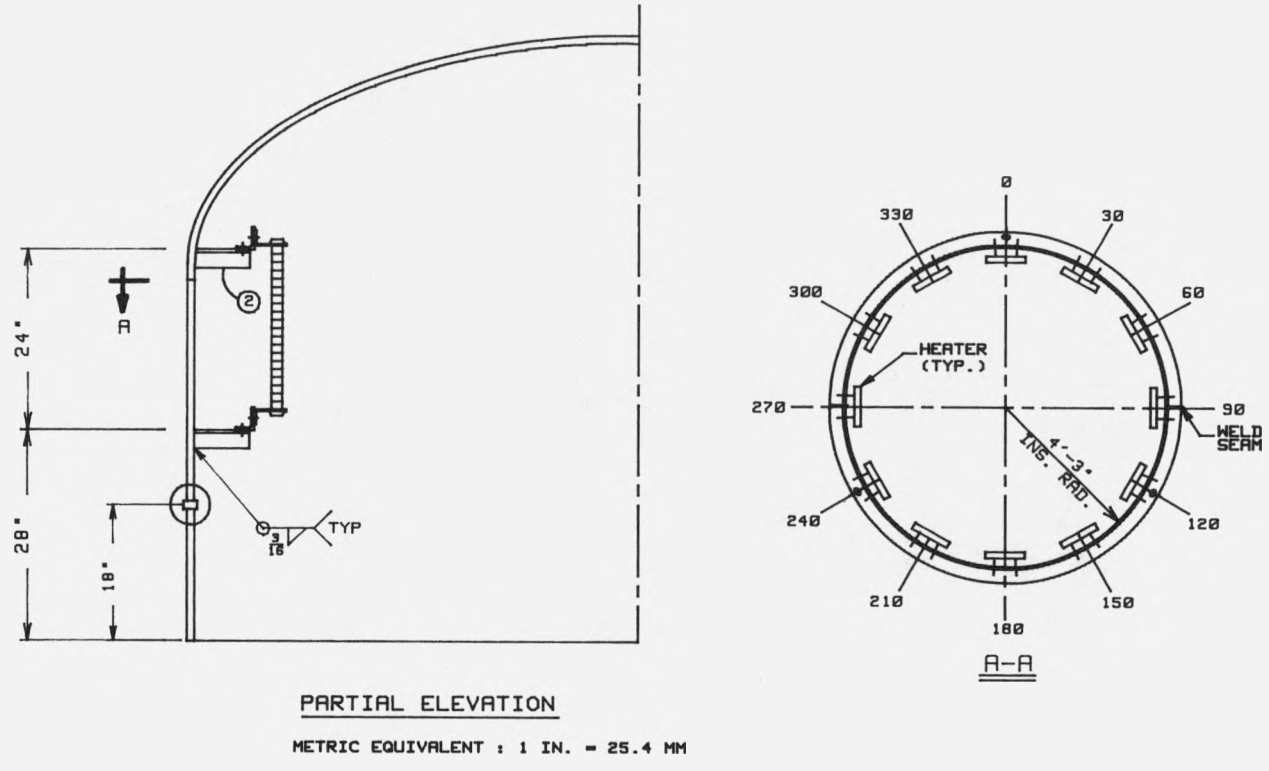

Figure 3.8 Partial Elevation of Chamber V-1 Detailing Oven Heater Assembly

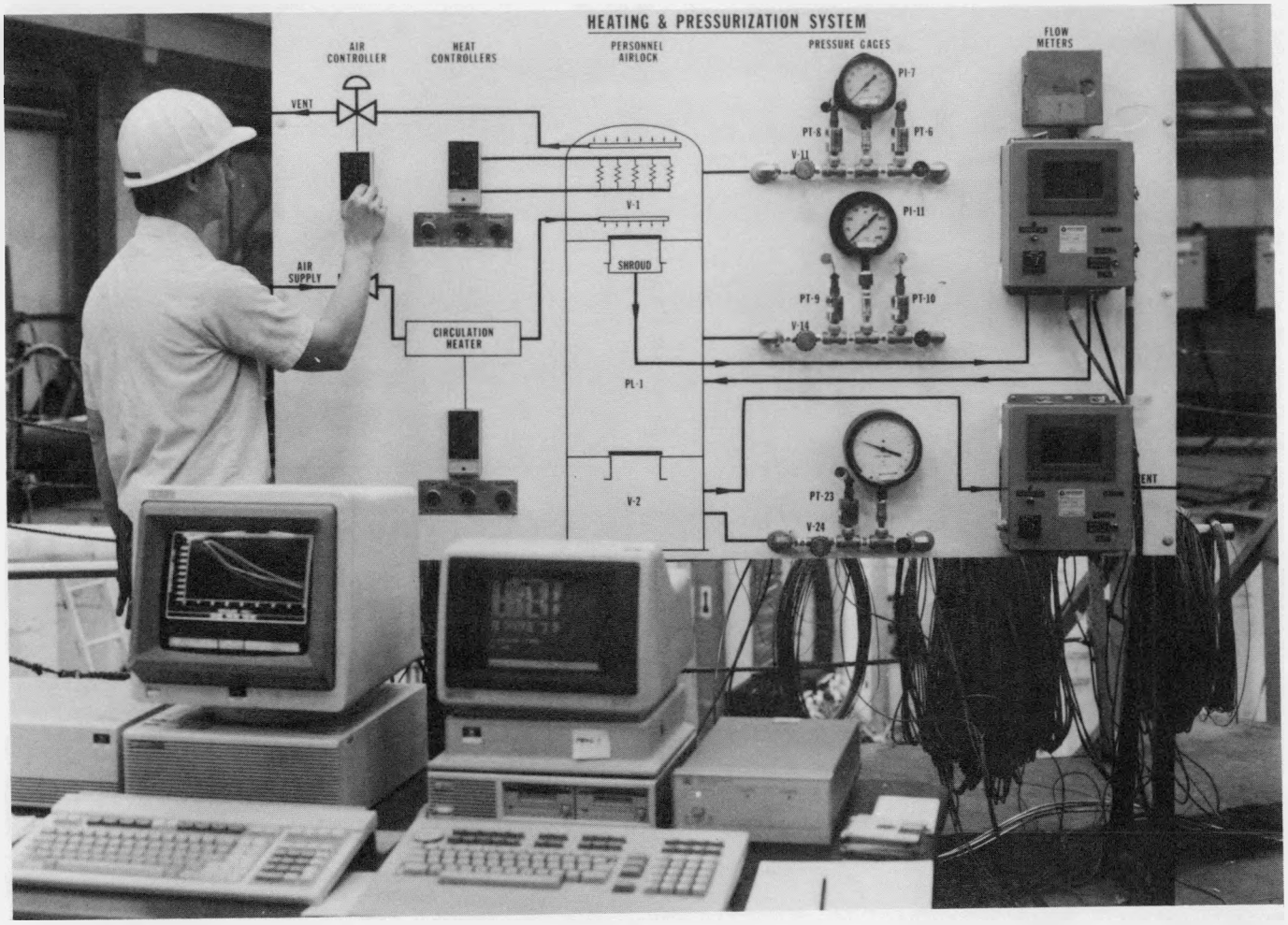

Figure 3.9 Control Panel and Computers

for storing data and plotting. The following paragraphs describe parameters and methods used to control pressure in Chamber V-1, the outlet temperature from the air circulation Heater H-1, and air temperature above the inner door of the airlock.

3.2.1 Chamber V-1 Pressure Control

Pressure inside the top chamber was controlled by a single Moore proportional integral derivative (PID) controller. The controller was set up internally to act as two controllers, one each for pressure control valves PCV-5A and PCV-5B. As shown in Figure 3.2, the air inlet pressure control valve PCV-5A allowed air into Chamber V-1 while the air outlet control valve PCV-5B allowed air to vent through the outlet header. By controlling the degree to which pressure control valve PCV-5B was open air circulation over the inner door seal could be controlled. Pressure Transducer PT-05 was used as a pressure sensor to send a feedback signal to the controller acknowledging pressure level in Chamber V-1. Pressure control valve PCV-5A was opened or closed as necessary to maintain pressure at the desired set point. The air outlet pressure control valve PCV-5B was configured to allow air to discharge out of Chamber V-1 so air would move at a nominally constant rate over the inner door gasket. The maximum amount that pressure control valve PCV-5B was opened or closed could be changed at any time during the test. Since pressure control valves PCV-5A and PCV-5B were controlled separately, each valve opened or closed independently of the other.

3.2.2 Heating System Control

Both the air circulation heater outlet temperature and the air temperature above the inner door were controlled with two separate Moore PID controllers. Each heating system had a dedicated PID controller that used temperature from a thermocouple as the feedback signal and sent a 4-20 mA signal to a silicon controlled rectifier (SCR) that controlled power input to the heating elements. Each SCR had a high limit temperature cutoff to prevent overheating of the heating elements. As shown in Figure 3.2, the Type "K" thermocouple used in the controller feedback loop for Heater H-1 was located at the outlet. The thermocouple sensor used to control the oven heat in Chamber V-1 was located above the center of the inner door above the hinge-beam assembly.

4.0 INSTRUMENTATION AND DATA ACQUISITION

During each test, combinations of different types of transducers were used to monitor the airlock pressures, temperatures, strains, deflections, and leakage. Electronic instruments were used to monitor these parameters. In the case of pressure, dial pressure gages were used as a backup/verification of the electronic pressure devices. All transducers were either factory calibrated or calibrated at CBIRC prior to use. Those devices that were factory calibrated were tested to verify the factory calibration.

Data was acquired on command and required the use of a data acquisition system and two computers. One computer monitored selected transducers during the test. The second computer was used to record data from all transducers, reduce to engineering units, store data on floppy disk and hard disk, and plot selected transducers. A total of 475 channels of data were scanned for 331 transducers used during the test. The following paragraphs are a general description of the types of instrumentation used during the test, verification tests of factory calibrated devices, and the data acquisition system setup.

4.1 Instrumentation

4.1.1 Flow Meters

Two flow meter systems were used to measure leak rates of air that bypassed the inner and outer doors. The two flow meter systems consisted of: (1) Rheotherm flow meters, and (2) orifice plate flow meters. Originally the Rheotherm flow meter was chosen for use, however, the meter was not capable of meeting the temperature ramping requirements. An orifice plate flow meter system was designed to replace the Rheotherm flow meters. Both systems were used during testing. The Rheotherm flow meters were used for Tests 1A, 1B, 1AA, and 1BB, and the orifice plate flow meters were used for Tests 2A, 2B, 2C, 3A, and 3B.

Rheotherm flow meters (Model No. LFI-111D-ID-TU1(BP)), manufactured by Intek* of Columbus, Ohio, were used during Tests 1A, 1B, 1AA, and 1BB. The Rhectherm flow meters were specified to operate within the ranges shown in Table 4.1.

The Rheotherm flow meters were dual range meters that operated between 0.7 to 11 SCFM (19.8 to 311 l/min) on Range 1, and 11 to 174 SCFM (311 to 4927 l/min) on Range 2. Switching ranges was performed manually. The flow meter was calibrated to output a DC proportional voltage signal from 0 to 10 volts for each flow range. Two calibration factors were required for each flow meter so that the voltage signal could be converted to a flow for each of the ranges. This system was originally selected for its simplicity and purported accuracy.

It was discovered during a verification of the factory calibrated Rheotherm flow meters that thermal transients resulted in unacceptable errors in the

* Mention of specific products and/or manufacturers in this document implies neither endorsement or preference nor disapproval of the use of a specific product for any purpose by the U.S. Government, any of its agencies, or Sandia National Laboratories.

meter output, rendering them useless for the high temperature testing. However, they were accurate for testing performed at steady-state temperature conditions. For Tests 1A, 1B, 1AA, and 1BB, the results reported are accurate to within ±5% of the reading.

Orifice plate flow meters were used in place of the Rheotherm flow meters for subsequent testing. Although more complex than the Rheotherm system, this flow measurement system was chosen for several reasons: reliability; insensitivity to changes in temperature; accuracy of flow measurements; and the wide range of flows that could be measured. Table 4.2 defines the flow range over which each meter could measure.

The orifice plate flow metering loops for the inner door consisted of four Daniel precision honed flow sections (Model No. H-1905W) in parallel while the flow metering loops for the outer door consisted of three sections in parallel as shown in Figure 4.1. Each honed flow section had an orifice plate with a precision center hole. Differential pressure transducers Sensotec Model No. A-5 (one dedicated to each array) with a range of ±10 psi, were used to measure the pressure drop across the orifice plate. Solenoid valves were used to isolate flow through a selected honed flow section and isolate the measurement of the pressure drop across the selected orifice plate. The solenoid valves were controlled using an Omron programmable logic controller (PLC). The equations used to calculate flow rates were based on the ASME Committee report on flow measurements.[12]

Verification tests of the inner door flow meter indicated that for conditions under which Tests 2C and 3A were performed, the leak rates reported herein can be as much as 6% less than the reported value. This was due to the failure of the gasket seal and coating of the orifice plates with a residue from the gasket. This was verified after completion of Test 3B.

The orifice plate flow meter array concept worked well for the variety of conditions it was subjected. Due to the interaction of the Omron programmable controller and the computer/data acquisition system, a computer dedicated to operating the arrays would have decreased reaction time and increased the speed with which the flow sections were isolated.

4.1.2 Strain Gages

The strain gages used during this test program were Eaton high temperature weldable strain gages (Eaton Part No. SG425). A total of 123 strain gages were installed in the airlock test assembly. The Eaton SG425 strain gage is a half bridge strain sensor with one active element and the other element used for temperature compensation. Each gage was factory calibrated and was provided with an apparent strain curve that defines the compensation for the difference in thermal expansion coefficients of the strain gage flange material and the base material to which the strain gage was attached. Coefficient of thermal expansion for the airlock steel was provided to Eaton by CBIRC and was based on tests of samples from the airlock cylinder wall.

A schematic of the strain gage completion circuitry is shown in Figure 4.2. In addition to the apparent strain curve and gage factor, each strain gage is provided with a balancing resistor, R_{BAL}, and a temperature compensating resistor, R_{TCM}. These resistors minimized the reported apparent strain for

Table 4.1

Rheotherm Flow Meter Operating Range Specification

	Inner Door Meter	Outer Door Meter
Fluid	Air	Air
Flow Range, SCFM	0.7 to 174	0.7 to 174
Temperature Range, °F	70 to 700	70 to 400
Pressure Range, psig	0 to 300	0 to 15
Temperature Increase Rate, °F/min	7	7

Metric Equivalents:
1 psi = 6.895 kPa
1 SCFM = 28.317 l/m
°C = 5/9 *(°F-32)

Table 4.2

Flow Rate Range for Inner and Outer Door Orifice Plate Flow Meters

Airlock Door	Honed Flow Section I.D. (in.)	Orifice Plate Bore Dia. (in.)	Flow Range (SCFM)
Inner	0.570	0.0855	0.5 - 4
	0.765	0.2065	3 - 27
	0.765	0.4666	14 - 148
	1.530	1.071	76 - 818
Outer	0.765	0.1836	0.5 - 4.9
	0.765	0.4513	3.4 - 31
	1.308	1.0464	21 - 196

Figure 4.1 Orifice Plate Flow Metering Loops

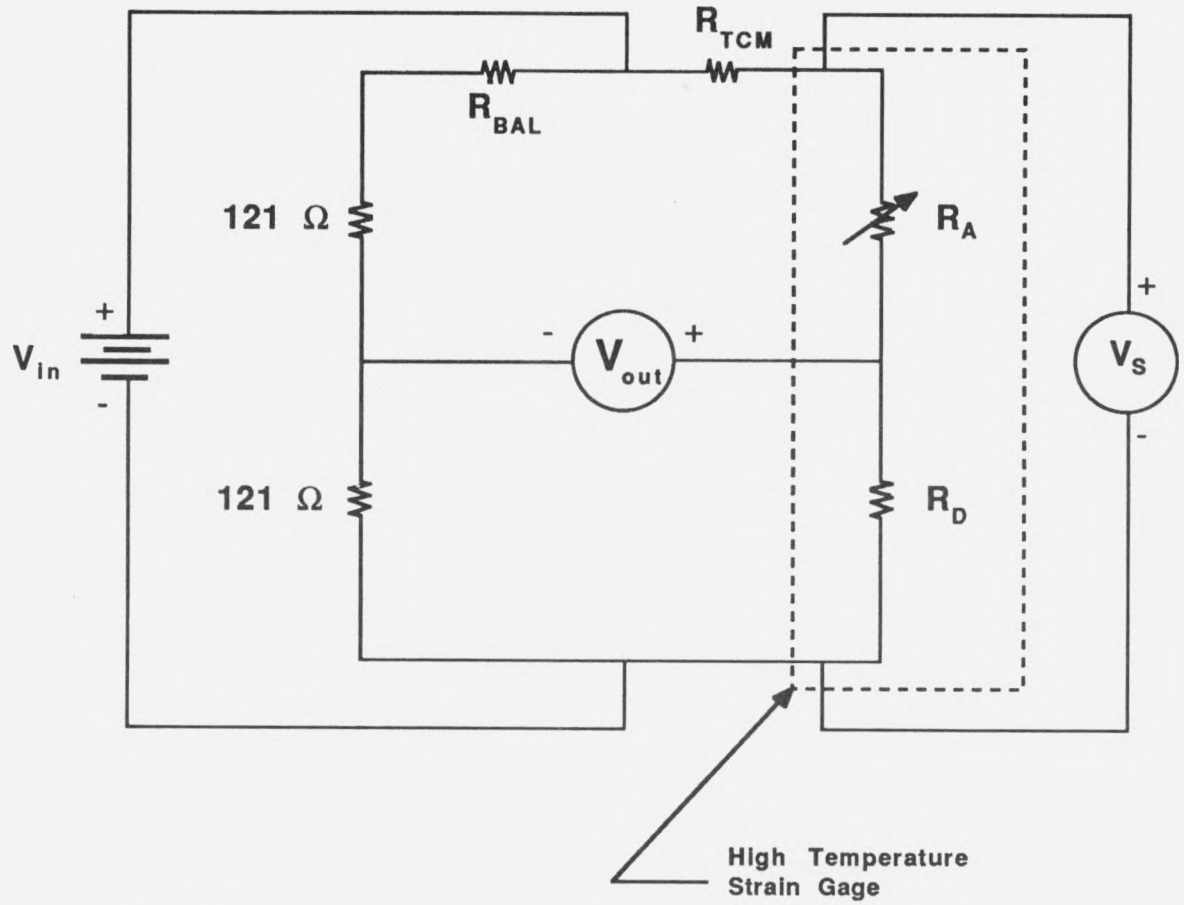

LEGEND:

V_{in} = Bridge excitation voltage

V_{out} = Bridge output voltage

V_S = Strain gage voltage

R_{TCM} = Temperature compensating resistor

R_{BAL} = Bridge balancing resistor

R_D = Dummy temperature compensating strain gage element

R_A = Active strain gage element

Figure 4.2 Schematic of Five Wire Strain Gage System

each gage and balanced the Wheatstone bridge. The sense voltage, which is the voltage across the strain gage, is also a refinement in temperature compensation for long leadwire lengths exposed to elevated temperatures. Strain gages were factory calibrated for an operating range of 40 to 800°F (4 to 427°C). Accuracy of the gages was reported by the manufacturer as ±3%. Installation of the strain gage began with laying out the exact location of the strain gage using a template. The strain gage was held in position by welding tabs of thin sheet stainless steel to the base material to which the strain gage was attached. The strain gage itself was then welded to the bulkhead or door by welding the strain gage flange with tiny spot welds that overlap and form a continuous bead along both sides of the strain tube. Schematic of a typical installation is shown in Figure 4.3.

As part of the contract requirements, six strain gages were tested to verify the strain gage operation as follows:

(1) Strains at ambient conditions,
(2) Strains at 600°F (316°C),
(3) Apparent strains, and
(4) Residual strains (effects of spot welding).

Testing was performed by first constructing a constant strain beam deflection assembly and an oven for the high temperature heating.

The constant strain beam had two high temperature strain gages attached opposite each other such that one gage was in compression while one was in tension. The constant strain beam test assembly inside the heating oven is shown in Figure 4.4. The strains generated for a deflection cycle at ambient and a deflection cycle at a constant temperature of 600°F (316°C) were in good agreement. This included both tension and compression. This indicated that the five wire correction system to account for changes in gage factor and leadwire resistance was performing as required.

The apparent strain test results were completed by heating the beam and strain gage and recording the strain gage output at temperatures over the operating range of the gage. The results of the apparent strain tests indicated poor agreement with the apparent strain data provided by the gage vendor. The difference was traced to a difference in the coefficient of thermal expansion of the airlock steel used by Eaton in the calculation of the apparent strain. A sample of the airlock cylinder wall steel was tested for coefficient of thermal expansion. The measured value reported by Harrop Industries, Inc. was 8.3×10^{-6}/°F (14.9×10^{-6}/°C) which was approximately 1.6×10^{-6}/°F (2.9×10^{-6}/°C) lower than the value used by Eaton. Eaton recalculated the apparent strain curves for each gage and replaced the temperature compensatory resistor and the balancing resistor for each gage. Apparent strain tests were performed again with the new set of resistors and the apparent strains measured were in agreement with Eaton's reported values.

Ambient tests of strains were performed on strain gages and compared with calculated strains for the constant strain beams. In comparison with the calculated strains, the average error was -0.38%, the maximum error 7.4%, the minimum error -9.4%, and a standard deviation of 4.9%. These results take into account tensile and compressive strains at ambient conditions and at 600°F (316°C).

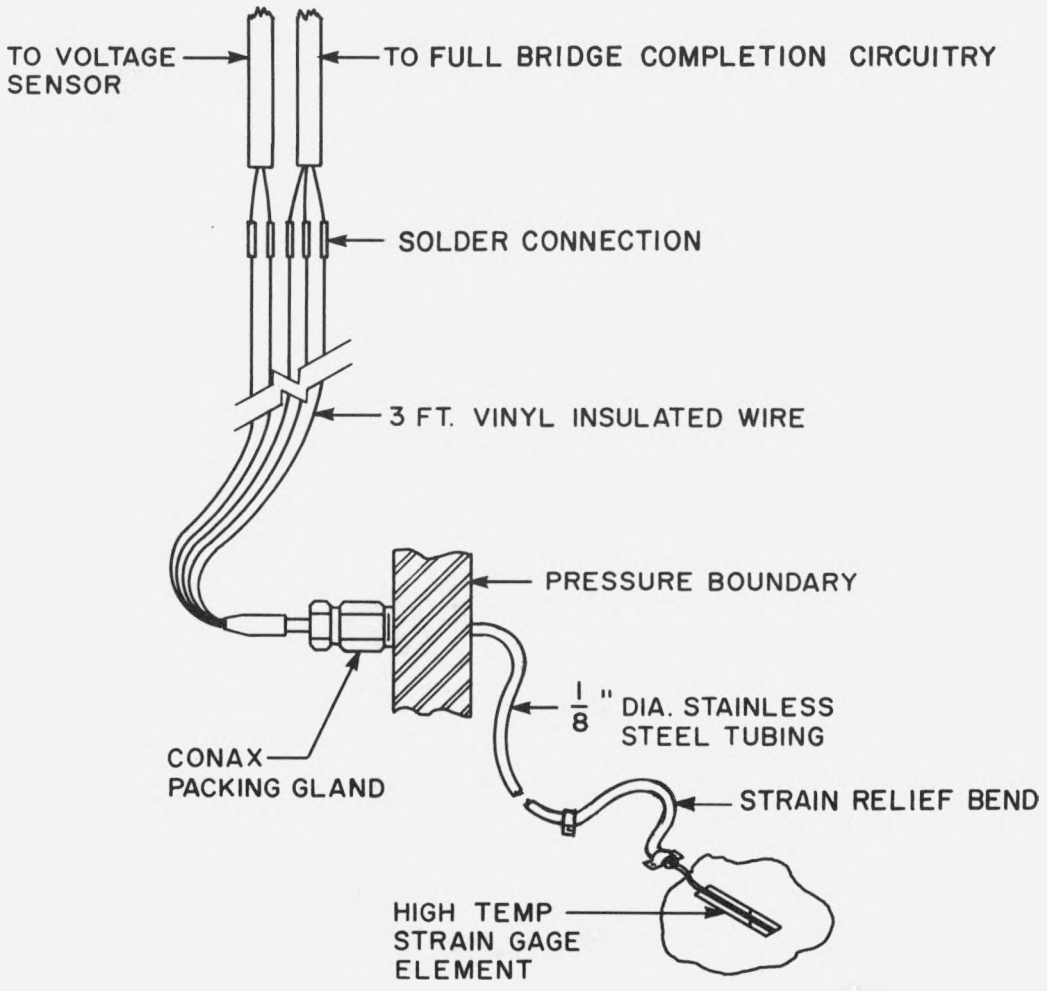

Figure 4.3 Typical High Temperature Strain Gage Installation

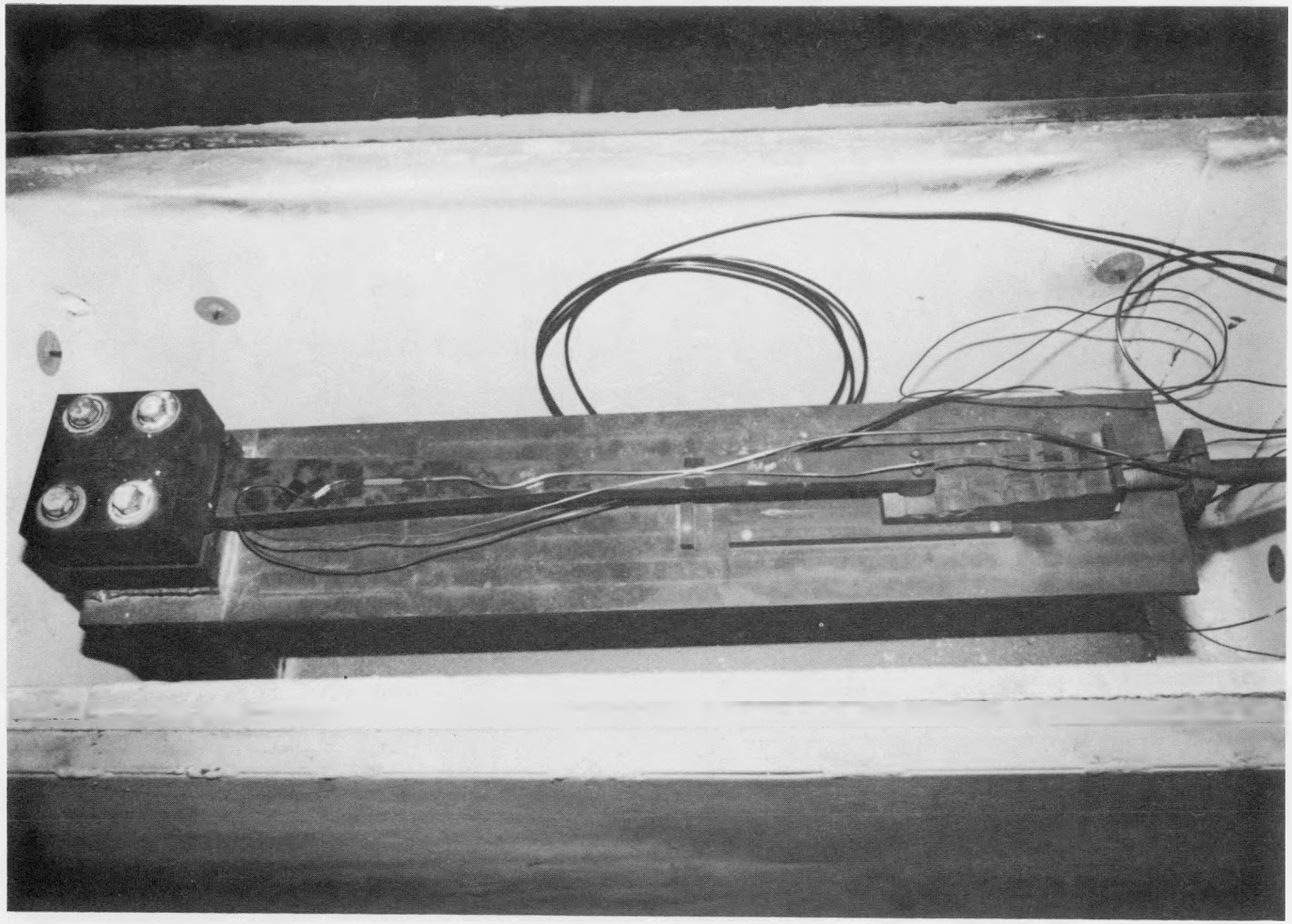

Figure 4.4 Constant Strain Beam Strain Gage Verification Assembly

The strain gages installed in the airlock and bulkheads were oriented in a 0°-45°-90° rosette. In addition, thermocouple elements were positioned near the strain gage rosette locations for temperature compensation as shown in Figure 4.5. Strain gage locations for the inner and outer bulkheads, stiffeners, and doors, and the cylinder wall of Chamber V-1 are shown in Figure 4.6 through 4.8.

4.1.3 Capacitance Displacement Transducers

Gap and rotation of the inner and outer doors relative to the bulkhead and out-of-plane movement of the doors and bulkheads relative to a reference frame were measured using a high temperature displacement transducer that operates on a capacitance principle. Additionally, slip of the door relative to the bulkhead and the growth of the door frame were also monitored using these probes. A total of eighty-four Capacitec Model No. HPC-375I high temperature probes and Capacitec Model No. 3200-S amplifier cards were used for this purpose. The probes had an operating range of 0.025 to 0.25 in. (0.64 to 6.4 mm) of a gap between the probe and the target surface. Although the operating range was up to 0.25 in. (6.4 mm), the gage had a repeatable non-linear range up to 0.40 in. (10 mm).

Each probe consisted of the transducer head and a length of coaxial cable sheathed in a stainless steel tube. An extension cable was provided with each probe assembly. The coaxial extension cable was sheathed with a flexible insulator. Each probe was paired with an extension cable and was calibrated as a total assembly. Calibration setup is shown in Figure 4.9.

Each transducer was calibrated individually at ambient temperatures and pressures. The curve that relates output voltage from the amplifier to the gap between the probe head and target surface is slightly non-linear. A fifth order polynomial was fit to each calibration curve to optimize the accuracy of the transducer output. For ambient conditions the gages are typically accurate to within ±0.5% of full scale. Figure 4.10 shows a typical set of calibration data and a fifth order polynomial curve fit for a capacitance displacement transducer.

Six capacitance probes were chosen at random and tested to determine the effects of elevated temperatures on the following:

(1) Zero drift,
(2) Probe mounting bracket, and
(3) Displacements at elevated temperatures.

Zero drift was measured by placing a target at a constant distance from the probe head and measuring the change in voltage of the probe output as temperature was increased to 700°F (371°C). All tests indicated that the zero drift amounted to less than 0.001 in. (0.03 mm) over a 630°F (332°C) temperature difference.

The mounting brackets used to hold the probe in place during the airlock test were tested to determine if the mounting system induced fictitious displacements. Temperature compensation was determined to result in a change of displacement measurement of 0.4% over the full range of temperatures

Figure 4.5 Strain Gage Rosettes and Thermocouple

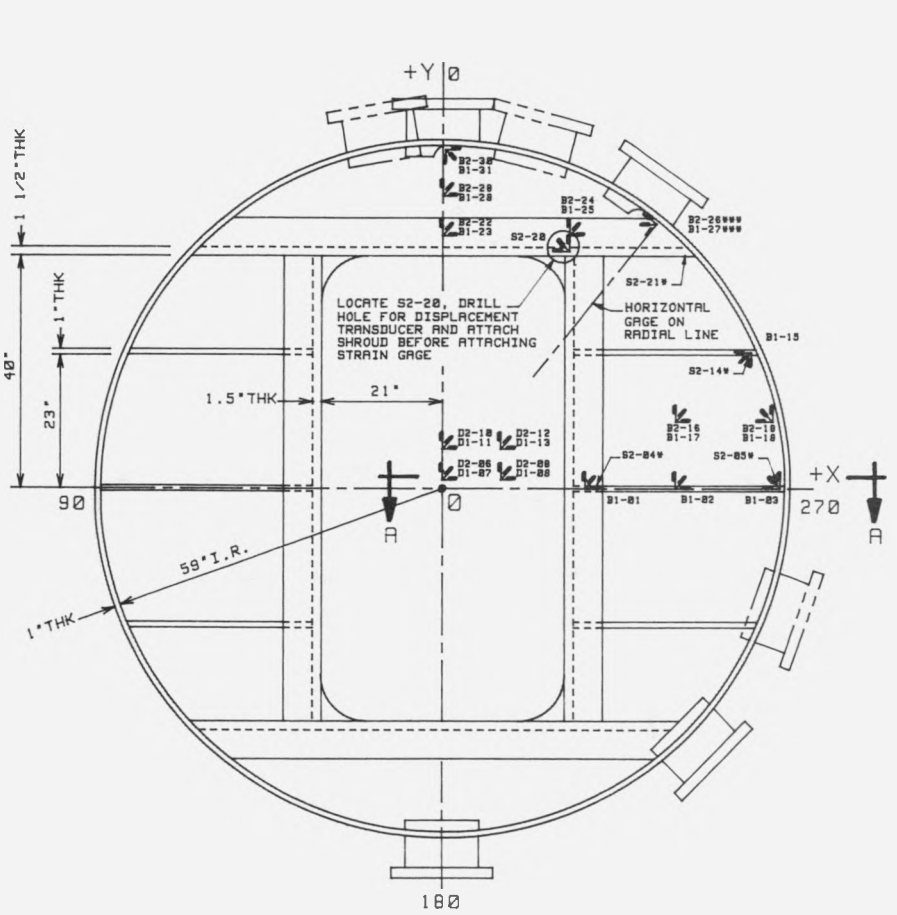

LOCATING POINT

EACH ID* REPRESENTS A GROUP OF 3 STRAIN GAGES (IN A ROSETTE PATTERN)	INSTRUMENTATION IDENTIFICATION	X (IN.)	Y (IN.)	TC'S FOR TEMPERATURE COMPENSATION INSTR. *
	SGB1-001	24.5000	0	107
	SGB1-002	40.0000	0	108
	SGB1-003	58.0000	0	109
	SGS2-004 *	24.5000	0.5000	011
	SGS2-005 *	58.0000	0.5000	012
	SGD2-006	0	1.5000	001
	SGD1-007	0	1.5000	001
	SGD2-008	10.0000	1.5000	001
	SGD1-009	10.0000	1.5000	001
	SGD2-010	0	6.8125	013
	SGD1-011	0	6.8125	013
	SGD2-012	10.0000	6.8125	013
	SGD1-013	10.0000	6.8125	013
	SGS2-014 *	53.0000	23.0000	113
	SGB1-015	53.0000	23.5000	112
	SGB2-016	40.0000	11.5000	015
	SGB1-017	40.0000	11.5000	015
	SGB2-018	56.7500	11.5000	111
	SGB1-019	56.7500	11.5000	110
	SGS2-020	21.7500	48.7500	023
	SGS2-021 *	42.3400	48.0000	024
	SGB2-022	0	43.5000	028
	SGB1-023	0	43.5000	028
	SGB2-024	21.7500	43.5000	026
	SGB1-025	21.7500	43.5000	026
	SGB2-026 ***	36.0000	45.5000	114
	SGB1-027 ***	36.0000	45.5000	016
	SGB2-028	0	58.2500	027
	SGB1-029	0	58.2500	027
	SGB2-030	0.5000	58.0000	025
	SGB1-031	0.5000	58.0000	115

SG [a] [b] - [*]

METRIC EQUIVALENT: 1 IN. = 25.4 MM

(a) SURFACE:
- D - DOOR
- B - BULKHEAD
- S - STIFFENER
- V - SLEEVE
- E - ENVIRONMENT
- T - TRANSDUCER

(b) CHAMBER:

* - SEE SECTION A-A FOR ORIENTATION

*** - HORIZONTAL LEG IN RADIAL DIRECTION
VERTICAL LEG IN TANGENTIAL DIRECTION

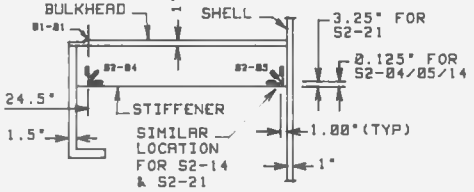

SECTION A-A

Figure 4.6 Strain Gage Locations on Inner Door and Bulkhead

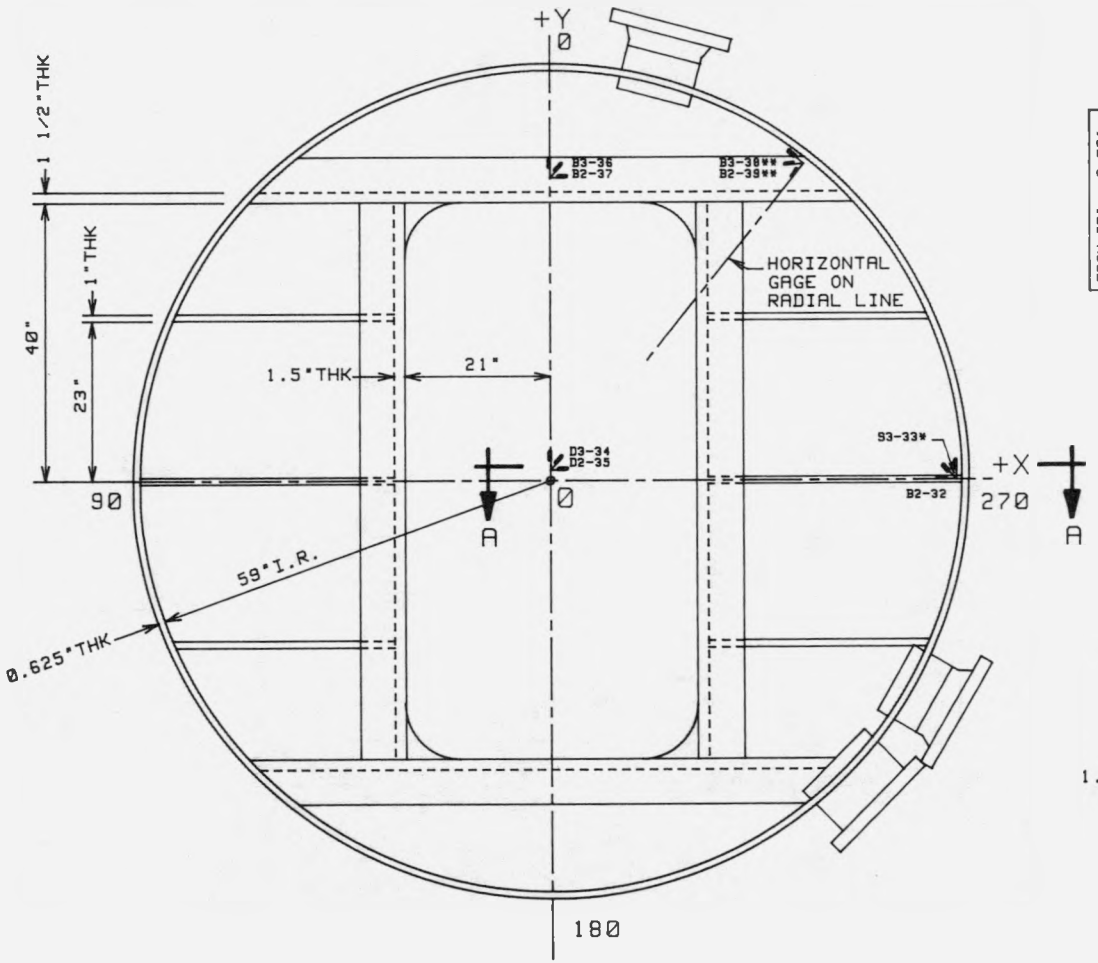

EACH ID# = 3 SG's (IN A ROSETTE)	INSTRUMENTATION IDENTIFICATION	X (IN.)	Y (IN.)	TC'S FOR TEMPERATURE COMPENSATION INSTRUMENT NO.
	SGB2-032	58.0000	0	040
	SGS3-033 *	58.0000	0.5000	039
	SGD3-034	0	1.5000	041
	SGD2-035	0	1.5000	042
	SGB3-036	0	43.5000	049
	SGB2-037	0	43.5000	050
	SGB3-038 **	36.0000	45.5000	051
	SGB2-039 **	36.0000	45.5000	052

LOCATING POINT

SG [a] [b] - [#]

METRIC EQUIVALENT : 1 IN. = 25.4

(a) SURFACE:

D - DOOR
B - BULKHEAD
S - STIFFENER
V - SLEEVE
E - ENVIRONMENT
T - TRANSDUCER

(b) CHAMBER:

1
2 4
3

* - SEE SECTION A-A FOR ORIENTATION
** - HORIZONTAL LEG IN RADIAL DIRECTION
VERTICAL LEG IN TANGENTIAL DIRECTION

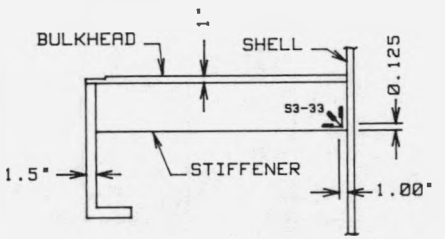

SECTION A-A

Figure 4.7 Strain Gage Locations on Outer Door and Bulkhead

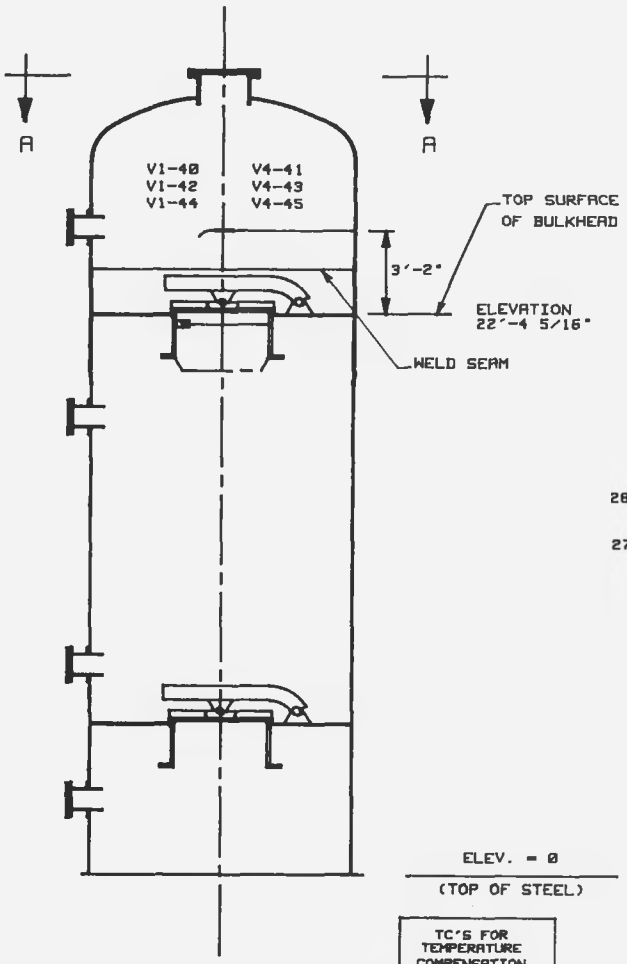

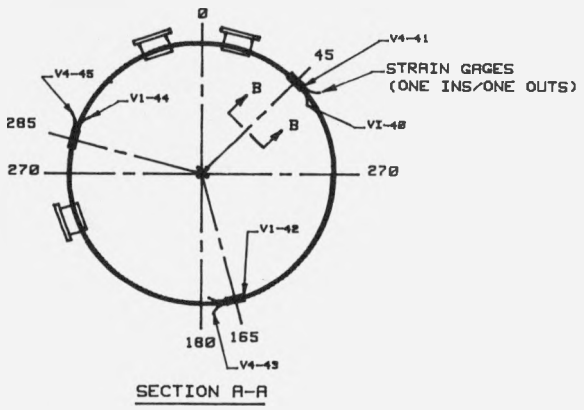

SECTION A-A

	INSTRUMENTATION IDENTIFICATION	ELEVATION ABOVE WELD SEAM	AZIMUTH	TC'S FOR TEMPERATURE COMPENSATION INSTRUMENT #
EACH ID # - 1 STRAIN GAGE	SGV1-040	1'-6"	45	090
	SGV4-041	1'-6"	45	090
	SGV1-042	1'-6"	165	091
	SGV4-043	1'-6"	165	091
	SGV1-044	1'-6"	285	092
	SGV4-045	1'-6"	285	092

TD [a] [b] - [#]

(a) SURFACE:

D - DOOR
B - BULKHEAD
S - STIFFENER
V - SLEEVE
E - ENVIRONMENT
T - TRANSDUCER

(b) CHAMBER:

METRIC EQUIVALENT : 1 FT. = 0.305 M
1 IN. = 25.4 MM

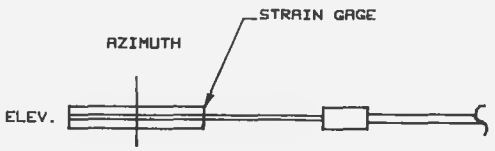

SECTION B-B

Figure 4.8 Strain Gage Locations on Chamber V-1 Cylinder Wall

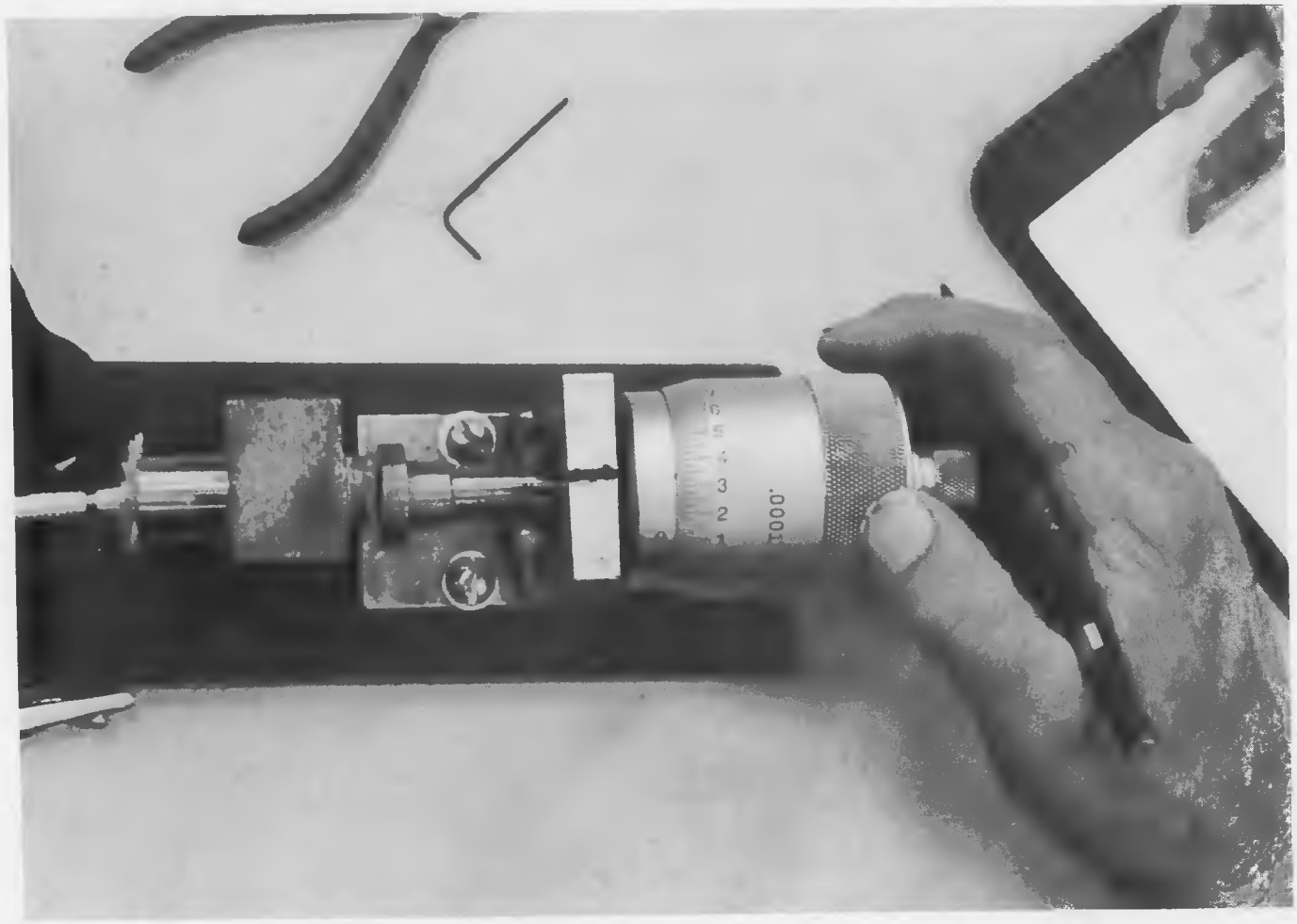

Figure 4.9 Capacitance Probe Calibration Setup

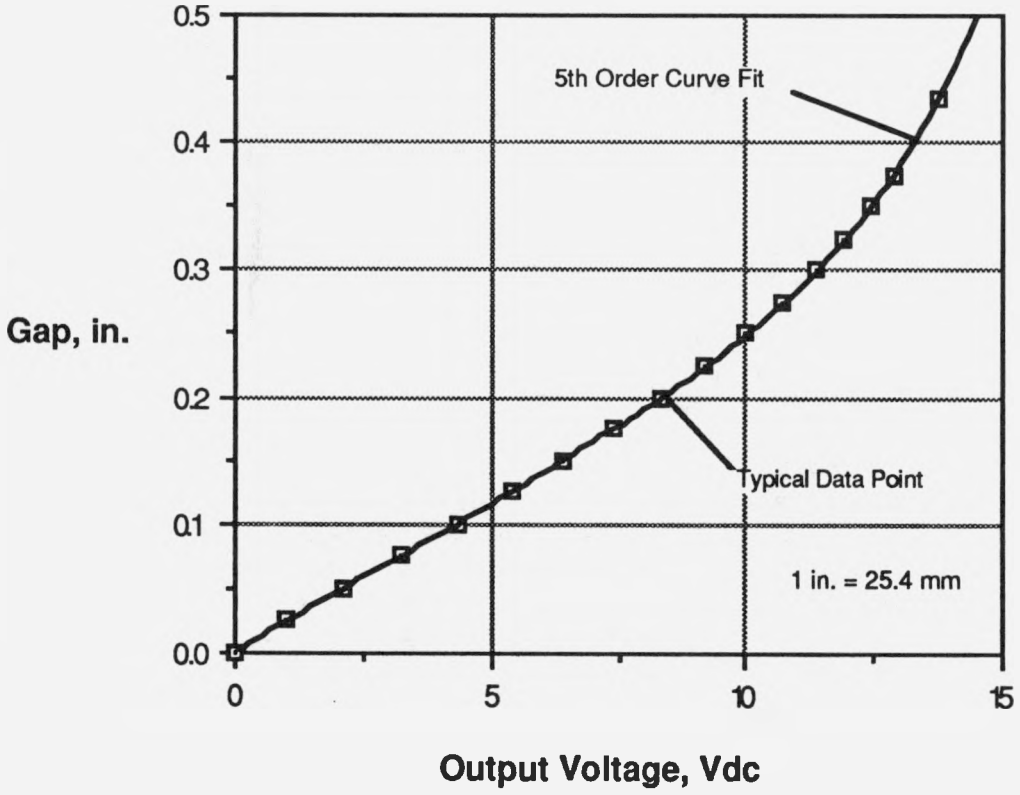

Figure 4.10 Typical Calibration Data and Fifth Order Polynomial Fit for Capacitance Displacement Transducer

The probe heads were heated to approximately 700°F (371°C) and then run through the full range of displacements and compared with a similar ambient calibration. The end points of the calibration, which ranged from 0.025 to 0.25 in. (0.64 to 6.4 mm), had the largest error. Five capacitance probes were evaluated. The average variation when compared to full scale ambient calibration was 1.2% with a maximum of 1.8% and a minimum of 0.7% for a gap between the probe and target of 0.025 in. (0.64 mm). For a gap between the probe and target of 0.25 in. (6.4 mm), the average variation was -0.06% with a maximum of 0.9% and a minimum of -0.5%.

There were major difficulties with these particular probes during installation in the airlock test assembly. The stainless steel sheathing is part of the electronic circuit and carries an AC signal to the probe. The sheathing was provided with a Nextel insulator. However, where the probe penetrated the airlock shell, the Nextel fiber jacket was removed. In its place two layers of Kapton high temperature insulating tape were wrapped around the stainless steel sheath. When inserted in the Conax multiple feed through gland, the Kapton tape was inadvertantly scraped off the probe cable, interrupting the probe signal. If this was an intermittent problem and was thought to have been fixed, the probe signal could possibly have been affected during testing yielding erroneous data.

Additionally, capacitance probes located in the lowest part of the deep test cell required long extension cables. The length of these extension cables increased the relative capacitance of the probe. Although the probe and cable combination were calibrated, the total length of the probe conductor and extension cable was approaching the limits of total capacitance.

The probes were sensitive to moisture infiltration in high humidity environments. Dehumidifiers were installed inside of both the airlock and Chamber V-2. There was also a problem with the BNC coaxial cable connectors between the probe and extension cable and the extension cable and the conditioning circuitry rack. A large amount of time was spent trouble shooting these problems. Results for probes in Chamber V-2 were more erratic than the probes located in the airlock and Chamber V-1 as a result of the higher humidities and combined effects of these difficulties. Typical gap/rotation and out-of-plane capacitance probe installation in the airlock is shown in Figure 4.11. Locations of capacitance type displacement transducers are shown in Figures 4.12 through 4.18. Mounting brackets and T-frame details are shown in Figures 4.19 through 4.22.

4.1.4 Thermocouples

Type "K" thermocouples were used for monitoring temperatures of the airlock doors, bulkheads, stiffeners, and the air inside and outside the airlock. A total of 115 thermocouples were installed inside and outside the airlock and surrounding chambers. In addition, Type "K" thermocouples were also used to monitor the temperature of air leaking past either door seal. A typical thermocouple is shown in Figure 4.5.

Thermocouples that were installed on the interior of the airlock and Chambers V-1 and V-2, were Omega Type "K" thermocouples (Omega Part No. TJ36-CASS-11GG), sheathed with a 1/16 in. (1.6 mm) diameter stainless steel tube, with the temperature sensing element grounded to the sheath. This thermocouple

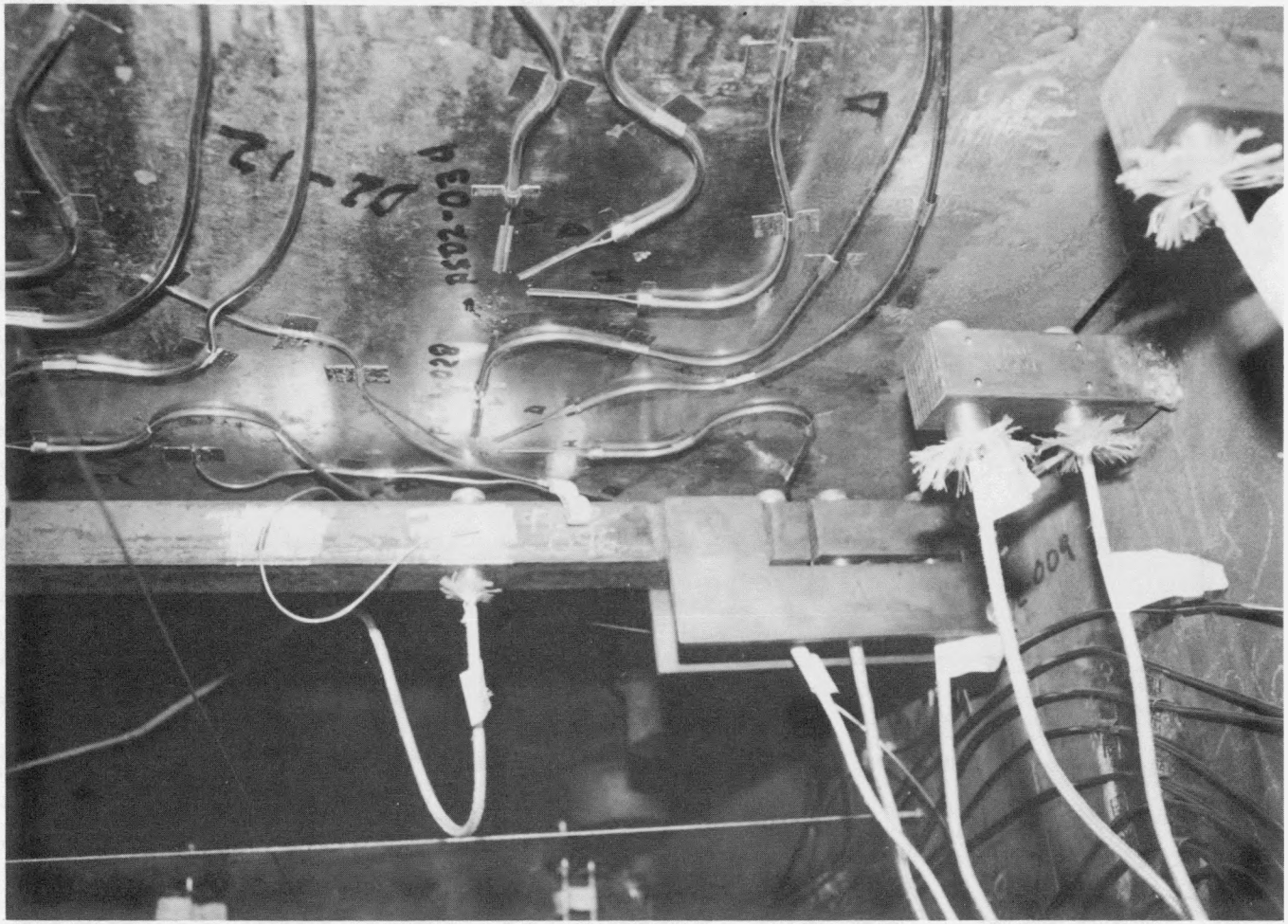

Figure 4.11 Typical Gap/Rotation and Out-of-Plane Capacitance Probe Installation

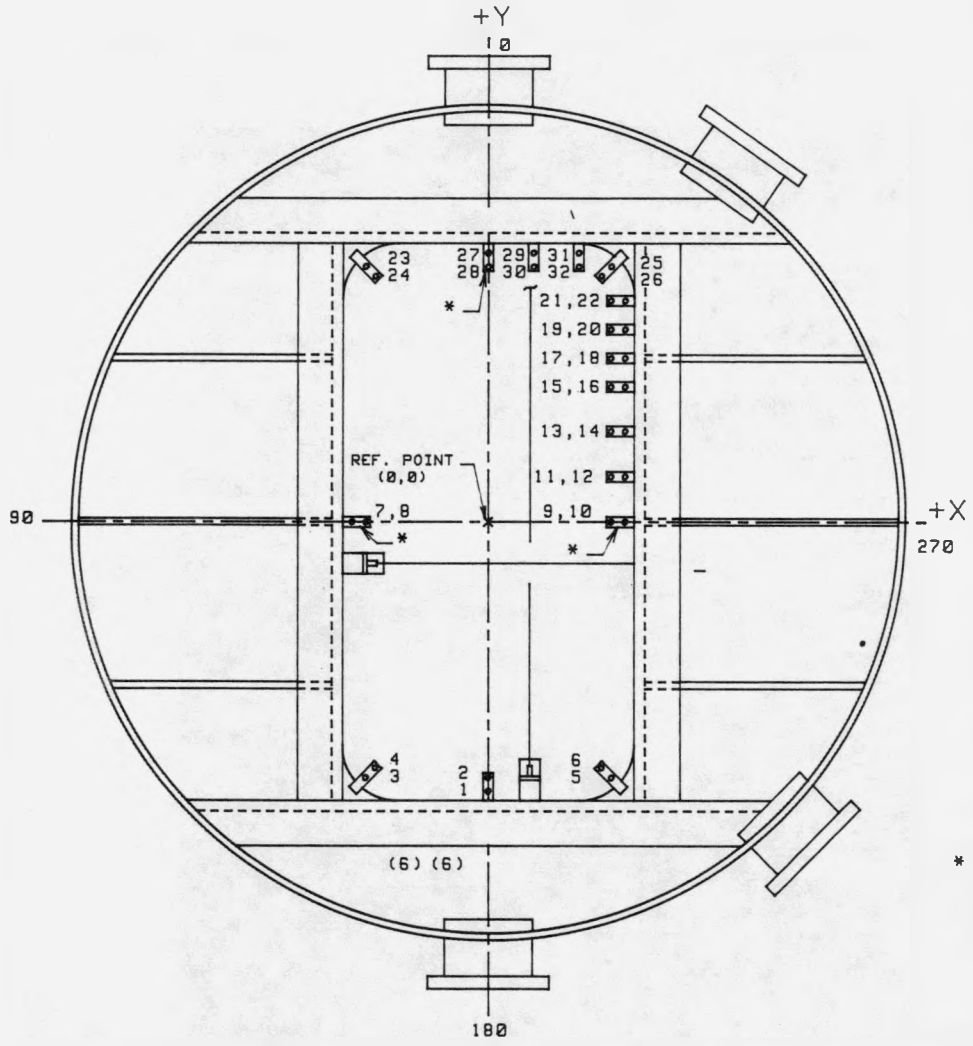

INSTRUMENTATION IDENTIFICATION	X (IN.)	Y (IN.)	TC'S FOR TEMPERATURE COMPENSATION INSTR. #
TGD2-001	0	-38.6250	021
TRD2-002	0	-36.6250	021
TGD2-003	-17.6846	-36.6846	003
TRD2-004	-16.2704	-35.2704	003
TGD2-005	17.6846	-36.6846	005
TRD2-006	16.2704	-35.2704	005
TGD2-007 *	-19.6250	0	007
TRD2-008	-17.6250	0	007
TRD2-009 *	17.6250	0	009
TGD2-010	19.6250	0	009
TRD2-011	17.6250	6.5000	009
TGD2-012	19.6250	6.5000	009
TRD2-013	17.6250	13.0000	009
TGD2-014	19.6250	13.0000	009
TRD2-015	17.6250	19.3750	019
TGD2-016	19.6250	19.3750	019
TRD2-017	17.6250	23.5000	019
TGD2-018	19.6250	23.5000	019
TRD2-019	17.6250	27.6250	019
TGD2-020	19.6250	27.6250	019
TRD2-021	17.6250	31.7500	019
TGD2-022	19.6250	31.7500	019
TGD2-023	-17.6846	36.6846	017
TRD2-024	-16.2704	35.2704	017
TGD2-025	17.6846	36.6846	019
TRD2-026	16.2704	35.2704	019
TGD2-027 *	0	38.6250	021
TRD2-028	0	36.6250	021
TGD2-029	6.5000	38.6250	021
TRD2-030	6.5000	36.6250	021
TGD2-031	13.0000	38.6250	019
TRD2-032	13.0000	36.6250	019

METRIC EQUIVALENT: 1 IN. =25.4 MM

* - BRACKET DOUBLES AS A SUPPORT FOR TRANSDUCER FRAME A

TG[a][b]-[#] (OR) TR[a][b]-[#]

(a) SURFACE:

- D - DOOR
- B - BULKHEAD
- S - STIFFENER
- V - SLEEVE
- E - ENVIRONMENT
- T - TRANSDUCER

(b) CHAMBER:

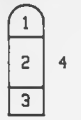

Figure 4.12 Gap/Rotation Transducer Locations on Inner Door

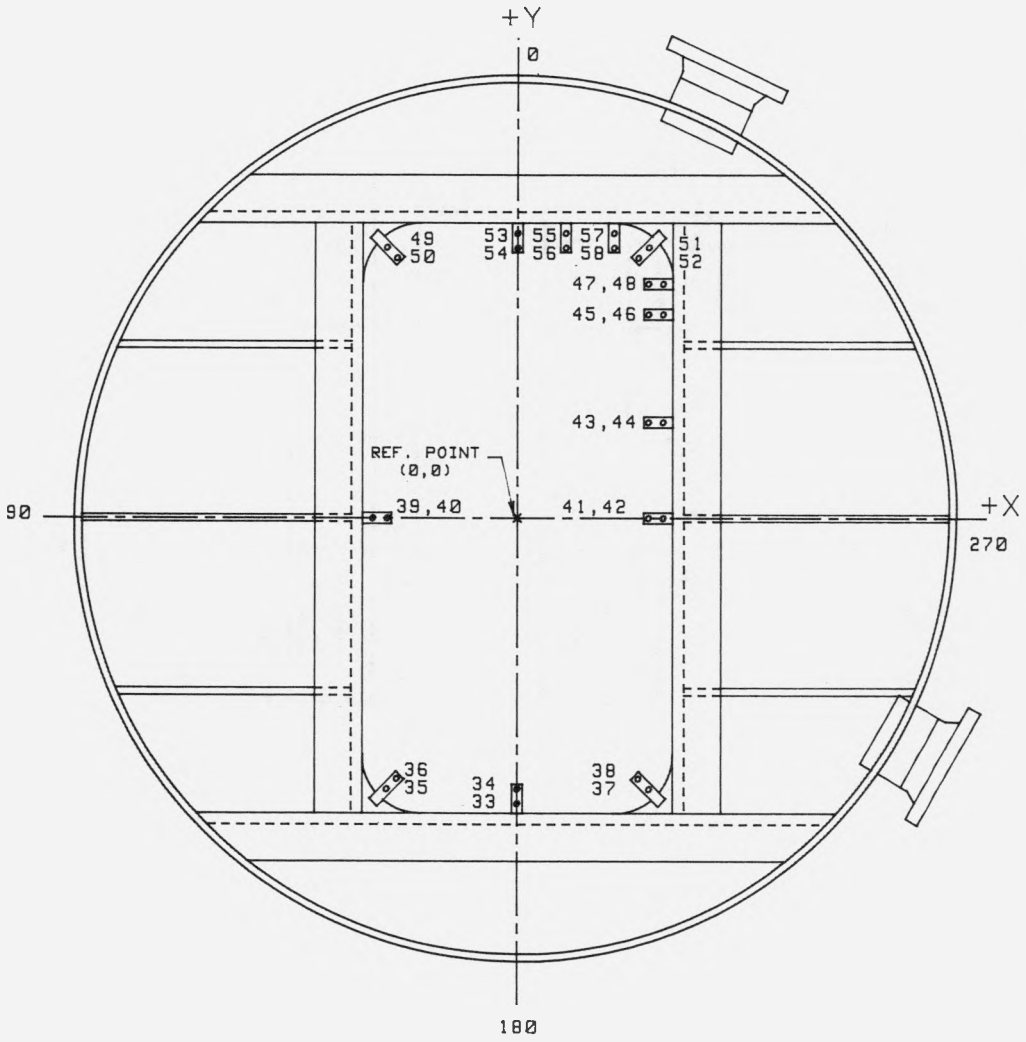

INSTRUMENTATION IDENTIFICATION	X (IN.)	Y (IN.)	TC'S FOR TEMPERATURE COMPENSATION INSTR. #
TGD3-033	0	-38.6250	029
TRD3-034	0	-36.6250	029
TGD3-035	-17.6846	-36.6846	031
TRD3-036	-16.2704	-35.2704	031
TGD3-037	17.6846	-36.6846	033
TRD3-038	16.2704	-35.2704	033
TGD3-039	-19.6250	0	035
TRD3-040	-17.6250	0	035
TRD3-041	17.6250	0	037
TGD3-042	19.6250	0	037
TRD3-043	17.6250	13.0000	037
TGD3-044	19.6250	13.0000	037
TRD3-045	17.6250	27.6250	045
TGD3-046	19.6250	27.6250	045
TRD3-047	17.6250	31.7500	045
TGD3-048	19.6250	31.7500	045
TGD3-049	-17.6846	36.6846	043
TRD3-050	-16.2704	35.2704	043
TGD3-051	17.6846	36.6846	045
TRD3-052	16.2704	35.2704	045
TGD3-053	0	38.6250	047
TRD3-054	0	36.6250	047
TGD3-055	6.5000	38.6250	047
TRD3-056	6.5000	36.6250	047
TGD3-057	13.0000	38.6250	045
TRD3-058	13.0000	36.6250	045

METRIC EQUIVALENT : 1 IN. = 25.4 MM

TG[a][b]-[#] (OR) TR[a][b]-[#]

(a) SURFACE:

- D - DOOR
- B - BULKHEAD
- S - STIFFENER
- V - SLEEVE
- E - ENVIRONMENT
- T - TRANSDUCER

(b) CHAMBER:

Figure 4.13 Gap/Rotation Transducer Locations on Outer Door

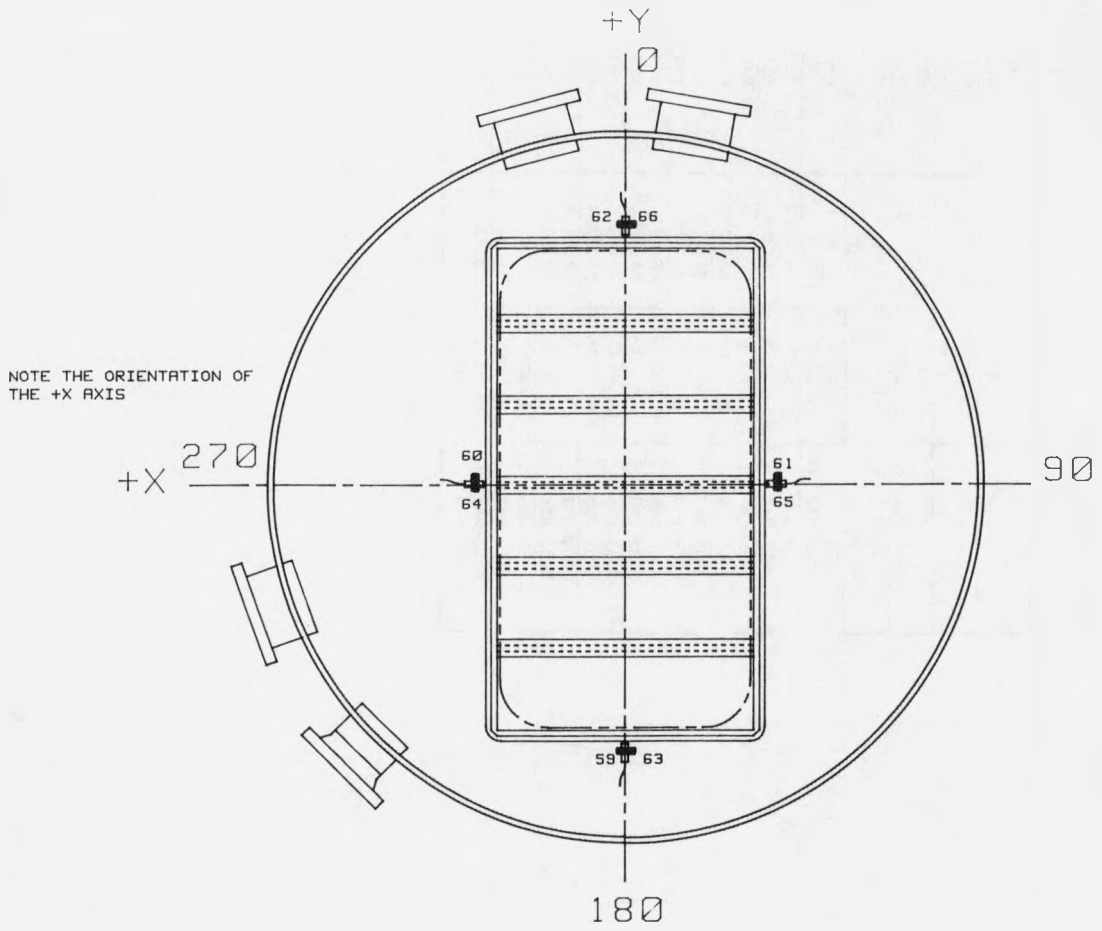

INNER DOOR			TC'S FOR TEMPERATURE COMPENSATION	
INSTRUMENTATION IDENTIFICATION	X (IN.)	Y (IN.)	INSTR. #	CHANNEL #
TSD1-059	0	-42.2500	002	281
TSD1-060	23.2500	0	008	287
TSD1-061	-23.2500	0	010	289
TSD1-062	0	42.2500	022	401

OUTER DOOR			TC'S FOR TEMPERATURE COMPENSATION
INSTRUMENTATION IDENTIFICATION	X (IN.)	Y (IN.)	INSTR. #
TSD2-063	0	-42.2500	030
TSD2-064	23.2500	0	036
TSD2-065	-23.2500	0	038
TSD2-066	0	42.2500	040

METRIC EQUIVALENT : 1 IN. = 25.4 MM

TS[a][b]-[#]

(a) SURFACE:

D - DOOR
B - BULKHEAD
S - STIFFENER
V - SLEEVE
E - ENVIRONMENT
T - TRANSDUCER

(b) CHAMBER:

Figure 4.14 Slip Transducer Locations on Inner and Outer Doors

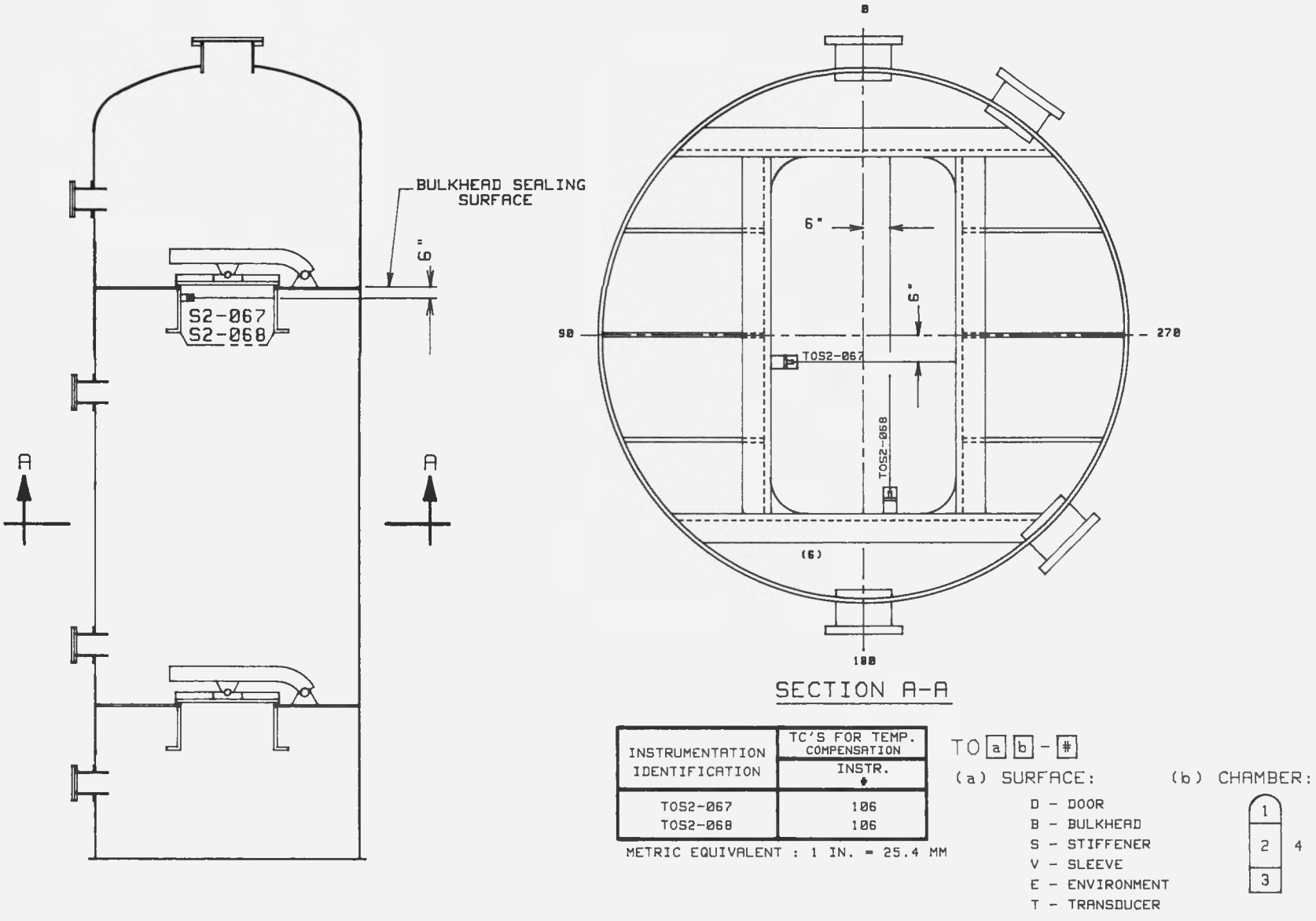

Figure 4.15 Inner Door Structural Stiffener Frame Transducers

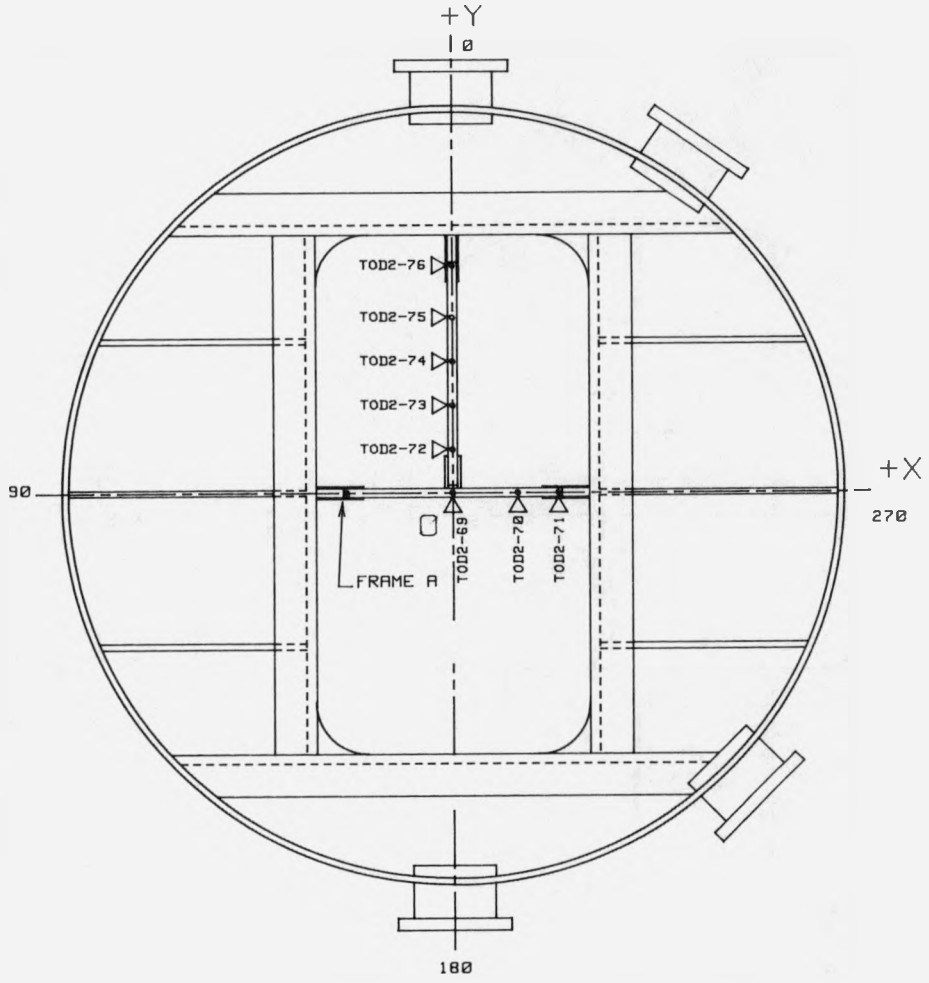

INSTRUMENTATION IDENTIFICATION	X (IN.)	Y (IN.)	TC'S FOR TEMPERATURE COMPENSATION INSTR. ♦
TOD2-069	0	0	097
TOD2-070	10.0000	0	096
TOD2-071	16.2500	0	096
TOD2-072	0	6.8125	097
TOD2-073	0	13.6250	097
TOD2-074	0	20.4375	098
TOD2-075	0	27.2500	098
TOD2-076	0	35.2500	099

METRIC EQUIVALENT : 1 IN. = 25.4 MM

TO [a] [b] - [♦]

(a) SURFACE:

- D - DOOR
- B - BULKHEAD
- S - STIFFENER
- V - SLEEVE
- E - ENVIRONMENT
- T - TRANSDUCER

(b) CHAMBER:

▷ - INDICATES A TRANSDUCER LOCATION

Figure 4.16 Out-of-Plane Transducers for Inner Door (Inside Shroud)

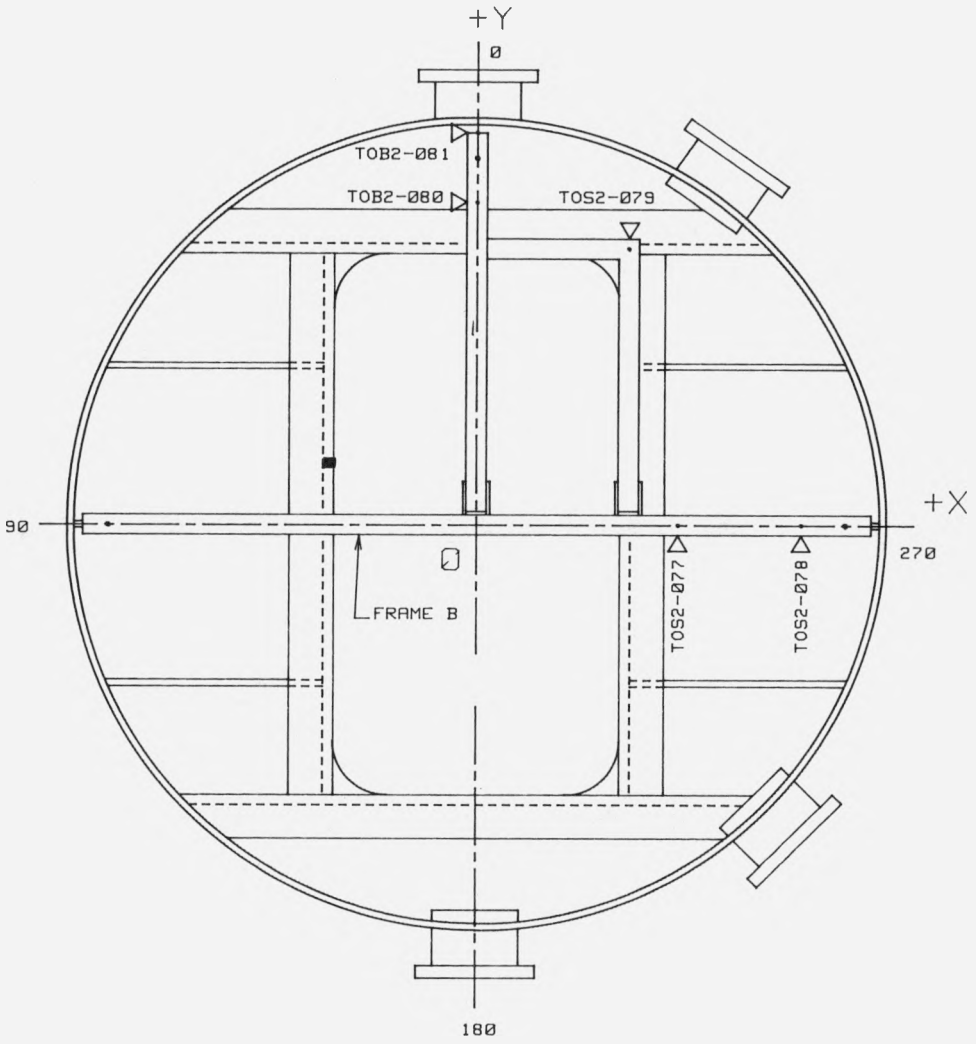

INSTRUMENTATION IDENTIFICATION	X (IN.)	Y (IN.)	TC'S FOR TEMPERATURE COMPENSATION INSTR. #
TOS2-077	29.5000	0	100
TOS2-078	49.0000	0	100
TOS2-079	21.7500	40.7500	101
TOB2-080	0	47.5000	102
TOB2-081	0	57.7500	102

METRIC EQUIVALENT : 1 IN = 25.4 MM

TO [a] [b] - [#]

(a) SURFACE:

- D - DOOR
- B - BULKHEAD
- S - STIFFENER
- V - SLEEVE
- E - ENVIRONMENT
- T - TRANSDUCER

(b) CHAMBER:

1
2 4
3

▷ - INDICATES A TRANSDUCER LOCATION

Figure 4.17 Out-of-Plane Transducers for Inner Door Bulkhead/Stiffener

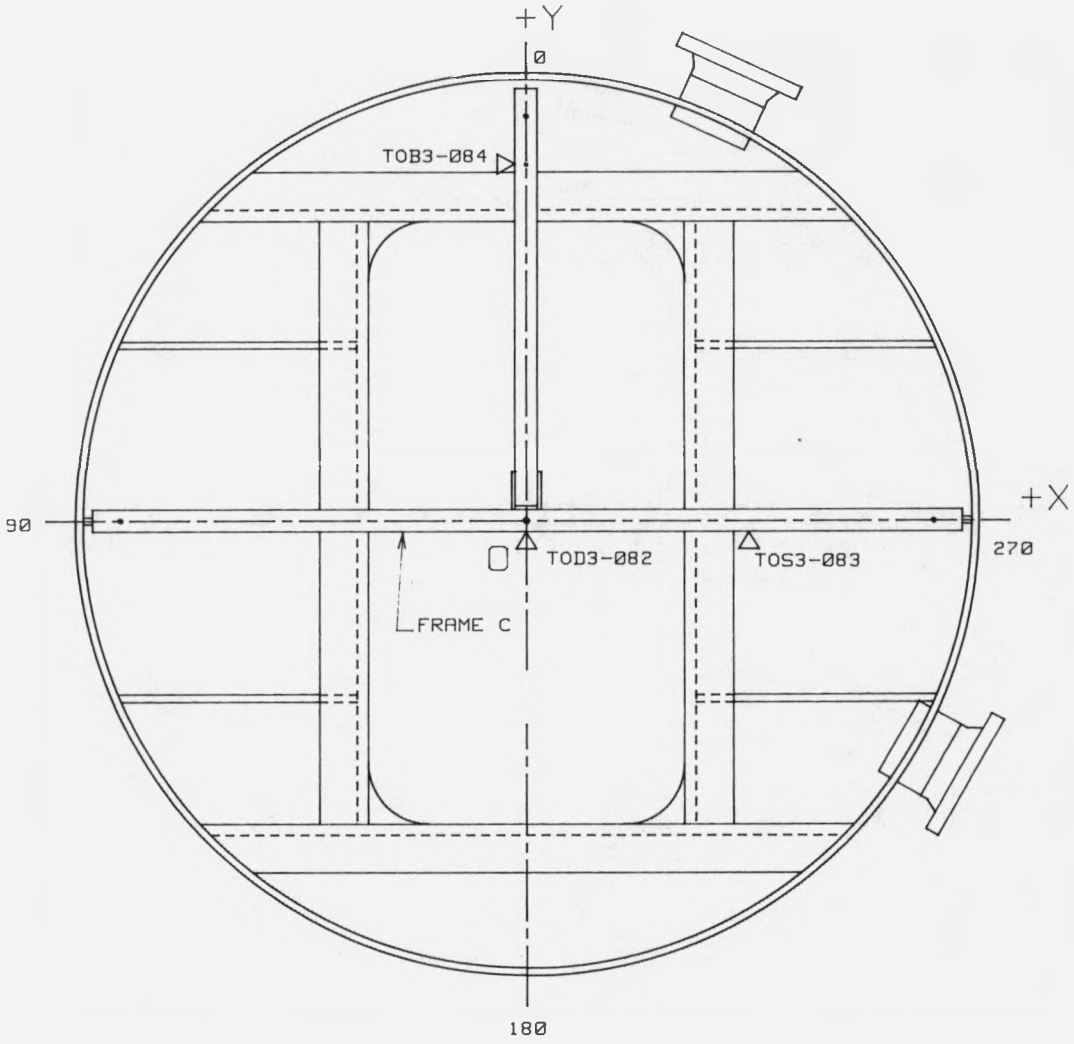

INSTRUMENTATION IDENTIFICATION	X (IN.)	Y (IN.)	TC'S FOR TEMPERATURE COMPENSATION INSTR. #
TOD3-082	Ø	Ø	103
TOS3-083	29.5000	Ø	104
TOB3-084	Ø	47.5000	105

METRIC EQUIVALENT : 1 IN = 25.4 MM

TO [a] [b] - [#]

(a) SURFACE:

D - DOOR
B - BULKHEAD
S - STIFFENER
V - SLEEVE
E - ENVIRONMENT
T - TRANSDUCER

(b) CHAMBER:

▷ - INDICATES A TRANSDUCER LOCATION

Figure 4.18 Out-of-Plane Transducers for Outer Door and Bulkhead/Stiffener

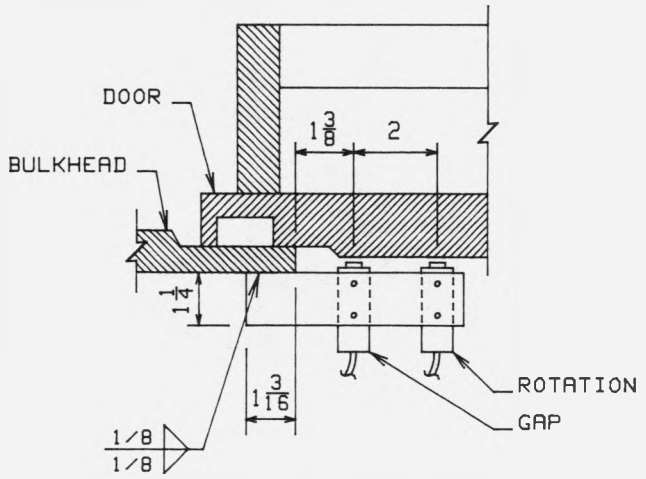

TRANSDUCER BRACKET FOR
GAP/ROTATION AT THE DOOR CORNERS

METRIC EQUIVALENT : 1 IN. = 25.4 MM

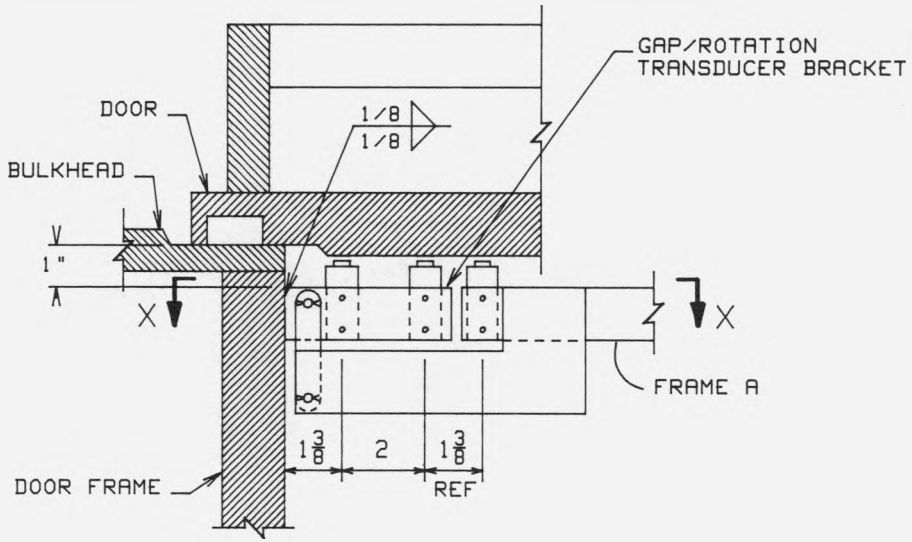

TRANSDUCER BRACKET FOR GAP/ROTATION

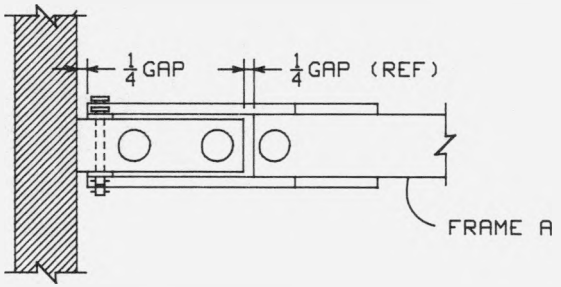

SECTION X-X

Figure 4.19 Gap/Rotation Transducer Bracket for Inner and Outer Doors and Out-of-Plane T-Frame A

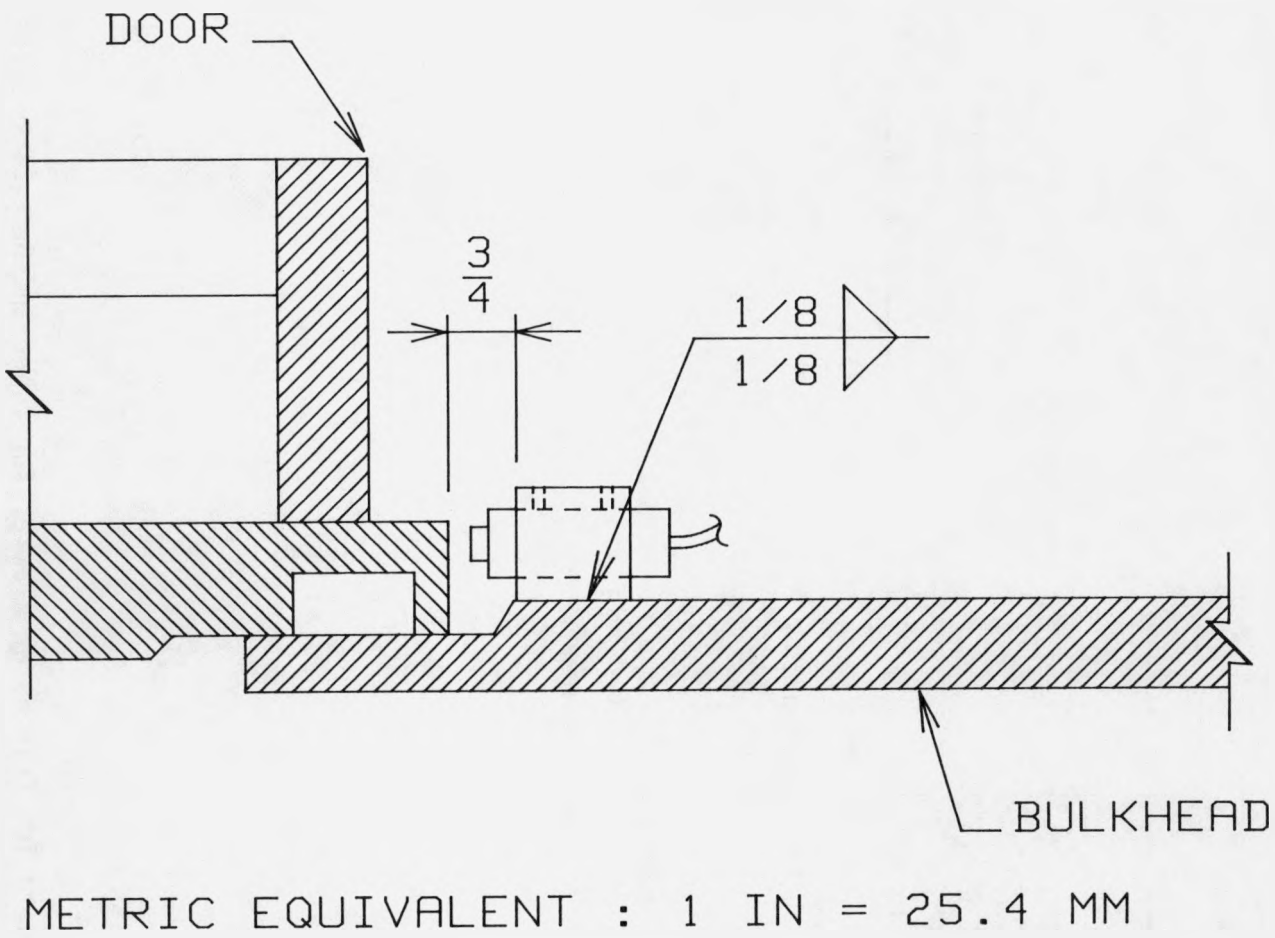

Figure 4.20 Door Slip Transducer Bracket

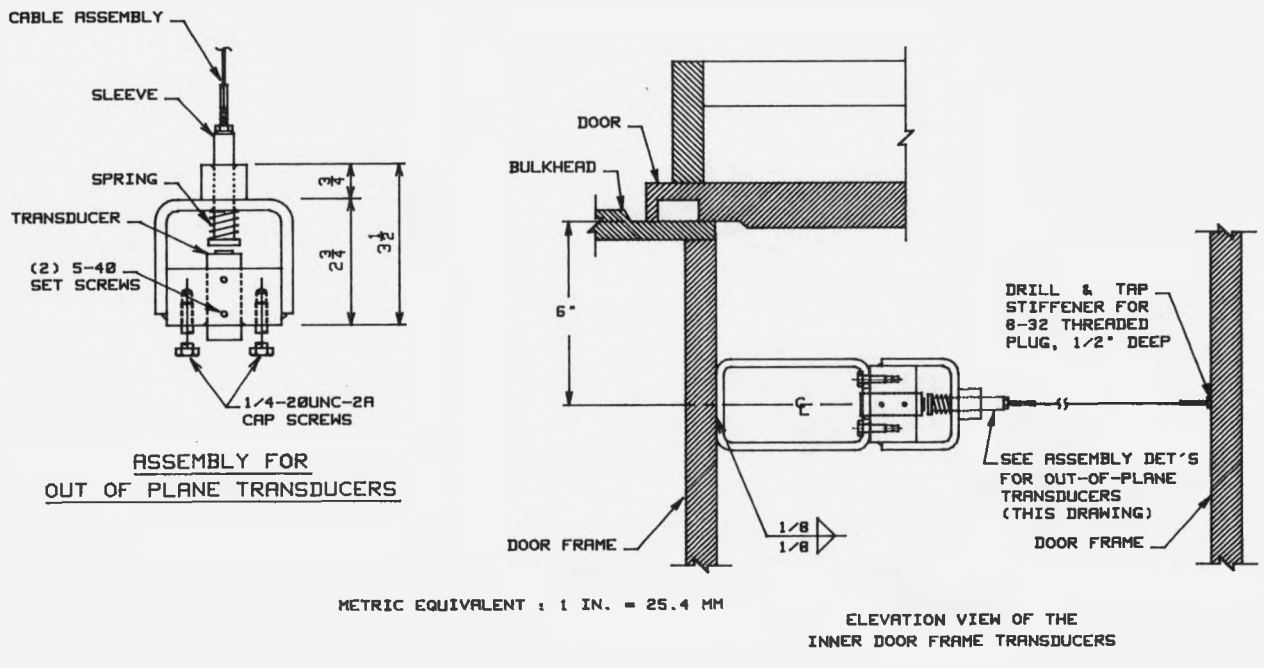

Figure 4.21 Inner Door Frame Out-of-Plane Transducer Bracket

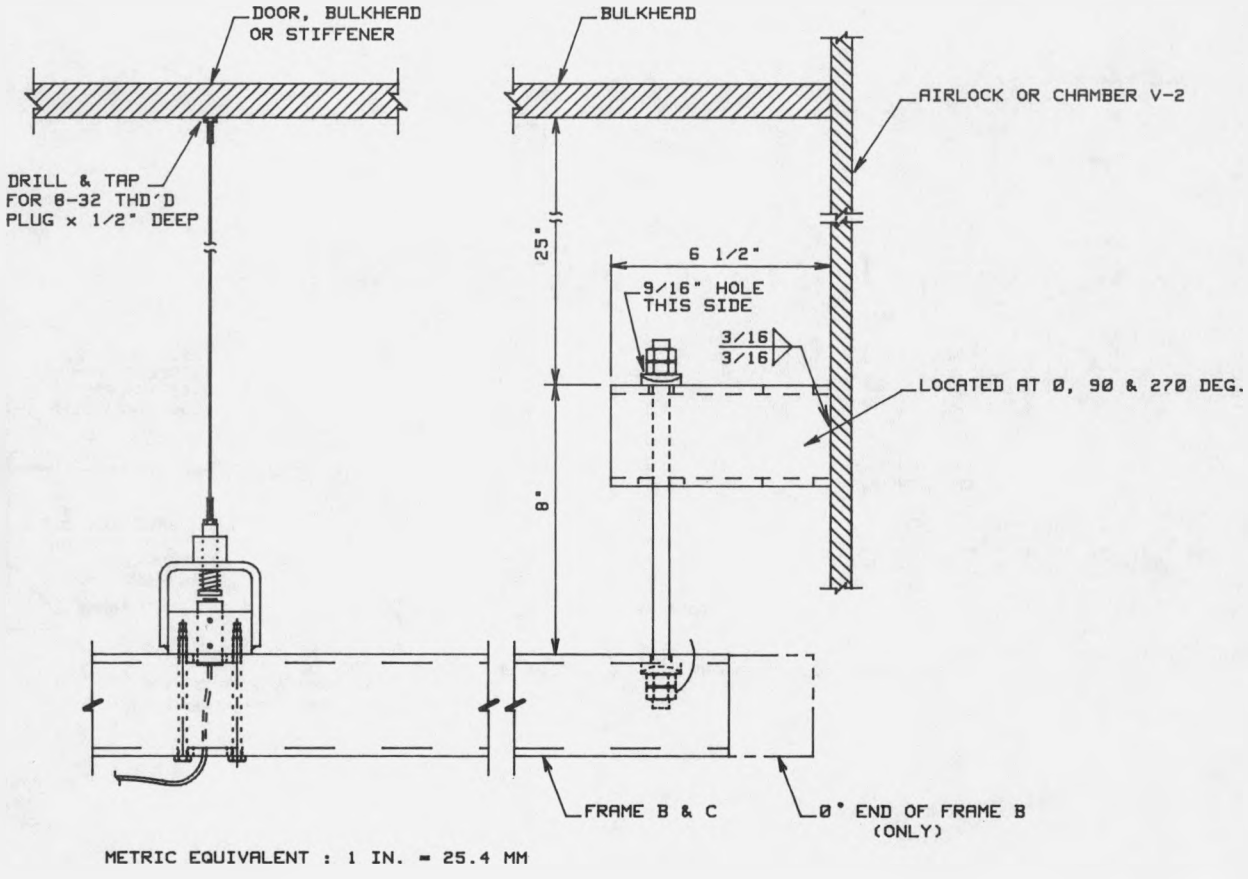

Figure 4.22 Out-of-Plane Transducer Bracket Details for T-Frames B and C

design was chosen to provide a leak tight seal. The thermocouples installed outside of the airlock assembly consisted of custom made thermocouples made of Type "K" 22 ga. thermocouple wire.

Thermocouples measuring air temperature were suspended in the air at their predetermined position. Thermocouples installed on the surface of the doors, bulkheads, or stiffeners were fixed to the surface using a metal strap spot welded to the steel surface. This tie down system was the same one used for the strain gages. Thermocouples were accurate to within ±4°F (2.2°C) of the reading over the temperature range 32 to 530°F (0 to 277°C) and ±0.75% of the reading over the temperature range 530 to 2300°F (277 to 1260°C). Thermocouple locations are shown in Figures 4.23 through 4.29.

4.1.5 Pressure Transducers

Pressure transducers used to monitor pressures in Chambers V-1, V-2, and the airlock were manaufactured by Sensotec. Pressure Transducers PT-06, PT-08, PT-09, and PT-10 were Sensotec Model Z general purpose gage pressure transducers with a pressure range of 0 to 500 psig (0 to 3.45 MPa). The accuracy of these pressure transducers was within ±1.0% of the full scale. Pressure Transducers PT-06 and PT-09 were the most accurate transducers used to measure pressures in Chamber V-1 and the airlock, respectively. Pressure Transducer PT-23 was also a Sensotec Model Z general purpose gage pressure transducer with a pressure range of 0 to 15 psig (0 to 103.4 kPa).

Since the operating temperature of these transducers was much lower than the temperatures anticipated during the high temperture test, the pressure transducers were located on the control panel in the trailer approximately 250 ft (76.2 m) from the airlock. Pressure transducers were calibrated just prior to Test 2C. General locations where pressures were measured in the system are shown in Figure 3.2.

4.1.6 Cantilever Beam Displacement Sensors

The overall diameter growth of Chamber V-1 just below the weld seam between the airlock and Chamber V-1 cylinder wall was measured using a cantilever type displacement transducer. The cantilever beam transducers were designed, fabricated, and calibrated by CBIRC. The transducers were calibrated in place. The cantilever beam was connected to the airlock by a length of INVAR wire rod. The transducers were located 4 ft (1.22 m) from the outside surface of Chamber V-1 cylinder wall. Air temperatures at a distance of 18 in. (457 mm) from the outer surface of Chamber V-1 did not exceed 124°F (51°C). INVAR is thermally stable with a very low coefficient of expansion. These transducers were not temperature compensated. The cantilever beam displacement transducers are accurate to within ±1.0% of the reading. Cantilever beam displacement transducer locations are shown in Figure 4.30.

4.2 Computers and Data Acquisition System

The overall computer and data acquisition system setup is shown schematically in Figure 4.31. The data acquisition system consisted of an HP3497A data acquisition unit with three HP3498A extender units.

The data acquisition system was located in the building with the airlock while the computers were located in the trailer approximately 250 ft (76.2 m) away. A remote extender unit was used to transmit data from the data acquisition system to Computer No. 1.

Computer No. 1 performed the following tasks:

(1) Continuously monitored a small number of selected transducers,
(2) Relayed the process signal from the Omron controller to the appropriate isolated honed flow section, and
(3) On command by operator, scanned all data channels and transmitted voltage data to Computer No. 2.

Computer No. 1 returned to the monitoring mode after Computer No. 2 received the data and acknowledged data transfer was complete. Computer No. 2 then performed the following tasks:

(1) Reduced voltage data for each transducer into engineering units,
(2) Stored voltage and engineering data on floppy disk,
(3) Stored voltage and engineering data on hard disk,
(4) Printed engineering data on paper, and
(5) Updated a plot of the output from up to eight selected transducers that was displayed on the computer screen.

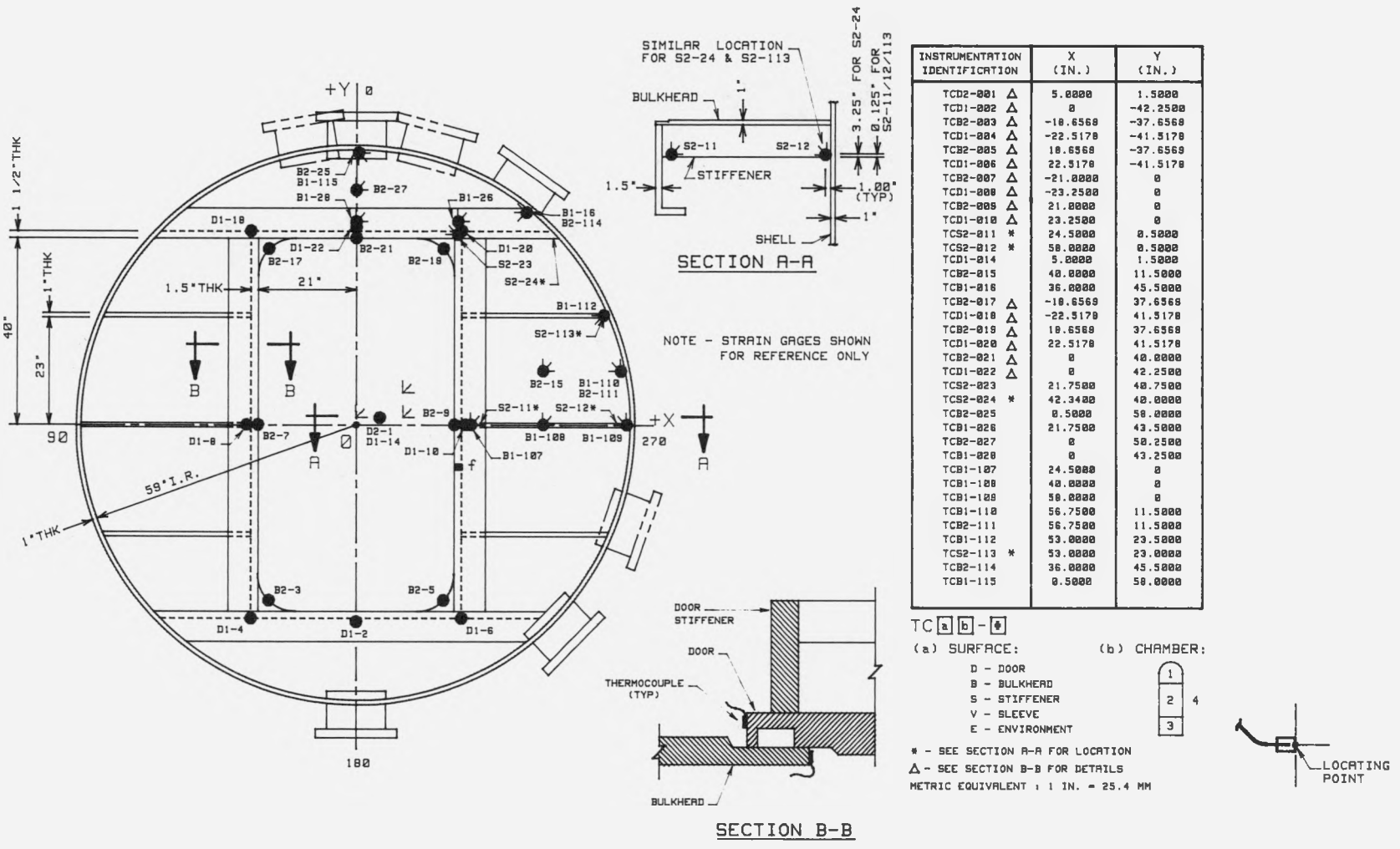

INSTRUMENTATION IDENTIFICATION		X (IN.)	Y (IN.)
TCD2-001	Δ	5.0000	1.5000
TCD1-002	Δ	0	-42.2500
TCB2-003	Δ	-18.6568	-37.6568
TCD1-004	Δ	-22.5178	-41.5178
TCB2-005	Δ	18.6568	-37.6568
TCD1-006	Δ	22.5178	-41.5178
TCB2-007	Δ	-21.0000	0
TCD1-008	Δ	-23.2500	0
TCB2-009	Δ	21.0000	0
TCD1-010	Δ	23.2500	0
TCS2-011	*	24.5000	0.5000
TCS2-012	*	58.0000	0.5000
TCD1-014		5.0000	1.5000
TCB2-015		40.0000	11.5000
TCB1-016		36.0000	45.5000
TCB2-017	Δ	-18.6568	37.6568
TCD1-018	Δ	-22.5178	41.5178
TCB2-019	Δ	18.6568	37.6568
TCD1-020	Δ	22.5178	41.5178
TCB2-021	Δ	0	40.0000
TCD1-022	Δ	0	42.2500
TCS2-023		21.7500	40.7500
TCS2-024	*	42.3400	40.0000
TCB2-025		0.5000	58.0000
TCB1-026		21.7500	43.5000
TCB2-027		0	50.2500
TCB1-028		0	43.2500
TCB1-107		24.5000	0
TCB1-108		40.0000	0
TCB1-109		58.0000	0
TCB1-110		56.7500	11.5000
TCB2-111		56.7500	11.5000
TCB1-112		53.0000	23.5000
TCS2-113	*	53.0000	23.0000
TCB2-114		36.0000	45.5000
TCB1-115		0.5000	58.0000

TC [a] [b] - [#]

(a) SURFACE:
D - DOOR
B - BULKHEAD
S - STIFFENER
V - SLEEVE
E - ENVIRONMENT

(b) CHAMBER: 1, 2, 3, 4

* - SEE SECTION A-A FOR LOCATION
Δ - SEE SECTION B-B FOR DETAILS
METRIC EQUIVALENT : 1 IN. = 25.4 MM

LOCATING POINT

Figure 4.23 Thermocouple Locations on Inner Door and Bulkhead

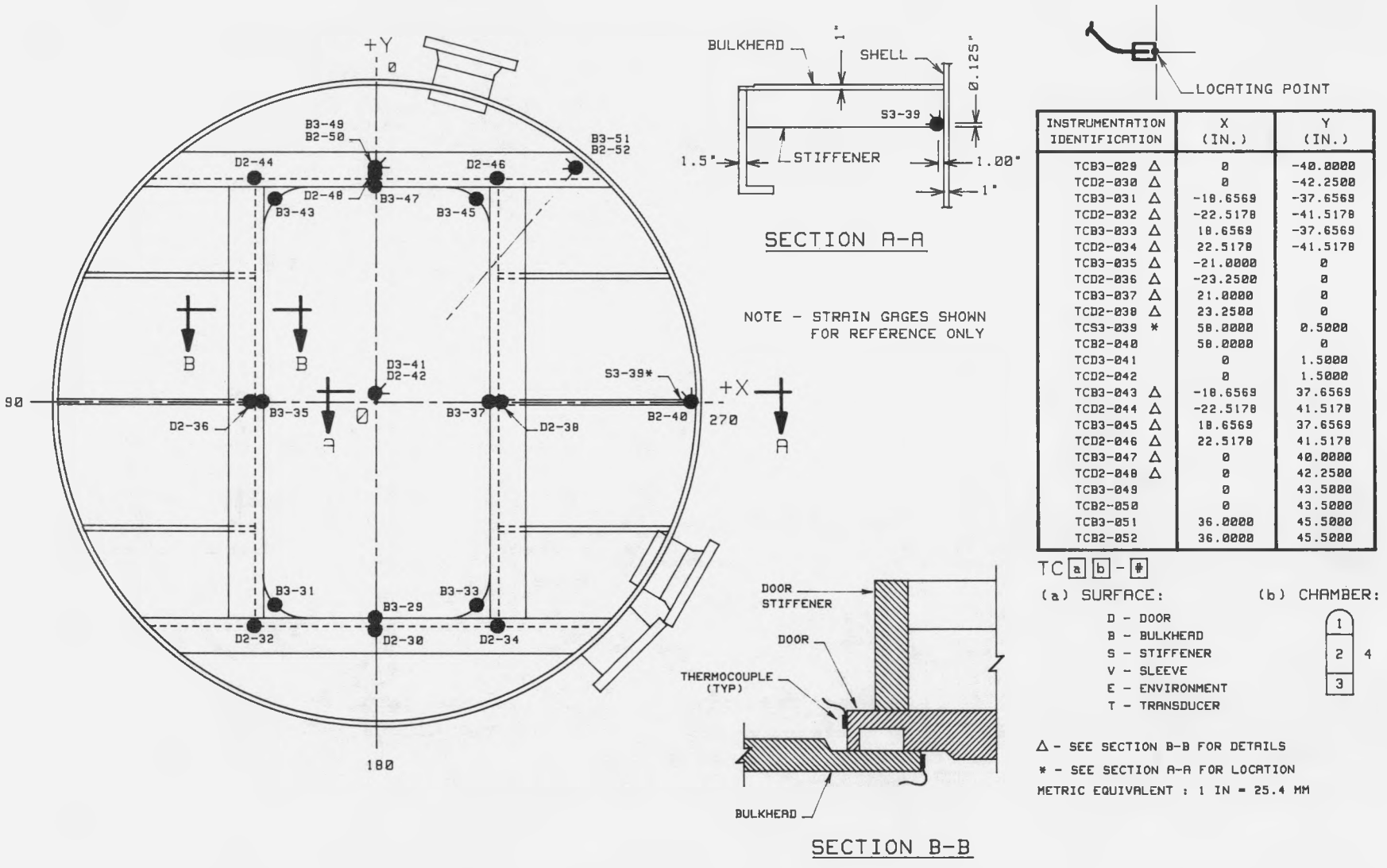

INSTRUMENTATION IDENTIFICATION	X (IN.)	Y (IN.)
TCB3-029 △	0	-40.0000
TCD2-030 △	0	-42.2500
TCB3-031 △	-18.6569	-37.6569
TCD2-032 △	-22.5178	-41.5178
TCB3-033 △	18.6569	-37.6569
TCD2-034 △	22.5178	-41.5178
TCB3-035 △	-21.0000	0
TCD2-036 △	-23.2500	0
TCB3-037 △	21.0000	0
TCD2-038 △	23.2500	0
TCS3-039 *	58.0000	0.5000
TCB2-040	58.0000	0
TCD3-041	0	1.5000
TCD2-042	0	1.5000
TCB3-043 △	-18.6569	37.6569
TCD2-044 △	-22.5178	41.5178
TCB3-045 △	18.6569	37.6569
TCD2-046 △	22.5178	41.5178
TCB3-047 △	0	40.0000
TCD2-048 △	0	42.2500
TCB3-049	0	43.5000
TCB2-050	0	43.5000
TCB3-051	36.0000	45.5000
TCB2-052	36.0000	45.5000

TC [a] [b] - [#]

(a) SURFACE:
- D - DOOR
- B - BULKHEAD
- S - STIFFENER
- V - SLEEVE
- E - ENVIRONMENT
- T - TRANSDUCER

(b) CHAMBER:
1
2 4
3

△ - SEE SECTION B-B FOR DETAILS

* - SEE SECTION A-A FOR LOCATION

METRIC EQUIVALENT : 1 IN = 25.4 MM

Figure 4.24 Thermocouple Locations on Outer Door and Bulkhead

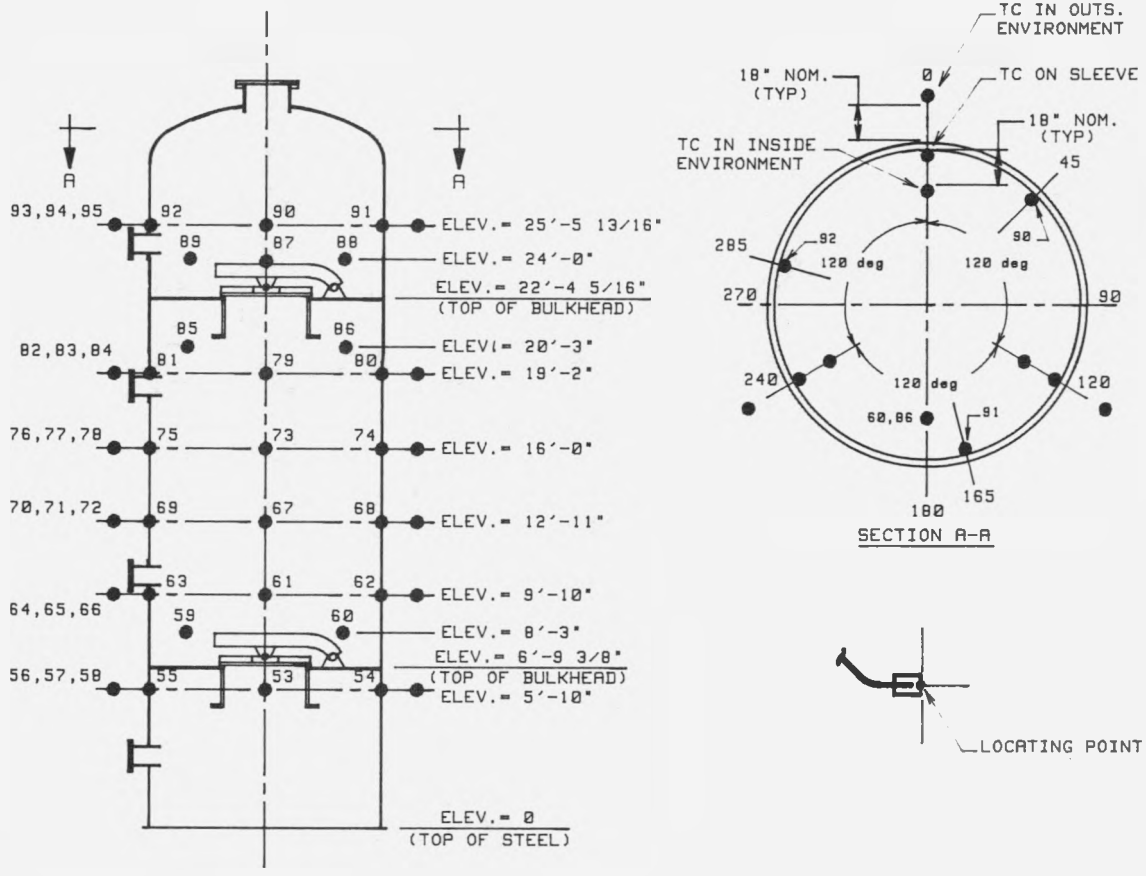

INSTRUMENTATION IDENTIFICATION	ELEVATION	AZIMUTH
TCV3-053	5'-10"	0
TCV3-054	5'-10"	120
TCV3-055	5'-10"	240
TCE4-056	5'-10"	0
TCE4-057	5'-10"	120
TCE4-058	5'-10"	240
TCE2-059	8'-3"	0
TCE2-060	8'-3"	180
TCV2-061	9'-10"	0
TCV2-062	9'-10"	120
TCV2-063	9'-10"	240
TCE4-064	9'-10"	0
TCE4-065	9'-10"	120
TCE4-066	9'-10"	240
TCV2-067	12'-11"	0
TCV2-068	12'-11"	120
TCV2-069	12'-11"	240
TCE4-070	12'-11"	0
TCE4-071	12'-11"	120
TCE4-072	12'-11"	240
TCV2-073	16'-0"	0
TCV2-074	16'-0"	120
TCV2-075	16'-0"	240
TCE4-076	16'-0"	0
TCE4-077	16'-0"	120
TCE4-078	16'-0"	240
TCV2-079	19'-2"	0
TCV2-080	19'-2"	120
TCV2-081	19'-2"	240
TCE4-082	19'-2"	0
TCE4-083	19'-2"	120
TCE4-084	19'-2"	240
TCE2-085	20'-3"	0
TCE2-086	20'-3"	180
TCE1-087	24'-0"	0
TCE1-088	24'-0"	120
TCE1-089	24'-0"	240
TCV1-090	25'-5 13/16"	45
TCV1-091	25'-5 13/16"	165
TCV1-092	25'-5 13/16"	285
TCE4-093	25'-5 13/16"	0
TCE4-094	25'-5 13/16"	120
TCE4-095	25'-5 13/16"	240

TC [a] [b] - [#]

(a) SURFACE:

D - DOOR
B - BULKHEAD
S - STIFFENER
V - SLEEVE
E - ENVIRONMENT
T - TRANSDUCER

(b) CHAMBER:

METRIC EQUIVALENT : 1 IN. = 25.4 MM
1 FT. = 0.305 M

Figure 4.25 Locations of Environmental Thermocouples and Cylinder Wall Surface Thermocouples

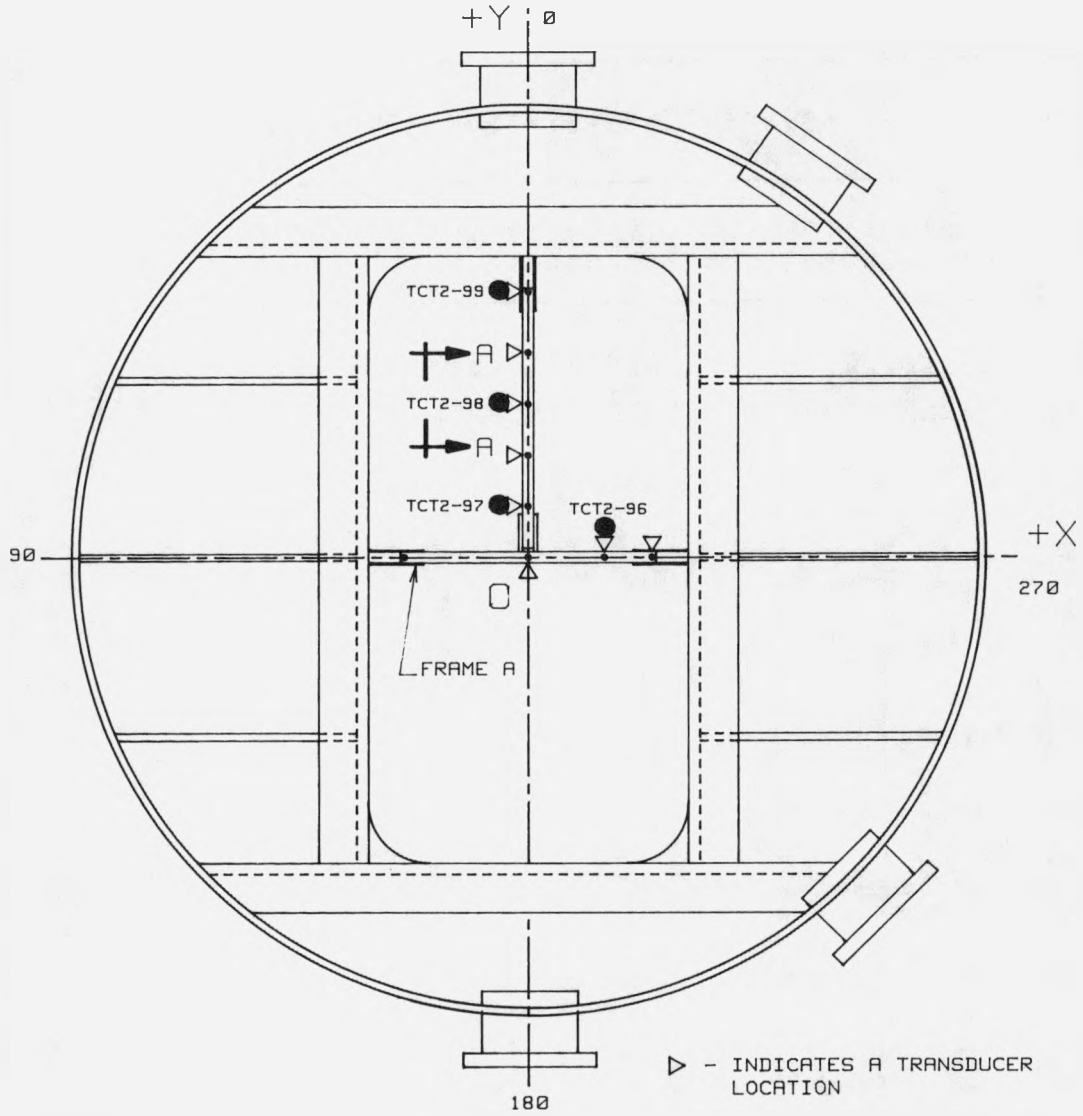

INSTRUMENTATION IDENTIFICATION	TRANSDUCER MOUNTED NEAR
TCT2-096	TOD2-070
TCT2-097	TOD2-072
TCT2-098	TOD2-074
TCT2-099	TOD2-076

METRIC EQUIVALENT : 1 IN = 25.4 MM

TC [a] [b] - [#]

(a) SURFACE: (b) CHAMBER:

D - DOOR
B - BULKHEAD
S - STIFFENER
V - SLEEVE
E - ENVIRONMENT
T - TRANSDUCER

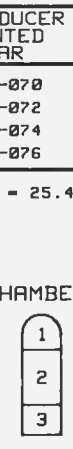

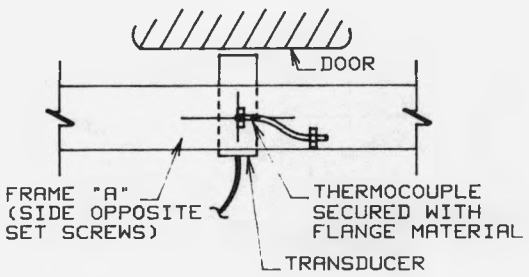

VIEW A-A

Figure 4.26 Thermocouple Locations on Capacitance Transducer Frame A

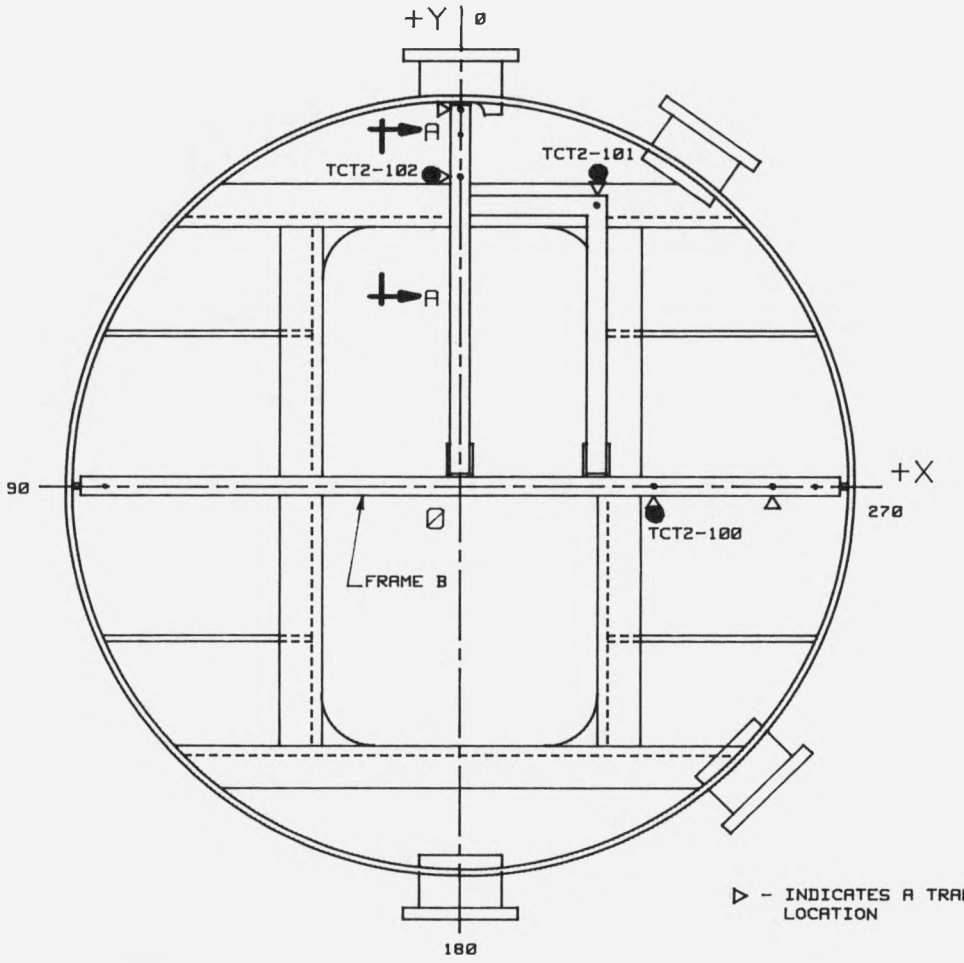

INSTRUMENTATION IDENTIFICATION	TRANSDUCER MOUNTED ON
TCT2-100	TOS2-77
TCT2-101	TOS2-79
TCT2-102	TOB2-80

TC [a] [b] - [#]

(a) SURFACE:

D - DOOR
B - BULKHEAD
S - STIFFENER
V - SLEEVE
E - ENVIRONMENT
T - TRANSDUCER

(b) CHAMBER:

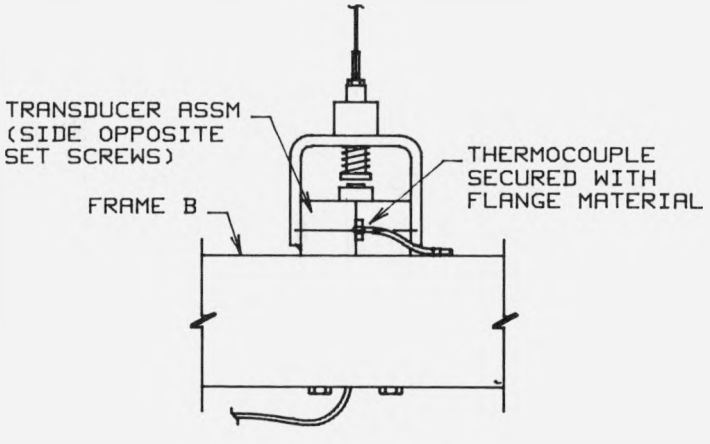

VIEW A-A

Figure 4.27 Thermocouple Locations on Capacitance Transducer Frame B

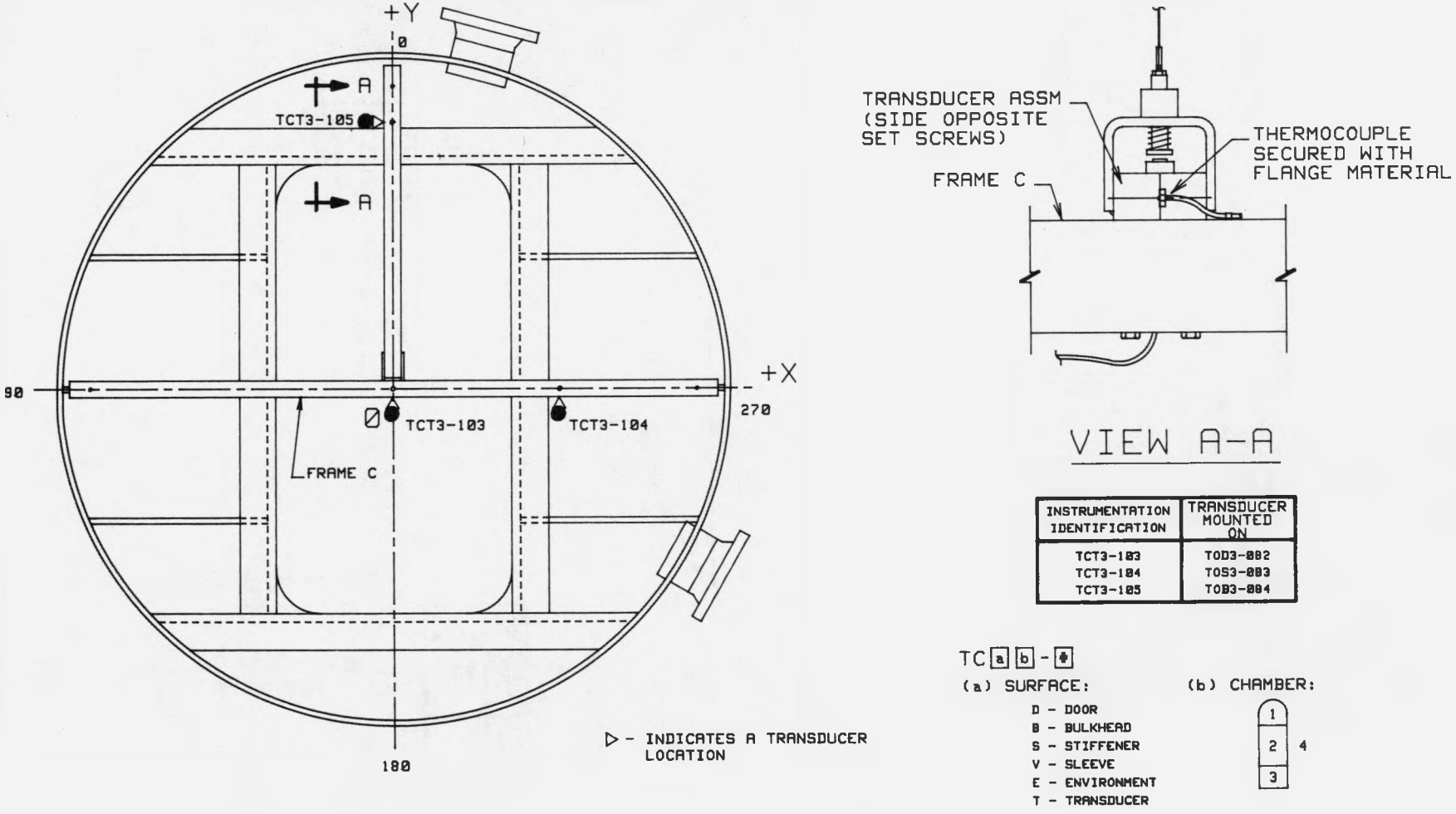

Figure 4.28 Thermocouple Locations on Capacitance Transducer Frame C

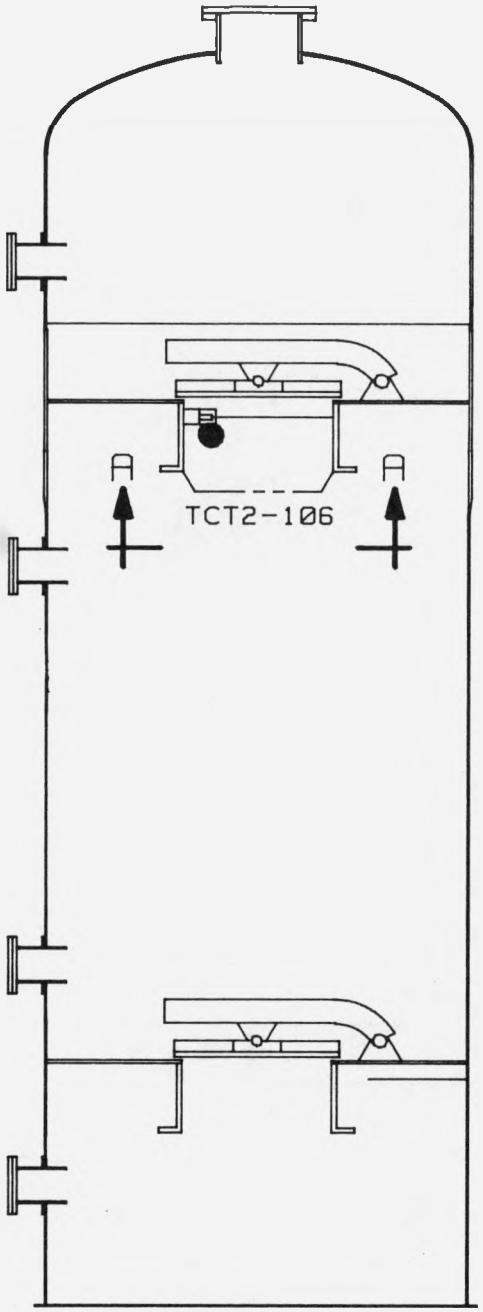

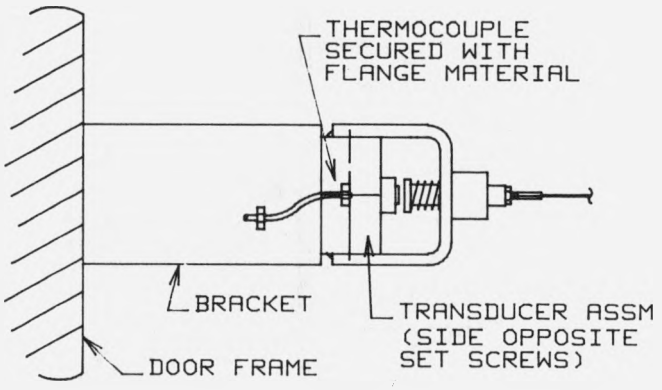

VIEW A-A

INSTRUMENTATION IDENTIFICATION	TRANSDUCER MOUNTED ON
TCT2-106	TDS2-067

TC [a] [b] - [#]

(a) SURFACE:

- D - DOOR
- B - BULKHEAD
- S - STIFFENER
- V - SLEEVE
- E - ENVIRONMENT
- T - TRANSDUCER

(b) CHAMBER:

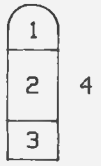

Figure 4.29 Thermocouple Location on Inner Door Frame Capacitance Transducer

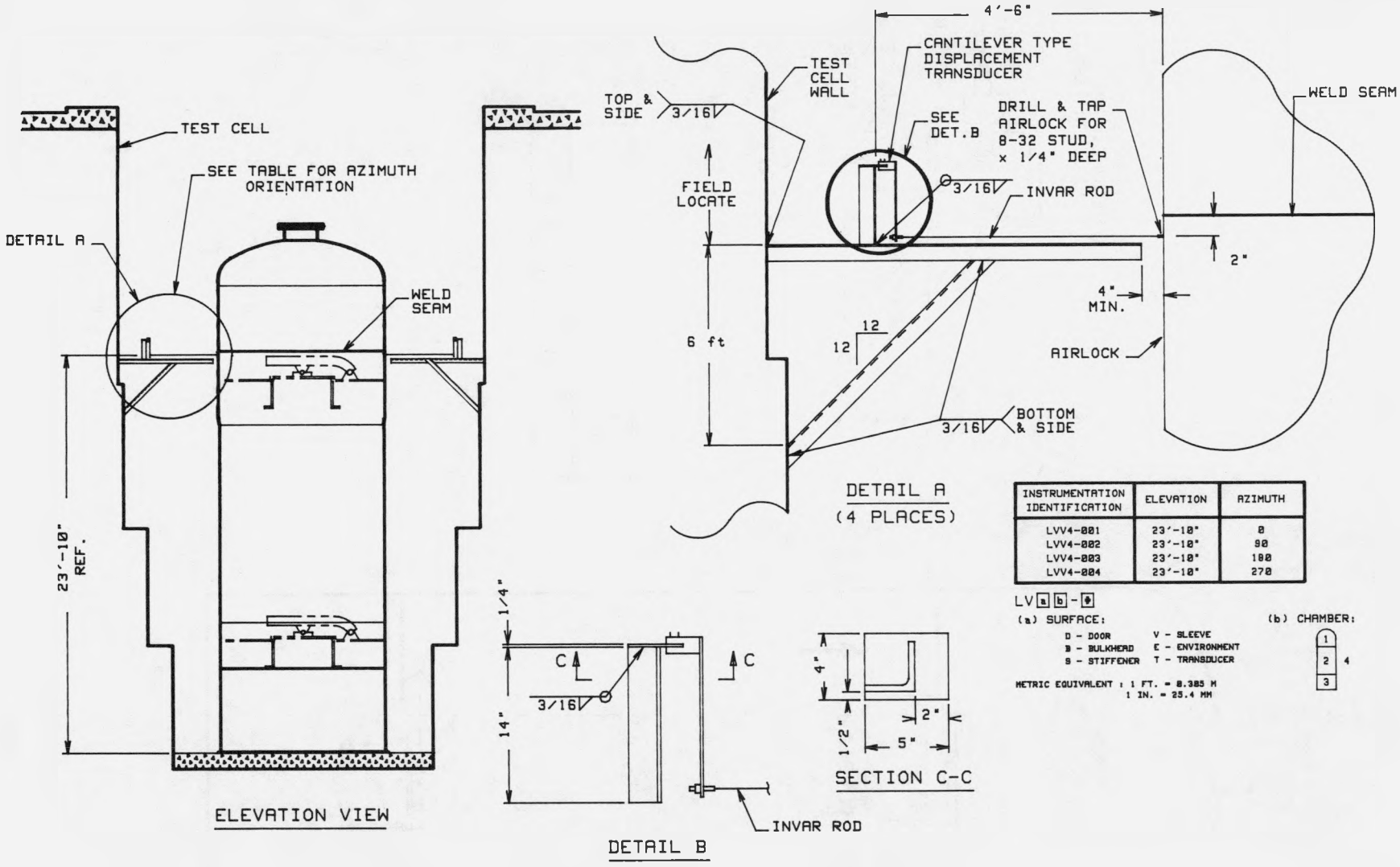

INSTRUMENTATION IDENTIFICATION	ELEVATION	AZIMUTH
LVV4-001	23'-10"	0
LVV4-002	23'-10"	90
LVV4-003	23'-10"	180
LVV4-004	23'-10"	270

LV [a] [b] - [4]

(a) SURFACE:
D - DOOR
B - BULKHEAD
S - STIFFENER
V - SLEEVE
E - ENVIRONMENT
T - TRANSDUCER

(b) CHAMBER: 1, 2, 3

METRIC EQUIVALENT : 1 FT. = 0.305 M
1 IN. = 25.4 MM

Figure 4.30 Cantilever Beam Displacement Transducer Locations

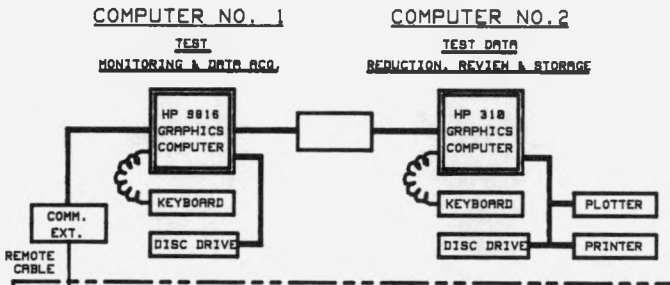

	# CHANNELS	GENERAL DESCRIPTION	# AND TYPE OF CARD USED	SLOTS USED	CHANNELS USED
COMM. EXT.					TEST BUILDING
DC POWER HP 3497A #1 DATA ACQUISITION UNIT	100 CHANNELS	(CAP)	5 OPTION 020	SLOTS 0 - 4	CHANNELS 0-93
[1] CAPACITEC 3210-A0 CONDITIONING	10 CHANNELS	(CAP)	8 CAPACITEC OPTION 3200-S	-	CHANNELS 0-17
[2] CAPACITEC 3210-A0 CONDITIONING	10 CHANNELS	(CAP)	8 CAPACITEC OPTION 3200-S	-	CHANNELS 10-35
[3] CAPACITEC 3210-A0 CONDITIONING	10 CHANNELS	(CAP)	8 CAPACITEC OPTION 3200-S	-	CHANNELS 36-53
[4] CAPACITEC 3210-A0 CONDITIONING	10 CHANNELS	(CAP)	8 CAPACITEC OPTION 3200-S	-	CHANNELS 54-71
[5] CAPACITEC 3210-A0 CONDITIONING	12 CHANNELS	(CAP)	6 CAPACITEC OPTION 3200-S	-	CHANNELS 72-83
DC POWER HP 3498A #2 EXTENDER	60 CHANNELS 60 CHANNELS 20 CHANNELS	(FULL BRIDGE) (VS) (TC)	6 OPTION 070 3 OPTION 020 1 OPTION 020	SLOTS 0 - 5 SLOTS 6,7 & 8 SLOT 9	CHANNELS 100-109, 120-129, 140-149, 160-169, 180-189, 200-209 CHANNELS 220-279 CHANNELS 280-299
DC POWER HP 3498A #3 EXTENDER	60 CHANNELS 60 CHANNELS 20 CHANNELS	(FULL BRIDGE) (VS) (TC)	6 OPTION 070 3 OPTION 020 1 OPTION 020	SLOTS 0 - 5 SLOTS 6,7 & 8 SLOT 9	CHANNELS 300-309, 320-329, 340-349, 360-369, 380-389, 400-409 CHANNELS 420-479 CHANNELS 480-499
DC POWER HP 3498A #4 EXTENDER	10 CHANNELS 20 CHANNELS 80 CHANNELS 10 CHANNELS 20 CHANNELS	(FULL BRIDGE) (VS) (TC) (FULL BRIDGE) (VS)	1 OPTION 070 1 OPTION 020 4 OPTION 020 1 OPTION 070 1 OPTION 020	SLOT 0 SLOT 1 SLOTS 2,3,4 & 5 SLOT 6 SLOT 7	CHANNELS 500-502 CHANNELS 520-522 CHANNELS 540-619 CHANNELS 620-629 (620-623 FOR CBDT'S & 624-629 FOR PRES.TRANS) CHANNELS 640-641 (FOR FLOWMETERS)

Figure 4.31 Computer and Data Acquisition System

5.0 ACCELERATED AGING OF DOOR GASKET SEALS

The gaskets used in the airlock door seals were subjected to an accelerated aging process to simulate both in-service radiation and thermal aging over a 40-year service life and a loss-of-coolant-accident (LOCA). Radiation aging was not practical due to the size of the door. Accelerated aging of both the inner and outer door gaskets was achieved by heating the gasket while in the door with the door closed and latched. Heating elements were installed under the doors between the main structural stiffeners. The bulkheads, doors, and cylinder walls were insulated to contain the heat around the gasket seal and force the heat distribution to be more uniform around the gasket. The gasket aging heating system is shown in Figure 5.1. Heating control was accomplished using the same heating control system as described in Section 3.0 of this report.

Thermocouples, made up at CBIRC from Type "K" thermocouple wire, were installed in eight locations on both the inner and outer doors as shown in Figure 5.2. Thermocouples were attached to the structure using spot welded metal straps, shown in Figure 5.3. The thermocouples were then covered with a layer of Kaowool insulation to protect the thermocouple from radiant heat exposure and to more realistically measure the structural steel surface temperatures.

The thermocouples were scanned and resultant temperatures recorded every fifteen minutes for the duration of the aging process with an HP71 computer and an HP3421A digital data acquisition system. Each door had a separate system to record temperatures and a hard copy of data was printed out and stored on floppy disk immediately after each scan.

The original goal of the accelerated aging process was to heat the gasket seal for 168 hours (7 days) at a temperature of 370°F (188°C). D. Clauss of SNL defined the temperature and time period over which the gasket should be exposed to achieve the desired aging. In his derivation, Clauss states:

> "Based on data obtained from Presray,[13] the compression set retention in EPDM E603 is affected more strongly by radiation aging than thermal aging. The compression set retention in E603 o-ring gaskets after exposure to 200 Mrad is 95%; for 100 Mrad it reduced only slightly to 92.5%. It was assumed that compression set retention from radiation aging and from thermal aging could not be superposed. Thus, accelerated thermal aging corresponding to approximately 95% compression set retention was desired to simulate the effect of radiation and thermal aging for a 40 year service life and a LOCA. The time and temperature were related by using the Arrhenius model with the constants determined by extrapolating available data. The equation is:
>
> $$t = Be^{\theta/kT} \quad 5\text{-}1$$
>
> where t is time in hours, B is a constant corresponding to 95% compression set retention (1.56×10^{-9}), θ is the apparent activation energy (1.01 eV), k is Boltzmann's constant (8.63×10^{-5} eV/°K) and T is the temperature in °K. In order to minimize the time required for aging, t was arbitrarily chosen to be 168 hours; then, equation 5.1 is satisfied with T equal to 370°F."

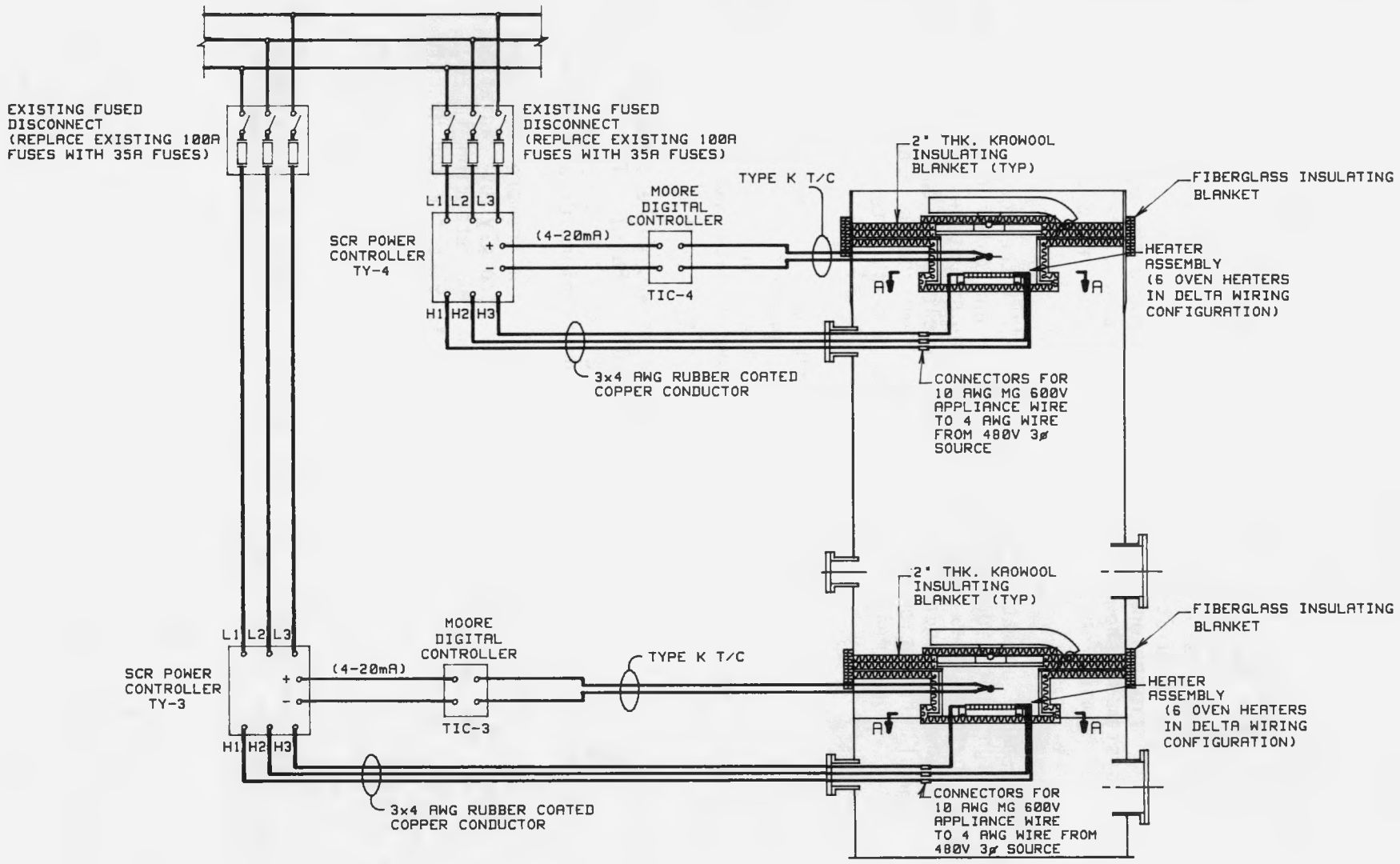

Figure 5.1 Seal Aging Heater Hardware and Control Assembly

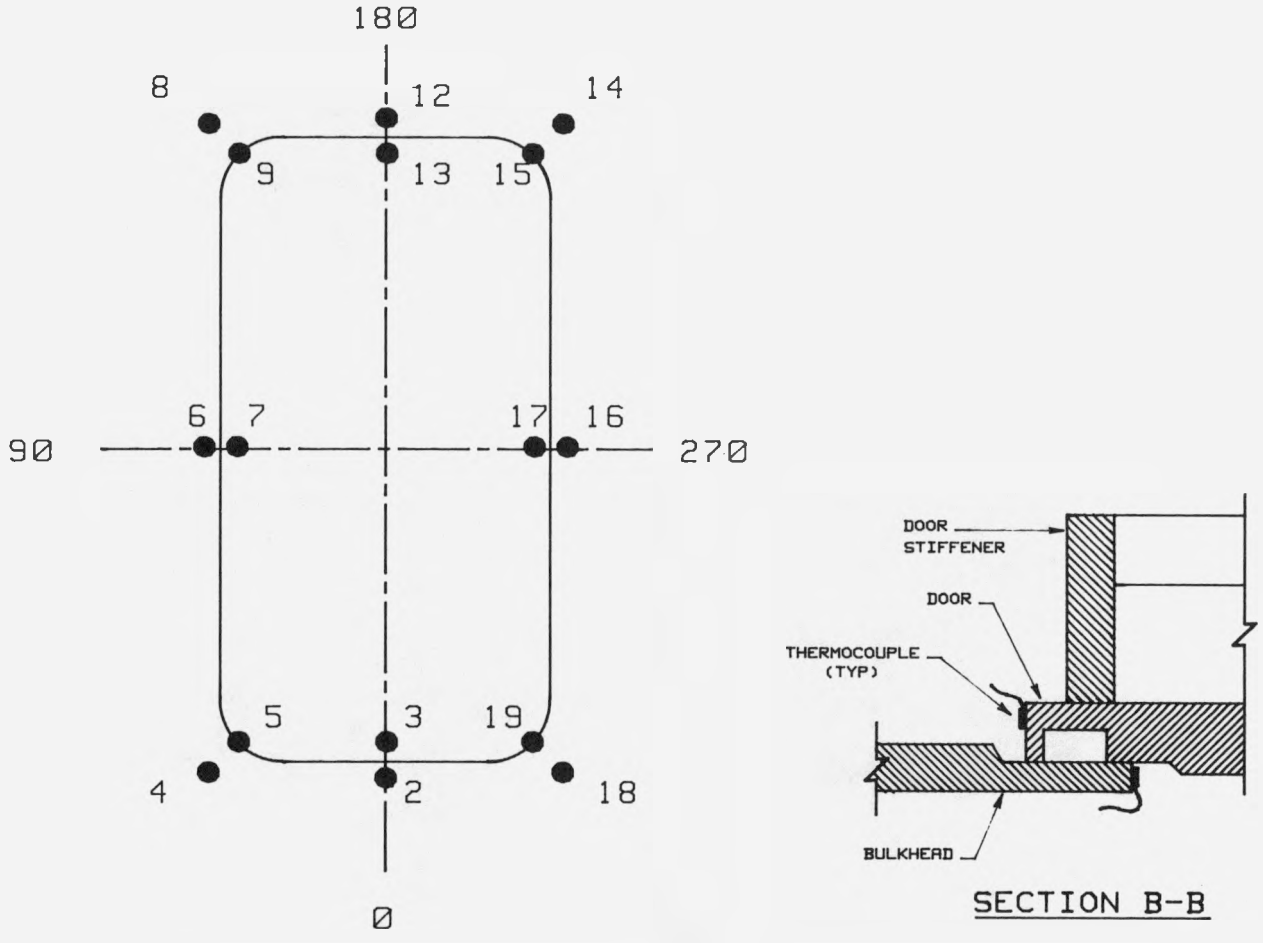

Figure 5.2 Thermocouple Locations for Gasket Seal Aging

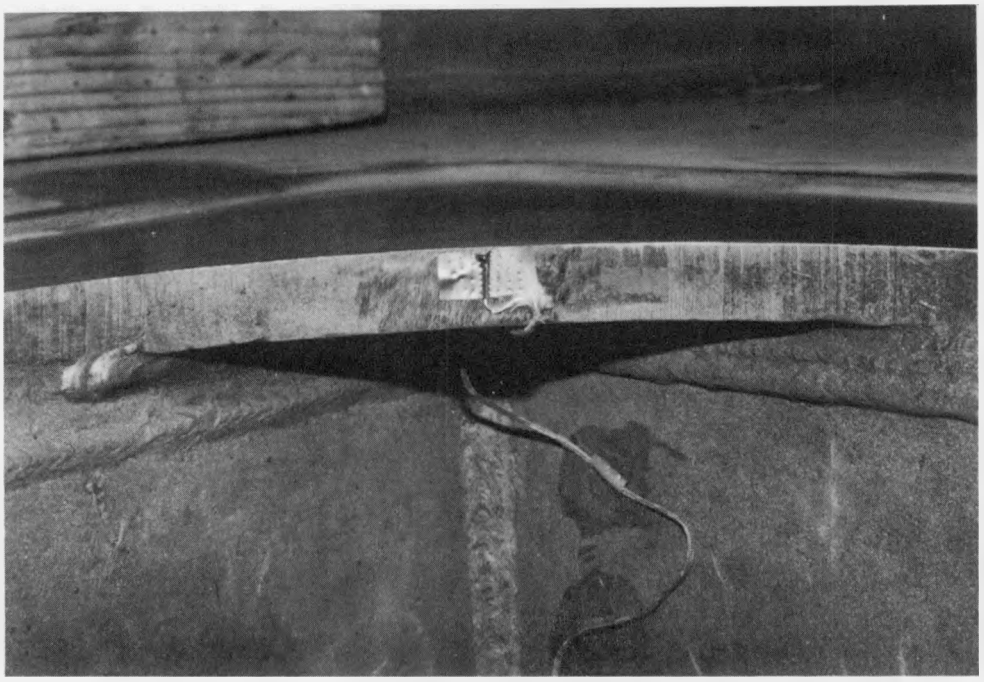

A. Thermocouple Installation

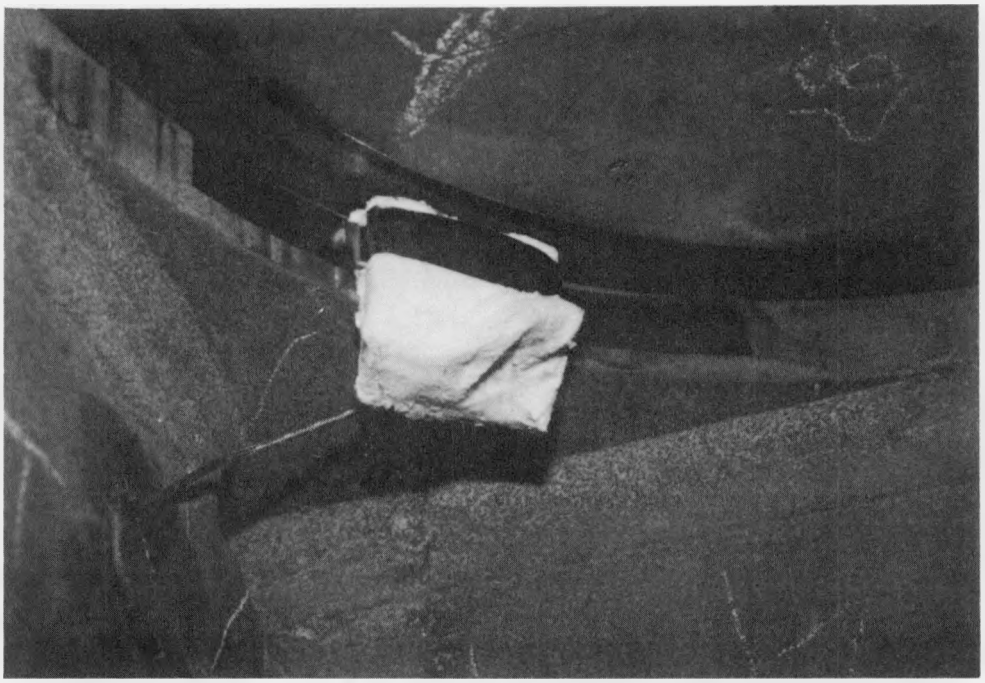

B. Thermocouple Covered with Kaowool Insulation

Figure 5.3 Thermocouple Installation for Seal Aging

Real time events required gradual heating of the surrounding bulkhead and door up to the target temperature and adjusting heating control and insulation to get the proper heating distribution. After the heaters were turned off, insulation was removed and the bulkheads were allowed to cool to ambient.

Aging is normally done under a fixed deformation condition. The dead weight of the door was on the gasket as well as the force imparted on the door by the latching mechanism, with no constraint on deformation. This is a more realistic boundary condition for the gasket seal as the doors in the airlock are normally latched closed.

The actual heating period, average temperature, maximum and minimum variations from average, and ramp time for temperature increase are listed in Table 5.1.

Table 5.1

Gasket Seal Aging Summary

Door Location	Avg Temp. (°F)	Maximum	Temp. Variation (°F) Minimum	Ramp	Heating Duration (Hr) @ Temp.
Inner	369	+14	-21	12	172
Outer	365	+17	-32	16	172

Metric Equivalent: °C = 5/9 *(°F - 32)

The temperature versus time relationship for the inner and outer door heating is shown in Figure 5.4. The duration of heating was 172 hours rather than 168 hours. The average temperature was initially approximately 350°F (177°C) for almost 30 hours for each door. The additional 4 hours were included to offset the effect of the lower initial temperatures.

As a result of the accelerated aging process, the seals were deformed to the point that the interspace gap and the double dog ear cross-section were no longer recognizable. At several locations around the door perimeter the aged gasket flowed into the space between the door and the bulkhead. This material between the door and the bulkhead prevented full compression of the gasket and metal-to-metal contact between the door and bulkhead. Condition of the gasket before and after accelerated aging is shown in Figure 5.5.

There was concern about the sealing capability of the aged gaskets. CBIRC and SNL considered replacing the aged gasket seals with the spare set of new gaskets. However, it was agreed that damage to the gaskets as a result of thermal aging should be expected, regardless of the circumstances. Therefore, two additional tests were added to the test plan, known as Tests 1AA and 1BB. The objective of these tests was to observe the sealing capability of each of the aged gaskets at ambient temperatures. The gasket seals were installed in the door, and the appropriate chamber was pressurized to 69 psig (475 kPa). Leak rates for each door were measured. Since no leakage for either door was observed, the thermally aged gaskets were used for the remaining tests.

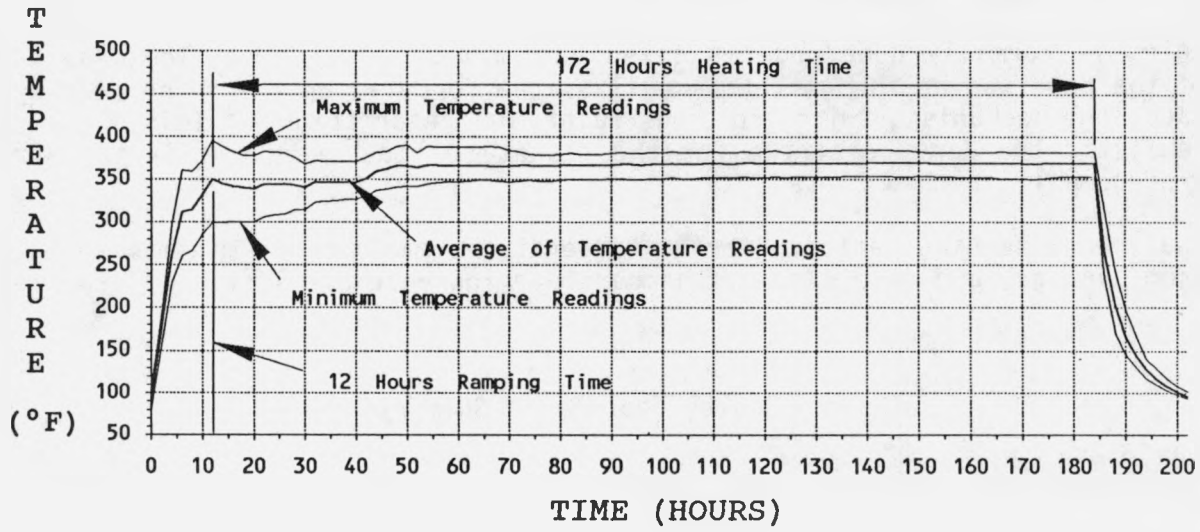

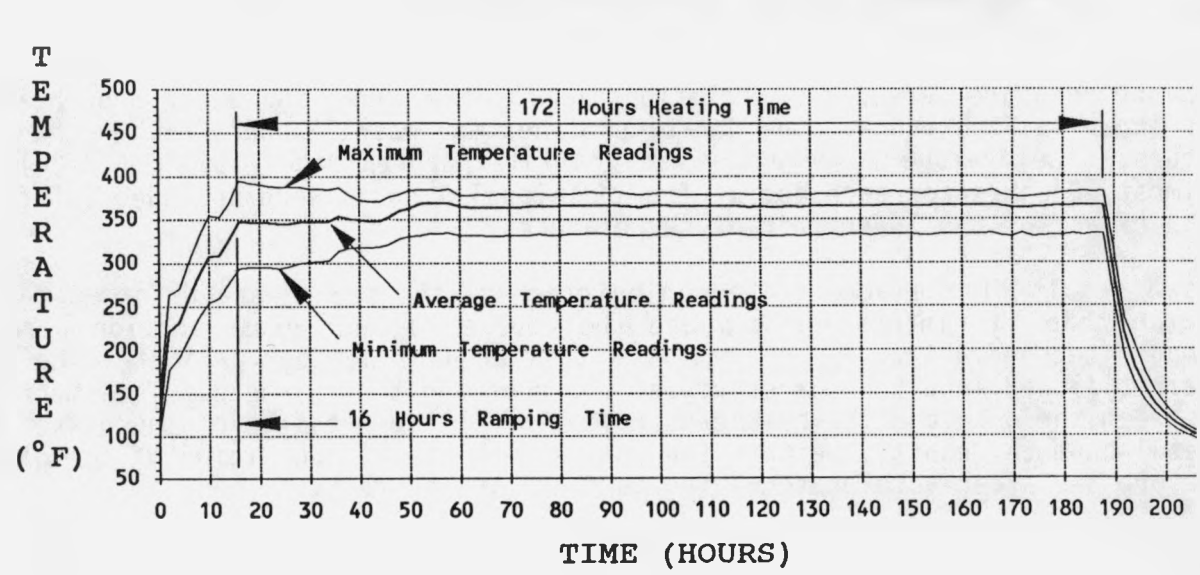

Figure 5.4 Average Temperature versus Time for Accelerated Aging of Gasket Seals

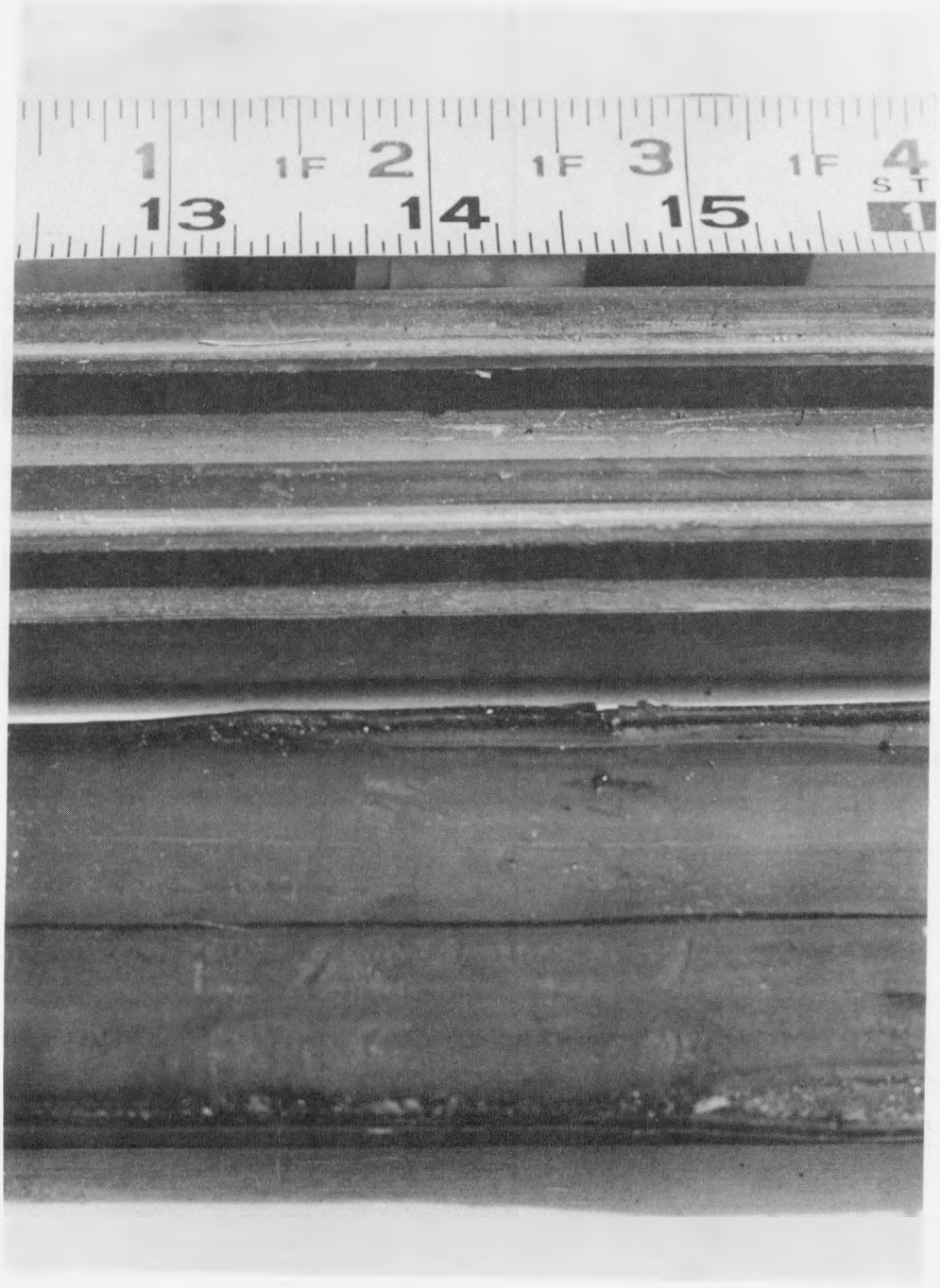

Figure 5.5 Gasket Seal Before and After Accelerated Aging

6.0 COMPRESSION SET RETENTION MEASUREMENTS

Compression set retention is the physical dimensional measurement of the permanent deflection retained by the flexible gasket seal as a result of long term sustained loads. In particular, the gasket seals were under sustained thermal and physical loadings during accelerated aging and during the high temperature and pressure test. Compression set retention measurements establish time dependent permanently retained deformations. The measurements that were made for compression set retention were loosely based on ASTM Designation: D395-78. Fixed deformations or constant loads were not applied, nor were the time limitations set in the procedure followed.

Prior to making compression set retention measurements, the doors were closed without the gaskets in place. With the doors in metal-to-metal contact with the bulkhead, the doors were shimmed for proper alignment. High spots in the machined surfaces were identified and ground down. The doors were then closed and the gaps between the metal-to-metal contact were measured using feeler gages. Results of these measurements are shown in Figures 6.1 and 6.2. The gaps at several locations between the door and bulkhead were greater than 0.005 in (0.13 mm), which were greater than design allowables. CBI Services staff, with field experience in maintaining personnel airlocks, confirmed that this nonconformity was also observed in actual installations and that the nonconformance was often accepted since it did not preclude a good seal. However, Tests 1AA and 1BB established that the gaskets formed an adequate seal.

Compression set retention measurements were taken for both the inner and outer doors at ambient temperatures. As a baseline measurement, the door was latched shut for a minimum of 12 hours. In the latched position, the gap between the machined surfaces of the door and bulkhead were measured using feeler gages, as shown in Figure 6.3.

Next, the door was unlatched and allowed to remain in the unlatched position for a minimum of 1 hour with the dead weight of the door on the seal. Gaps between the door and bulkhead were again measured for each door.

After accelerated aging of the gasket seals was completed and the temperatures had returned to ambient, the door was unlatched and allowed to remain in the closed position with the dead weight of the door on the gasket for a minimum of one hour. Gaps between the door and bulkhead were again measured for each door.

Following Test 3B and after approximately 8 months had elapsed (due to a contract delay following Test 3B), the final compression set retention measurements were taken. The door was unlatched and allowed to remain in the closed position with the dead weight of the door on the gasket for a minimum of 1 hour. Gaps between the door and bulkhead were again measured for each door.

Results of these measurements are shown in Tables 6.1 and 6.2. Those measurements missing for the inner door in Table 6.1 are a result of the seal extruding into the gap and not leaving any room to take the measurement. Additionally, the depth of gasket seal gland for both doors is also presented in Tables 6.1 and 6.2.

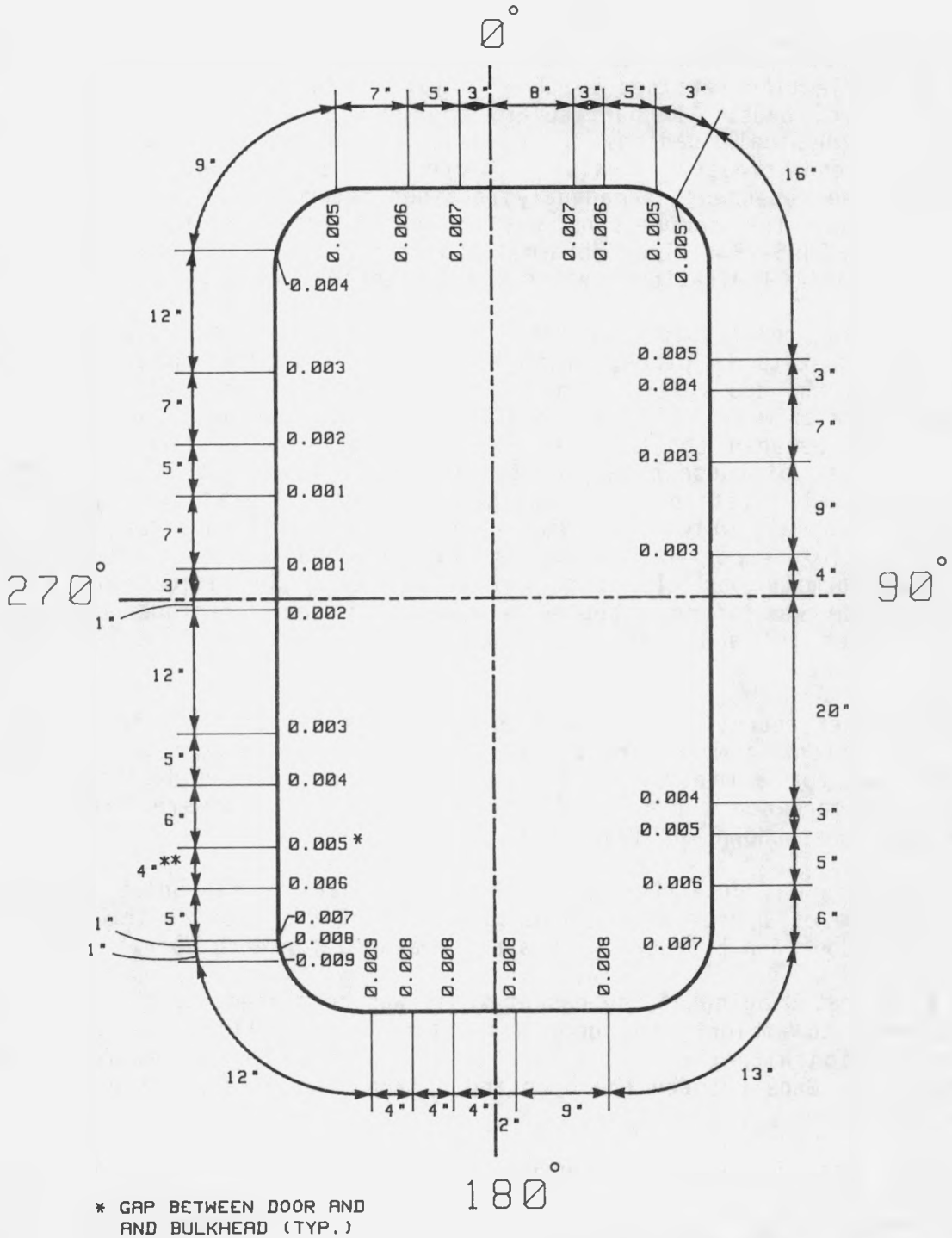

Figure 6.1 Gap Between Inner Door and Bulkhead When in Metal-to-Metal Contact

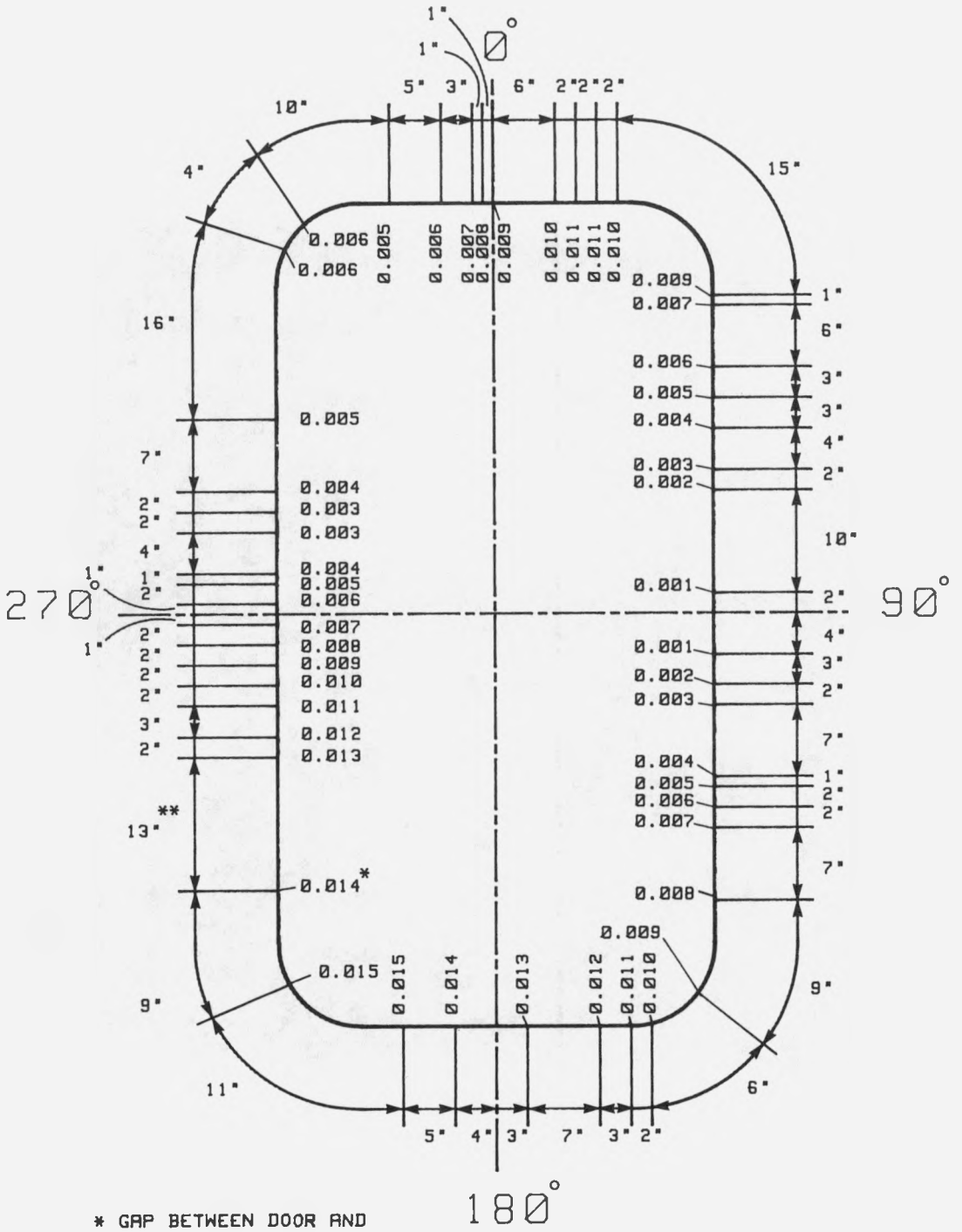

* GAP BETWEEN DOOR AND AND BULKHEAD (TYP.)

** LENGTH ALONG DOOR/BULKHEAD INTERFACE WHERE GAP IS BETWEEN 0.013 AND 0.014 IN. (TYP.)

METRIC EQUIVALENT : 1 IN. = 25.4 MM

Figure 6.2 Gap Between Outer Door and Bulkhead When in Metal-to-Metal Contact

Figure 6.3 Gap Measurement Between Bulkhead and Door

Table 6.1

Inner Door Compression Set Retention Measurements

Location	Groove Depth (in.)	Gap Measurement (in.)			
		Prior to Aging		After Seal Aging Unlatched h_{au}	After Test 3B Unlatched h_{au}
		Door Latched h_{ul}	Door Unlatched h_{uu}		
27 (0°)	0.6900	0.115	0.160	0.067	---
23	0.6919	0.109	0.160	0.059	---
7 (90°)	0.6918	0.086	0.185	0.055	0.032
3	0.6931	0.123	0.213	0.076	0.042
1 (180°)	0.6928	0.133	0.218	0.084	0.044
5	0.6875	0.128	0.217	0.086	0.043
10 (270°)	0.6918	0.087	0.187	0.062	0.030
12	0.6941	0.086	0.182	0.061	---
14	0.6942	0.087	0.179	0.061	---
16	0.6938	0.089	0.174	0.062	---
18	0.6932	0.092	0.171	0.063	---
20	0.6921	0.095	0.168	0.064	0.010
22	0.6923	0.100	0.165	0.066	---
25	0.6915	0.106	0.162	0.067	---
31	0.6905	0.109	0.159	0.066	---
29	0.6900	0.113	0.160	0.066	---

Metric Equivalent: 1 in. = 25.4 mm

To convert to "compression set retention", use the equation below:

$$C_B = \frac{h_{uu} - h_{au}}{h_{uu} - h_{ul}} \times 100$$

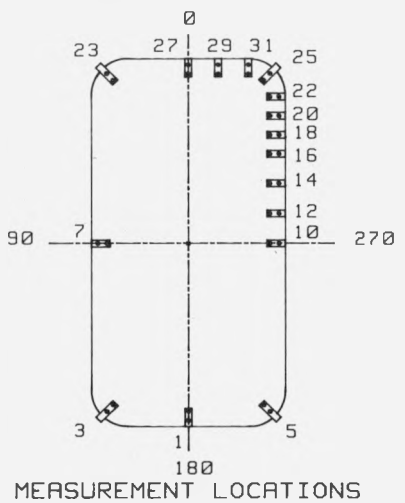

MEASUREMENT LOCATIONS

Table 6.2

Outer Door Compression Set Retention Measurements

Location	Groove Depth (in.)	Gap Measurement (in.)			
		Prior to Aging		After Seal Aging Unlatched h_{au}	After Test 3B Unlatched h_{au}
		Door Latched h_{ul}	Door Unlatched h_{uu}		
53 (0°)	0.6873	0.130	0.174	0.074	0.045
49	0.6869	0.129	0.173	0.071	0.045
39 (90°)	0.6875	0.107	0.187	0.058	0.040
35	0.6870	0.134	0.206	0.074	0.050
33 (180°)	0.6874	0.135	0.198	0.070	0.041
37	0.6870	0.126	0.191	0.064	0.040
42 (270°)	0.6878	0.097	0.174	0.050	0.029
44	0.6888	0.096	0.177	0.056	0.032
46	0.6889	0.102	0.173	0.061	0.034
48	0.6890	0.104	0.172	0.063	0.039
51	0.6874	0.108	0.170	0.064	0.040
57	0.6885	0.115	0.169	0.070	0.038
55	0.6872	0.126	0.171	0.072	0.041

Metric Equivalent: 1 in. = 25.4 mm

To convert to "compression set retention", use the equation below:

$$C_B = \frac{h_{uu} - h_{au}}{h_{uu} - h_{ul}} \times 100$$

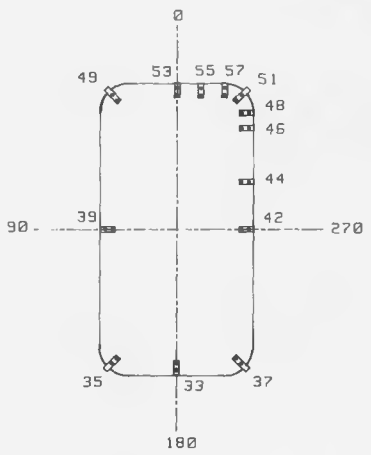

MEASUREMENT LOCATIONS

7.0 TEST PROCEDURES

During this test program there were three main test configurations. Tests 1A, 1AA, 2A, and 3A were performed using one procedure. Tests 1B, 1BB, 2B, and 3B were performed using a procedure similar to Tests 1A, 1AA, 2A, and 3A. Test 2C was performed using a separate test procedure. This section describes the three basic test procedures used for this test program. Table 7.1 lists each test performed in chronological order and gives a brief description of the test.

7.1 Tests 1A, 1AA, 2A, and 3A

Chamber V-1 was pressurized to 40 psig (276 kPa) in 5 psi (34.5 kPa) increments. Chamber V-1 was then pressurized in 10 psi (69.0 kPa) increments to 60 psig (414 kPa) and was then pressurized to approximately 69 psig (476 kPa) on the final pressure increment. Data were recorded prior to beginning pressurization, and after each increment of pressure. After pressure had reached its maximum and data were recorded, pressure was decreased in several increments to atmospheric conditions. Strain gages, thermocouples, and displacement transducers were not installed for Tests 1A and 1AA.

7.2 Test 1B, 1BB, 2B, and 3B

Chamber V-1 and the airlock were pressurized to 40 psig (276 kPa) in 5 psi (34.5 kPa) increments. Chamber V-1 and the airlock were then pressurized in 10 psi (69.0 kPa) increments to 60 psig (414 kPa) and was then pressurized to approximately 69 psig (476 kPa) on the final pressure increment. Data were recorded prior to beginning pressurization, and after each increment of pressure. After pressure had reached its maximum and data were recorded, pressure was decreased in several increments to atmospheric conditions. Strain gages, thermocouples, and displacement transducers were not installed for Tests 1B and 1BB.

7.3 Test 2C

The beyond design test was performed in accordance with the basic test outline described in Section 1.1, "Test Philosophy". This test was completed in three distinct load cycles that included target air temperature plateaus of 400°F (204°C) and 800°F (427°C), and pressures in Chamber V-1 of up to 300 psig (2.07 MPa).

The first load cycle began by establishing a pressure in Chamber V-1 of 10 psig (69 kPa). Temperature controller setpoints were set at 400°F (204°C). The air temperature above the inner door in Chamber V-1 was allowed to stabilize. By partially opening pressure control valve PCV-5B, heated air was blown on the inner door seal. After temperatures of air and steel had stabilized at the first temperature plateau, pressure in Chamber V-1 was increased to 300 psig (2.07 MPa) in 10 psi (69 kPa) increments. Pressure was then reduced to 10 psig (69 kPa) in approximately 25 psi (172 kPa) increments. This load cycle established that the airlock could survive a pressure greater than any pressure an LWR containment is likely to survive. In addition, the integrity of the gasket seal was tested when exposed to a temperature that may have caused leakage due to degradation resulting from thermal aging.

Table 7.1

Chronological Order and Description of Testing

Test Designation	Test Description
1A	Leak rate test of airlock inner door without the gasket. The inner door was subjected to a pressure of 69 psig (476 kPa) at ambient temperature.
1B	Leak rate test of airlock outer door without the gasket. The outer door was subjected to a pressure of 69 psig (476 kPa) at ambient temperature.
1AA	Leak rate test of airlock inner door with accelerated aged gasket in place. The inner door was subjected to a pressure of 69 psig (476 kpa). Not originally planned.
1BB	Leak rate test of airlock outer door with accelerated aged gasket in place. The outer door was subjected to a pressure of 69 psig (476 kpa). Not originally planned.
2A	Leak rate test of airlock inner door with gasket in place and full instrumentation. The inner door was subjected to 69 psig (476 kPa) at ambient temperature.
2B	Leak rate test of airlock outer door with gasket in place and full instrumentation. The outer door was subjected to 69 psig (476 kPa) at ambient temperature.
2C	Leak rate test of the entire airlock subjected to severe accident conditions. The airlock inner door was subjected to 300 psig (2.07 MPa) and 850°F (454°C).
3A	Leak rate test of the airlock inner door after Test 2C. The gasket was undisturbed and the inner door was subjected to a maximum pressure of approx. 16 psig (110 kPa). Could not reach 69 psig (476 kPa) due to leaking seal.
3B	Leak rate test of the airlock outer door after Test 2C. The gasket was undisturbed and same pressure as Test 2B.

The second load cycle began by changing the temperature controller setpoints to 800°F (427°C). Pressure in Chamber V-1 was maintained at approximately 10 psig (69 kPa). The air temperature above the inner door in Chamber V-1 was allowed to stabilize. Pressure control valve PCV-5B was again partially opened. After temperatures of air and steel had stabilized at the second temperature plateau, pressure in Chamber V-1 was increased to 300 psig (2.07 MPa) in 10 psi (69 kPa) increments. Pressure was then reduced to 10 psig (69 kPa) in 25 psi (172 kPa) increments.

While pressurizing Chamber V-1 in the second load cycle, the temperatures in Chamber V-1 dropped sharply. When the pressure was decreased to 10 psig (69 kPa) the temperatures in Chamber V-1 began to climb. Temperatures on the door dropped from 641°F (338°C) to 561°F (294°C) and air temperature above the bulkhead 18 in. (460 mm) from the cylinder wall dropped from 755°F (401°C) to 613°F (323°C) when maximum pressure was achieved. Air temperatures increased during depressurization after the pressure in Chamber V-1 was decreased to 288 psig (1.98 MPa) and held at that pressure for approximately 96 minutes. Pressure control valve PCV-5A was closed and PCV-5B was used to vent Chamber V-1.

A third cycle was added to the test as a result of the decreasing temperatures during pressurization and since the gasket seal remained intact during full pressurization. However, during the heating period, the following was done to increase the relative temperature in Chamber V-1:

(1) Increased the temperature controller setpoints to 850°F (454°C).
(2) Pressure control valve PCV-5B was 100% closed.

Setting the controller setpoints to 850°F was approaching the heat output capacity of the air circulation heater and the oven heaters located in Chamber V-1. Closing pressure control valve PCV-5B prevented heat loss through vent piping. Air and steel temperatures were allowed to stabilize. To reduce heat loss during pressurization, pressure was increased in 25 psi (172 kPa) increments up to 300 psig (2.07 MPa). When the inner door gasket seal failed, the airlock chamber was pressurized through the leaking gasket by way of the inner door flow meter loop. When the airlock and Chamber V-1 reached the same pressure, both chambers were simultaneously pressurized up to 300 psig (2.07 MPa).

Data were recorded prior to the beginning of the test, at regular intervals during the heating phase, and after each increment of pressure. After the test was completed and the airlock had reached ambient temperature and zero pressure conditions, data were recorded to measure the final condition of the airlock.

8.0 DISCUSSION OF TEST RESULTS

Results of this test program are divided into two main categories. The first category discusses tests performed at ambient temperature conditions, i.e., Tests 1A, 1AA, 2A, 3A, 1B, 1BB, 2B, and 3B. The second category discusses Test 2C which was performed at temperatures and pressures beyond the airlock design and simulated "generic" severe accident conditions.

The gasket seals used during this test program were subjected to an accelerated aging process that simulated in-service radiation and thermal aging over a 40-year service life and a LOCA. The following sections discuss results of testing performed on the airlock doors with and without the thermally aged gasket seals.

8.1 Pressure Tests at Ambient Temperatures

This section discusses the results of tests performed on the personnel airlock at ambient temperatures and pressures up to 15% beyond design. These tests were defined to:

(1) Establish the before and after effects of elevated pressures and temperatures on the airlock,
(2) Establish a baseline leak rate to evaluate the effectiveness of the gaskets, and
(3) Understand the effect, if any, of observed permanent deformations.

This section is divided into two parts. The first part is a presentation of basic results of tests performed at ambient temperature conditions. The second part is a discussion of comparisons of test results. Leak rates discussed in this section converted to percent volume per day are based on a 1 million ft^3 (28,300 m^3) containment building.

8.1.1 Test Results for Ambient Temperature Pressure Tests

Results for each ambient temperature pressure test are presented herein. Results for Tests 1A, 1B, 1AA, and 1BB are presented in their entirety herein. Plots and tabulations for remaining tests are presented in Appendix B of this report.

8.1.1.1 Test 1A

Prior to testing, the gasket seal for the inner door was removed. In this test, pressure in Chamber V-1 was increased from 0 to 69 psig (476 kPa) at ambient temperature conditions. Air leaking past the inner door was collected in the airlock, routed to the flow meter, and then vented to atmosphere. Transducers that were monitored for this test are as follows:

Temperature:	TE-24
Pressure:	PT-06, PT-08, PT-09, PT-10
Flow:	FT-16

Locations of these transducers are shown in the process and instrument diagram of Figure 3.2. Results for Test 1A are shown in Figure 8.1 and are also tabulated in Table 8.1. Maximum leak rate measured past the inner door was

45.3 SCFM (1280 l/min), or 6.5% volume/day, at a pressure in Chamber V-1 of 68.7 psig (474 kPa).

8.1.1.2 Test 1B

Prior to testing, the gasket seal for the outer door was removed. In this test, the pressure in Chamber V-1 and the airlock was increased from 0 to 69 psig (474 kPa) at ambient temperature conditions. Air leaking past the outer door was collected in Chamber V-2, routed to the flow meter, and then vented to atmosphere. Transducers that were monitored are as follows:

Temperature:	TE-25
Pressure:	PT-06, PT-08, PT-23
Flow:	FT-21

Locations of these transducers are shown in the process and instrument diagram of Figure 3.2. Results for Test 1B are shown in Figure 8.2 and are tabulated in Table 8.2. Maximum leak rate measured past the outer door was 30.4 SCFM (861 l/min), or 4.4% volume/day, at a pressure in Chamber V-1 and the airlock of 69.2 psig (477 kPa).

8.1.1.3 Test 1AA

Test 1AA was a repeat of Test 1A with the thermally aged gasket installed in the inner door. The same transducers as listed in Section 8.1.1.1 "Test 1A", were monitored. Maximum pressure achieved was 70.1 psig (483 kPa). There was no measurable leakage past the inner door during this test.

8.1.1.4 Test 1BB

Test 1BB was a repeat of Test 1B with the thermally aged gasket installed in the outer door. The same transducers as listed in Section 8.1.1.2 "Test 1B", were monitored. Maximum pressure achieved was 69.7 psig (481 kPa). There was no measurable leakage past the outer door.

8.1.1.5 Test 2A

Prior to testing, the gasket seal in the inner door was installed. In this test, pressure in Chamber V-1 was increased from 0 to 69 psig (0 to 476 kPa) at ambient temperature conditions. Air leaking past the inner door was collected in a shroud, routed to the flow meter, and then vented to atmosphere.

All transducers were installed and monitored with the exception of the cantilever beam displacement transducers described in Section 4.0, "Instrumentation and Data Acquisition". Tabulations and plots for each active transducer are presented in Appendix B, "Data Plots and Tabulations".

The maximum pressure applied was 68.8 psig (474 kPa). There was no measurable leakage past the inner door. Maximum compressive strain on the inner door/bulkhead recorded at maximum pressure was -296 microstrain at strain gage location SGB1-17V. Maximum tensile strain on the inner door/bulkhead recorded was 281 microstrain at strain gage location SGB2-24V.

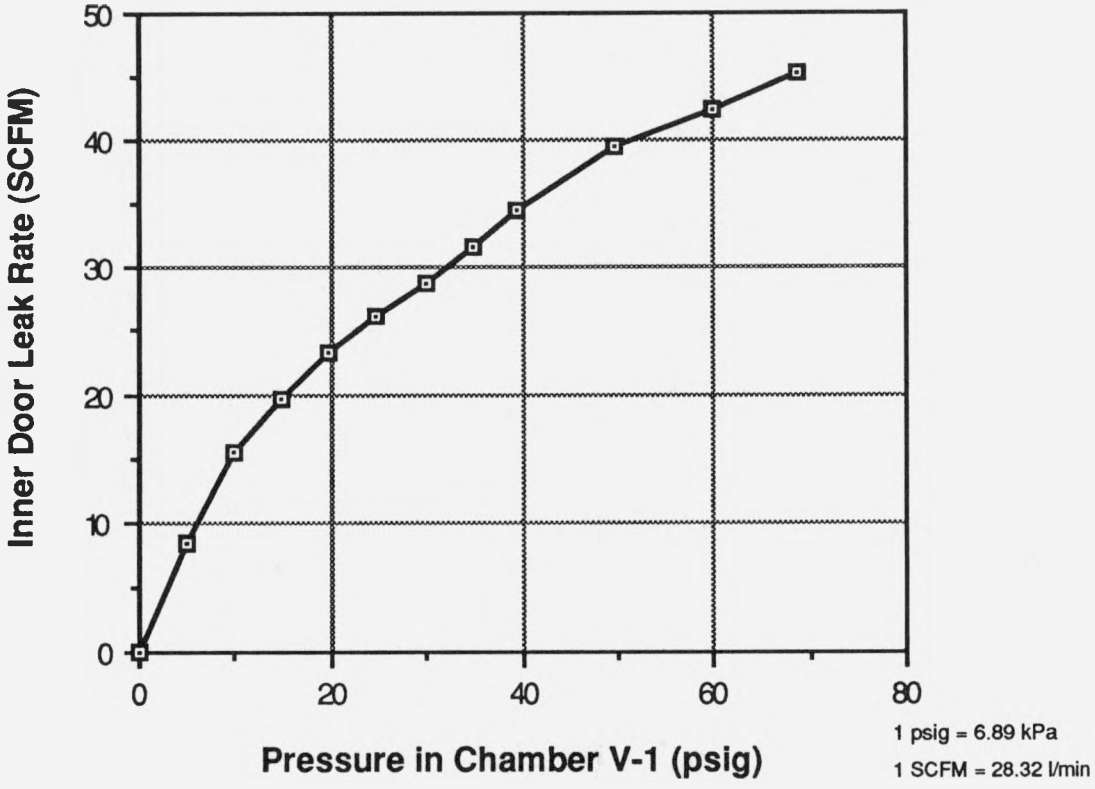

Figure 8.1 Leak Rate versus Pressure for Test 1A

Table 8.1

Test 1A: Leak Rate and Pressure

Pressure in Chamber V-1 (psig)	Inner Door Leak Rate (SCFM)
0	0
4.8	8.5
9.9	15.5
14.9	19.7
19.6	23.3
24.5	26.1
30.1	28.9
35.0	31.7
39.4	34.6
49.8	39.5
59.9	42.3
68.7	45.3

Metric Equivalent: 1 psig = 6.89 kPa

1 SCFM = 28.32 l/min

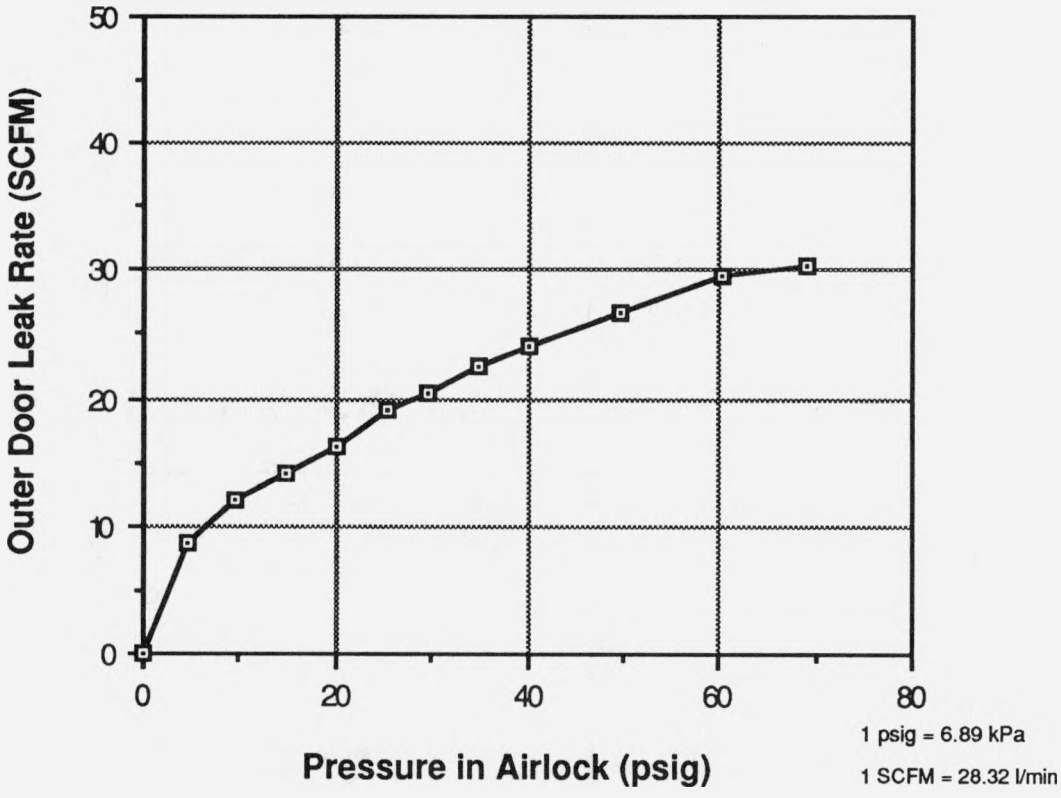

Figure 8.2 Leak Rate versus Pressure for Test 1B

Table 8.2

Test 1B: Leak Rate and Pressure

Pressure in Airlock (psig)	Outer Door Leak Rate (SCFM)
0	0
4.5	8.7
9.5	12.0
14.9	14.2
20.0	16.2
25.2	19.1
29.6	20.5
34.9	22.6
40.0	24.0
49.8	26.8
60.1	29.7
69.2	30.4

Metric Equivalents: 1 psig = 6.89 kPa

1 SCFM = 28.32 l/min

Gap/rotation transducers indicate a small reduction in the gap between the door and bulkhead. Maximum displacements were -0.016 in. (-0.41 mm). Out-of-plane displacement transducers for the inner door and bulkhead show a maximum displacement of -0.036 in. (-0.91 mm). Slip transducers on the inner door, locations TSD1-060 and TSD1-061, indicated movement of the door in the 270° to 90° direction. The maximum movement was recorded on the 90° side of the door with a change in location of the door of -0.012 in. (-0.30 mm).

8.1.1.6 Test 2B

Prior to testing, the gasket seal in the outer door was installed. In this test, pressure in Chamber V-1 and the airlock was increased from 0 to 69 psig (0 to 476 kPa) at ambient temperature conditions. Air leaking past the outer door was collected in Chamber V-2, routed to the flow meter, and then vented to atmosphere.

All transducers were installed and monitored with the exception of the cantilever beam displacement transducers, described in Section 4.0, "Instrumentation and Data Acquisition". Tabulations and plots for each active transducer are presented in Appendix B, "Data Plots and Tabulations".

The maximum pressure applied in the airlock and Chamber V-1 was 68.8 psig (474 kPa). There was no measurable leak past the outer door. Maximum compressive strain on the outer door/bulkhead was -205 microstrain at strain gage location SGB2-37H. The maximum tensile strain on the outer door/bulkhead was 221 microstrain at strain gage location SGB3-36V.

Gap/rotation transducers indicate relatively small reductions in the gap between the outer door and bulkhead, with the maximum gap change -0.030 in. (-0.8 mm). Out-of-plane transducers at the center of the outer door indicated a total deflection of -0.069 in. (-1.8 mm). Slip transducers indicated a relative motion of the outer door in the 270° to 90° direction.

8.1.1.7 Test 3A

This test was a repeat of Test 2A to compare the before and after behavior characteristics of the airlock after it had been exposed to pressures and temperatures beyond the design basis. Transducer locations are described in Section 4.0, "Instrumentation and Data Acquisition". Tabulations and plots for each active transducer are presented in Appendix B, "Data Plots and Tabulations".

The maximum pressure achieved in Chamber V-1 was 16.4 psig (113 kPa). The inner door leak rate at this pressure was 326.6 SCFM (9248 l/min), or 47% volume/day. Leak rate as a function of pressure is shown in Figure 8.3. Strains were very small at this pressure. Deflections at active transducers were near zero for gap and rotation transducers and for out-of-plane transducers across the inner door. Out-of-plane transducers measuring movement of the bulkhead indicated deflections no greater than -0.007 in. (-0.178 mm).

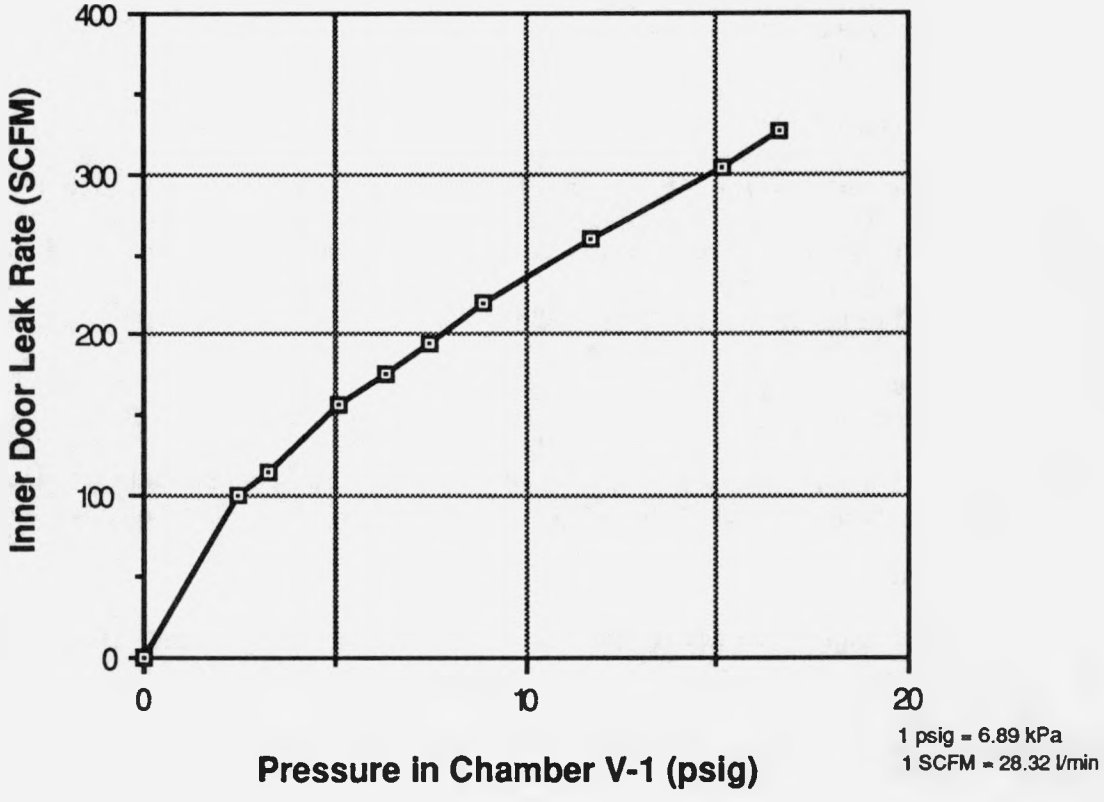

Figure 8.3 Leak Rate versus Pressure for Test 3A

8.1.1.8 Test 3B

This test was a repeat of Test 2B to compare the before and after behavior characteristics of the airlock after it had been exposed to pressures and temperatures beyond the design basis. Transducer locations are described in Section 4.0, "Instrumentation and Data Acquisition". Tabulations and plots for each active transducer are presented in Appendix B, "Data Plots and Tabulations.

The maximum pressure applied in the airlock and Chamber V-1 was 70.8 psig (488 kPa). There was no measureable leak past the outer door. Maximum compressive strain on the outer door/bulkhead was -210 microstrain at strain gage location SGB2-37H. The maximum tensile strain on the outer door/bulkhead was 226 microstrain at strain gage location SGB3-36V.

Gap/rotation transducers indicated relatively small reduction in the gap between the door and bulkhead, with a maximum gap change of -0.021 in. (-0.53 mm). Out-of-plane transducers at the door center showed a change in displacement of -0.070 in. (-1.78 mm).

8.1.2 Discussion of Pressure Tests at Ambient Temperature

The following is a brief discussion comparing leak rates, strains, and displacements that occurred during the design pressure tests at ambient temperature conditions.

8.1.2.1 Leak Rates

No measurable leakage was recorded past the inner door in Tests 1AA and 2A. The resulting leak rates recorded for Test 1A, where the door was in metal-to-metal contact with the bulkhead and the gasket absent from the inner door gland, and Test 3A, where the inner door gasket seal had failed previously in Test 2C, is shown in Figure 8.4.

The leak rates shown in Figure 8.4 do not reflect the relative size of the openings through which the pressurized air passed through the seal. After the inner door seal failed during Test 2C, the apparent flow area was 1.85 $in.^2$ (1190 mm^2). Based on the results of the gap measurements between the inner doors and bulkhead, the total open area for Test 1A before pressurization was approximately 1.18 $in.^2$ (760 mm^2). Although the measured leak rates are not proportional to the estimated opening through which the pressurized air bypassed the inner door, it is possible the actual opening in Test 1A became considerably smaller during pressurization. It is also possible that the failed seal opening for Test 3A was larger than the area measured where the seal failed after all tests were completed. Although there was no visible evidence, other areas of the seal may have leaked, to a much lesser degree, during Test 3A. Leak rate for Test 1B is also shown in Figure 8.4. The leak rates for Tests 1A and 1B are similar in magnitude, however, there is no apparent correlation of leak rate and open flow area between the doors and bulkheads.

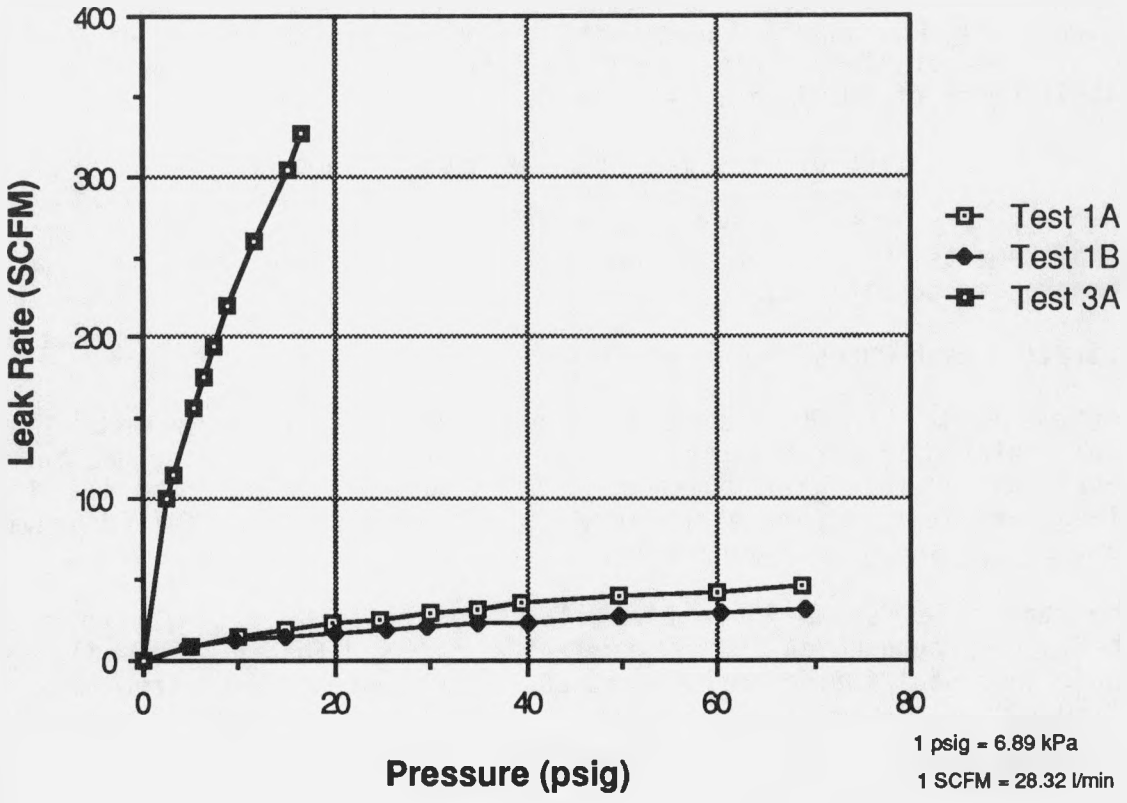

Figure 8.4 Comparison of Leak Rates for Tests 1A, 1B, and 3A

8.1.2.3 Displacements

A number of capacitance type displacement transducers were used to measure the relative change in gap between the doors and bulkheads, movement of the doors in the plane of the bulkheads relative to the bulkheads, and the out-of-plane movement of the doors and bulkheads relative to a reference frame.

The profile of the inner door during Tests 2A and 3A is shown in Figures 8.5 through 8.7. In general, the gap between the inner door and bulkhead closed during pressurization. Results are presented in each figure for Test 2A at maximum pressure in Chamber V-1. In addition, these changes in gap results are also presented for Test 2A at a pressure of 14.3 psig (98.6 kPa) for comparison of results for Test 3A. The maximum pressure reached during Test 3A was 16.4 psig (113 kPa), however, results for Test 3A are shown for a pressure in Chamber V-1 of 14.8 psig (102 kPa) for comparison purposes.

Results for Test 3A yield virtually no change in gap between the inner door and bulkhead. It is clear that the elevated temperatures and pressures during Test 2C did have an effect on the deflection characteristics of the inner door gasket seal.

Deflections of the inner door along the long and short centerline directions are shown in Figure 8.5.

Change in gap along the edge of the inner door is shown in Figures 8.6 and 8.7. In general, in the long direction of the door, the corners of the door compressed more during pressurization than the center of the door along the edge. Along the short direction of the door on the edge, the gap became smaller in the center of the door than at the corners.

Change in gap for the outer door in Tests 2B and 3B are shown in Figures 8.8 and 8.9. The change in gap did not show any pattern, although the gap between the outer door and bulkhead closed more during Test 2B than in Test 3B.

There are some relative differences in the change in gap (as measured from the zero reference) before and after Test 2C on the inner door. These differences could be due to one or a combination of any of the following:

(1) Before Test 2C, the inner door was simply supported on an elastic foundation (gasket) around the entire perimeter. After Test 2C, the inner door was simply supported on three sides (the gasket was completely eroded on the fourth side after Test 2C).
(2) Gasket material underwent a chemical change resulting from high temperature exposure causing a change in the elastic properties of the gasket (i.e., the gap between door and bulkhead was smaller therefore support conditions stiffer).
(3) When the seal failed, the amount of solid particulates in the airlock and shroud chamber increased. Since the displacement transducers used to measure change in gap operated on a capacitance principle using air as the dielectric, it is possible the transducer output was significantly altered after being coated with solid particulates from the gasket.

8.1.2.2 Strains

During Tests 2A, 2B, 3A, and 3B, the strain gages indicated purely linear elastic behavior. Maximum strains were small for Test 3A as a result of the low maximum pressures. Strains were repeatable for Tests 2B and 3B, with small variations in magnitude of the resultant strains between tests. Strain gage readings at all locations did not indicate yielding during Tests 2A, 2B, 3A, and 3B. Comparison of selected strain gages before and after Test 2C are shown in Figure 8.10. These strain gages are representative of the largest tensile and compressive strains recorded during Tests 2A, 2B, 3A, and 3B.

8.2 Elevated Pressure and Temperature Testing of Personnel Airlock

The personnel airlock tested was designed for a pressure of 60 psig (410 kPa) and a temperature of 340°F (171°C). During Test 2C the maximum pressure reached was 300 psig (2.07 MPa). The maximum surface temperature recorded on the door during heating of Chamber V-1 was 784°F (418°F).

Test 2C consisted of three combined thermal and pressure cycles. The first cycle started by ramping the air temperature above the inner door to 400°F (204°C). Temperatures of the steel inner door and bulkhead were allowed to stabilize. Pressure inside Chamber V-1 was increased to 300 psig (2.07 MPa) in 10 psi (69 kPa) increments. There was no measurable leakage of the inner door seal during pressurization. Pressure was decreased in 25 psi (170 kPa) increments, ending the first test cycle.

The second cycle started by ramping the air temperature above the inner door to 800°F (427°C). Temperatures of the steel inner door and bulkhead were allowed to stabilize. Pressure inside Chamber V-1 was increased to 300 psig (2.07 MPa) in 10 psi (69 kPa) increments. There was no measurable leakage of the inner door seal during pressurization. During pressurization, the temperature of the air and, to a lesser degree, the steel door and bulkhead, decreased as pressure in Chamber V-1 increased. Temperatures of the steel door around the gasket seal, where air was blown directly from the air inlet header, suggest that air colder than 800°F (427°C) was exiting the header. There was no indication of this from the thermocouple used to control the heated air leaving the air circulation heater as the thermocouple output displayed on the controller was nominally at 800°F (427°C). Pressure was decreased in 25 psi (170 kPa) increments, ending the second test cycle.

One of the objectives of this test program was to subject the airlock to beyond design basis loads. Another objective was to establish the point at which the gasket failed to seal the airlock chamber from the containment building. The third and final test cycle was added to the test program due to these results following the first and second cycles:

(1) The gasket seal remained intact and withstood 300 psig (2.07 MPa) in Chamber V-1.
(2) The air and steel surface temperatures dropped considerably while increasing pressure during the second load cycle.

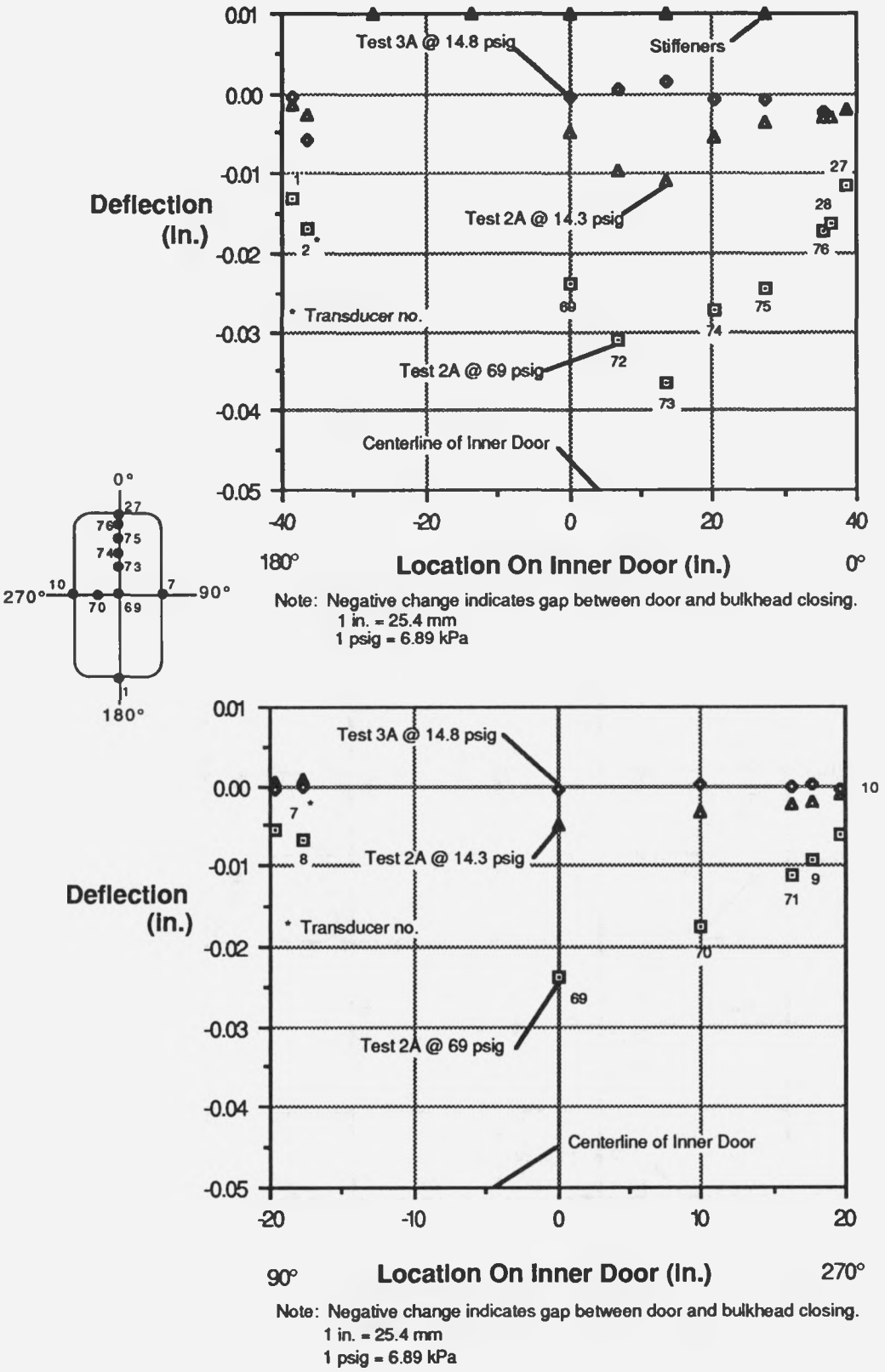

Figure 8.5 Deflection of Inner Door Centerline Along the 0°-180° and 90°-270° Axis for Tests 2A and 3A

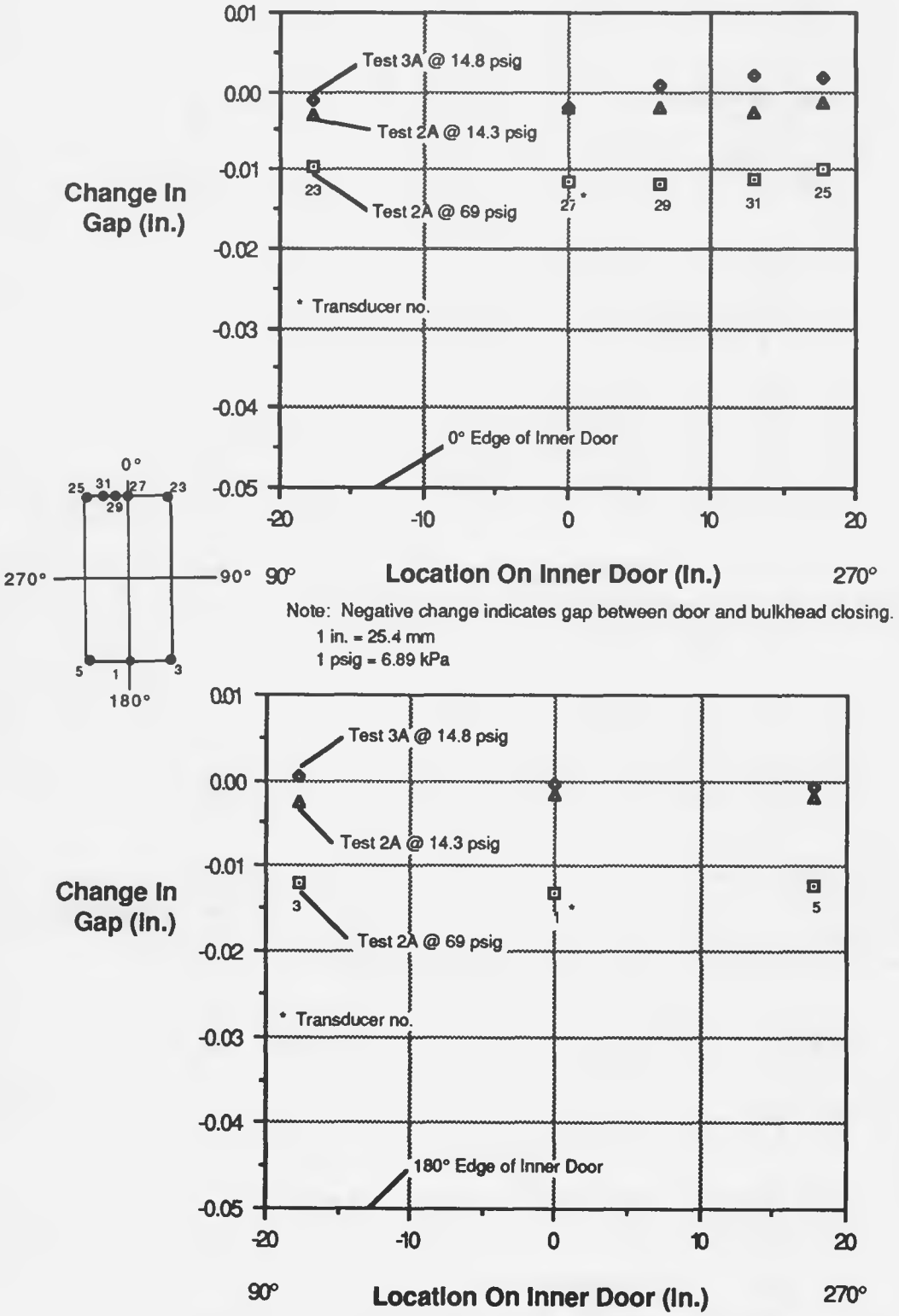

Figure 8.6 Gap Change on the Inner Door Along the 0° and 180° Edges of the Door

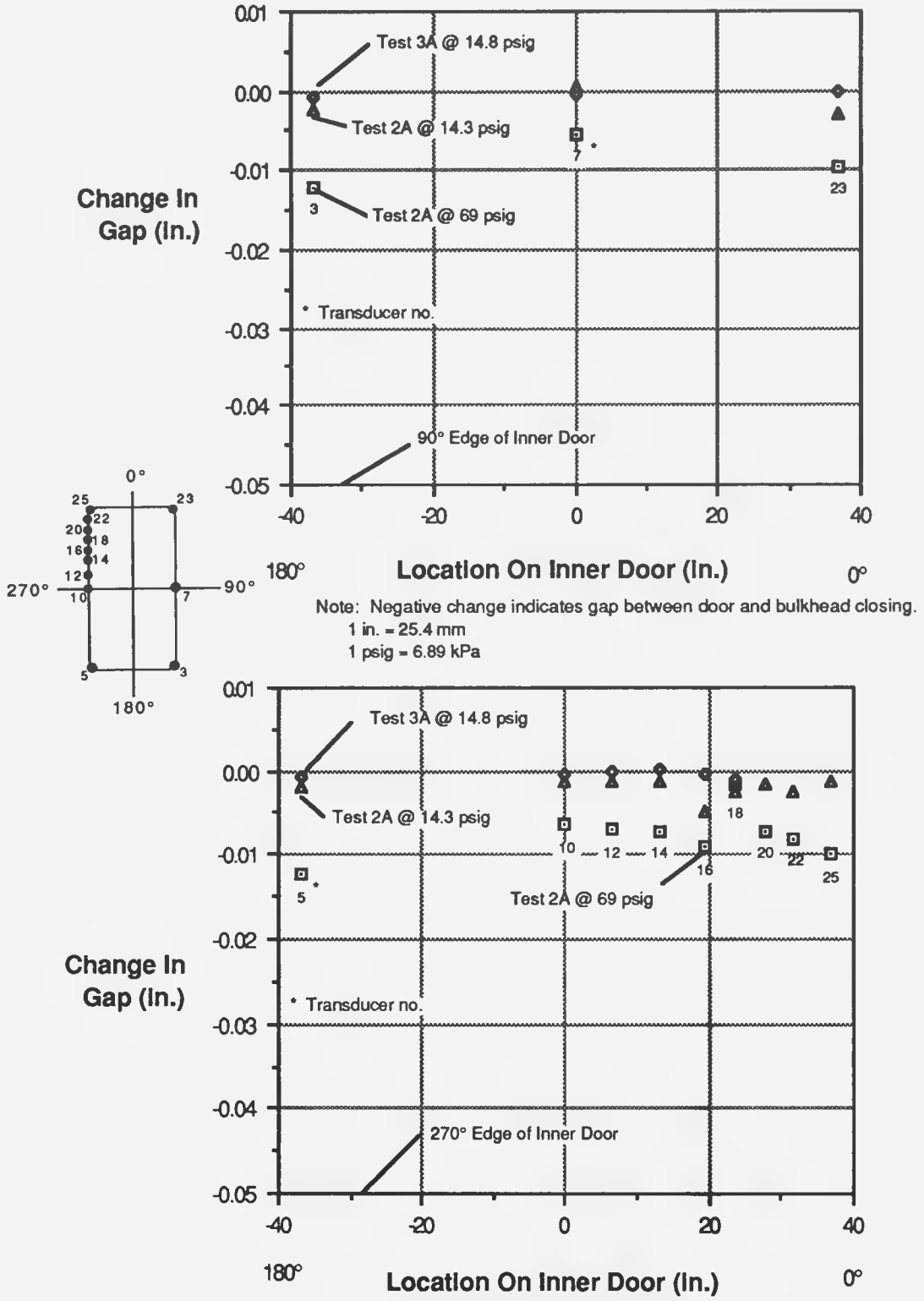

Figure 8.7 Gap Change on the Inner Door Along the 90° and 270° Edges of the Door

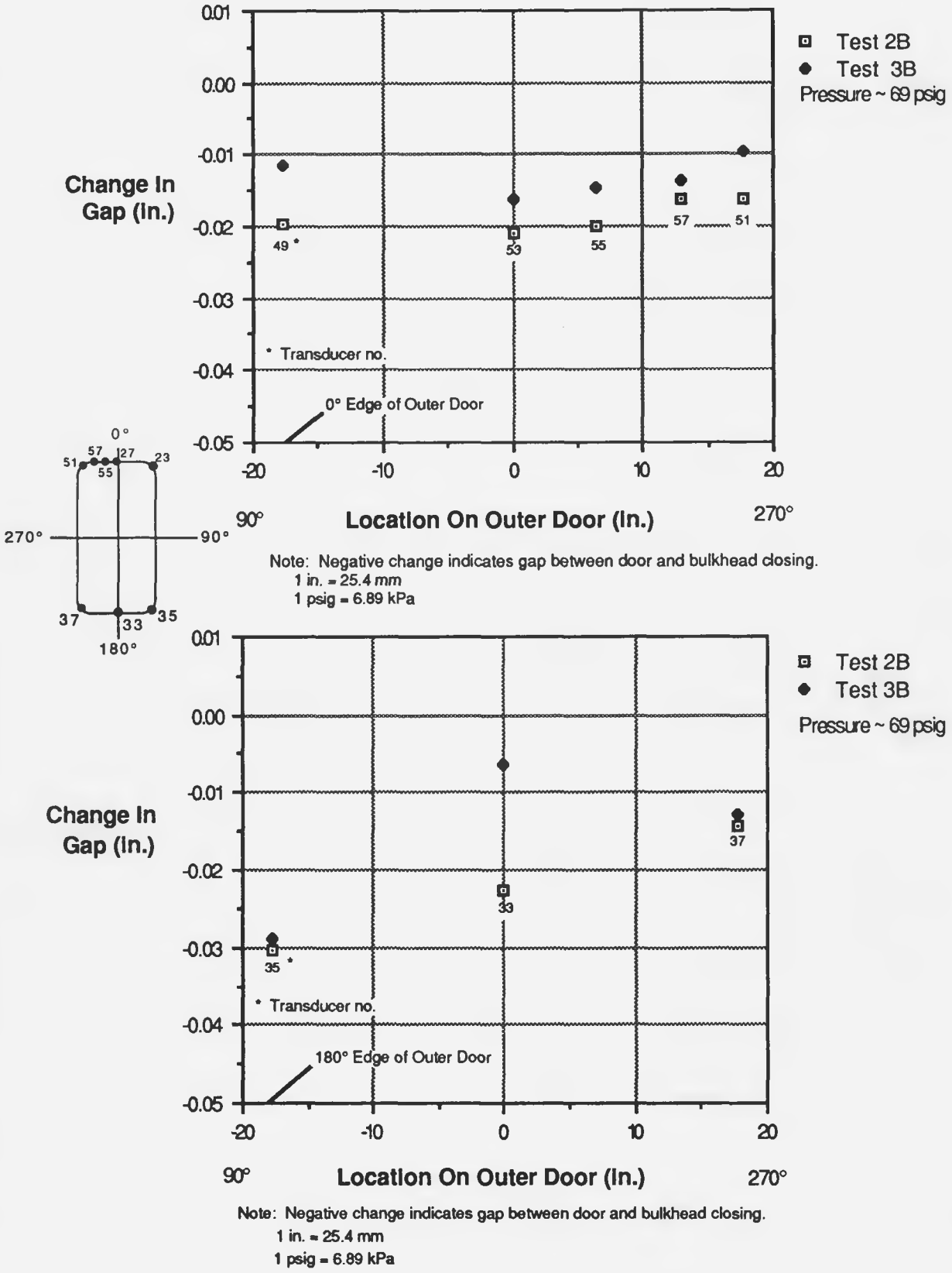

Figure 8.8 Gap Change on the Outer Door Along the 0° and 180° Edges of the Door

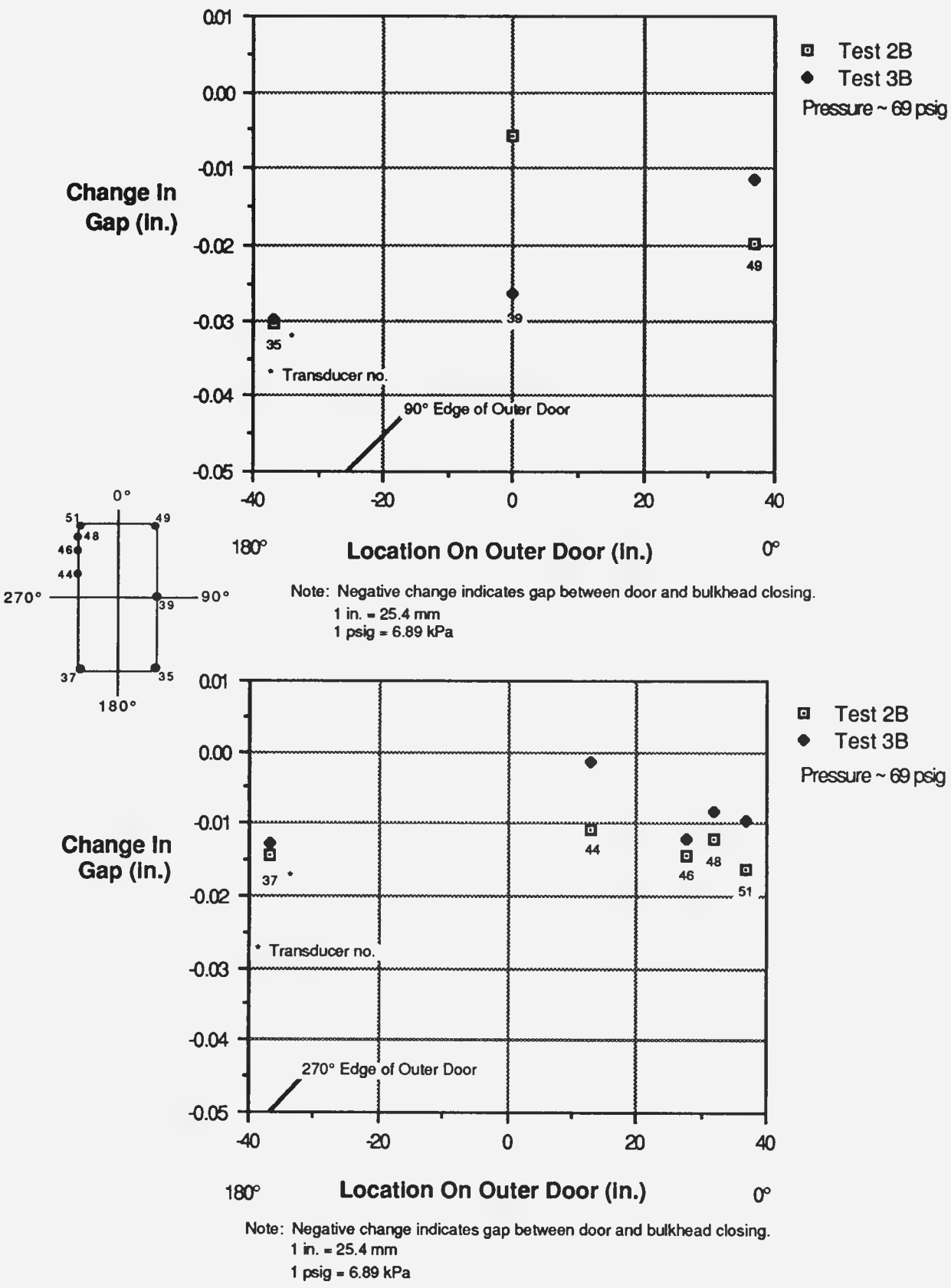

Figure 8.9 Gap Change on the Outer Door Along the 90° and 270° Edges of the Door

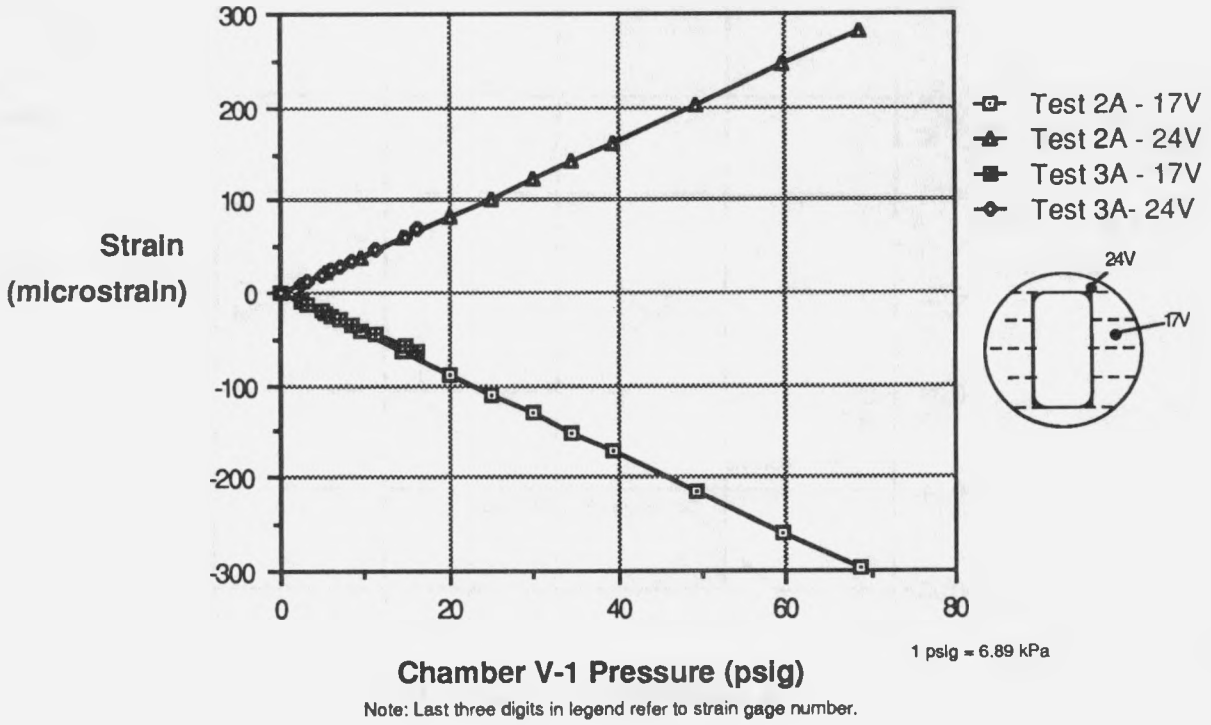

Note: Last three digits in legend refer to strain gage number.

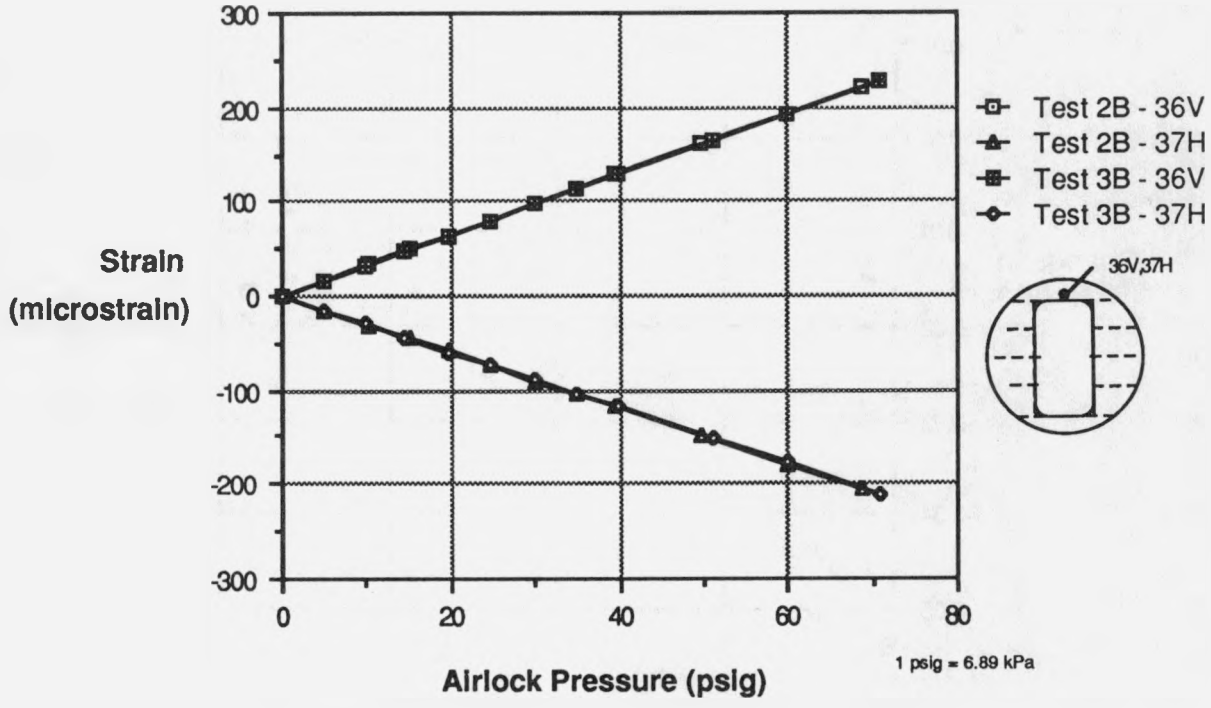

Note: Last three digits in legend refer to strain gage number.

Figure 8.10 Strain versus Pressure for Measured Strains on Inner and Outer Door Bulkheads During Tests 2A, 2B, 3A, and 3B

A drop in temperature during the second load cycle was not anticipated. This may have contributed to the gasket seal not reaching the threshold temperature at which the gasket material becomes unstable. The threshold temperature at which the EPDM E603 compound from which the gasket was manufactured was approximately 620°F (327°C). This threshold temperature was established in tests performed by SNL[5].

Clearly, the airlock could easily survive pressures up to 300 psig (2.07 MPa). The third load cycle, which was not part of the original test plan, was added to determine the seal system temperature limitations. The temperature controller setpoints were set at 850°F (454°C) for both the air circulation heater and the heater array in Chamber V-1. Vent valve PCV-5B was completely closed, so all of the heat input was from the heating elements in Chamber V-1. The time that elapsed between the end of the second load cycle and when pressurization began during the third load cycle was nearly 12 hours. This was at 52.70 hours after the test began.

After 53.27 hours from the start of the test, the limit pressure of 151 psig (1.04 MPa) was reached on the third pressure cycle. The seal failure occurred suddenly, however, there was evidence that the seal was beginning to leak at lower pressure. During the third pressurization cycle, at a pressure of 51 psig (350 kPa), the pressure in the airlock began to increase. There was a small increase of flow rate measured past the inner door, but it was out of the range of the flow meter accuracy. Pressures in the airlock increased from 2.34 to 6.48 psig (16.1 to 44.7 kPa) while pressure in Chamber V-1 increased from 51 to 149 psig (350 to 1.03 MPa). A portion of this pressure increase may be attributable to temperature increase in the airlock. While increasing pressure from 149 psig to 175 psig (1.03 to 1.21 MPa), the seal failed completely at a pressure of 151 psig (1.04 MPa). The seal eroded quickly, creating a leak path. When the seal failed, the maximum leak rate recorded was 706 SCFM (20,000 l/min), or 102% volume/day. However, continuous recording of the leak rate was not possible during pressurization and leak rates may have been greater. It is probable that leak rates exceeded 706 SCFM (20,000 l/min) after the inner door seal was effectively bypassed.

The following is a discussion of the temperature, deflection, and strain data recorded during Test 2C. Typical temperature and pressure curve versus time is shown in Figure 8.11. The temperature shown in Figure 8.11 was recorded from a thermocouple located in Chamber V-1 18 in. (460 mm) from the cylinder wall and 19.75 in. (500 mm) above the inner door bulkhead.

8.2.1 Effect of High Temperatures on the Gasket

The temperature profile along the length of the airlock and across the inner door and bulkhead for several different times in the test is shown in Figure 8.12. The most significant effect that elevated temperatures had was on the inner door gasket seal. Not only did the seal fail due to exposure to temperatures at which the gasket material becomes unstable, the gasket material exhibited expansion characteristics far in excess of any anticipated.

In tests performed by SNL on Presray's EPDM E603 seal material, it was determined that the temperature at which the material deteriorates is approximately 620°F (327°C)[5]. As shown in Figure 8.13, the temperature profile measured on the door was fairly uniform except at 0 and 180° which had

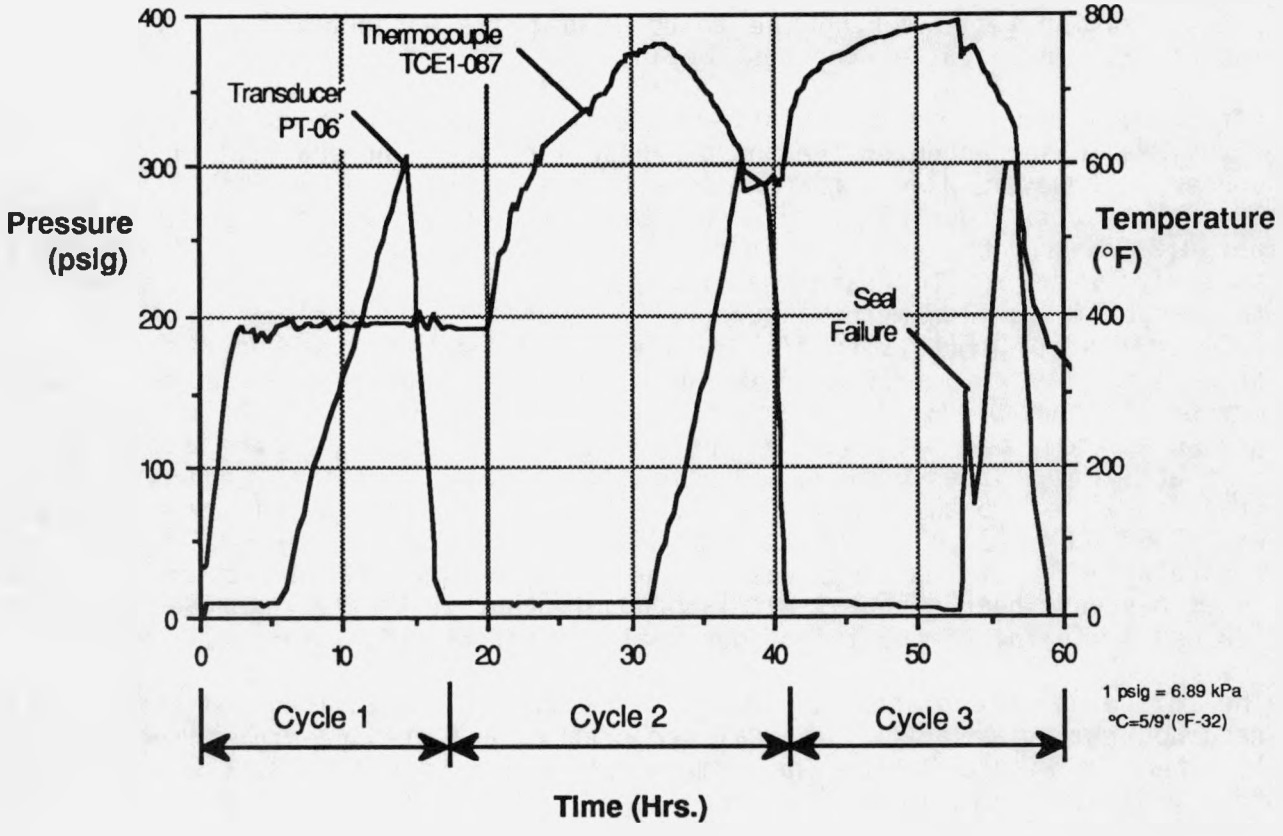

Figure 8.11 Pressure and Temperature Versus Time Relationship for Test 2C

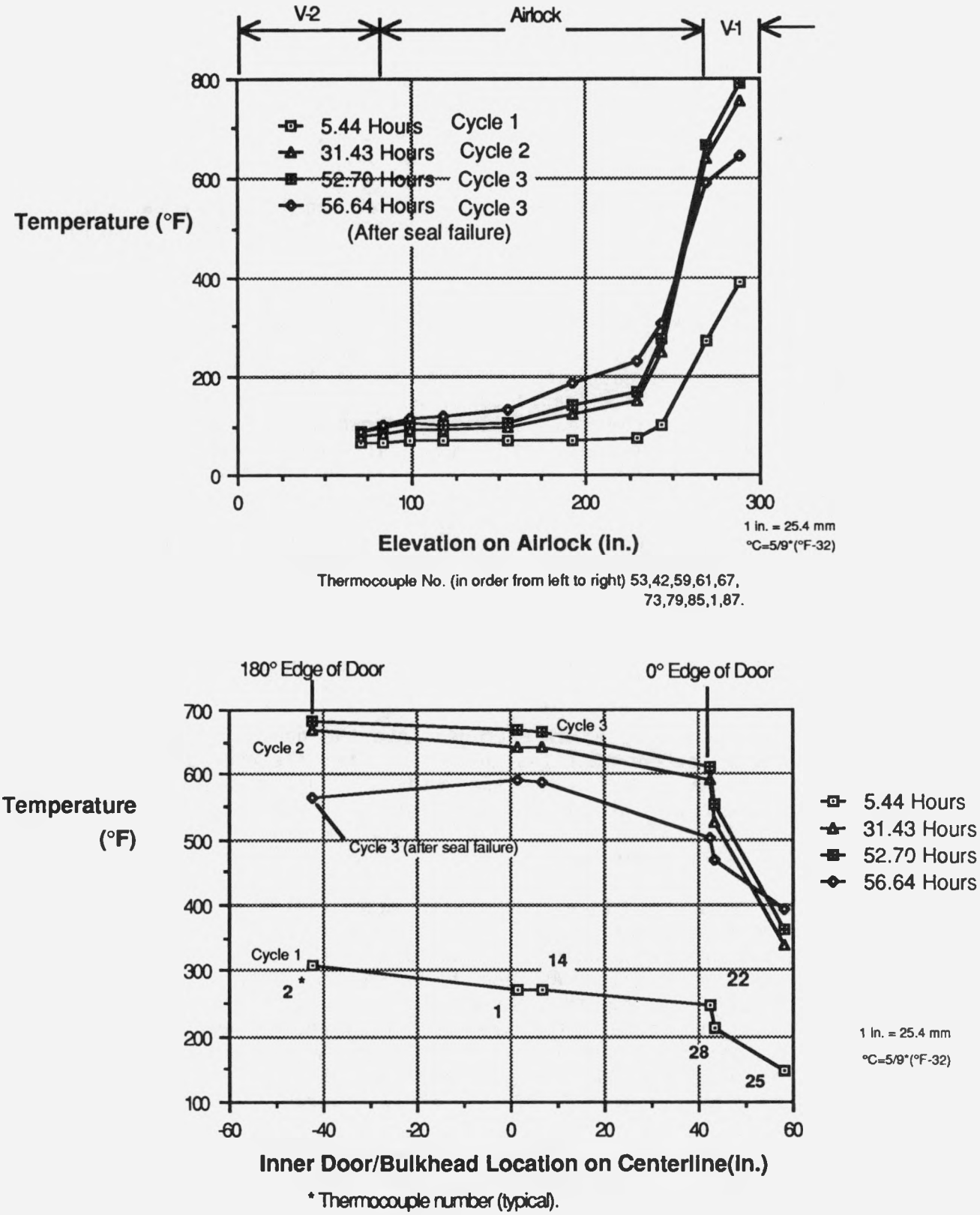

Figure 8.12 Temperature Profiles Along Length of Airlock and Across Inner Door Bulkhead

the lowest and highest temperatures, respectively. It is clear that, prior to pressurization of the third cycle, the temperatures on the door measured in Chamber V-1 were all near the temperature at which the seal material degrades. Pressure was increased from 4.6 psig (32 kPa) to 149 psig (1.03 MPa) and the elapsed time was 34 minutes. The temperature increased at 180° orientation but decreased in every other location. The temperature increase discussed was not gradual but was represented by a spike in the temperature time relationship for the thermocouple element at the 180° orientation. The seal failed at 180° orientation and is indicated by the shaded area in Figure 8.13.

The actual seal failure is shown in Figures 8.14 through 8.17. The entire area where the seal failed is shown in Figure 8.14. The machined surface was clean except for the powdery residue of what remained from the gasket. The gasket disintegrated from each of the corners and about 3 to 5 in. (75 to 130 mm) beyond the capacitance transducer brackets. The remains of the gasket seal at the corner where the seal failed is shown in Figure 8.15. Remains from the gasket were charred in this area. The white residue and charred remains crumbled when touched. The remaining gasket, mainly intact, adhered to the inner door bulkhead and is shown in Figure 8.16. The gasket material was cracked and was brittle near the cracked areas. Between the cracks the consistency of the gasket was rather gummy, and did not rebound and return to its initial shape when deformed. The material appears to have lost all elasticity. Data describing a sudden, irregular increase in temperature at the failure location, the charred remains of the gasket, and the sooty byproduct from the gasket, is consistent with either smoldering or combustion of the gasket due to outgassing of combustible by-products during high temperature exposure.*

During Test 2C the gasket material extruded into the gap between the door and bulkhead to a greater extent than that observed after the accelerated aging of the gasket seal. Figure 8.17 shows the residue of the gasket material that extruded between the door and bulkhead and adhered to the inner door.

8.2.2 Deflections of Inner Door

Displacements of both the inner and outer door relative to the bulkhead stiffener were measured during the test. Figures 8.18 through 8.20 are isometric views of the door showing displacement of the inner door relative to the original zero position. As can be seen in these glimpses of the displacement geometry during the three test cycles, there are two major driving forces causing these displacements: elevated temperatures and high surface pressure on the inner door. The load cycle, time, pressure and average temperature around the door perimeter are documented. Displacements have been magnified by a factor of 100 for these figures.

As shown in Figure 8.19, during the second load cycle at 31.43 hours after the test began and prior to pressurization, the inner door had moved away from the bulkhead, opening the gap between the inner door and bulkhead. The center of the door moved 0.036 in. (0.91 mm) away from the bulkhead. Displacements that

---

* Observation speculated by SNL.

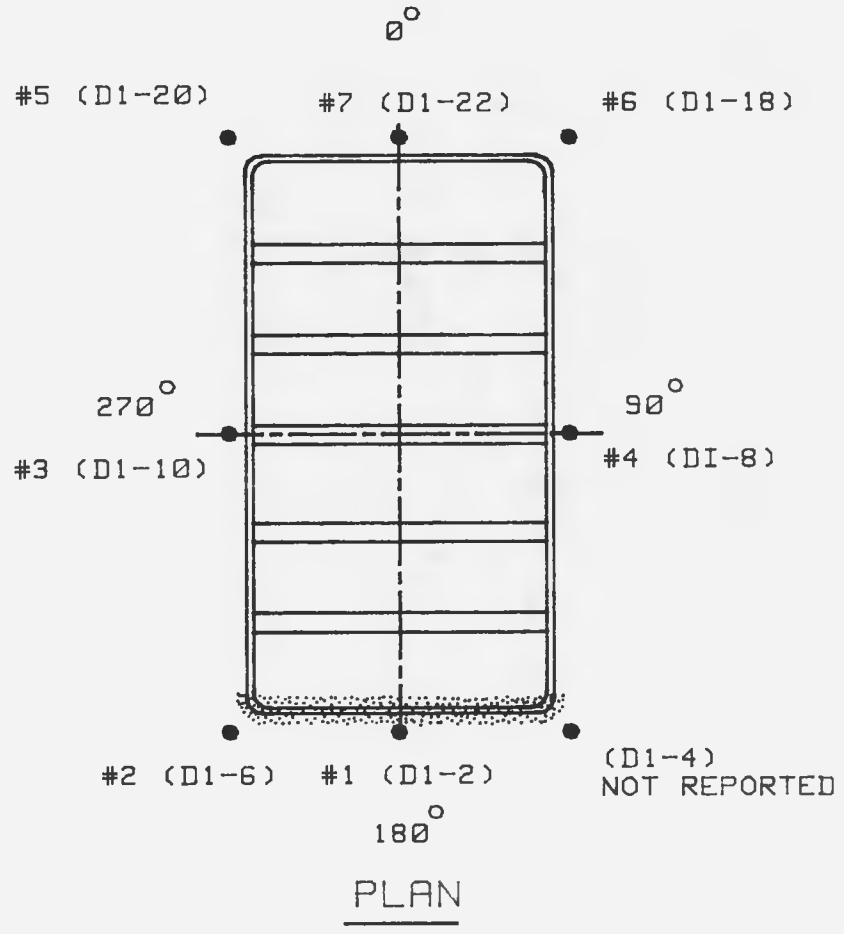

PLAN

THERMOCOUPLE LOCATION	TEMPERATURE (°F)	
	T=52.7 HRS P=4.6 PSIG	T=53.3 HRS P=148.5 PSIG
1	682.9	730.8
2	667.8	642.7
3	655.4	615.9
4	645.6	633.4
5	657.3	616.7
6	657.8	576.6
7	611.3	569.7

NOTE: SHADED AREA DENOTES LOCATION WHERE SEAL FAILED.

Figure 8.13 Temperature Profile Around Inner Door

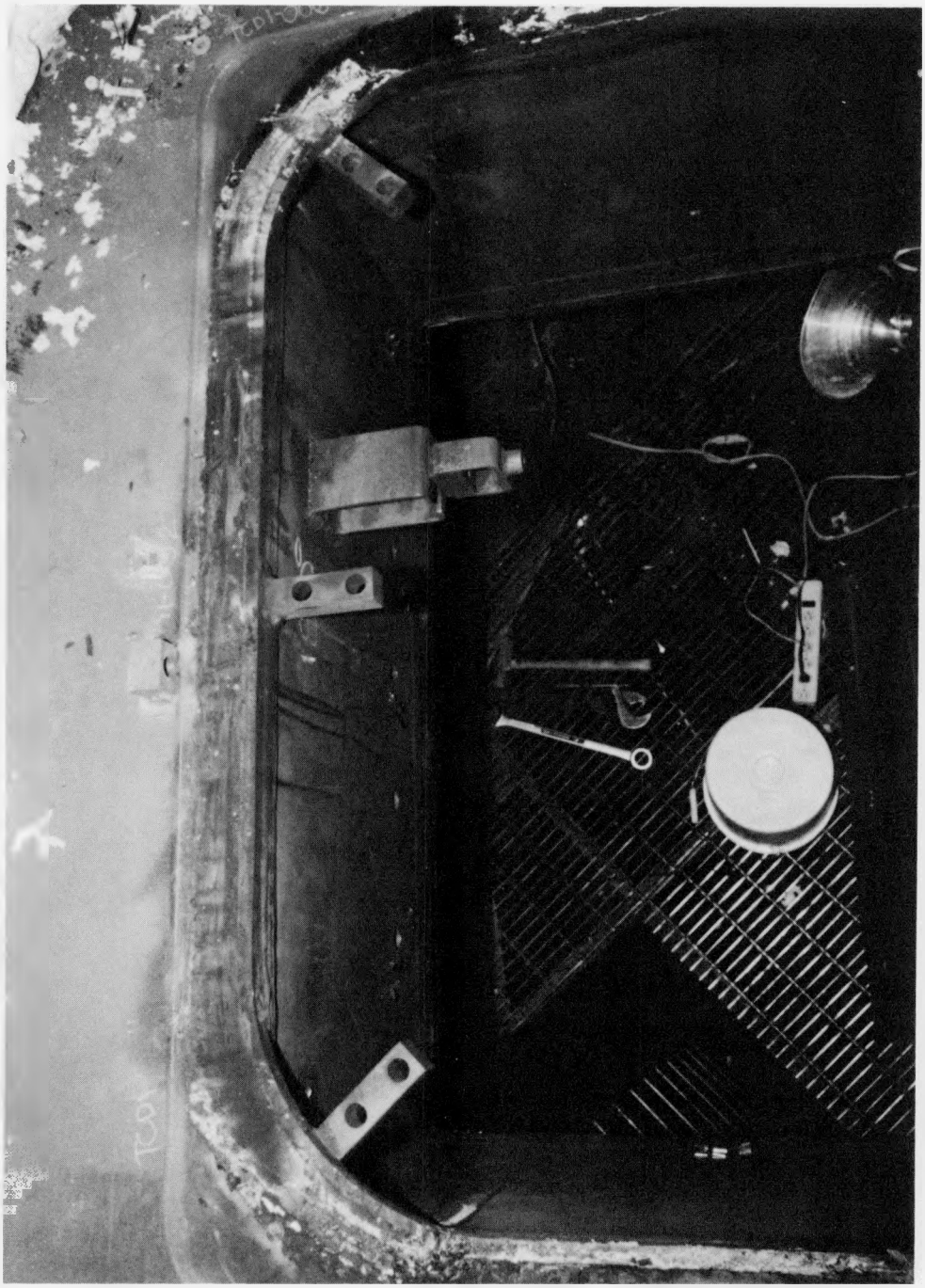

Figure 8.14 Inner Door Gasket Seal Failure Location

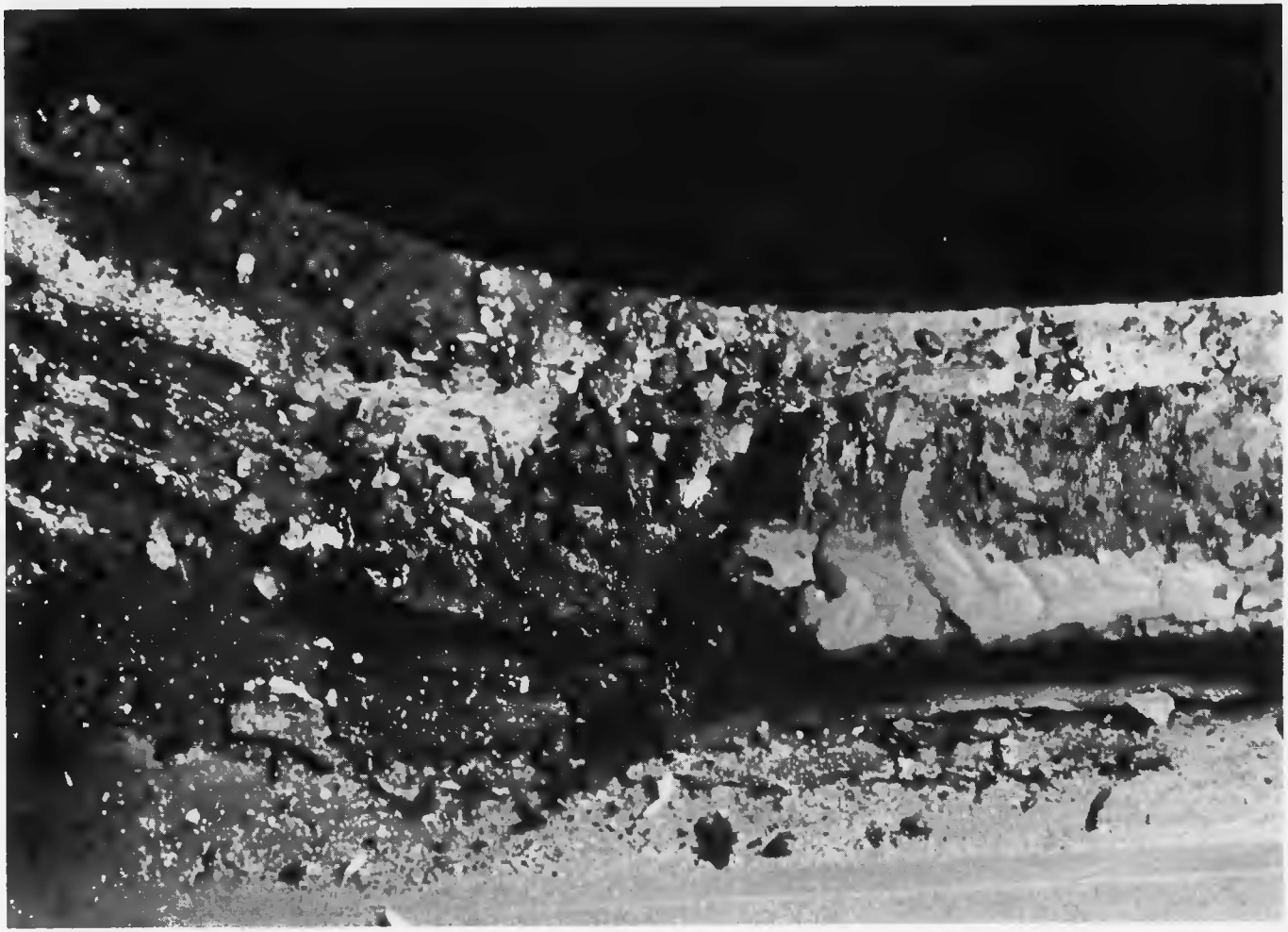

Figure 8.15 Charred Remains of Gasket Seal After Seal Failure

Figure 8.16 Gasket Seal Outside of Failure Area

Figure 8.17 Extruded Seal Remains Intact on Inner Door

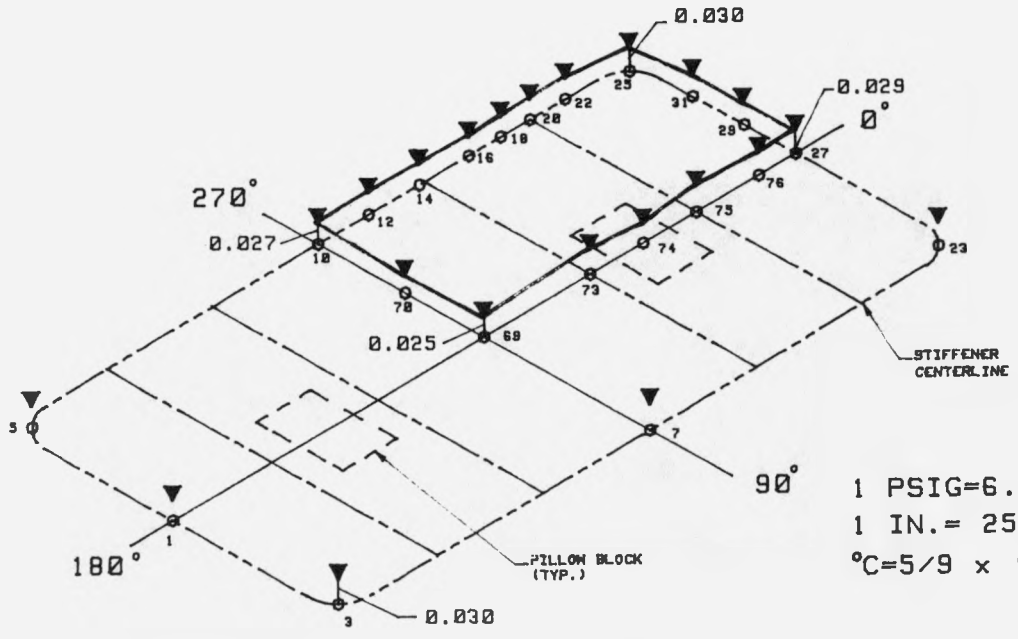

CYCLE NO. 1
TIME: 5.44 HRS

PRESSURE: 9.1 PSIG
(DOOR AVG. PERIMETER
SURFACE TEMP.: 280.2 F)

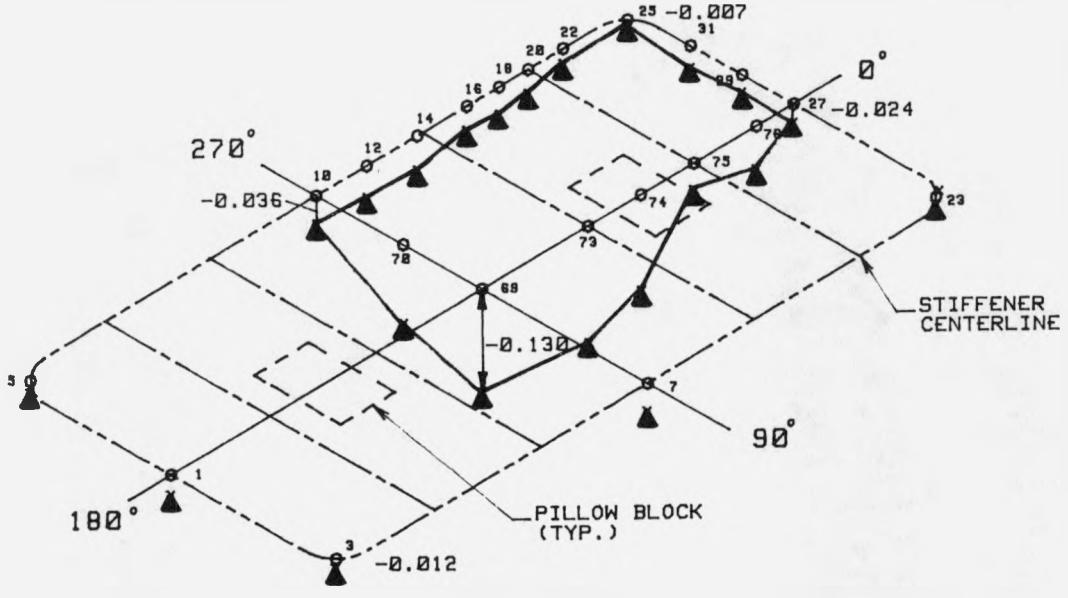

CYCLE NO. 1
TIME: 14.42 HRS

PRESSURE: 305.9 PSIG
(DOOR AVG. PERIMETER
SURFACE TEMP.: 284° F)

Figure 8.18 Profiles of Inner Door Displacement During the First Load Cycle

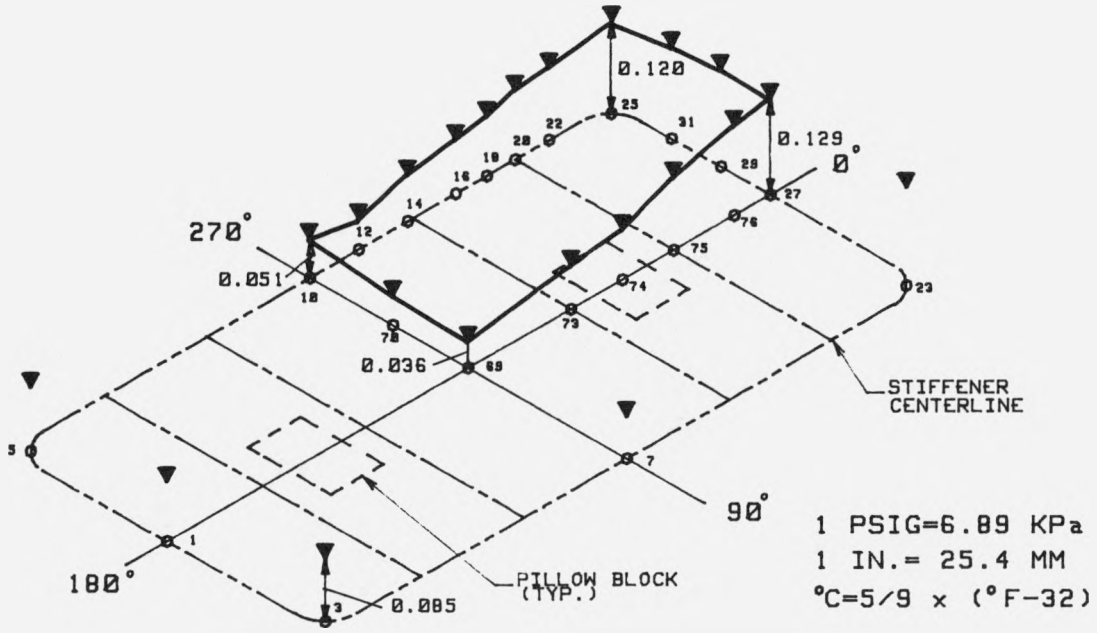

CYCLE NO. 2 PRESSURE: 10.0 PSIG
TIME: 31.43 HRS (DOOR AVG. PERIMETER
SURFACE TEMP.: 640.2 F)

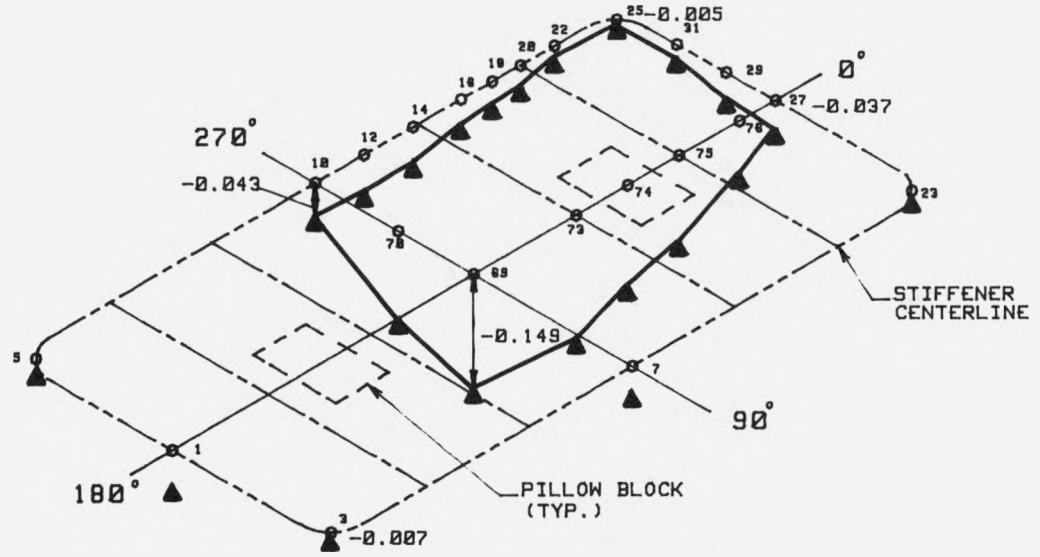

CYCLE NO. 2 PRESSURE: 301.6 PSIG
TIME: 37.67 HRS (DOOR AVG. PERIMETER
SURFACE TEMP.: 485.3 F)

Figure 8.19 Profiles of Inner Door Displacement During the Second Load Cycle

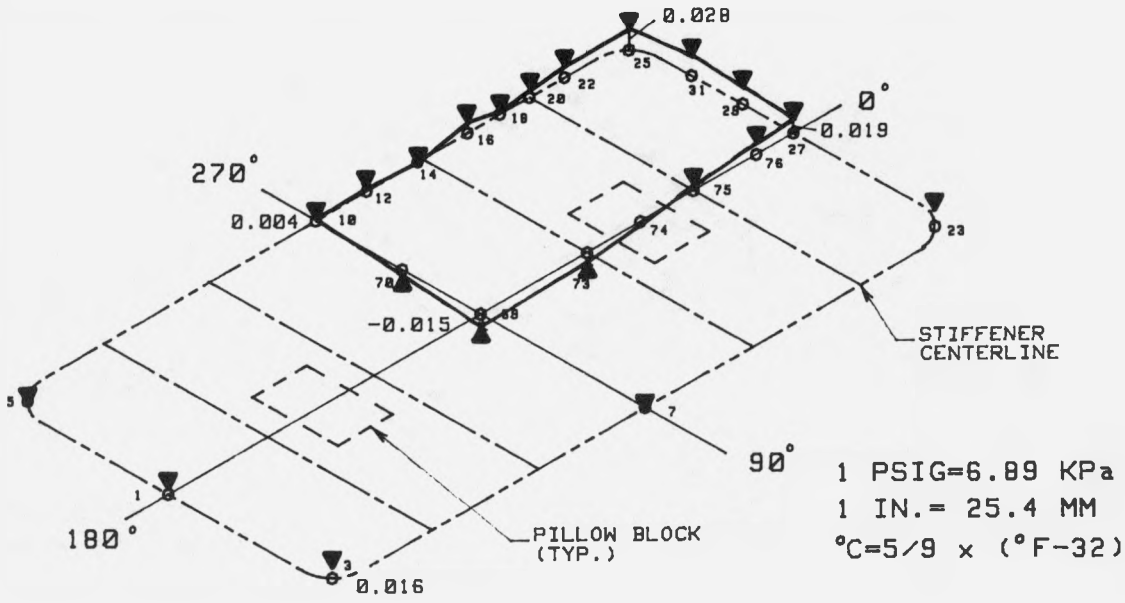

CYCLE NO. 3 PRESSURE: 4.5 PSIG
TIME: 52.70 HRS (DOOR AVG. PERIMETER
SURFACE TEMP.: 654.0 F)

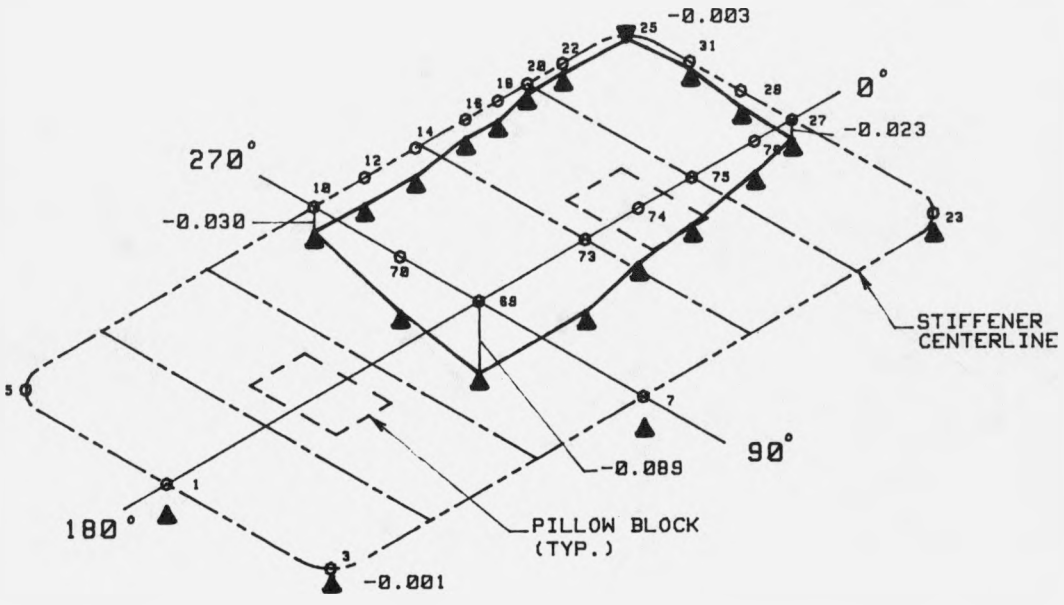

CYCLE NO. 3 PRESSURE: 148.2 PSIG
TIME: 53.27 HRS (DOOR AVG. PERIMETER
SURFACE TEMP.: 626.5 F)

Figure 8.20 Profiles of Inner Door Displacement During the Third Load Cycle

occurred at 0° and 180° were 0.129 in. (3.3 mm) and 0.080 in. (2.0 mm), respectively. At 90° the displacement was 0.056 in. (1.4 mm). The shape of the displacements indicates two-way plate bending, however, upon inspection of the 0° - 270° quadrant, displacements along the 0° - 180° centerline and along the door edge parallel to the centerline indicate a definite inflection point. This inflection point coincides with the door hinge pillow block attachment to the door. The downward force of the air pressure was overcome by an upward acting force. Temperatures through the thickness of the steel door were relatively uniform, with a temperature differential between the hot and cold sides of 26°F (14°C). It is clear that the latching mechanism was engaged and provided the restraint necessary to cause the door to take on the shape reported herein.

These glimpses of the inner door profile provide some insight into the structural interaction of the door, the latching mechanism, the effect of high surface pressures on the inner door, and the expanding gasket. To fully separate the effect of the driving forces of elevated temperatures and high surface pressures on the inner door, selected displacement transducers around the perimeter of the door were compared with the surface temperature of the door, which are shown in Figures 8.21 and 8.22. As can be seen in these figures, the most dramatic effect of increasing temperature on the gasket seal occurred during the second load cycle. As shown in Figure 8.21, the increase in gap between the door and bulkhead reached an upper limit of 0.130 in (3.3 mm), and then suddenly dropped off in magnitude. Displacement transducers for Figure 8.22 show no sudden drop off during heating. It can be surmised that, with the apparent sudden loss of structural stability of the gasket and a closing of the gap, the gasket material had reached the point at which the material became unstable. Although the gasket material may have initiated a phase change, there was no measurable loss of the seal across the pressure boundary. Both transducers along the 180° edge show this phenomena. Based on earlier discussions, the gasket seal failed along the 180° edge of the door, which is consistent with the drop off in load carrying capability shown in Figure 8.21.

The increase in gap indicated for the first load cycle is continued in the second load cycle. The offset is due to compression caused by high pressures exerted on the door. The gap increase during the third load cycle was negligible in comparison. At this point, the entire gasket had been exposed to temperatures beyond the original design and sufficient volume of the gasket reached material instability.

Expansion of the seal within the gland could account for the upward movement observed. Temperature of the seal was most likely very close to the temperature of the inner door. Thermal expansion characteristics of the EPDM E603 material are reported for temperatures up to 375°F (191°C). The reported value of thermal coefficient of expansion for EPDM E603 is 8.9×10^{-5}/°F (16×10^{-5}/°C) In this test the seal was constrained to move in one direction: towards the bulkhead. It is true that as the gap between the door and bulkhead seal surface increases the potential for the gasket material to extrude into the gap increases, just as the gasket material extruded into the gap during thermal aging of the gasket. However, it was observed after testing that the gasket was firmly adhered to the seal surface, most likely as a result of the gasket being exposed to temperatures in excess of the material instability threshold temperature and high compressive forces on the gasket.

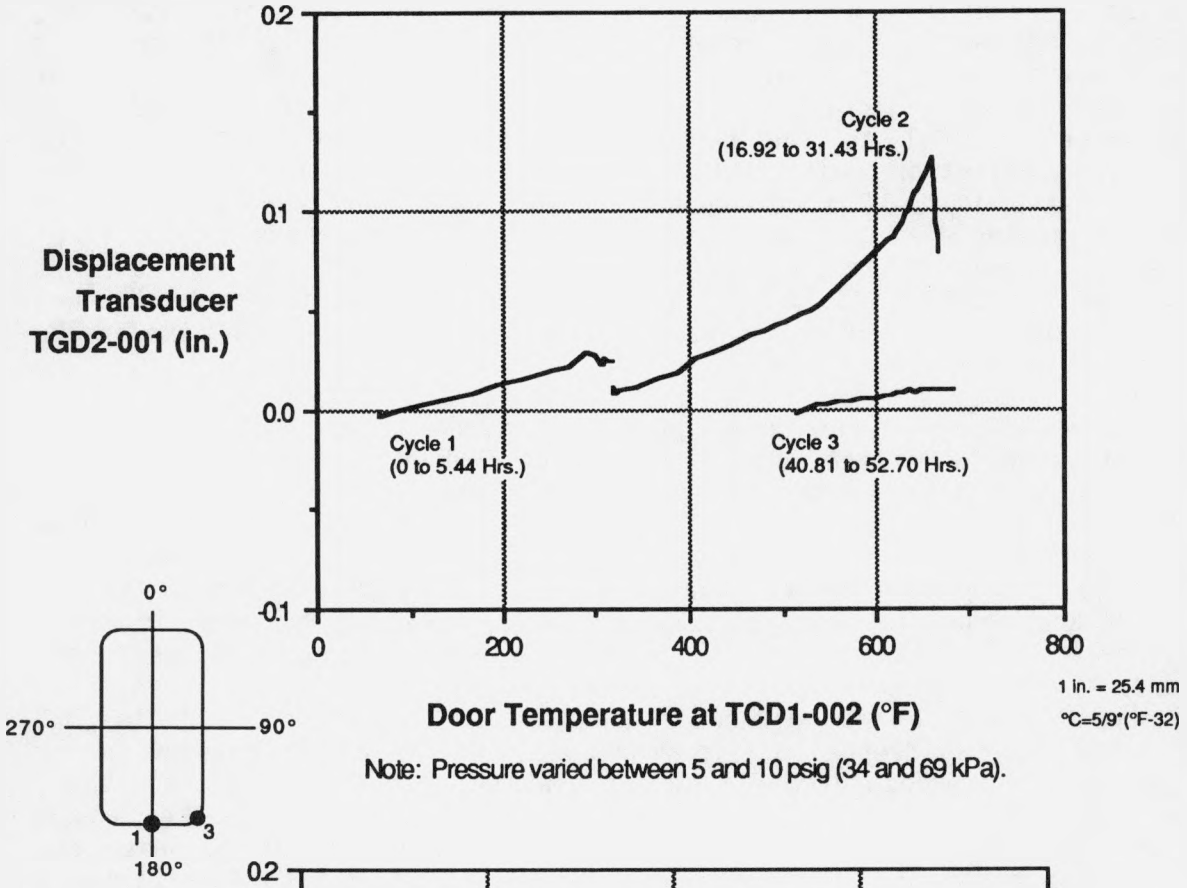

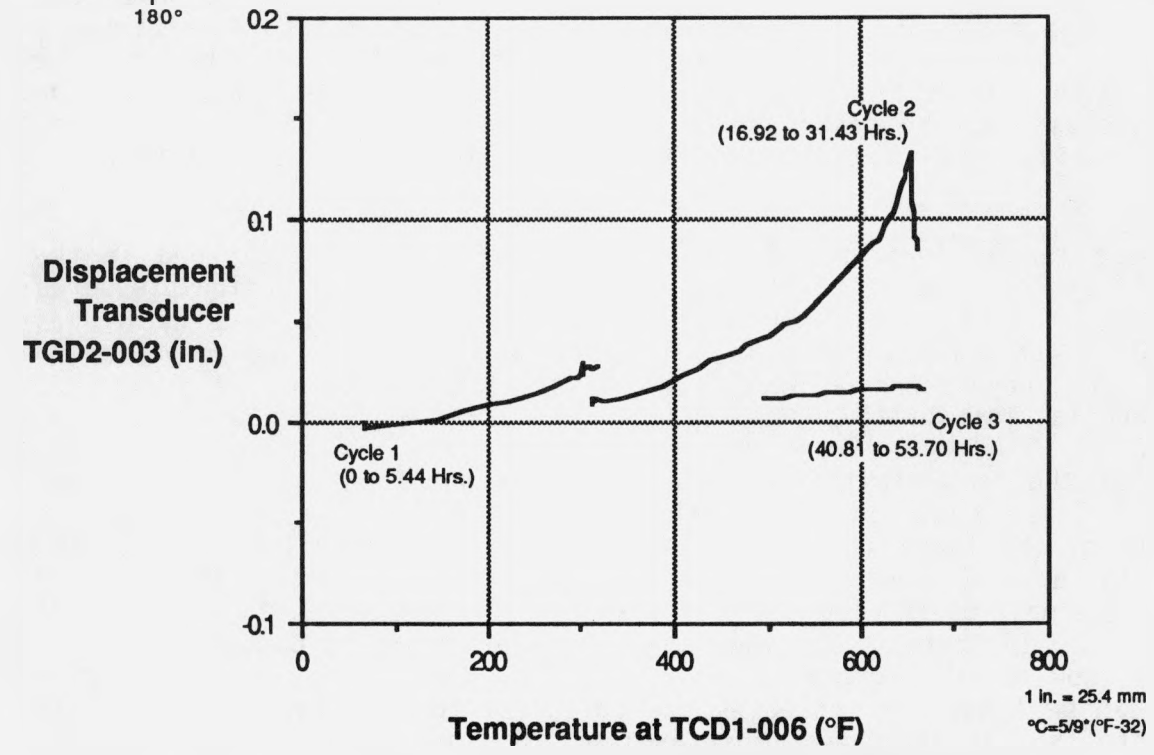

Figure 8.21 Displacement versus Temperature for Capacitance Probe Transducers TGD2-001 and TGD2-003

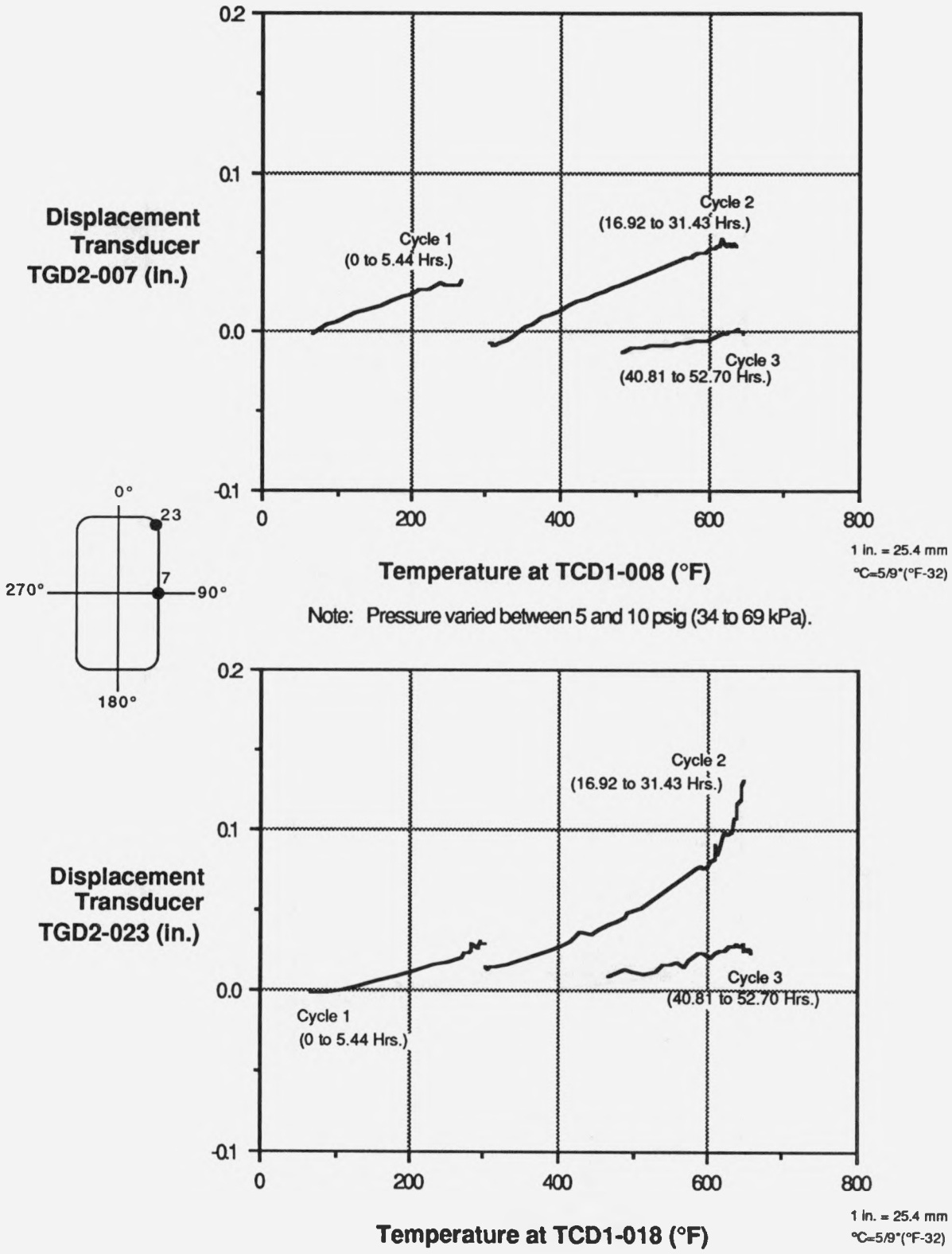

Figure 8.22 Displacement versus Temperature for Capacitance Probe Transducers TGD2-007 and TGD2-023

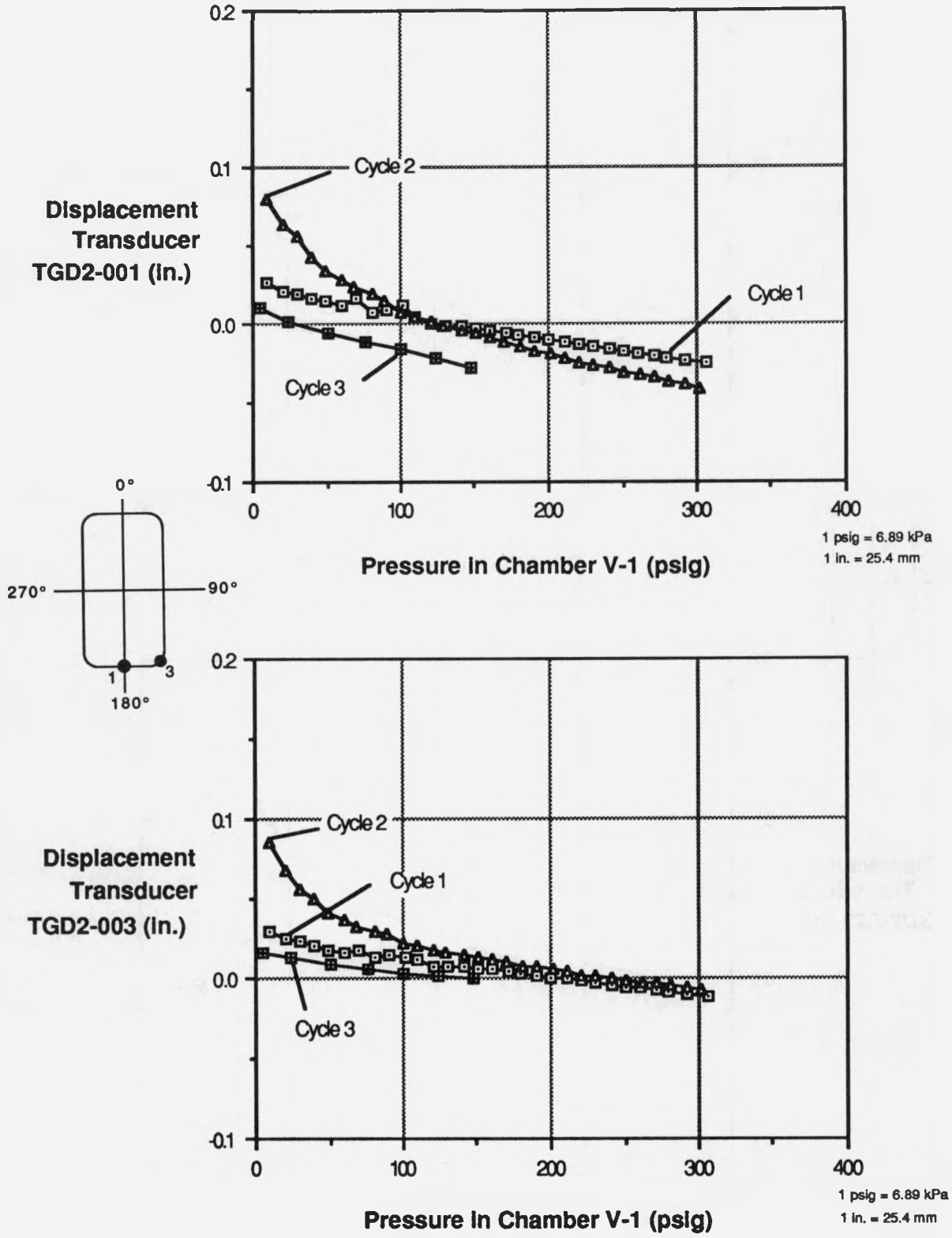

Figure 8.23 Displacement versus Pressure for Capacitance Probe Transducers TGD2-001 and TGD2-003

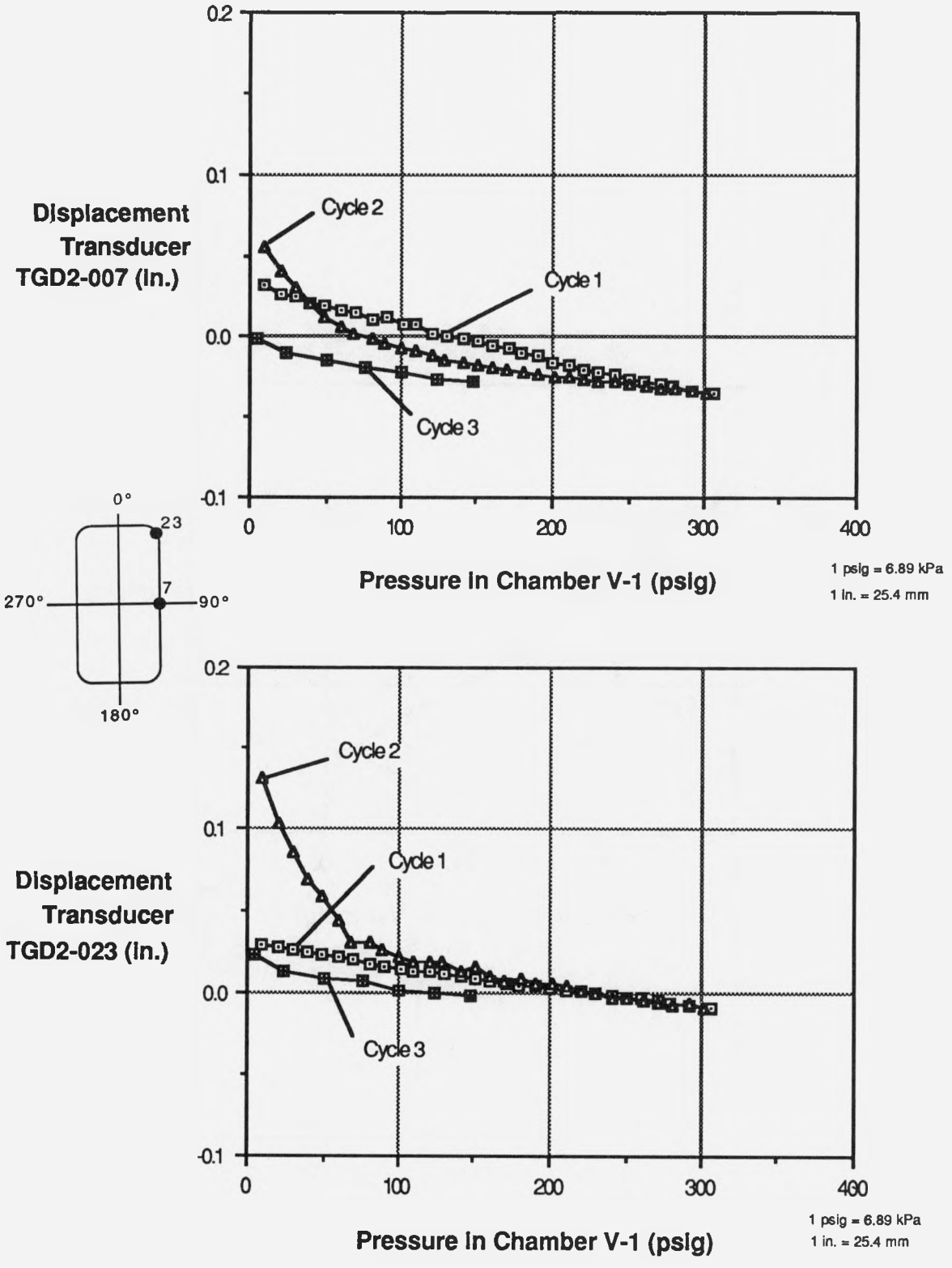

Figure 8.24 Displacement versus Pressure for Capacitance Probe Transducers TGD2-007 and TGD2-023

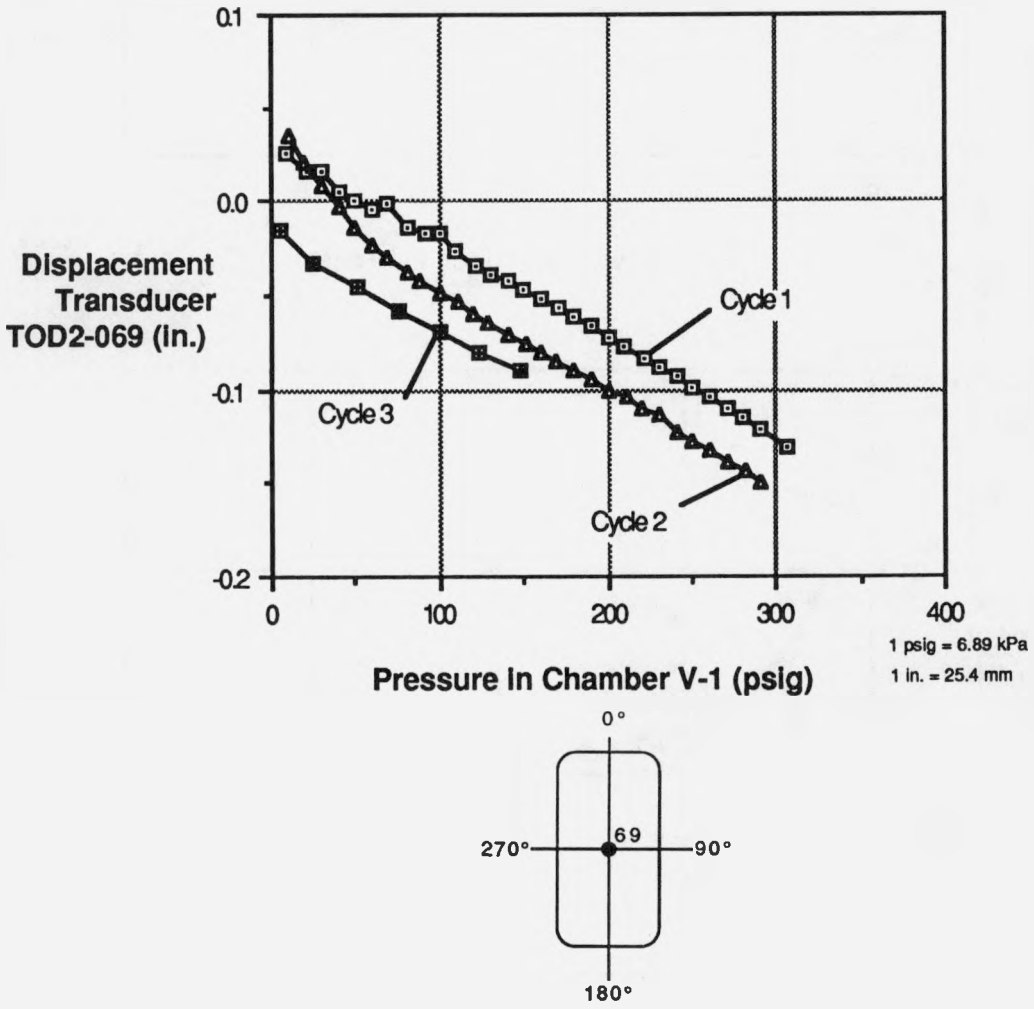

Figure 8.25 Displacement versus Pressure for Capacitance Probe Transducer TOD2-069

If the EPDM E603 material is assumed to be incompressible, the net volume after expansion must remain constant. If a unit length of the seal, with a net cross-section equal to the seal gland, was allowed to expand freely in the direction of the bulkhead and constrained in the other two directions, the net total expansion would be 0.137 in. (3.5 mm) The maximum recorded displacement was 0.13 in. (3.3 mm), with the majority of the deflections around the door perimeter from 0.05 to 0.09 in. (1.3 to 2.3 mm). Although this data was not available, the coefficient of thermal expansion may be greater at temperatures above 375°F (191°C) which may have caused greater expansion, hence larger forces on the restrained door.

The effect of pressure on the gap between the door is shown in Figures 8.23, 8.24, and 8.25. As can be seen in Figures 8.18, 8.19, and 8.20, profiles of the deformed inner door indicate classical plate bending due to high pressure exposures. Figure 8.25 shows the deflection of the center of the inner door at transducer location TOD2-069. The center of the door showed maximum deflection while exposed to the high pressures. From the beginning of the pressurization cycle until 300 psig (2.07 MPa) was reached during the second load cycle, the center of the inner door moved from 0.036 in (0.91 mm) to -0.149 in (3.8 mm), yielding a total movement of 0.185 in (4.7 mm). This deflection of the inner door was in part due to compression of the gasket seal, and part due to flexural deformations of the door.

At transducer locations TGD2-003 and TGD2-023, which are corner locations on the door, the overall deflection due to high pressures was less than the other locations. This may be a result of two-way plate bending where the corners of the plate curl up. The reinforcement configuration of the inner door does not appear to fully prevent the curling up of the corners.

8.2.3 Measured Strains During Test 2C

Measured strains had two components which contributed to the resultant recorded strains. The first component resulted from temperature differential in the airlock and resultant internal restraints. Two strain gages, SGB1-31V and SGB1-17V are plotted against their respective thermocouple temperature output used for temperature compensation, as shown in Figure 8.26. Each curve is representative of the time period in each load cycle prior to pressurization. Duration of heating period is shown in each figure. The magnitude of these strains due to differential temperatures was dependent on temperature and restraint conditions. If the airlock was allowed to achieve uniform temperatures throughout the airlock, the strains due to internal restraint would go to zero. Maximum offset due to thermally induced strains for strain gage SGB1-17V was -681 microstrain near the end of the third cycle. Maximum offset due to thermally induced strains for strain gage SGB1-31V was -375 microstrain at the end of the third cycle, as shown in Figure 8.26.

The second component that contributed to the resultant strain recorded strains was due to pressurization of Chamber V-1 and the airlock. The results of strain plotted against pressure is shown in Figure 8.27. Two items are immediately apparent:

(1) The curves appear to be very linear, and have nominally the same slope.

(2) The strain gage output shows an offset, i.e., they do not start at zero strain.

Although the slope is virtually the same, the curves do not fall right on top of each other for the same strain gage. The offset is a result of the thermally induced strains and internal restraint. Maximum compressive strain recorded was -1659 microstrain, which is very close to the yield point, and the maximum tensile strain recorded was 1242 microstrain.

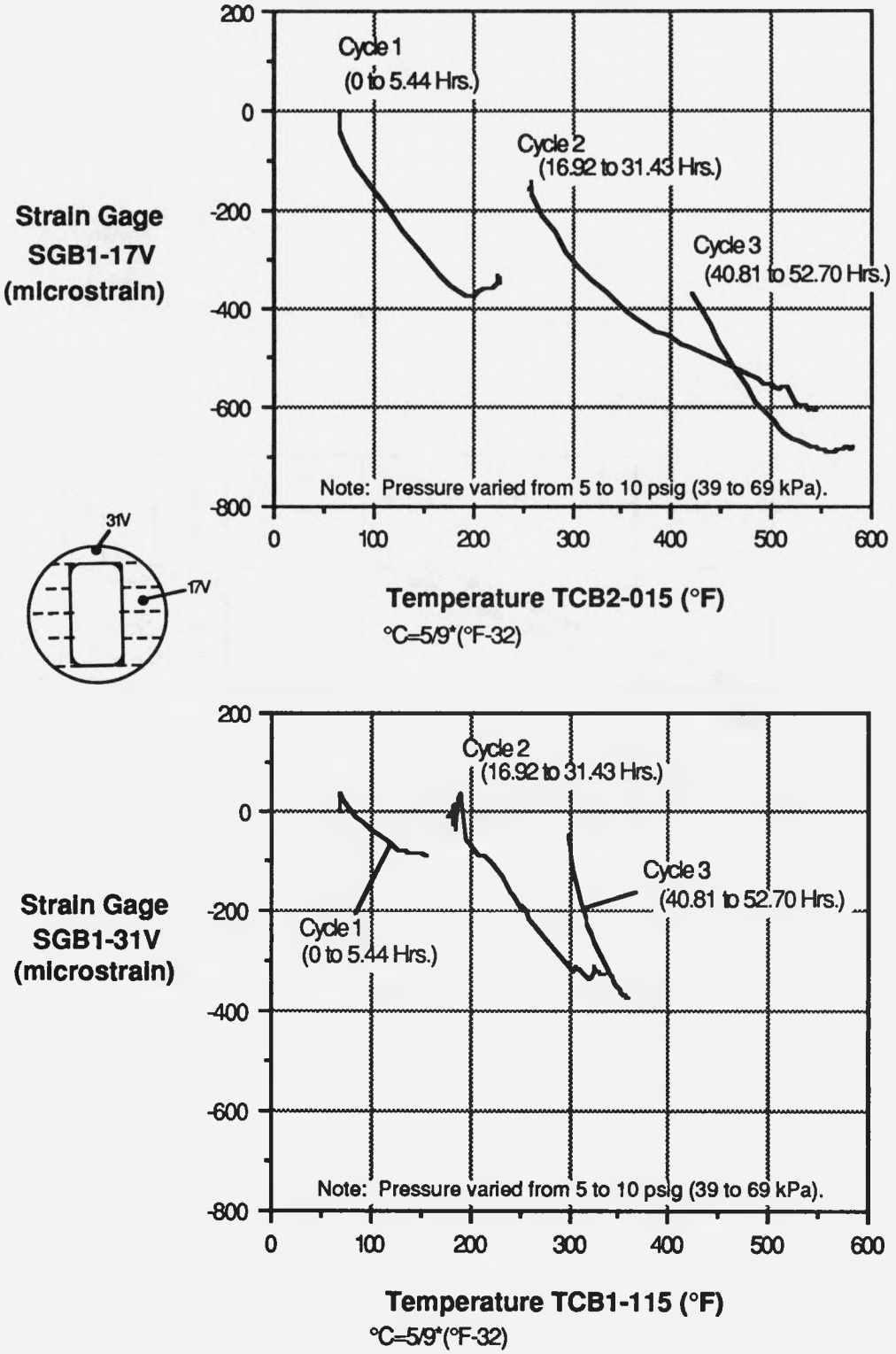

Figure 8.26 Strain versus Temperature for Measured Strains on Inner Door Bulkhead During Test 2C

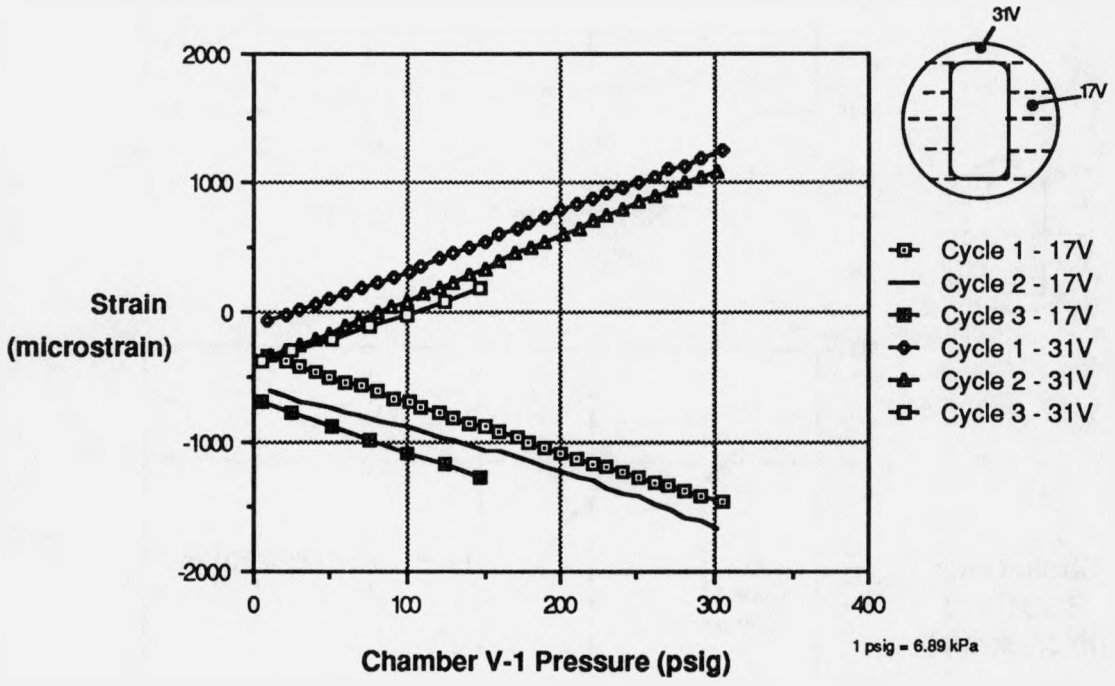

Note: The last three digits in legend refer to strain gage number.

Figure 8.27 Strain versus Pressure for Measured Strains on Inner Door Bulkhead During Test 2C

9.0 SUMMARY AND COMMENTS

In previous studies, the gasket seal in a personnel airlock assembly was identified as a potential weak link in overall containment integrity.[3,4] As a result of testing performed on a full size airlock, the following summarize the test results:

(1) The airlock was designed for 60 psig (410 kPa) and 340°F (171°C). Testing exposed the airlock to 300 psig (2.07 MPa) and an air temperature above the inner door of 850°F (454°C). Although the gasket was degraded by an accelerated aging process, no leakage of the airlock door occurred for pressures from 0 to 300 psig (0 to 2.07 MPa) while the gasket was subjected to temperatures less than its ignition temperature (approximately 620°F (327°C)).

(2) Degradation and subsequent failure of the gasket seal was related to temperatures in excess of the temperatures at which EPDM E603 elastomer is stable. When the gasket failed it was quickly eroded by an onrush of hot air. The gasket was reduced to a powdery consistency in the area that the seal was breached.

(3) Test results indicate that the gasket expanded while increasing air temperature above the door from 400 to 800°F (204 to 427°C) causing significant upward deflection of the inner door and resulting in larger gaps between the inner door and bulkhead.

(4) The personnel airlock survived 300 psig (2.07 MPa) internal pressurization. All strain gages indicated elastic behavior throughout the airlock from stresses induced by the elevated pressures and temperatures.

(5) The condition of the gasket due to accelerated aging did not appear to affect sealing ability at high temperatures and pressures. However, extrusion of the gasket material between the inner door and bulkhead during accelerated aging and high temperature heating, as in Item (3) above, prevented metal-to-metal contact between the door and bulkhead.

(6) The outer door at 300 psig (2.07 MPa) did not leak. Temperatures measured on the outer door were below 200°F (93°C). Heat transfer conditions have an important effect on the temperature distribution. The temperature of the inner door and bulkhead reached an average surface temperature of approximately 611°F (322°C) when the air temperature was 800°F (427°C), even under forced convection conditions. The outer door and bulkhead temperatures were lower for this test than might be expected due to the effect of the airlock orientation.

10.0 REFERENCES

[1] Sebrell, W.A., "The Potential for Containment Leak Paths Through Electrical Penetration Assemblies Under Severe Accident Conditions," NUREG/CR-3234, SAND83-0538, Sandia National Laboratories, Albuquerque, NM, July 1983.

[2] Clauss, D.B., Horschel, D.S., and Blejwas, T.E., "Insights into the Behavior of LWR Steel Containment Buildings During Severe Accidents," Nuclear Engineering and Design 100 (1987) p. 189.

[3] Shackelford, M.H., et al., "Characterization of Nuclear Reactor Containment Penetrations - Final Report," NUREG/CR-3855, SAND84-7180, Sandia National Laboratories, Albuquerque, NM, January 1985.

[4] Barnes, B.L., et al., "Leak Area Estimates for Power Reactor Containments During Severe Accident Conditions," Idaho National Engineering Laboratory, EGG-EA-6753, 1984.

[5] Brinson, D.A., and Graves, G.A., "Evaluation of Seals for Mechanical Penetrations of Containment Buildings," NUREG/CR-5096, SAND88-7016, Sandia National Laboratories, Albuquerque, NM, 1988.

[6] Norris, O.E., Chicago Bridge & Iron Company, "RFQ 64-7523 Personnel Lock for NRC Containment Penetrating Leak Testing Program," April 30, 1985 (Letter).

[7] ASME Boiler and Pressure Vessel Code, Section II, "Material Specifications," American Society of Mechanical Engineers, 1974 (No Addenda).

[8] ASME Boiler and Pressure Vessel Code, Section III, "Rules for Construction of Nuclear Power Plant Components," American Society of Mechanical Engineers, 1974 (No Addenda).

[9] ASME Boiler and Pressure Vessel Code, Section V, "Nondestructive Examination," American Society of Mechanical Engineers, 1974 (No Addenda).

[10] ASME Boiler and Pressure Vessel Code, Section IX, "Welding and Brazing Qualifications," American Society of Mechanical Engineers, 1974 (No Addenda).

[11] Peters, S.W., CBI Industries, Inc., "Thermal Analysis Results for Temperature Increase to 800°F," January 27, 1987 (Letter).

[12] ASME Committee on Flow Measurement, "Flowmeters, Their Theory and Applications," 6th Edition, 1971.

[13] Orwick, P.E., "Aging Characteristics of Presray Seal and Gasket Material," Presray, March 1986.

APPENDIX A

NOTES ON QUALITY ASSURANCE

"Statement of Work for Testing a Personnel Airlock", Document No. 56-6713, Attachment I dated July 18, 1986 requires that a quality assurance plan in accordance with the intent of EP 401414 be approved by SNL prior to any testing. CBIRC received approval for and implemented for this testing contract the quality control system as outlined in Issue 1 of the "Manual for Research and Development Quality Control System". This system provides activities which invoke a quality assurance program consistent with 10 CFR 50 Appendix B as required by EP 401414.

CBIRC's execution of the personnel airlock test invoked all the activities in the quality control system from design control through the eighteen point criteria of 10 CFR 50 Appendix B up to, but not including, internal audits. Internal audits were excepted by Change No. 8 of Contract Amendment No. 01. Records are maintained by CBIRC which furnish evidence of the activities performed for this contract in accordance with the quality control system.

APPENDIX B - DATA PLOTS AND TABULATIONS

TABLE OF CONTENTS

B.0 DATA PLOTS AND TABULATIONS

The results of each of Tests 2A, 2B, 2C, 3A, and 3B are presented herein. Results are presented in both tabular form and as plots. Results of Tests 1A, 1AA, 1B, and 1BB are presented in their entirety in Section 8.0, "Discussion of Test Results". Reference locations of all transducers are discussed in Section 4.0, "Instrumentation and Data Acquisition".

For Tests 2A, 2B, 3A, and 3B, plots are made with reference to the controlling parameter pressure. Tabulated data is presented for each scan. Results for Test 2C are presented by plotting transducer results versus time and tabulating every fourth data point recorded during the test. Only those transducers which were active during the test will be plotted and tabulated. Active means that the transducer was attached to or targeted at a structure under pressure or combined pressure and thermal loading.

During testing, some transducers clearly failed before testing began. Those transducers that failed are not reported but are omitted in the plots and tabulation. Those transducers that were operational when the test began but failed prior to the end of the test will be plotted or tabulated until the point of failure. Active transducers and a list of those transducers that were not reported or had erratic behavior but were reported herein are tabulated in Tables B.1 through B.5.

B.1 Transducer Sign Conventions

The sign convention for thermocouples is self-explanatory, however, for clarification the numerical sign convention for transducers is defined below.

- Strain Gages: "+" - tensile strains "-" - compressive strains
- Capacitive Displacement Transducers:

Gap/Rotation Transducers:	"+"	Gap between door and bulkhead increasing
	"-"	Gap between door and bulhead decreasing
Slip Transducers:	"+"	Gap between door edge and transducer increasing
	"-"	Gap between door edge and transducer decreasing
Inner Door Frame Transducers:	"+"	Door frame growing
	"-"	Door frame shrinking
Out-of-Plane Transducers:	"+"	Gap between door/bulkhead/stiffener and reference frame increasing
	"-"	Gap between door/bulkhead/stiffener and reference frame decreasing

• Cantilever Type Displacement Transducers:	"+"	increase in Chamber V-1 diameter
	"-"	decrease in Chamber V-1 diameter
• Pressure Transducers:	"+"	Positive internal pressure in Chamber V-1 or airlock
• Flow Meters:	"+"	Flow direction from Chamber V-1 to airlock or airlock to Chamber V-1

Table B.1

Test 2A Active Transducers

Active Transducers

Pressure:	PT-06, PT-08, PT-09, PT-10
Leak Rate:	FT-16
Gap/Rotation:	TGD2-001 through TRD2-032
Door Slip:	TSD1-059 through TSD1-062
Door Frame:	TOS2-067, TOS2-068
Out-of-Plane:	TOD2-069 through TOD2-076, TOS2-077 through TOS2-079, TOB2-080, and TOB2-081
Strain Gages:	SGB1-01 through SGB1-031, SGV1-040 through SGV4-045

Transducer	Comments
TGD2-016	Noise in transducer response
TRD2-017	Not reported due to transducer malfunction
TGD2-018	Not reported due to transducer malfunction
TGD2-025	Noise in transducer response
TRD2-026	Noise in transducer response
TOS2-067	Not reported due to transducer malfunction

Table B.2

Test 2B Active Transducers

Active Transducers

Pressure:	PT-06, PT-08, PT-09, PT-10, PT-23
Leak Rate:	FT-21
Gap/Rotation:	TGD2-033 through TRD3-058
Door Slip:	TSD2-063 through TSD2-066
Out-of-Plane:	TOD3-082, TOS3-083, TOB3-084
Strain Gages:	SGB2-32 through SGV4-045

Transducer	Comments
TRD3-041	Not reported due to transducer malfunction
TGD3-042	Not reported due to transducer malfunction
TRD3-056	Not reported due to transducer malfunction

Table B.3

Test 2C Active Transducers

Active Transducers

All pressure, leak rate, displacement, temperature, and strain gage transducers discussed in Section 4.0, "Instrumentation and Data Acquisition", were considered active.

Transducer	Comments
	Capacitance Probes
TGD2-001	Gap after seal failure unrealistic
TRD2-002	Gap after seal failure unrealistic
TGD2-016	Noise in transducer response
TRD2-017	Not reported due to transducer malfunction
TRD2-026	Noise in transducer response
TRD2-028	Three readings after test require smoothing
TRD2-030	Not reported due to transducer malfunction
TGD2-031	Not reported due to transducer malfunction
TGD3-033	Not reported due to transducer malfunction
TGD3-034	Not reported due to transducer malfunction
TGD3-035	Noise in transducer response
TRD3-036	Noise in transducer response
TGD3-037	Noise in transducer response
TRD3-038	Not reported due to transducer malfunction
TGD3-039	Noise in transducer response
TRD3-040	Not reported due to transducer malfunction
TRD3-041	Not reported due to transducer malfunction
TGD3-042	Noise in transducer response
TRD3-043	Noise in transducer response

Table B.3 (continued)

Transducer	Comments
TGD3-044	Not reported due to transducer malfunction
TRD3-053	Not reported due to transducer malfunction
TRD3-058	Not reported due to transducer malfunction
TSD1-060	Transducer may have come in contact with door
TSD2-066	Not reported due to transducer malfunction
TOS2-067	Not reported due to transducer malfunction
TOD2-071	Transducer may have come in contact with door at high pressures
TOD2-072	Not reported due to transducer malfunction
	Thermocouples
TCD1-014	Not reported due to transducer malfunction
TCE4-056	Electrical noise during heating
TCE4-057	Electrical noise during heating
TCE4-058	Electrical noise during heating
TCE4-064	Electrical noise during heating
TCE4-065	Electrical noise during heating
TCE4-066	Electrical noise during heating
TCE4-070	Electrical noise during heating
TCE4-071	Electrical noise during heating
TCE4-072	Electrical noise during heating
TCE4-076	Electrical noise during heating
TCE4-077	Electrical noise during heating
TCE4-078	Electrical noise during heating
TCE4-082	Electrical noise during heating
TCE4-083	Electrical noise during heating
TCE4-084	Electrical noise during heating
TCE4-093	Electrical noise during heating
TCE4-094	Electrical noise during heating
TCE4-095	Electrical noise during heating

Table B.3 (continued)

Transducer	Comments
	Strain Gages
SGD1-07V*	Temperature compensation thermocouple failed
SGD1-07D*	Temperature compensation thermocouple failed
SGD1-07H*	Temperature compensation thermocouple failed
SGD1-09V*	Temperature compensation thermocouple failed
SGD1-09D*	Temperature compensation thermocouple failed
SGD1-09H*	Temperature compensation thermocouple failed

* A thermocouple adjacent to the strain gage location was used in recalculating strains.

Table B.4

Test 3A Active Transducers

Active Transducers

Pressure:	PT-06, PT-08, PT-09, PT-10
Leak Rate:	FT-16
Gap/Rotation:	TGD2-001 through TRD2-032
Door Slip:	TSD1-059 through TSD1-062
Door Frame:	TOS2-067, TOS2-068
Out-of-Plane:	TOD2-069 through TOB2-081
Strain Gages:	SGB1-01 through SGB1-031, SGV1-040 through SGV4-045
Canilever Beam Displacements:	LVV4-001 through LVV4-004

Transducer	Comments
TRD2-016	Not reported due to transducer malfunction
TRD2-017	Not reported due to transducer malfunction
TGD2-018	Not reported due to transducer malfunction
TRD2-019	Not reported due to transducer malfunction
TOS2-067	Not reported due to transducer malfunction

Table B.5

Test 3B Active Transducers

Active Transducers	
Pressure:	PT-06, PT-08, PT-09, PT-10, PT-23
Leak Rate:	FT-21
Gap/Rotation:	TGD2-033 through TRD3-058
Door Slip:	TSD2-063 through TSD2-066
Out-of-Plane:	TOD3-082, TOS3-083, TOB3-084
Strain Gages:	SGB2-32 through SGV4-045
Cantilever Beam Displacements:	LVV4-001 through LVV4-004

Distribution:

J. F. Costello (20 Copies)
USNRC/RES
Mail Stop NL/S-217A
5650 Nicholson Lane
Rockville, MD 20852

H. L. Graves, III
USNRC/RES
Mail Stop NL/S-217A
5650 Nicholson Lane
Rockville, MD 20852

US Department of Energy
Office of Nuclear Energy
Attn: A. Millunzi
Bernard J. Rock
D. Giessing (3 copies)
Mail Stop B-107
NE-540
Washington, DC 20545

CBI NaCon, Inc.
Attn: Thomas J. Ahl
800 Jorie Boulevard
Oak Brook, IL 60521

Wilfred Baker Engineering
Attn: Wilfred E. Baker
218 E. Edgewood Pl.
P. O. Box 6477
San Antonio, TX 78209

Battelle Columbus Laboratories
Attn: Richard Denning
505 King Avenue
Columbus, Ohio 43201

Bechtel Power Corporation
Attn: Asadour H. Hadjian
12400 E. Imperial Highway
Norwalk, CA 90650

Bechtel Power Corp.
Attn: T. E. Johnson, Subir Sen
K. Y. Lee (3 copies)
15740 Shady Grove Rd.
Gaithersburg, MD 20877

Babcock & Wilcox Co.
Attn: James R. Farr
20 S. van Buren Ave.
Barberton, OH 44203

CBI Research Corp.
Attn: J. T. Julien (10 copies)
S. W. Peters (10 copies)
1501 N. Division Street
Plainfield, IL 60544-8929

City College of New York
Dept. of Civil Engineering
Attn: C. Costantino
140 Street and Convent Ave.
New York, NY 10031

1245 Newmark CE Lab
University of Illinois
Attn: Prof. Mete A. Sozen
208 N. Romine
MC-250
Urbana, IL 61801

Stevenson & Associates
Attn: John D. Stevenson
9217 Midwest Ave.
Cleveland, Ohio 44125

United Engineers & Constructors, Inc.
Attn: Joseph J. Ucciferro
30 S. 17th St.
Philadelphia, PA 19101

Electrical Power Research Institute
Attn: H. T. Tang, Y. K. Tang
Raf Sehgal, J. J. Taylor,
W. Loewenstein (5 copies)
3412 Hillview Avenue
PO Box 10412
Palo Alto, CA 94304

School of Civil & Environ. Engr.
Attn: Professor Richard N. White
Hollister Hall Cornell University
Ithaca, NY 14853

NUTECH Engineers, Inc.
Attn: John Clauss
1111 Pasquinelli Drive, Suite 100
Westmont, Illinois 60559

Iowa State University
Department of Civil Engineering
Attn: L. Greimann
420 Town Engineering Bldg.
Ames, IA 50011

TVA
Attn: D. Denton, W9A18
400 Commerce Ave.
Knoxville, TN 37902

Los Alamos National Laboratories
Attn: C. Anderson
PO Box 1663
Mail Stop N576
Los Alamos, NM 87545

EQE Inc.
Attn: M. K. Ravindra
3300 Irvine Aveune
Suite 345
Newport Beach, CA 92660

University of Illinois
Attn: C. Siess
Dept. of Civil Engineering
Urbana, IL 61801

EBASCO Services, Inc.
Attn: Robert C. Iotti
Two World Trade Center
New York, NY 10048

EG&G Idaho
Attn: B. Barnes, T. L. Bridges
(2 copies)
Willow Creek Bldg. W-3
PO Box 1625
Idaho Falls, ID 83415

Sargent & Lundy Engineers
Attn: A. Walser
P. K. Agrawal (2 copies)
55 E Monroe St.
Chicago, IL 60603

General Electric Company
Attn: E. O. Swain, D. K. Henrie,
R. Gou (3 copies)
175 Curtner Ave.
San Jose, CA 95125

Westinghouse Electric Corp.
Attn: Vijay K. Sazawal
Waltz Mill Site
Box 158
Madison, PA 15663

Quadrex Corporation
Attn: Quazi A. Hossain
1700 Dell Ave.
Campbell, CA 95008

ANATECH International Corp.
Attn: Y. R. Rashid
3344 N. Torrey Pines Court
Suite 320
LaJolla, CA 92037

Oak Ridge National Laboratory
Attn: Steve Hodge
PO Box Y
Oak Ridge, TN 37830

Brookhaven National Laboratory
Attn: C. Hofmayer,T. Pratt
M. Reich (3 copies)
Building 130
Upton, NY 11973

Argonne National Laboratory
Attn: J. M. Kennedy,
R. F. Kulak,
R. W. Seidensticker (3 copies)
9700 South Cass Avenue
Argonne, IL 60439

Tennessee Valley Authority
Attn: Nathaniel Foster
400 Summit Hill Rd.
W9D24C-K
Knoxville, Tennessee 37902

University of Wisconsin
Nuclear Engineering Dept.
Attn: Prof. Michael Corradini
Madison, WI 53706

Brookhaven National Laboratory
Attn: Ted Ginsberg
Building 820M
Upon, NY 11973

Dept. of Chemical & Nuclear Engr.
Univ. of California Santa Barbara
Attn: T. G. Theofanous
Santa Barbara, CA 93106

Northern Illinois University
Mechanical Engineering Dept.
Attn: A. Marchertas
DeKalb, IL 60115

Institut fur Mechanik
Universitaet Innsbruck
Attn: Prof. G. I. Schueller
Technikerstr. 13
A-6020 Innsbruck
AUSTRIA

Nuclear Studies & Safety Dept.
Ontario Hydro
Attn: W. J. Penn
700 University Avenue
Toronto, Ontario
M5G 1X6
CANADA

University of Alberta
Dept. of Civil Engineering
Attn: Prof. D. W. Murray
Edmonton, Alberta
CANADA T6G 2G7

Commissariat a L'Energie Atomique
Centre d'Etudes Nucleaires de Saclay
Attn: M. Livolant, P. Jamet (2 copies)
F-91191 Gif-Sur-Yyette Cedex
FRANCE

Institut de Protection et de
Surete Nucleaire
Commissariat a l'Energie Atomigue
Attn: M. Barbe
F-92660 Fontenay-aux-Roses
FRANCE

Kernforschungszentrum Karlsruhe GmbH
Attn: R. Krieg, P. Gast (2 copies)
Postfach 3640
D-7500 Karlsruhe
FEDERAL REPUBLIC OF GERMANY

Lehrstuhl fuer Reakordynamik
und Reaktorsicherheit
Technische Universitaet Muenchen
Attn: Prof. H. Karwat
D-8046 Garching
FEDERAL REPUBLIC OF GERMANY

Staatliche Materialpruefungsanstalt (MPA)
University of Stuttgart
Attn: Prof. K. F. Kussmaul
Pfaffenwaldring 32
D-7000 Stuttgart 80 (Vaihingen)
FEDERAL REPUBLIC OF GERMANY

Gesellschaft fuer Reaktorsicherheit
Attn: H. Schulz, A. Hoefler,
F. Schleifer (3 copies)
Schwertnergasse 1
D-5000 Koeln 1
FEDERAL REPUBLIC OF GERMANY

Kraftwerk Union AG
Attn: M. Hintergraber
Hammerbacherstr. 12-14
D-8520 Erlangen
FEDERAL REPUBLIC OF GERMANY

Ente Nazionale per l'Energia Elettrica
Attn: Francesco L. Scotto
v. le Regina Margherita, 137
Rome, ITALY

ISMES
Attn: A. Peano
Viale Giulio Cesare 29
I-24100 Bergamo
ITALY

ENEA-DISP
ACO-CIVME
Attn: Giuseppe Pino
Via Vitaliano Brancati, 48
I-00144 Roma
ITALY

Nuclear Equipment Design Dept.
Hitachi Works, Hitachi, Ltd.
Attn: O. Oyamada
3-1-1 Saiwai-Cho
Hitachi-Shi
Ibaraki-ken
JAPAN

Division of Technical Information
Japan Atomic Energy Research Institute
Attn: Jun-ichi Shimokawa
2-2, Uchisaiwai-cho 2-chome
Chiyoda, Tokyo 100
JAPAN

University of Tokyo
Institute of Industrial Science
Attn: Prof. H. Shibata
22-1, Roppongi 7
Minatu-ku, Tokyo
JAPAN

Civil Engineering Laboratory
Central Research Institute of
Electric Power Industry
Attn: Yukio Aoyagi
1646 Abiko Abiko-Shi Chiba
JAPAN

Kajima Corporation
Attn: K. Umeda
No. 1-1, 2-Chome Nishishinjuku
Shinjuku-ku
Tokyo 160
JAPAN

Muto Institute of Structural Mechanics
Attn: Tadashi Sugano
Room 3005 Shinjuku Mitsui Building
Shinjuku-ku
Tokyo, 163
JAPAN

Nuclear Power Engineering Test Center
Attn: Yoshio Tokumaru
6-2, 3-Chome, Toranomor
Minatoku
Tokyo 105
JAPAN

Japan Atomic Energy Research Inst.
Attn: Kunihisa Soda
Toshikuni Isozaki (2 copies)
Tokai-Mura, Ibaraki-Ken 319-11
JAPAN

Shimizu Construction Co., Ltd.
Attn: Toshihiko Ota
No. 4-17, Etchujima 3-Chome
Koto-Ku
Tokyo 135
JAPAN

Shimizu Construction Co., Ltd.
Attn: Toshiaki Fujimori
No. 18-1, Kyobashi 1-Chome
Chuo-ku
Tokyo 104
JAPAN

Universidad Politecnica
Escuela Tecnica Superior
de Ingenieros Industriales
Attn: Agustin Alonso
Madrid
SPAIN

Unidad Electrica S.A.
Attn: Jose Puga
UNESA
ES-28020 Madrid
SPAIN

Principia Espana, SA
Attn: Joaquin Marti
Orense, 36-2
28020 Madrid
SPAIN

Studsvik Energiteknik AB
Attn: Kjell O. Johansson
S-611 82 Nykoping
SWEDEN

Swedish State Power Board
Nuclear Reactor Safety
Attn: Hans Cederberg
Per-Eric Ahlstrom
Ralf Espefaelt (3 copies)
S-162 87 Vallingby
SWEDEN

Swiss Federal Institute of Technology
Institute of Structural Engineering
Attn: W. Ammann
ETH-Hoenggerberg, HIL
CH-8093 Zurich
SWITZERLAND

Motor-Columbus Consulting Engineers, Inc.
Attn: K. Gahler, A. Huber
A. Schopfer (3 copies)
Parkstrasse 27
CH-5401 Baden
SWITZERLAND

EIR (Swiss Federal Institute for
Reactor Research)
Attn: O. Mercier
P. Housemann (2 copies)
CH-5303 Wuerlingen
SWITZERLAND

Swiss Federal Nuclear Safety Inspectorate
Federal Office of Energy
Attn: S. Chakraborty
CH-5303 Wuerenlingen
SWITZERLAND

Swiss Federal Institute of Technology
Attn: Prof. F. H. Wittmann
Chemin de Bellerive 32
CH-1007 Lausanne
SWITZERLAND

Elektrowatt Ingenieurunternehmung AG
Attn: John P. Wolf
Bellerivestr. 36
CH-8022 Zurich
SWITZERLAND

Atomic Energy Establishment
Attn: Peter Barr
Winfrith
Dorchester Dorset
DT2 8DH
UNITED KINGDOM

Atomic Energy Authority
Safety and Reliability Directorate
Attn: D. W. Phillips
Wigshaw Lane
Culcheth
Warrington WA3 4NE
UNITED KINGDOM

HM Nuclear Installation Inspectorate
Attn: R. J. Stubbs
St. Peter's House
Stanley Precinct
Bootle L20 3LZ
UNITED KINGDOM

Taylor Woodrow Construction Limited
Attn: Carl C. Fleischer
Richard Crowder (2 copies)
345 Ruislip Road
Southall, Middlesex
UB1 2QX
UNITED KINGDOM

Central Electricity Generating Board
Attn: J. Irving
Barnett Way
Barnwood, Gloucester
GL4 7RS
UNITED KINGDOM

Central Electricity Generating Board
Attn: Carl Lomas
Booths Hall
Chelford Road
Knutsford, Cheshire
WA16 8QG
UNITED KINGDOM

HM Nuclear Installations Inspectorate BrC
Attn: Iain Todd
St. Peter's House
Bootle, Mereyside L20 3LZ
UNITED KINGDOM

3141	S. A. Landenberger (5)
3151	W. I. Klein
3153	R. Gardner
6400	D. J. McCloskey
6410	N. R. Ortiz
6420	J. V. Walker
6422	T. Fuketa
6440	D. A. Dahlgren
6442	W. A. von Riesemann (30)
6442	D. B. Clauss
6442	R. N. Eyers
6442	D. S. Horschel
6442	L. D. Lambert
6442	M. B. Parks
6442	J. J. Westmoreland
6447	M. P. Bohn
8524	J. A. Wackerly

NRC FORM 335 (2-84) NRCM 1102, 3201, 3202

U.S. NUCLEAR REGULATORY COMMISSION

BIBLIOGRAPHIC DATA SHEET

SEE INSTRUCTIONS ON THE REVERSE.

1. REPORT NUMBER (Assigned by TIDC, add Vol. No., if any)

NUREG/CR-5118
SAND88-7155

2. TITLE AND SUBTITLE

Leak and Structural Test of Personnel Airlock for LWR Containments Subjected to Pressures and Temperatures Beyond Design Limits

3. LEAVE BLANK

4. DATE REPORT COMPLETED

MONTH	YEAR
February	1989

5. AUTHOR(S)

James T. Julien, CBI
Steven W. Peters, CBI

6. DATE REPORT ISSUED

MONTH	YEAR
May	1989

7. PERFORMING ORGANIZATION NAME AND MAILING ADDRESS (Include Zip Code)

CBI Research Corporation
1501 N. Division Street
Plainfield, IL 60544-8929

Under Contract to:
Sandia National Laboratories
Albuquerque, NM 87185

8. PROJECT/TASK/WORK UNIT NUMBER

9. FIN OR GRANT NUMBER

FIN A-1375

10. SPONSORING ORGANIZATION NAME AND MAILING ADDRESS (Include Zip Code)

Division of Engineering
Office of Nuclear Regulatory Research
U.S. Nuclear Regulatory Commission
Washington, DC 20555

11a. TYPE OF REPORT

Topical

b. PERIOD COVERED (Inclusive dates)

12. SUPPLEMENTARY NOTES

13. ABSTRACT (200 words or less)

As part of the U.S. Nuclear Regulatory Commission's (USNRC) Containment Integrity Program, a leak rate test was performed on a full size personnel airlock for a nuclear containment building. The airlock was subjected to conditions simulating severe accident conditions. Testing was performed by CBI Research Corporation (CBIRC) under contract to Sandia National Laboratories (SNL) which manages the Containment Integrity Program for the USNRC.

The objective of the test was to characterize the performance of airlock door seals when subjected to conditions that simulate a severe accident condition. The gaskets tested had a cross-section known as a "double dog-ear" configuration and were made from EPDM E603. The seals were aged at an accelerated rate to simulate aging that might occur during 40 years of continuous service and a loss of coolant accident (LOCA). The data obtained from this test will be used by SNL as a benchmark for development of analytical methods. In addition to leak rate data, strain, temperature, displacement, and pressure data were measured and recorded from over 330 transducers.

A total of nine tests were performed on the airlock. In the most rigorous of these tests, the airlock inner door was subjected to pressures and temperatures of 300 psig (2.07 MPa) and 850°F (454°C).

14. DOCUMENT ANALYSIS – a. KEYWORDS/DESCRIPTORS

personnel airlock
leak rate test

b. IDENTIFIERS/OPEN-ENDED TERMS

15. AVAILABILITY STATEMENT

Unlimited

16. SECURITY CLASSIFICATION

(This page) Unclassified

(This report) Unclassified

17. NUMBER OF PAGES

18. PRICE